# INVESTIGATION OF ENVIRONMENTAL PARAMETERS INFLUENCING THE PERFORMANCE OF SOLAR PANEL AND TO OPTIMIZE ITS PERFORMANCE IN DUSTY ENVIRONMENT

Thesis

Submitted in partial fulfillment of the requirements for the degree of

DOCTOR OF PHILOSOPHY

by

ABHISHEK KUMAR TRIPATHI



DEPARTMENT OF MINING ENGINEERING
NATIONAL INSTITUTE OF TECHNOLOGY KARNATAKA
SURATHKAL, MANGALURU - 575 025

July-2019

*This Thesis is dedicated*

*to*

*my family and my better half*

# D E C L A R A T I O N

I hereby *declare* that the Research Thesis entitled **"Investigation of Environmental Parameters Influencing the Performance of Solar Panel and to Optimize Its Performance in Dusty Environment"** which is being submitted to the **National Institute of Technology Karnataka, Surathkal** in partial fulfilment of the requirements for the award of the Degree of **Doctor of Philosophy** in **Department of Mining Engineering** is a *bonafide report of the research work carried out by me.* The material contained in this Research Thesis has not been submitted to any University or Institution for the award of any degree.

**Abhishek Kumar Tripathi**
**Reg. No. 155135MN15F01**
**Department of Mining Engineering**

Place: NITK, Surathkal

Date:

# C E R T I F I C A T E

This is to *certify* that the Research Thesis entitled **"Investigation of Environmental Parameters Influencing the Performance of Solar Panel and to Optimize Its Performance in Dusty Environment"** submitted by **Mr. Abhishek Kumar Tripathi** (**Register Number: 1551357MN15F01**) as the record of the research work carried out by him, is *accepted as the Research Thesis submission* in partial fulfilment of the requirements for the award of degree of **Doctor of Philosophy.**

**Research Guides**

**Dr. Ch. S. N. Murthy**
Professor
Dept. of Mining Engg.

**Dr. M. Aruna**
Associate Professor
Dept. of Mining Engg.

**Chairman - DRPC**

Date:

# ACKNOWLEDGEMENTS

I most gratefully thank my parents **Mr. Kali Dutt Tripathi** and Mrs. **Grish Tripathi** for staying in my heart and their continuous support in each step of my life, without which it would have been impossible for me to reach this stage.

My special thanks to my elder brother Avinash, Younger brother Ashish, my sisters Neelam and Vinita, Brothers in-law Mr. Ajay and Mr. Jitnerda for their love and affection.

My heartfelt thanks to my dear childhood friend **Hari** for his strong believe in me and for always supporting me at every up and down in my life.

I owe my deepest gratitude towards my better half for her continuous support, motivation and understanding of my goals. Her love and support have always been my strength. Her patience and sacrifice will remain my inspiration throughout my life and my love for her will always increase just like entropy of universe. Without her help, I would not have been able to complete much of what I have done. It would be ungrateful on my part if I don't thank **Namrata** in these few words.

And above all, I am thankful to the Almighty **Lord Shree Krishna** for his grace.

I am sure I have forgotten someone. I assure you that this is a shortcoming on my part and not on yours. I beg you to forgive me for my oversight.

<div align="right">

**Abhishek Kumar Tripathi**

</div>

# ABSTRACT

The performance of PV panel is primarily dictated by the solar radiation falling on its surface. This research study showed that the power output of the panel decreases almost linearly with the decrease in intensity of solar radiation falling on its surface. Whenever the panel experiences shading across its surface, the solar radiation reaching its surface reduces, which degrades its performance. Moreover, the experimental results indicated that the continuous shading of other cells in the PV panel increases the temperature of an un-shaded cell and glass substrate.

The surface temperature of PV panel has an adverse impact on its electrical parameters. In this regard, an experiment was carried out to investigate the influence of PV panel surface temperature on its electrical parameters. The results of this study showed a significant reduction in the performance of PV panel with an increase in its surface temperature. A 5 W polycrystalline PV panel experienced a 0.39% decrease in open circuit voltage for every 1℃ increase in panel surface temperature. Similarly, there was 0.72% and 0.49% decrease in maximum power output and fill factor, respectively.

Humidity is also one of the environmental parameters that affect the performance of PV panel. A laboratory study was carried out to understand the effect of relative humidity on the performance of a 20 W polycrystalline PV panel. The results of the experiments demonstrated that with 32.80% (i.e., from 65.40% to 98.20% relative humidity) increase in relative humidity level the panel power output reduced by 35.82%.

The accumulated airborne dust particles on the panel surface creates a barrier in the path of sunlight, which significantly reduces the amount of solar radiation falling on the panel surface. The present study proved that the deposition of smaller size dust particles on the panel surface blocks the solar radiation more prominently compared to larger size dust particles. This reveals that the reduction in the panel performance due to the accumulation of smaller size dust particles is higher than that of the larger size dust particles. Moreover, the performance of PV panel was studied under three types of dust pollutants, namely red soil dust, lime stone dust and iron ore dust. The results of

this study demonstrated that the performance of PV panel not only affected by the mass of dust deposition on its surface but it also influenced by the type of dust pollutants.

The reduction in short circuit current and maximum power output due to mass of dust deposition (i.e., 12.86 gm of dust deposition) on the panel surface (i.e., of area 0.1489 m$^2$) were respectively, 39.58% and 43.18%, compared to a clean panel, after five days of its exposure to outside regime (in surface iron ore mines). However, the reduction in open circuit voltage was 4.35%, which is not of much significance when compared to short circuit current and maximum power output. To validate these field results, a laboratory study was conduted which showed 44% reduction in short circuit current and 44.75% reduction in maximum power output with 13gm of dust deposition (nearer to the field conditions) on the panel surface. Similar to field study the reduction in open circuit voltage was also low (i.e., 5.47%) in laboratory study. Thus, the deposition of dust on the panel surface having a negavative impact on its performance. Therefore, an automatic dust cleaning system was developed to clean the accumulated dust from the surface of the panel. The laboratory study was conducted with the help of developed cleaning system, using a 10W polycrystalline PV panel (which is having an area of 0.0952m$^2$), under 442W/m$^2$ solar radiation. This study showed an improvement of 25% in the short circuit current of a cleaned panel with respect to a dusty panel (which is created by deposition of 3gm of iron ore dust). Moreover, there was improvement in open circuit voltage and maximum power output by 2.80% and 27.98%, respectively.

**Keywords:** PV panel; Solar radiation; Shading; Temperature; Humidity Dust.

# TABLE OF CONTENTS

# LIST OF FILGURES

# LIST OF TABLES

# LIST OF ABBREVIATIONS

| | |
|---|---|
| A | Area of PV panel |
| $a_0$ | Intercept of the line (regression constant) |
| $a_1$ | Slope of the line (regression constant) |
| AC | Alternating current |
| °C | Degree Celsius |
| DC | Direct current |
| FF | Fill factor |
| G | Solar radiation falling on the panel surface |
| $G_r$ | Reference solar radiation |
| Gs | Simulated solar radiation |
| ICSP | In-circuit serial programmer |
| $I_d$ | Current through diode |
| $I_m$ | Maximum output current of a solar PV panel |
| $I_o$ | Reverse saturation current |
| $I_{ph}$ | Photo or light generated current |
| $I_{sc}$ | Short circuit current |
| $I_{sc\ clean}$ | Short circuit current of clean panel |
| $I_{sc\ dusty}$ | Short circuit current of dusty panel |
| K | Boltzmann's constant |
| N | Total number of shaded cells |
| NA | Not applicable |
| n | Number of observations |
| $P_c$ | Power output of clean panel |
| $P_d$ | Power output of dusty panel |

| | |
|---|---|
| $P_i$ | Input power to the PV panel surface |
| $P_{max}$ | Maximum power output of a solar PV panel |
| $P_N$ | Normalized power output |
| PWM | Pulse width modulation |
| q | Absolute value of electric charge |
| RCTUC | Rate of change of temperature of un-shaded cell |
| RCTUG | Rate of change of temperature of glass surface |
| RH | Relative Humidity |
| RSCC | Reduction in short circuit current |
| RTC | Real time clock |
| $R_{sh}$ | Shunt resistance |
| $R_s$ | Series resistance |
| T | Surface temperature of PV panel |
| $\Delta T$ | Change in temperature |
| $V_d$ | Voltage across diode |
| $V_m$ | Maximum output voltage of a solar PV panel |
| $V_{oc}$ | Open circuit voltage |
| $\eta$ | Efficiency of solar PV panel |
| w.r.t. | With respect to |
| UARTs | Universal Asynchronous Receiver Transmitter |

# CHAPTER 1

# INTRODUCTION

## 1.1 GENERAL

Water, power and health are the three most essential things for the development of any country. Apart from water and health, power is utmost important not only for every person but also every country. The economic growth of a country crucially depends upon its power generation capacity and also on the per capita energy consumption (Ozturk et al. 2010). Due to the fast growing population, it is very difficult to fulfil the energy consumption demand in the present scenario (Zabel and Economics 2009). India is now facing an acute shortage of power, especially in the industrial sector. Due to this, the country's economy is not growing as per expectation. As compared to many countries, India's per capita energy consumption is far below.

In India, the total installed capacity of power is 315GW. This installed capacity of power is divided into two different types of energy sources, namely, the renewable energy and non-renewable energy and is shown in Figure 1 (Sector 2016). At present, 70% of the installed power is being generated using non-renewable sources, such as coal, natural gas, diesel, nuclear energy etc., and 30% is being generated using renewable sources such as geothermal, hydro, wind, biomass, solar etc.
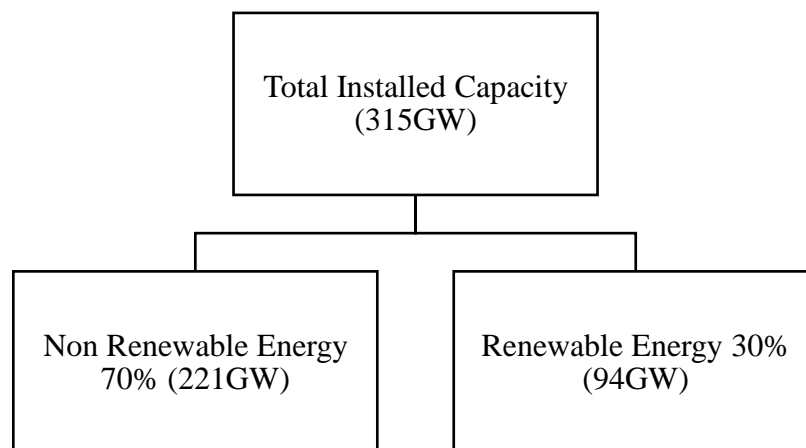


Figure 1.1. Power generation scenario in India

The power generated by non- renewable energy sources (conventional power) has an adverse impact on the environment. In conventional power generation, large amount of sulphur oxides ($So_x$), nitrogen oxides ($No_x$) and suspended particulate matter (SPM) are generated which are responsible for pollution of the environment and it also deteriorates the health of human beings, animals as well as plants. This emitted gas also augments the global warming. On the other hand, there is a continuous increment in energy consumption, cost of fossil fuel and global warming all over the world. Hence, green and renewable energy technology is very much essential for fulfilling the energy demand of world consumers, which is also drawing attention day by day in both academic and industrial sectors.

There are many available renewable energy sources, such as biomass, hydro, geothermal, wind and solar. Among all these renewable energy sources, solar energy is the most vital source that can be used to generate electric power. Solar energy has experienced a rapid growth and popularity in the last one decade because of its huge advantages, like availability of raw material in abundance, non-emission of pollutants, usability in remote areas, no generation of loud noise and easy installation of panels (Bayod-Rújula et al. 2011; Chueco-Fernández and Bayod-Rújula 2010; Mekhilef et al. 2011; Oliver and Jackson 2001; Ozturk et al. 2010).

Energy coming from the sun is called solar energy which is in the form of light and heat. In the solar energy system, solar power can be converted into electrical power by the use of solar photovoltaic panels, which are usually made from silicon (Dincer 2011). Photovoltaic (PV) is a technology in which light is converted into electrical power. Whenever sunlight falls on PV cell surface, it excites the electrons of the valence band to move to from valence band to conduction band (Green 2002). This generates hole in valence band and as a result photo current starts flowing to the external circuit. A photovoltaic module consists of several number of PV cells and a PV panel consists of several number of PV modules. Most of the researchers have concentrated on the design of PV cells, due to which there is a continuous decrement in the cost of PV cells with improvement in its performance.

In remote areas it is very difficult to provide electric power and also it is very expensive. In such cases, solar energy could be a good choice for providing electrical power (Chakrabarti and Chakrabarti 2002). In general, the mining industries are situated in remote areas, where the electrical power is provided either from transmission line (Grid) or from a diesel generator (DG) set. Since, the price and utilization charges of both of these energy sources are continuously increasing, solar energy technology could be the best alternative energy source for the mining industry. Looking at the worst condition encountered in the mines, a detailed study of environmental parameters which are responsible for degradation of PV panel performance has to be carried out before its installation in the mines.

The PV panel installation requires vast land which is easily assessable in the mining areas in the form of waste dump yard, abandoned mine area, pit bottom area, tailing ponds etc. In these areas PV panels can be effectively installed and utilized. The electricity thus generated by solar energy can be utilized for spot lighting, haul road lighting, lighting crusher and office premises, beneficiary plant, pumping area etc. But due to dusty and bad environment prevailing in the mines PV panel may not perform well as ensured by the manufactures. In fact, the performance of PV panel degrades with time due to such dusty and bad environment (Tripathi et al. 2017b).

## 1.2 SCOPE OF THE WORK

One of the promising applications of solar energy technology is the installation of photo-voltaic (PV) systems, which generates electrical power using sunlight (solar radiation) without emitting pollutants and consumption of no fuel. Much research has been performed on photo-voltaic systems in the last one decade so as to improve its performance, which would help to meet the demand of world energy consumers. Solar photovoltaic systems are rapidly growing in electricity markets due to the decline in the cost of PV modules, increase in efficiency of PV cells, manufacturing-technology enhancements and economics of scale. But, once the PV panel is installed in the site, its performance starts decreasing gradually due to the influence of surrounding environmental parameters. Therefore, to study the influence of environmental parameters on the performance of PV panel is the prime motive of this project.

3

**1.3 OBJECTIVES OF THE WORK**

1. To study the effect of dust, shading, humidity, temperature on PV panel performance.
2. To study the effect of tilt angle on the performance of PV panel.
3. To develop a method to minimize the dust deposition on PV panel surface.

**1.4 CONTENTS OF THE THESIS**

The thesis consists of nine chapters. The first chapter includes the general introduction followed by the origin, scope and objectives of the work. The second chapter gives the brief literature review which addresses the objectives of the work. The third chapter gives the information about experimental set-up and instrumentation used in the present study. Chapter four explains the effect of solar radiation on the performance of PV panel. In chapter five, the effect of shading on PV panel performance under various shading strengths is discussed. This chapter also explains the effect of continuous shading on the temperature variation of un-shaded cell in the string of PV panel. Chapter six discusses the effect of dust on PV panel performance, which is followed by chapter seven which discusses the effect of surface temperature of PV panel and humidity on the performance of PV panel. Chapter eight discusses the effect of tilt angle on the performance of PV panel. The last chapter of the thesis includes the overall discussions and conclusions of the present research work. This chapter also includes the scope of future work in this research field.

# CHAPTER 2

# LITERATURE REVIEW

## 2.1 ENERGY SCENARIO

Energy is one of the major inputs for the economic development of any country. The consumption of the energy in any country is directly affected by its population growth (i.e., growing populations consume more energy) (Kumar et al. 2014; Vlahinić-Dizdarević and Žiković 2010). India's energy sector is one of the most vital sectors that affect India's economic growth and thus it is also one of the largest industries in India. India's energy demand has grown at 3.6% per annum over the past 30 years. India has the 5th largest electricity generating capacity and it is the 6th largest energy consumer amounting for around 3.4% of global energy consumption in the year 2016 (Central Electricity Authority of India report).

As per the Ministry of Power (Central Electricity Authority of India report) the total installed energy capacity in India is 315 GW. Out of total installed capacity 70% of energy (i.e., 221 GW) is generated by non-renewable energy and 30% (i.e., 94 GW) is generated by renewable energy source. The installed energy capacity by various sources in India is presented in Table 2.1, Figure 2.1 shows the percentage share of the various sources (Sector 2016).

**Table 2.1** Installed capacity in different energy sectors

| Sl. No | Source of Energy | Installed Capacity (GW) |
|--------|------------------|--------------------------|
| 1 | Coal | 188.80 |
| 2 | Gas | 26.29 |
| 3 | Diesel | 0.84 |
| 4 | Nuclear | 5.80 |

| 5 | Hydro | 40.00 |
|---|-------|-------|
| 6 | Renewable | 54.88 |
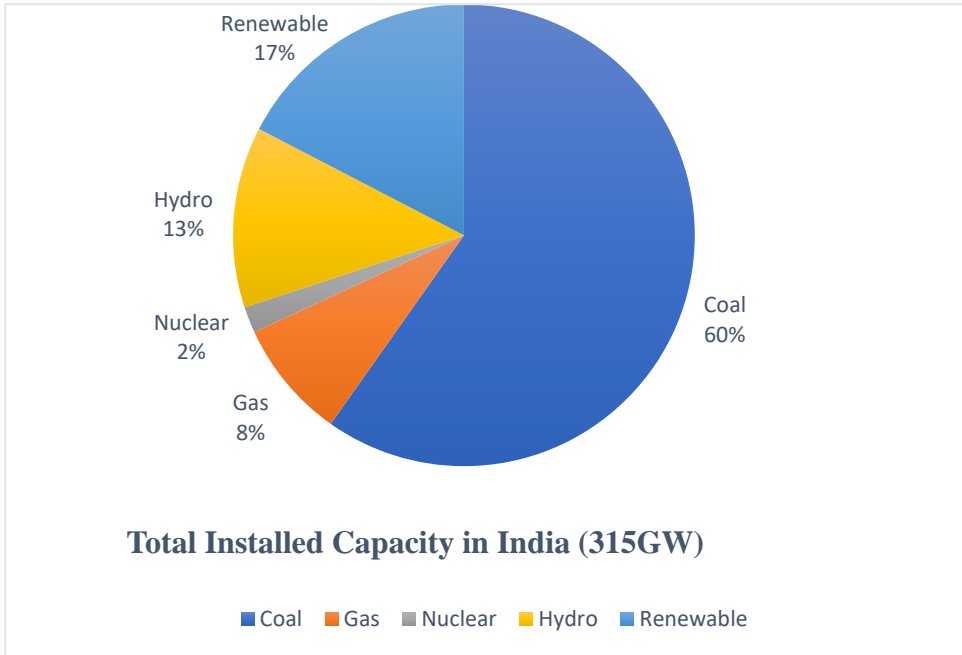


Figure 2.1 Percentage share of different energy sources in India

Due to the fast depletion of fossil fuel and unsafe activity of nuclear energy sources renewable energy sources could be a good choice for power generation in the future course of action. There are various types of renewable energy sources, such as biomass, geothermal, wind, hydro and solar (Sayigh 2009). Figure 2.2 shows the present renewable energy scenario in India (Sector 2016).
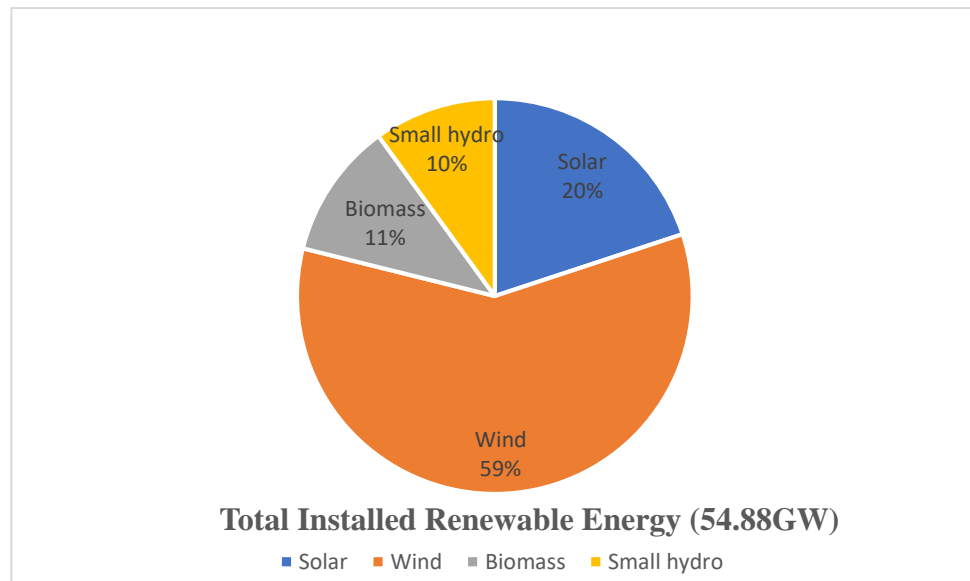
Figure 2.2 Percentage share of different renewable energy sources in India

## 2.2 SOLAR ENERGY

Solar energy is a very huge and infrangible source of energy. The power coming from the sun to the earth is approximately $1.8 \times 10^8$ GW, which is thousands of times larger than the present power consumption of the world consumers (Jones and Bouamane 2012). Therefore, solar energy could be a good choice of power generation in the future course of action. A broad classification of the various methods of solar energy utilisation is shown in Figure 2.3. As shown in Figure 2.3, the solar energy can be used directly and indirectly. The direct solar energy including thermal and photovoltaic conversions, wherein the energy generated is directly obtained from the sun. Similarly, indirect solar energy is the energy obtained from the sun indirectly, such as wind, hydro, wave energy, biomass etc (Sukhatme and Sukhatme 1996). In solar energy the device used in photovoltaic conversion is called solar PV cell. The major advantages associated with solar cells are that they have no moving parts, require less maintenance and are environmentally friendly.
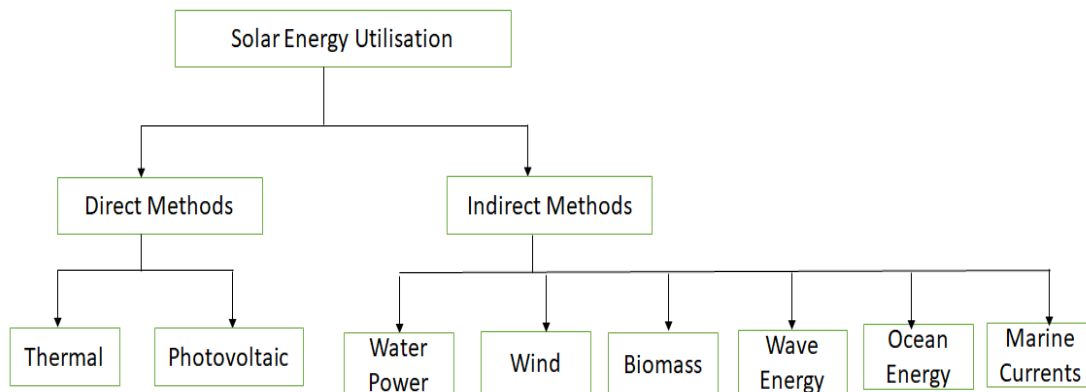
Figure 2.3 Classification of solar energy utilisation methods

## 2.3 HISTORY OF PV CELL

The term "photo" means light and "voltaic" means electricity. Thus, a photovoltaic cell is a device that converts sunlight directly into electricity. In 1839 a French physicist Edmond Becquerel first demonstrated experimentally the photovoltaic effect and later in 1876 Adams and Day observed the photovoltaic effect on the Selenium element. Thereafter, in 1883 an American scientist Charles Fritts developed the first solar PV cell by the coating of a thin layer of gold on the semiconductor selenium to form the junctions and the device was approximately 1% efficient. Further, in 1954 Chapin, Fuller and Pearson observed that as a PV cell material silicon is more efficient than selenium and they increased the PV cell efficiency up to 6% by adding some impurities to the silicon solar cell (Gevorkian 2007; Goetzberger et al. 2003; Jager-Waldau 2011; Mekhilef et al. 2011).

At present, there are two types of PV cell materials, such as crystalline and thin film cells. Crystalline solar cells are of three types, i.e., as mono crystalline (mono-Si), poly crystalline (p-Si) and gallium arsenide (GaAs) solar cells. Similarly, thin film solar cells are of different types, such as amorphous silicon (a-Si), cadmium telluride (CdTe), copper indium gallium selenide (CIS/CIGS) and organic photovoltaic cells (OPC) (Green 1982; Shah et al. 1999). These PV cells materials vary from each other in terms of light absorption capacity, energy conversion efficiency, manufacturing technique and cost of production. As of today, more than 90% of the solar PV cells are made of

crystalline silicon materials, because crystalline solar cells give higher efficiency and better withstand against the environment parameters over the thin film solar cells (Weller et al. 2010). Mono crystalline solar cells have higher energy conversion efficiency than those of poly crystalline solar cells, since, mono crystalline cells are made out of high grade silicon. Nevertheless, today the poly crystalline solar cells are more in practice than the mono crystalline solar cells due to less cost and simple production process (Contreras et al. 1999; Van Sark et al. 2007; Wu 2004).

## 2.4 TERMINOLOGIES USED IN SOLAR PV SYSTEM

**Open Circuit Voltage:** It is defined as an output voltage of a PV cell when load impedance is much larger than the device impedance, which means no current is flowing through the load. It is the maximum possible voltage of a PV cell. It is denoted as $V_{oc}$ and measured in volt.

**Short Circuit Current:** It is defined as an output current of a PV cell when load impedance is much smaller than the device impedance, which means no voltage developed across the load. It is the maximum possible current of a PV cell. It is denoted as $I_{sc}$ and measured in amp.

**Maximum Output Voltage:** It is the voltage across the load at which maximum output power of a PV cell is achieved. It is denoted as $V_m$ and measured in volt.

**Maximum Output Current:** It is the current flowing through the load at which the maximum output power is achieved. It is denoted as $I_m$ and measured in watt.

**Output Power:** It is the product of output current and output voltage of PV panel (equation 2.1). It is denoted as P and measured in the unit of watt.

$$P = V \times I \qquad\qquad (2.1)$$

where, *P*= Output power of PV panel (watt),

   *V*= Output voltage of PV panel (volt), and

   *I* = Output current of PV panel (amp).

**Theoretical Output Power:** It is the product of open circuit voltage and short circuit current of PV panel (equation 2.2). It is denoted as $P_t$ and measured in the unit of watt.

$$P_t = V_{oc} \times I_{sc} \qquad (2.2)$$

where, $P_t$ = Theoretical output power of PV panel (watt),

$V_{oc}$ = Open circuit voltage of PV panel (volt), and

$I_{sc}$ = Short circuit current of PV panel (amp).

**Maximum Output Power:** The product of maximum output voltage and maximum output current gives the maximum output power of a PV panel (equation 2.3). This output power increases with increase in the load, but after a particular load output power starts decreasing toward zero, at the maximum possible load. The power obtained at that particular load is termed as maximum output power of a PV cell. It is denoted as $P_m$ and measured in watt.

$$P_m = V_m \times I_m \qquad (2.3)$$

where, $P_m$ = Maximum output power of a solar PV panel (watt),

$V_m$ = Maximum output voltage of a solar PV panel (volt), and

$I_m$ = Maximum output current of a solar PV panel (amp).

**Input Power of PV cell:** It is defined as the product of solar radiation falling on PV cell surface and the surface area of the cell (equation 2.4). It is denoted as $P_i$ and measured in watt.

$$P_i = G \times A \qquad (2.4)$$

where, $P_i$ = Input power to the PV panel surface (watt),

$G$ = Solar radiation falling on the panel surface (W/m$^2$), and

$A$ = Surface area of the PV panel (m$^2$).

**Maximum Conversion Efficiency:** It is defined as the ratio of maximum output power to the incident input power to the solar PV cell, which is given by equation (2.5)

$$\eta = \frac{P_m}{P_i} = \frac{V_m \times I_m}{G \times A} \times 100 \qquad (2.5)$$

where, $\eta$ = Efficiency of a solar PV panel

$P_m$ = Maximum output power of a solar PV panel (watt),

$P_i$ = Input power to the PV panel surface (watt),

$V_m$ = Maximum output voltage of a solar PV panel (volt),

$I_m$ = Maximum output current of a solar PV panel (amp),

$G$ = Solar radiation falling on the panel surface (W/m$^2$), and

$A$ = Surface area of the PV panel (m$^2$).

**Fill Factor:** It is the ratio of maximum power output to the theoretical output power of PV panel. It is a dimension less quantity and denoted as FF. The mathematical representation of FF is given by equation (2.6).

$$FF = \frac{P_m}{P_t} = \frac{V_m \times I_m}{V_{oc} \times I_{sc}}$$

(2.6)

where, $FF$ = Fill factor of PV panel

$P_m$ = Maximum output power of PV panel (watt),

$P_t$ = Theoretical output power of PV panel (watt),

$V_m$ = Maximum output voltage of PV panel (volt),

$I_m$ = Maximum output current of PV panel (amp),

$V_{oc}$ = Open circuit voltage of PV panel (volt), and

$I_{sc}$ = Short circuit current of PV panel (amp).

**Maximum Power Point:** The point in the power voltage characteristic at which the PV panel attains the maximum power is called maximum power point. It is denoted as MPP.

## 2.5 FUNDAMENTALS OF SOLAR PV CELL

The solar PV cell is a silicon PN semiconductor and its working principle can be analysed as analogous to that of PN diode. There are two important steps involved in the principle of working of a solar cell.

I.   Creation of positive (hole) and negative (electron) charges due to the solar radiation falling on the PV cell surface.

II.  Separation of positive and negative charges due to the potential gradient within the cell.

The step by step working of the solar cell due to the absorbed solar radiation is demonstrated in Figure 2.4, Figure 2.5 and Figure 2.6. In Figure 2.4, when P and N type semiconductor material join together to form a PN junction, then the electron from N side combines with the holes of the P side and forms a space charge region across the PN junction as shown in Figure 2.5. In space charge region N side experiences, a positive potential and P side experiences a negative potential (because of their donor and acceptor nature). Whenever the sun light falls on the space charger region it creates free electrons and holes in this region. Due to the developed potential gradient in the solar cell, the created electrons move towards N side of the material and holes move towards P side of the material. Now, this generated charge on both sides of PV material can be collated through charge collector electrode.
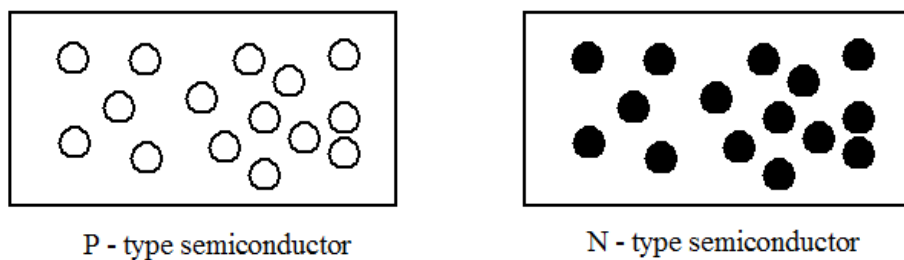


Figure 2.4 Representation of P and N type semiconductor
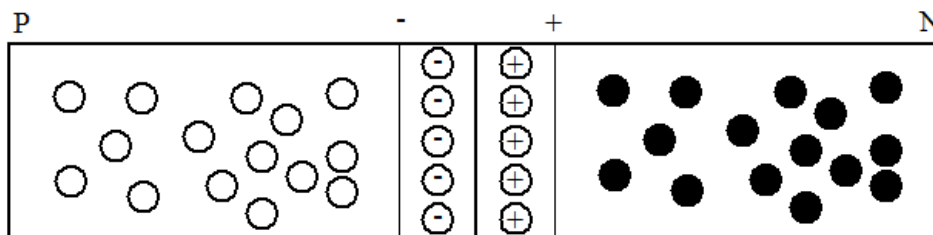


Figure 2.5 Formation of space charge region in P-N type semiconductors
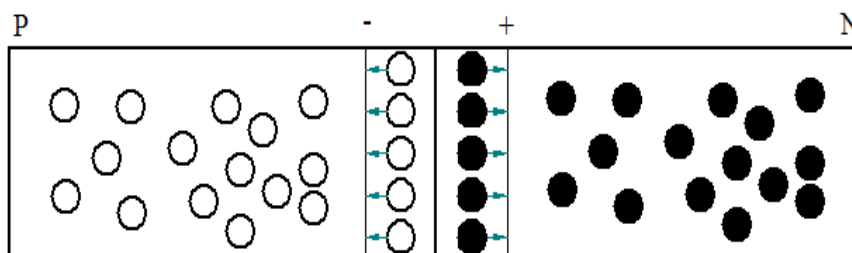


Figure 2.6 Separation of electrons and holes from the space charge region

The generated electric current by photovoltaic effect is strongly dependent on the solar radiation falling on the cells surface. As the sunlight consists of particles of energy called photons, the energy of a photon is measured in electron volts, which is designated as eV (one eV is equivalent to the energy gained by an electron when it accelerates through a one-volt potential difference). The electrons in the atoms of a solar cell need a specific amount of energy or wavelength from photons in order to be propelled into the circuit of a solar power system. Since, PV cells are made of silicon semiconductor materials which are insensitive to other wavelengths outside the visible range, the wavelength of the visible range (i.e., 0.38 µm-0.78 µm) in the spectrum is mostly responsible for powering of the PV cells (Dirnberger et al. 2015; Ghitas 2012; Gouvêa et al. 2017).

## 2.6 EQUIVALENT CIRCUIT OF SOLAR PV CELL

The performance of a solar PV cell can be analysed through it is equivalent circuit diagram, which is shown in Figure 2.7. The equivalent circuit diagram is based on one diode model which consists of a current source connected in parallel with a diode.
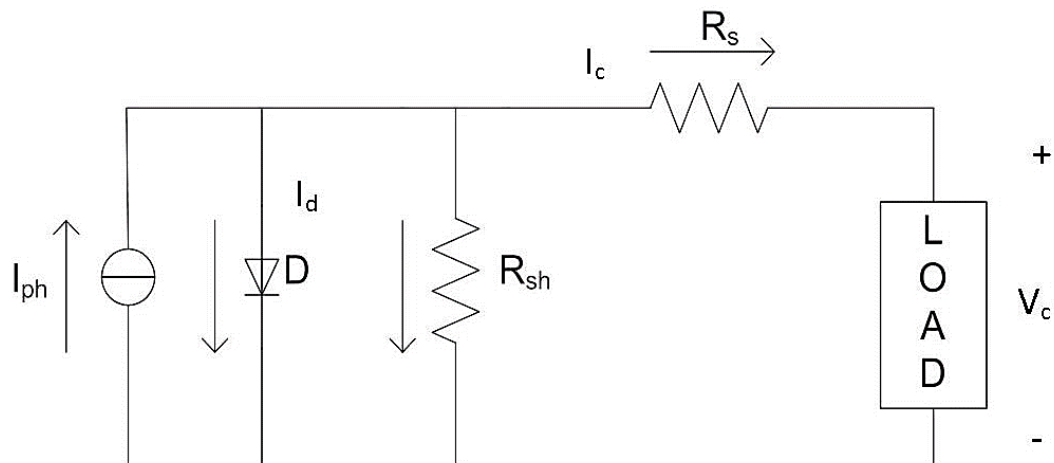


Figure 2.7 Equivalent circuit of a solar PV cell

$I_{ph}$ = Photo or light generated current (amp),

$I_d$ = Current through diode (amp),

$I_c$ = Current through the load or output current (amp),

$V_c$ = Voltage across the load or output voltage (volt),

$R_{Sh}$ = Shunt resistance ($\Omega$), and

$R_S$ = Series resistance ($\Omega$).

The shunt resistance $R_{Sh}$, is due to the manufacturing defect rather than poor solar cell design. Ideally its value should be infinite. The low value of shunt resistance causes significant power losses in solar cells by providing an additional path for the light-generated current. Due to this, the output current of a solar cell reduces which further reduces the output power of a solar PV cell. Thus, the shunt resistance of a solar cell should be low as possible for its efficient performance. The effect of a shunt resistance is particularly severe at low light levels, since, there will be less light-generated current. Therefore, the loss of the output current in this case would be much significant. Similarly, the series resistance $R_S$, is due to the resistance offered by the thin diffused layer on the top of the photovoltaic cell. Ideally it should be zero. Therefore, the modified equivalent circuit under ideal conditions ($R_{Sh}=\infty$ and $R_S=0$) is presented in Figure 2.8.
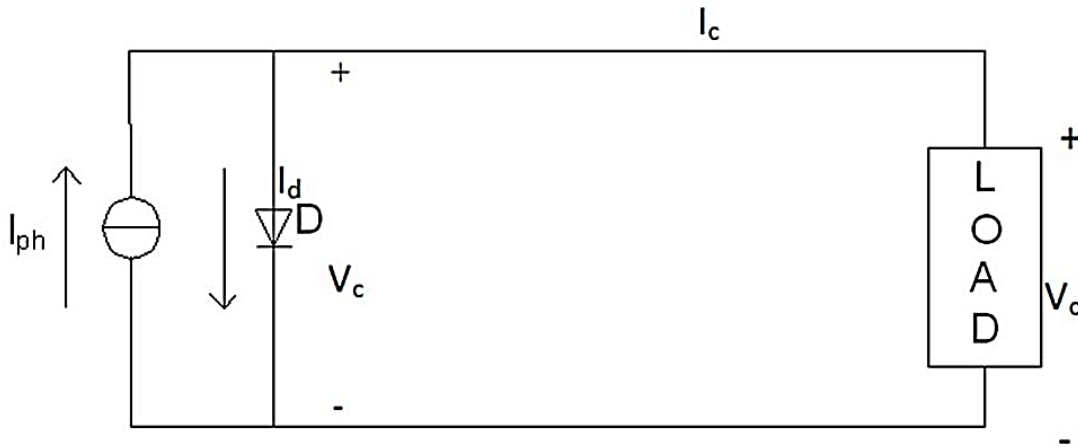


Figure 2.8 Modified circuit of a solar PV cell

As shown in Figure 2.8, the voltage across the diode is the same as the voltage across the load (i.e., $V_d=V_c$). The current through the diode is given by equation (2.7).

$I_d = I_0 \left[ exp \left( qV_d/KT \right) - 1 \right]$ (2.7)

where,

$I_d$= Current through the diode (amp),

$I_0$= Reverse saturation current (amp),

14

$V_d$= Voltage across the diode (volt),

$q$= Absolute value of electric charge (C),

$K$= Boltzmann's constant (J/K), and

$T$= Temperature (K).

By applying Kirchhoff's current law in Figure 2.8.

$I_{ph} = I_c + I_d$

$I_c = I_{ph} - I_d$

$I_c = I_{ph} - I_0 [exp\ (qV_d/KT)-1]$ $\hspace{3cm}$ (From equation 2.7)

Since, under ideal condition $V_d = V_c$

$\therefore I_c = I_{ph} - I_0 [exp\ (qV_c/KT)-1]$ $\hspace{4cm}$ (2.8)

$\quad I_c = I_{ph} - I_0\ exp\ (qV_c/KT) + I_0$

If the load is completely shorted which means the voltage across the load is zero (i.e., $V_c$=0) then, the obtained output current is termed as short circuit current '$I_{sc}$', which is given by equation (2.9).

$I_{sc} = I_{ph}$ $\hspace{8cm}$ (2.9)

Similarly, if the load is completely open i.e., zero output current ($I_c$=0), then the output voltage is termed as an open circuit voltage '$V_{oc}$', which is derived as shown below and given by equation (2.10).

$I_0\ exp\ (qV_{oc}/KT) = I_{ph} + I_0$ $\hspace{3cm}$ (From equation 2.8)

$exp\ (qV_{oc}/KT) = (I_{ph} + I_0)/I_0$

$qV_{oc}/KT = ln\ [(I_{ph} + I_0)/I_0]$

$V_{oc} = \dfrac{KT}{q}ln\left(\dfrac{I_{ph}+I_0}{I_0}\right)$

Since, $I_{ph} >> I_0$

$\therefore V_{oc} = \dfrac{KT}{q}ln\left(\dfrac{I_{ph}}{I_0}\right)$ $\hspace{6cm}$ (2.10)

## 2.7 DESIGN AND STRUCTURE OF SOLAR PV MODULE/PANEL

A number of solar cells electrically connected to each other and mounted on a supporting structure is called a photovoltaic (PV) module and one or more number of

PV module assembled as pre-wired unit is called a PV panel. For practical purposes, some of the manufacturers designated PV module as a PV panel. To avoid confusion among there terminology, PV panel and PV module are used analogous to each other in this entire thesis ("Solar cell" 2017).

### 2.7.1 Number of Solar Cells in a Panel

The panel manufacturing technology was developed intensively in 1980s. At that time, PV panels were designed for charging the batteries of 12 V terminal voltage. Therefore, the panel should provide enough voltage and current to charge a 12 V battery under typical daily solar radiation. This voltage required for charging batteries can be obtained by series connection of 36 Si-based solar cells in a string of PV panel. A commercially available solar cell generally has a $V_{oc}$ of about 0.55 V at 25°C. Thirty-six cells in series would have output about 20 V. This voltage is kept intentionally higher than the required charging voltage, so as to adjust the voltage limit in case of any environmental impact on the cells or the degradation of any cells in the panel. Similarly, 24 V output voltage solar panels require 72 individual solar cells connected in series (El Amrani et al. 2007; Solanki 2015).

### 2.7.2 Fabrication of a PV Panel

In order to ensure long life of the cells in a PV panel, they are required to be protected from the environment in which they are operated. Moisture in the environment can erode the metal contacts and affect the anti-reflective coating of the cells, resulting in a degradation in its performance. The cells in the panel should also be protected from dust, rain, mechanical shocks etc. In order to protect the panel from environmental damage, the PV panels are sealed using glass at the front side and polymer resin for encapsulation, for the back-side protection, which provide electrical isolation. At the back side, there could be a layer of polymer resin, glass, Al sheet, hard polymer or a combination of these layers. This protection should be good enough to protect the panels for over its life time, generally more than 25 years. A typical fabrication layering of Si-based PV panel is shown in the Figure 2.9 (Solanki 2015).
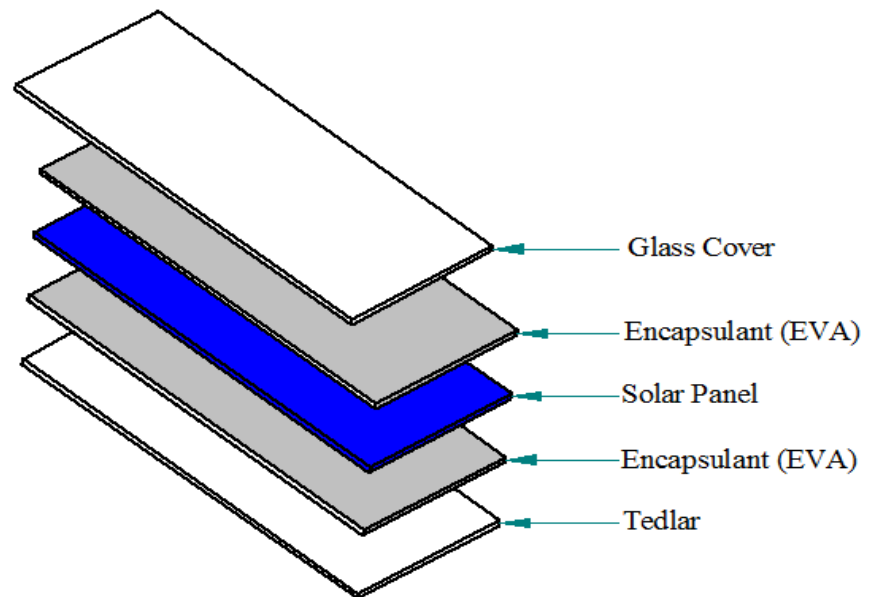
Figure 2.9 Layering of PV Si-based PV panel

## 2.8 PERFORMANCE OF A SOLAR PV PANEL

The performance of a solar PV panel can be evaluated by measuring its electrical responses, such as open circuit voltage, short circuit current, maximum power output, fill factor and conversion efficiency. The performance can be visualised by plotting its electrical characteristics, such as current-voltage (I-V) and power-voltage (P-V). A standard I-V and P-V characteristics curves of a panel is shown in Figure 2.10 ("Photovoltaic (PV) - Electrical Calculations" n.d.). The point in the characteristic curve at which maximum power ($P_{max}$) is obtained is called maximum power point (MPP). It is seen in Figure 2.10 that the current is almost the same before MPP. But with a small increase in voltage beyond MPP, there is a rapid reduction in current. Therefore, the PV panel characteristic behaves as current source before the MPP point and as a voltage source after the MPP point.
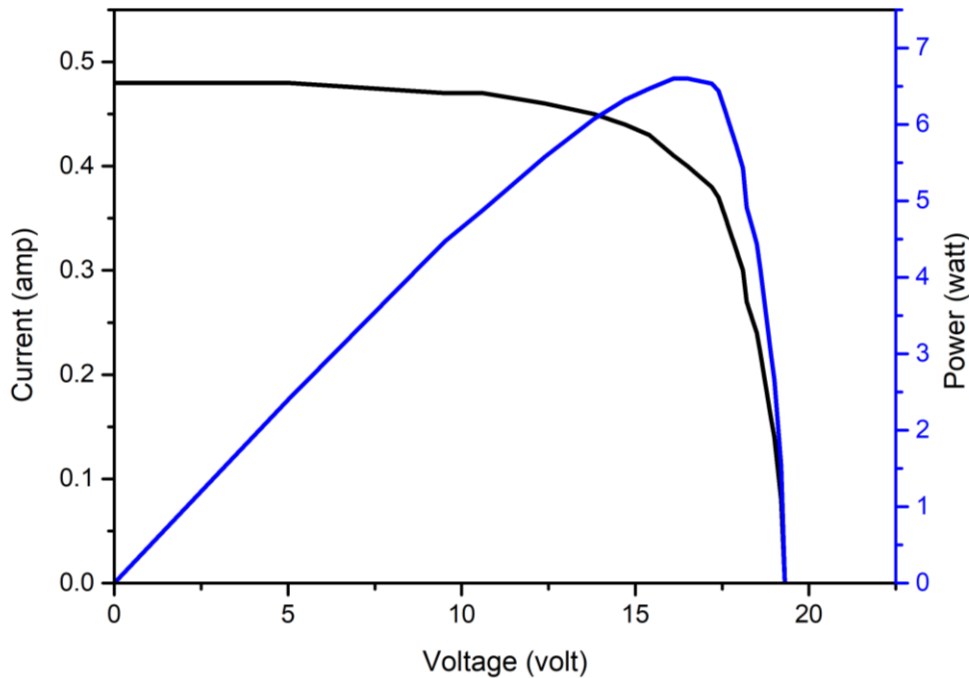
Figure 2.10 Electrical characteristic of PV panel

## 2.9 EFFECT OF ENVIRONMENTAL PARAMETERS ON THE PERFORMANCE OF A SOLAR PV PANEL

In general, the PV panel is operated in an open atmosphere, where it experiences a significant variation in its performance due to its surrounding environmental parameters (Jiang et al. 2011). The generation of electrical energy from the PV panel mainly depends upon its performance. The performance degradation of PV panel depends on internal and external parameters. The internal parameters that affect the performance of PV panels are surface temperature, panel configuration, tilt angle, corrosion and breaking of cells, delamination of the cells etc., and the external parameters are dust, humidity, ambient temperature, wind speed, solar radiation and the rate of shading across panel surface. Among all the external parameters, dust plays a significance role in reducing the PV panel performance, whereas atmospheric temperature, wind speed and humidity of the surrounding environment play a critical role in deposition and spreading of dust on the panel surface. Further, these parameters (i.e., atmospheric temperature, wind speed and humidity) solely affect the performance of PV panel.

The tilt angle of the PV panel also plays an important role in its performance. Moreover, as the tilt angle increases the dust settlement on PV panel decreases, which improves its performance. Thus, it is very important to orient the solar PV panel at an optimum tilt angle for any given location. Therefore, a detailed study of environmental parameters which are responsible for degradation of PV panel performance has to be carried out before its installation in the mines or in any harsh environment.

### 2.9.1 Effect of Solar Radiation on PV Panel Performance

The overall technical and economical performance of solar PV panel strongly depends on the solar radiation falling on its surface. Therefore, the measurement and estimation of solar radiation is an important aspect to determine the PV panel performance. The output power of the panel decreases almost linearly with the decrease in the intensity of solar radiation falling on its surface. Unfortunately, the solar radiation falling on the panel surface is not constant throughout the day time. In a normal sunny day, it increases from morning to noon and then decreases till sunset when radiation intensity falls to zero. Due to this variation in the solar radiation, the output power of the PV panel also changes and it is not uniform throughout the day. The output current produced by the PV panel is the linear function of the solar radiation falling on its surface (Arjyadhara et al. 2013; Hirata and Tani 1995). But the output voltage of the panel is a logarithmic function of the solar radiation falling on its surface (Mohanty et al. 2016; Villalva et al. 2009).

In solar PV panels, a number of solar cells are electrically connected to each other in the form of series or parallel configuration and all cells are required to be identical in terms of electrical parameters. If the solar radiation falling on the panel surface is not uniform, then some cells in the panel receive more solar radiation and some cells receive less. The cells which receives lesser radiation will generate less output current compared to the cells receiving higher radiation.

### 2.9.2 Effect of Dust on PV Panel Performance

Due to the fast industrialisation and urbanisation the effect of air pollution is becoming a very serious problem in the area of solar energy utilisation (Tian et al. 2007). Because

of the air pollution, the air borne dust particles get deposited on the surface of PV panel, and this is the main cause for its performance degradation (Adinoyi and Said 2013; Klugmann-Radziemska 2015; Mani and Pillai 2010). Dust creates a barrier between the PV panel surface and sunlight falling on its surface, which attenuates the part of the incoming sunlight (Kaldellis and Kapsali 2011). The attenuation of sunlight depends on the size of dust, density of dust and type of dust (Darwish et al. 2015). This attenuation of sunlight considerably reduces the performance of PV panel (Al-Hasan and Ghoneim 2005; Sulaiman et al. 2014).

In one study it was found that due to dust deposition on panel surface the power generation capacity and conversion efficiency of PV panel reduces to 92.11% and 89%, respectively (Rajput and Sudhakar 2013). A work carried out to study the effect of dust on transmittance of panel glass shown that there is a reduction in transmittance which ranges from 12.38% to 52.4% for 4.48 to 15.84 $g/m^2$ of dust deposition (Elminir et al. 2006). One more study reported that the reduction in conversion efficiency of PV panel due to dust deposition was 10%, 16% and 20%, respectively, for 12.5 $g/m^2$, 25 $g/m^2$ and 37.5 $g/m^2$ of dust density (El-Shobokshy and Hussein 1993).

According to the published literature, studies have been carried out on the twelve types of dust pollutants as given in Table 2.2, to understand its effect on the performance of the PV panel.

**Table 2.2** Different types of dust

| Sl. No | Type of Dust | Sl. No | Type of Dust |
|--------|--------------|--------|--------------|
| 1 | Red soil | 7 | Carbon |
| 2 | Sand | 8 | Mud |
| 3 | Limestone | 9 | Talcum |
| 4 | Ash | 10 | Natural Dust |
| 5 | Silica | 11 | Calcium carbonates |
| 6 | Cement | 12 | Clay |

A study carried out by Kaldellis and Kapsali (2011) demonstrated that the energy loss of PV module due to red soil, lime stone and ash is, respectively, 19%, 10% and 6%

(Kaldellis et al. 2011). Similarly one more study reported that the dust shows a minimum reduction of 0.9V output and a maximum of 4.7 V for ash, among five kinds of air pollutants, such as red soil, ash, sand, calcium carbonate and silica gel (Khatib et al. 2013).The performance degradation of PV panel due to the deposition of dust on its surface also depends on PV cell technology, like monocrystalline silicon (mc-Si), polycrystalline silicon (pc-Si) and amorphous silicon (a-Si)(NADH et al. 2014). A study reported that the reduction in PV module power output due to dust deposition is 77.75% for mc-Si module and 18.02% for pc-Si module (Ndiaye et al. 2013). One more study shows that due to the deposition of dust on the panel surface, its short circuit current reduced up to 41%, 4.79% and 7.34%, respectively for the monocrystalline, poly crystalline and amorphous PV panel(Chegaar and Mialhe 2008).

Even the exposure time of PV panel in real atmospheric environment is important for its efficient performance. Because the density of dust deposition on panel surface also depends on exposure time other than the local climatic conditions. In a study it was found that the reduction in spectral transmittance and overall glass transmittance of PV panel was 35% and 20% due to $5g/m^2$ of dust deposition on its surface with 45 days of exposure to real atmospheric environment (Said and Walwil 2014). One more study reported that there was power loss of 3% to 4% due to dust deposition on PV panel for 5 weeks of its exposure to the atmospheric condition (Appels et al. 2012). Similarly, another study indicated that the reduction in glass transmittance of PV panel was from 90.7% to 87.6% after 33 days of its exposure to the outside environment (Hee et al. 2012).

Further, one more study shown that the reduction in short circuit current and power output of PV panel was up to 28.6% and 30.6%, respectively after 12 days of its exposure to the atmospheric condition (El-Shobokshy et al. 1985). A study carried out by Motasem et al. (2016) shown that the reduction in maximum power current of a PV panel was ranging from 6.9% to 16.4% for one day to one month of its exposure in an open desert environment (Saidan et al. 2016).

### 2.9.3 Effect of Shading on PV Panel Performance

Shading of the panel surface affects its surface temperature and also the amount of solar radiation reaching the panel surface. Hence, shading is the major cause for the degradation of panel performance in an outdoor regime. Shading on PV panel may occur due to the passing clouds, deposited dust particles on its surface, permanent structures nearby panel area and shadow of other panels in its vicinity (Bruendlinger et al. 2006; Decker and Jahn 1997; Patel and Agarwal 2008a; b; Silvestre and Chouder 2008)

In the case of shading, the whole PV panel experiences non-uniform solar radiation and as a result of this the power output, current and voltage of the panel reduces (Ishaque and Salam 2013; Tabish and Ashraf 2017). A shaded cell receives the power through un-shaded cells and acts as a load rather than power generating source and because of this a significant amount of panel power output reduces (Bhattacharya et al. 2017; Sathyanarayana et al. 2015). The reduction in the power output of PV panel depends on the shaded area of the panel (Sera and Baghzouz 2008). According to Dolara et al. (2013) 50% shading of the single cell in a panel reduces 30% of the power output (Dolara et al. 2013). It was found that a large amount of power reduces during shading condition which represents two different peaks in the power-voltage characteristic (Sun et al. 2014). The deformation in the current-voltage and power-voltage curve increases with the amount of shading rate, thus the maximum power point moves towards the lower output voltage (Alonso-Garcia et al. 2006; Carannante et al. 2009).

Due to the partial shading, the shaded cell generates lesser current than the un-shaded cell in the string, which develops current mismatch phenomena in the PV panel operation. The current mismatch loss caused by the partial shading condition is not only influenced by the shaded area but it also depends on the shading pattern (Vengatesh and Rajan 2016). This current mismatch is the main cause for the hot spot problem. In general, the hot spot occurs in those lesser current generating cells (due to shading), which increases its temperature, and if this prolongs then it may damage that cell itself. It was found that hotspot heating rises the cell temperature of the shaded cell more than

20ºC over the other cells in the same string of PV module (Molenbroek et al. 1991). This leads to some destructive effects that degrade PV module performance.

Complete shading of one cell provides a non-uniform solar radiation over the surface of PV panel. Hot spot phenomenon heats the whole module instead of one cell.  But due to this localized heating of the cell hot spot temperature is not influenced very much by the other cells. The complete shading of a single cell is the worst condition of hotspot heating. To minimize these effects the panel should be mounted in such a way that it receives lesser shading effect on its surface. If the number of shaded cells in a module increases the performance of the panel significantly reduces. It was also observed that the number of shaded cells in the same string will not have that much effect on the performance of PV panel when compared to the cells which are shaded in other strings (Bishop 1988).

The shading phenomena not only affects the performance of shaded cells but also affects the performance of un-shaded cells. During the shading condition, the temperature of the un-shaded cell (s) also rises, which plays an anchor role in enhancement of panel surface temperature (Hee et al. 2012; Herrmann et al. 1997; Rahman et al. 2014; Tripathi et al. 2017a). The consequences of shading also vary with the panel configurations. Ramabadran and Mathur (2009) reported that the parallel configuration of the panels performs better than the series configuration under the same shading condition (Ramabadran and Mathur 2009).

It is quite difficult to study the effect of partial shading of the panel surface on its performance in an outdoor regime, because of its dependency on varying weather conditions. In this regard, a simulated experimental study is necessary to understand the partial shading effect on the panel performance.

## 2.9.4 Effect of Tilt Angle on PV Panel Performance

The PV panels or arrays are most efficient when they are directly facing the sun (Kamanga et al. 2014). Since, every individual location has their own geographical conditions (latitude and longitude), which affect the orientation or tilt of the solar

panels, for achieving maximum output power the determination of optimum tilt of the panel is essential before its installation. Therefore, tilt angle of PV panel is also a key parameter which decides its optimum performance. The tilt angle is dependent on the latitude of the particular site of installation and the season of installation of the solar panel.

Therefore, in the case of stand-alone PV systems, where PV panels are attached to a permanent structure, the tilt angle of panels should be determined to optimize their performance when sunlight is most scarce. In a study it was found that the panel efficiency was increased from 11.05% to 21% for tilt angle varying from 0° to 30° (Gandhi et al. 2014). The angle of incidence of light beam is inversely proportional to the tilt angle (Calabrò 2013). The tilt angle is measured from the horizontal surface and the incidence angle is measured from the position of light source (sun) to the direction normal to the surface of PV panel (i.e., incidence angle is taken as 90° when the light beam is normal to the panel surface).

Moreover, the soiling effect on the performance of PV panel also depends on its tilt angle. Because tilt angle significantly affects the PV panel yield via affecting the dust settlement on the panel surface. As the tilt angle increases the dust settlement on panel surface reduces, which improves its performance. A study on the performance of PV panel indicated that the reduction in performance due to soiling effect was 2.3%, 4.7% and 8% with 0°, 24° and 58° incidence angles (i.e., the tilt angle 90°, 66° and 32°), respectively (Hammond et al. 1997).

### 2.9.5 Effect of Temperature on PV Panel Performance

The panel surface temperature is a key environmental parameter that influences the performance of PV panel by changing its electrical parameters, such as open circuit voltage ($V_{oc}$), short circuit current ($I_{sc}$), maximum power output ($P_m$) and fill factor (FF) (Chander et al. 2015; Vergura et al. 2012). In general, PV panels are made up of silicon semiconductor material and like all semiconductor materials PV panels are also temperature sensitive. Therefore, temperature of PV panel is an important environmental parameter, which affects its performance. The panel surface temperature

depends on the encapsulating material, solar radiation, atmospheric temperature, humidity and wind speed (García and Balenzategui 2004).

As the temperature of PV panel increases its $V_{oc}$, $P_m$ and FF decreases. But, the $I_{sc}$ of PV panel experiences a very small increment with the rise in its surface temperature. As a result of this, the overall performance of PV panel reduces due to increase in its surface temperature (Migan 2013). Earlier study shown that the rise in panel temperature for crystalline silicon PV panel decreases its $V_{oc}$ at the rate of -0.45%/K (Virtuani et al. 2010). Similarly, the decrease in power output and fill factor are respectively at the rate of -0.65%/K and -0.2%/K, with increase in panel surface temperature (Radziemska 2003).

A study carried out by Bahaidarah et al. (2013) has shown that there was 9% increment in panel efficiency due to 20% reduction in the panel surface temperature (Bahaidarah et al. 2013). One more study conducted by Krauter (2004) has demonstrated that with 22ºC reduction in the panel surface temperature, its power output experienced a gain of 10.3% (Krauter 2004). The available literature shows that the surface temperature of PV panel is a vital parameter which affecting its performance and hence, in this thesis an attempt is made to study the influence of surface temperature on the performance of PV panel.

### 2.9.6 Effect of Humidity on PV Panel Performance

Humidity is an ambient parameter which is defined as the amount of water vapour present in the atmospheric air. To analyse the effect of humidity two scenarios, need to be considered. The first scenario is the effect of humidity on the solar radiation and the second scenario is humidity ingression to the solar cell enclosure. Whenever, the sunlight rays hit the water droplets they undergo the phenomena of refraction, reflection and diffraction. These effects alter and reduce the solar radiation reaching the panel surface in non-linear manner due to non-uniform distribution and random sizes of water droplets in the atmosphere (Gwandu and Creasey 1995). Thus, the overall performance of PV panel (i.e., output current, voltage and power) reduces with the increase in the humidity level in the environment (Kazem et al. 2012; Panjwani and Narejo 2014).

In the second scenario, when the PV panels are exposed to humidity for a long time, there may be a possibility of moisture ingression into the glass of the PV panel. In this case, when moisture enters the solar panel, it provides an additional shunt path for the output current of the cell. Thus, the effective shunt resistance of the cells in the panel reduces which further reduces the output current of the panel (Merten et al. 1999). This reduction of output current will be more significant if the series resistance of the cells increases due to the corrosion of the contact pads under the exposure of moisture. Sometimes, the moisture ingression into the cell of the panel reduces the life span of the crystalline cell by delamination, embrittlement and corrosion of encapsulant material of the PV cell (Mekhilef et al. 2011; Tan et al. 2010).

## 2.10 DUST CLEANING TECHNIQUES FROM PV PANEL SURFACE

The literature study shows that the accumulation of dust on PV panel surface is the main cause for its performance degradation. Therefore, an effective dust cleaning system is required in order to get the satisfactory performance from the PV panel. There are various dust cleaning systems, such as natural cleaning, manual cleaning with water, automatic cleaning and electrostatic cleaning system (Sayyah et al. 2014).

Rainfall is considered to be the most efficient natural cleaning system. Rainfall removes the accumulated dust particles from the panel surface and improves the panel performance. This cleaning system can be achieved by installing the panel other than the horizontal orientation. The study conducted in the higher latitude zone shows the significant improvements in the panel performance due to natural rainfall (Haeberlin and Graf 1998). But this cleaning system will be very ineffective where the rain fall events are infrequent i.e., semi-arid and desert areas where the rainfall occasionally happens. Moreover, low rainfall in the dusty environment followed by dusty wind increases the accumulation of dust on the panel surface, thus reduces its performance. The natural cleaning system of dust from the panel surface is not reliable and not efficient in low rainfall area.

Water often mixed with detergent followed by wiper of soft cloth is the most common practice for cleaning the PV panel surface in small scale installation (Mohamed and Hasan 2012; Zorrilla-Casanova et al. 2013). However, for large scale installation of PV plants, high-pressure water jet, followed by brushing has been reported in many investigations (Kimber 2007). It is considered as one of the most efficient cleaning systems among existing practices, because it is less harmful to the panel surface. One study reported that the manual cleaning with water brush arrangements increased the output power of the PV plant by 6.9% (Pavan et al. 2011). But, this cleaning system is quite expensive as it includes the cost of labour, water and also requires trained personnel. Moreover, this cleaning system is not applicable where the scarcity of water is the prime concern.

An automatic cleaning system is very effective in highly dusty environment. This system uses the computer controlled mechanical devices to clean the panel surface. This cleaning system is more efficient and reliable as it reduces the labour and water cost. A study conducted by (Tejwani and Solanki 2010) shown that the output power of panel was increased by 15% compared to the panel which is not having integrated automatic cleaning system.

The electrostatic dust cleaning is another method of cleaning of dust from the PV panel surface. It consists of series of alternating electrode, embedded in a transparent dielectric film and applied to the panel surface. Whenever, the panel surface is charged, the array will attract particles of opposite charge and repel particles of the same charge. This cleaning system requires high electric field for the short duration to generate a standing wave by an alternating electric field. The dust removal process requires no water and no moving parts. This method of cleaning is in the developmental stage (Kawamoto and Shibata 2015; Mazumder et al. 2013).

## 2.11 PV PANEL CONFIGURATIONS

PV panels are connected in series and parallel configurations to get higher output power. Series configuration is done in order to increase the output voltage, while parallel configuration is done in order to increase the output current. The series and

parallel configuration of the PV panels are shown in Figure 2.11 and Figure 2.12. In Figure 2.11, the negative terminal of the first panel is connected to the positive terminal of the second panel and the negative terminal of the second terminal is connected to the positive terminal of the third panel. Thereafter, the positive terminal of the first terminal and the negative terminal of the third panel are connected to the load.

The output voltage across the load is the sum of the output voltage produced by all the three panels, but the current flowing through the load will be the same as the current flowing through each panel. Similarly, in Figure 2.12 the positive terminal of all the three panels is connected to one side of the load and the negative terminal of all the panels is connected to the other side of the load. The output current flowing through the load will be the sum of the output currents produced by all the three panels, whereas the voltage across the load will be the same as the voltage across each panel.
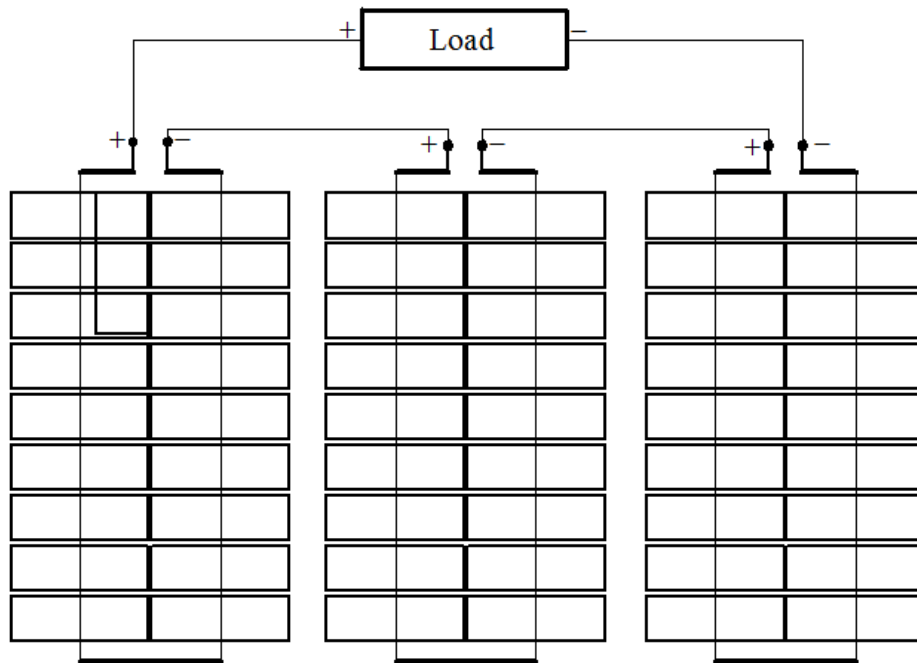


Figure 2.11 Series configuration of PV panels
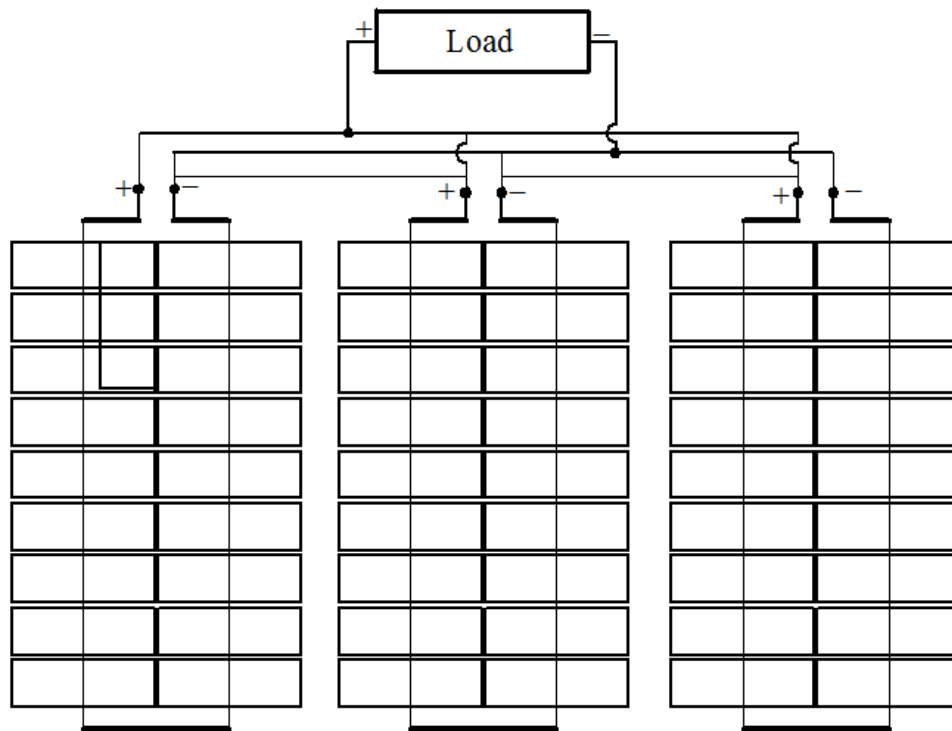
Figure 2.12. Parallel configuration of PV panels

In series and parallel configurations several panels are electrically connected with each other. In such situations all panels require to be operated identically at every operating condition. But, they usually differ from each other due to their operating conditions (i.e., non-uniform solar radiation, shading, dust, different surface temperature etc.) and internal property of the panels (i.e., different processing unit, breakage of glass, different manufacturer etc.). Due to this variation, current generated by each unit will not be same and the current mismatch phenomena may occur in this case. In the current mismatch phenomena, the lower current generating unit will act as a load rather than the power generating source and due to this the lower current generating unit experiences a reverse biasing effect. This reverse bias effect could be very strong depending on the amount of current mismatch. If the mismatch is more than the reverse bias effect will be more. This reverse bias effect generates a local heat, in the lower current generating unit, which increases its temperature. This is called hot spot heating (Bakhsh and Itako 2015; Gonzalez et al. 1984).

29

## 2.12 SOLAR POWER IN MINES

Most of the mining industries are located in the remote places, where access for power is very difficult, to power the mines two types of power sources are used. One is the power from electric grid lines and other is the power from diesel generator set. Both these power sources use fossil fuels which have a negative impact on the environment, and also supports the greenhouse gases. On the other hand, the usage of renewable energy sources minimizes the greenhouse gases in the environment and promotes the clean and green environment (Tripathi 2014). Therefore, many countries promote the usage of renewable energy system in abandoned mine sites, which further promotes the reuse and revitalization of abandoned mine lands (Simon and Mosey n.d.; Song and Choi 2015).

Abandoned mine lands (AMLs) are those lands where extraction, beneficiation or processing of ores and minerals has occurred (Mhlongo and Amponsah-Dacosta 2016; Song and Choi 2016). Song et al. (2015) studied and analysed the photovoltaic (PV) potentials at seven abandoned mine districts in South Korea. They found that the greenhouse gas reduction is proportional to the power production by the solar PV system. Their results also showed that the usage of solar PV power inside the mines not only promotes the green environment for the mines but also improves its cash flow economics by reducing the cost of power production (Song et al. 2015).

# CHAPTER 3

# EXPERIMENTAL SET-UP AND INSTURMENTATION

To investigate the performance of PV panel under the field and laboratory conditions, a PV panel mounting was fabricated, the details of which is discussed in the succeeding section.

## 3.1 Experimental Set-up

A mobile experimental set-up was designed and fabricated to investigate the performance of PV panel in the laboratory as well as in the field (in a surface mine in Hospet Sector of Karnataka State), under varied environmental and operational conditions. A pictorial front and isometric view of the experimental set-up are presented in Figure 3.1 and Figure 3.2.
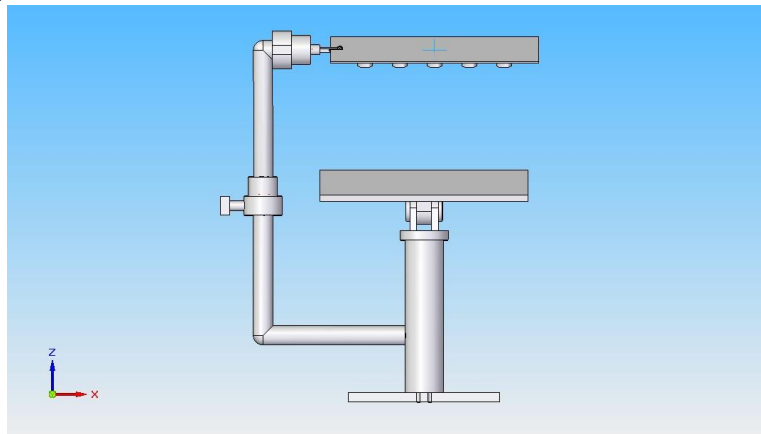


Figure 3.1 Front view of the experimental set-up
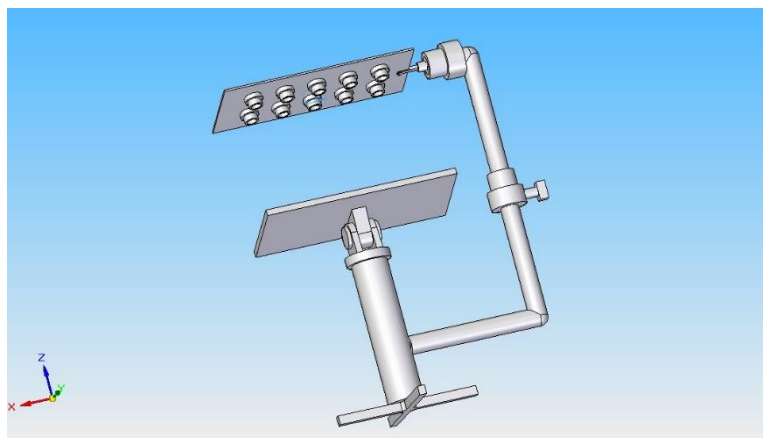


Figure 3.2 Isometric view of the experimental set-up

The experimental set-up consists of a stand of height 1 m with a flat frame on it to hold the panel. The surface of the frame can be tilted in a vertical plane, which can be set-up in any vertical angle, varying from 0º to 90º. A set of light sources which are acting as a solar simulator is placed above the panel surface. The solar simulators are used to generate an artificial solar radiation inside the laboratory. These simulators could generate a different range of constant solar radiation. The photographic view of the experimental set-up under normal and working condition is shown in Figure 3.3.
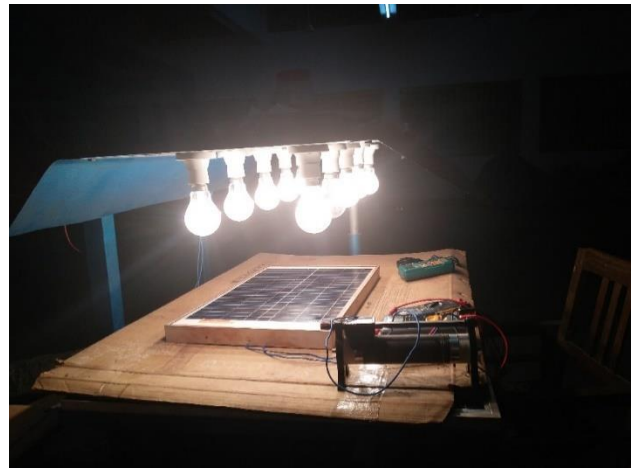


(a) Normal condition          (b) Working condition

Figure 3.3 Photograph of the experimental set-up

**3.2 Instruments Used in the Experiment**

To investigate the effect of environmental parameters, such as dust, shading, temperature and humidity on the performance of solar PV panel various instruments were used which are given below.

**3.2.1 PV Panels**

The PV panels used to generate electric power and its performance were measured under the influence of different environmental parameters. Based on the availability of the instruments and experimental limitations (with respect to the environmental parameters that were existing in the laboratory) the different size and rating of PV panels were used in this study, which are given in Table 3.1.

**Table 3.1** Different ratings of PV panel

| Sl. NO. | PV Panel Rating (watt) | Purpose |
|---------|------------------------|---------|
| 1 | 100 | To study the effect of tilt angle on PV panel performance |
| 2 | 20 | To study the effect of dust and shading on PV panel performance |
| 3 | 10 | To evolve a dust cleaning technique from the surface of PV panel |
| 4 | 5 | To study the effect of shading on the performance of PV panel, and the temperature on the performance of different types of PV panels |
| 5 | 2.5 | To study the effect of shading on the performance of different configurations of PV panel |

### 3.2.2 Solar Power Meter

Solar power meter is a device that measures the solar radiation falling on a particular surface. It measures the solar radiation in terms of BTU (British Thermal Unit) and $W/m^2$ (Watt/meter$^2$). The measured solar radiation in BTU is 3.155 times of $W/m^2$. The solar power meter used in the present study (Model: Tenmars TM-207), is shown in Figure 3.4. The technical specifications of TM-207 is given in Table 3.2.



Figure 3.4 TM-207 solar power meter

**Table 3.2** Technical specifications of TM-207 solar power meter

| Sl. No | Parameter/ Component | Rating/ Range |
|--------|---------------------|---------------|
| 1 | Display | 3½ digits, 2000 readings |
| 2 | Range | 2000 W/m$^2$ |
| 3 | Resolution | 0.1 W/m$^2$ |
| 4 | Accuracy | Typically, within +/- 10W/m$^2$ |
| 5 | Drift | < +/-3% per year |
| 6 | Sampling time | 0.25 second |
| 7 | Operating Temp | 40ºC a |
| 8 | Relative humidity | 80% |
| 9 | Power supply | Single 9V battery |
| 10 | Sensor wire | 1.5 meter |
| 11 | Size | 130×55×39mm (L×W×H) |
| 12 | Weight | 150g |

### 3.2.3 Voltmeter

A voltmeter was used (Model: Fluke 101 Digital multi-meter) to measure the output voltage of the PV panel which was connected across the load. The voltmeter could be able to measure the maximum DC voltage of up to 600 volts with an accuracy of 0.5%. Accuracy is specified for 1 year after calibration, at operating temperature range of 18 °C to 28 °C and at relative humidity of 0% to 90%. The FLUKE 101 digital multi-meter used as a voltmeter in the present study is shown in Figure 3.5.
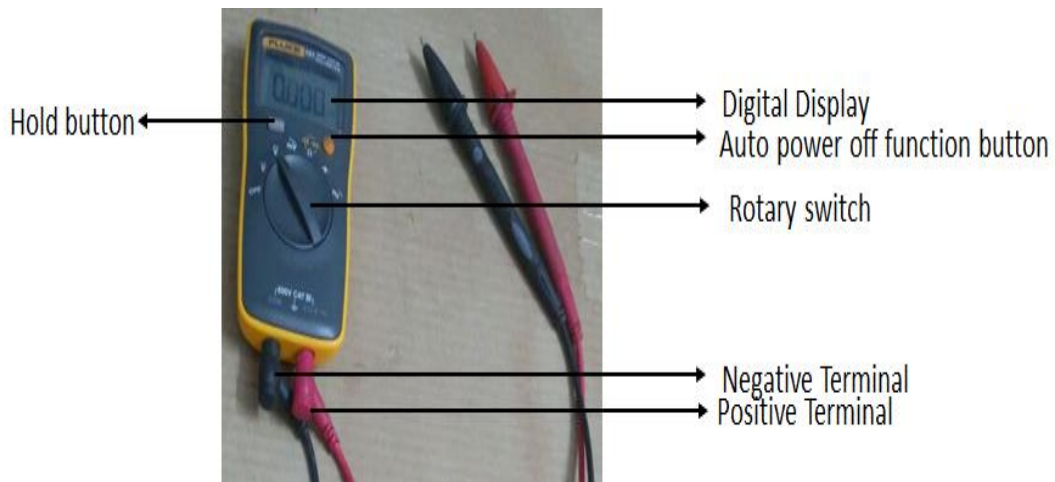
Figure 3.5 Fluke 101 Digital multi-meter

### 3.2.4 Ammeter

The purpose of ammeter in the study is to measure the output current of the PV panel and is connected in series with the load. The DT830 series digital multi-meter used as an ammeter is shown in Figure 3.6. The said ammeter could be able to measure the maximum direct current of up to 10 amps with an accuracy of 2%. Accuracy is specified for 1 year after calibration, at operating temperature range of 23°C to 28 °C, with less than 75% relative humidity.
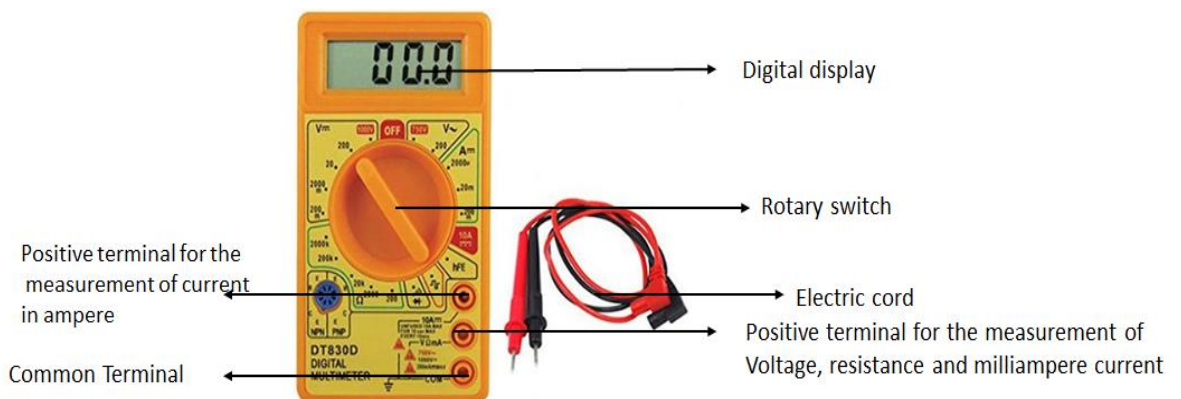

Figure 3.6 DT830 Series Digital multi-meter

### 3.2.5 Rheostat

Rheostat is an electrical instrument used to control current by varying the resistance. In the present study, 320 Ω slide wire rheostat of 1.2 amps current rating was used to control the current in solar panel circuit. Figure 3.7 shows the photograph of 320 Ω slide wire rheostat.
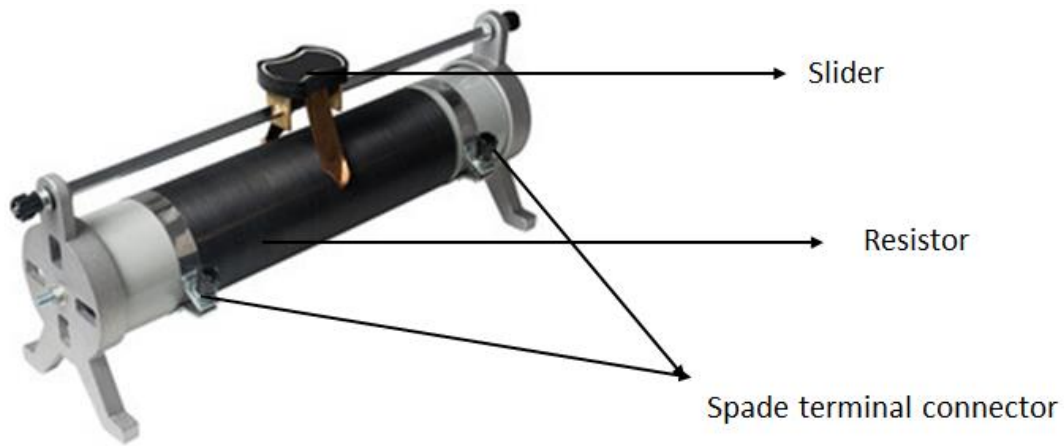
Figure 3.7 Slide wire rheostat

### 3.2.6 Pyrometer

Pyrometer is an instrument which is used to measure the surface temperature of PV panel. DT 500 non-contact digital pyrometer was used in the present study, which is shown in Figure 3.8. The technical specifications of the pyrometer are presented in the Table 3.3.



Figure 3.8 Infrared DT-500 digital non-contact thermometer gun Pyrometer

**Table 3.3** Technical specifications of DT-500 digital pyrometer

| Sl. No | Parameter | Rating/Range |
|--------|-----------|--------------|
| 1 | Temperature | -50°C-500°C |
| 2 | Accuracy | ±2°C or ±2% |
| 3 | Power supply | 2pcs of 1.5V battery |
| 4 | Resolution | 0.1°C or 0.1°F |
| 5 | Operating temperature | -10 to 40°C |
| 6 | Relative humidity | 10% to 90% |
| 7 | Response time | ≤0.8 second |
| 8 | Distance to Spot Ratio | 12: 1 |
| 9 | Size | Approx.145 × 80 × 35mm |
| 10 | Storage temperature | -10°C to 40°C |

### 3.2.7 Humidifier

A humidifier is a device that increases humidity (moisture) level in the atmosphere. A mini water spray fan was used as a humidifier in the present study. The said humidifier has a dimension of 21 cm×12 cm× 9 cm and requires power supply of 2.5 watt.  The photograph of the humidifier is shown in Figure 3.9.



Figure 3.9 Mini water spray fan

### 3.2.8 Hygrometer

A hygrometer is an instrument used for measuring the relative humidity level in the atmosphere. HTC Digital Thermo-hygrometer which is used in this study shown in Figure 3.10 and its specifications are given in Table 3.4.
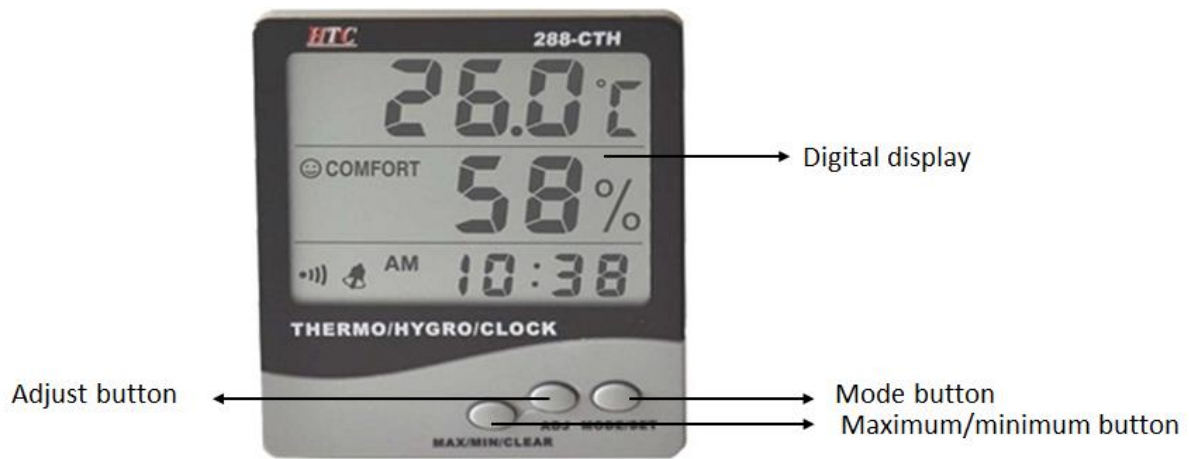


Figure 3.10 HTC Digital Thermo-hygrometer

**Table 3.4** Specifications of HTC digital thermos-hygrometer

| Sl. No | Parameter | Rating/Description |
|--------|-----------|--------------------|
| 1 | Humidity Accuracy | ±5% RH |
| 2 | Power | Battery AAA 1.5 V |
| 3 | Display | LCD display |
| 4 | Dimension (H×W×T) | $106 \times 92 \times 22$ mm |

# CHAPTER 4

# EFFECT OF SOLAR RADIATION ON PV PANEL PERFORMANCE

The performance of solar PV panel strongly depends on the solar radiation falling on its surface. Unfortunately, the solar radiation available throughout the day is not constant. In a cloudless day, it increases from morning to noon and then decreases till the sunset. Due to this variation in the solar radiation the output power of a PV panel is not uniform throughout a day. Therefore, the effect of solar radiation was studied in the laboratory which was presented in this chapter.

## 4.1 METHODOLOGY

A 20 W polycrystalline solar PV panel was used to study the effect of solar radiation on PV panel performance, which consists of two parallel strings and 18 cells in each string as shown in Figure 4.1. A set of 10 numbers of 200 W incandescent bulbs were used as solar radiation to generate an artificial solar radiation in the range from 449 W/m$^2$ to 920 W/m$^2$, as shown in Figure 4.2. The solar radiation falling on the panel surface were measured using solar power meter (as discussed in section 3.2.2), which is shown in Figure 4.3.  As seen in Figure 4.3, the sensor of solar power meter covers three cells of the panel at a time and hence in six solar readings were taken for one string. Thus, in total twelve readings were to cover the entire panel and the mean of twelve readings was considered as the average solar radiation falling on the panel surface.

Figure 4.1 Photographic view of 20 W PV panel



Figure 4.2 PV panel under an artificial solar radiation

Figure 4.3 Measurement of solar radiation falling on the PV panel surface

The electrical responses of PV panel, such as current, voltage and power output were measured for ten different intensity of solar radiation (i.e., 449 W/m$^2$, 516 W/m$^2$, 593 W/m$^2$, 608 W/m$^2$, 661 W/m$^2$, 719 W/m$^2$, 740 W/m$^2$, 788 W/m$^2$, 878 W/m$^2$ and 918 W/m$^2$) under varying output load conditions. The values of electrical responses of PV panel, such as output current, output voltage and output power under varying output load for ten different intensity of solar radiation are given in Table 4.1 to Table 4.10 in Appendix I. Table 4.11 gives the performance of PV panel subjected to ten different intensity of solar radiation.

**Table 4.11** Performance of PV panel under varying solar radiation

| Solar radiation (W/m$^2$) | Maximum power output (watt) | Short circuit current (amp) | Open circuit voltage (volt) |
|---|---|---|---|
| 449.58 | 3.42 | 0.27 | 18.85 |
| 516.22 | 3.73 | 0.31 | 19.15 |
| 593.70 | 4.35 | 0.35 | 19.35 |
| 608.63 | 4.97 | 0.37 | 19.50 |
| 661.49 | 5.13 | 0.39 | 19.95 |
| 719.60 | 6.18 | 0.44 | 20.10 |
| 750.50 | 6.71 | 0.48 | 20.30 |
| 788.49 | 6.89 | 0.49 | 20.60 |
| 878.67 | 7.24 | 0.54 | 20.75 |
| 918.10 | 8.48 | 0.63 | 20.95 |

## 4.2 RESULTS AND DISCUSSION

The I-V and P-V characteristics of a panel for four solar radiation level, i.e., 449 W/m$^2$, 661 W/m$^2$, 719 W/m$^2$ and 788 W/m$^2$, were plotted (which are shown in Figure 4.4 and Figure 4.5) instead of considering all the ten different radiations, as the graph looks very clumsy. As shown in Figure 4.4, for all the four-solar radiation level under consideration, the current initially decreases gradually (first stays more or less constant) with increase in voltage, then it drops suddenly to zero because of the internal characteristic of the PV panel, as discussed in Section 2.8 of Chapter 2. Similarly, the power-voltage characteristic of the panel is also shown in Figure 4.5. It is seen in Figure 4.5 that power increases more or less linearly from zero, reach the maximum value and then drops to zero (with steep slope) when the voltage corresponds to open circuit voltage.
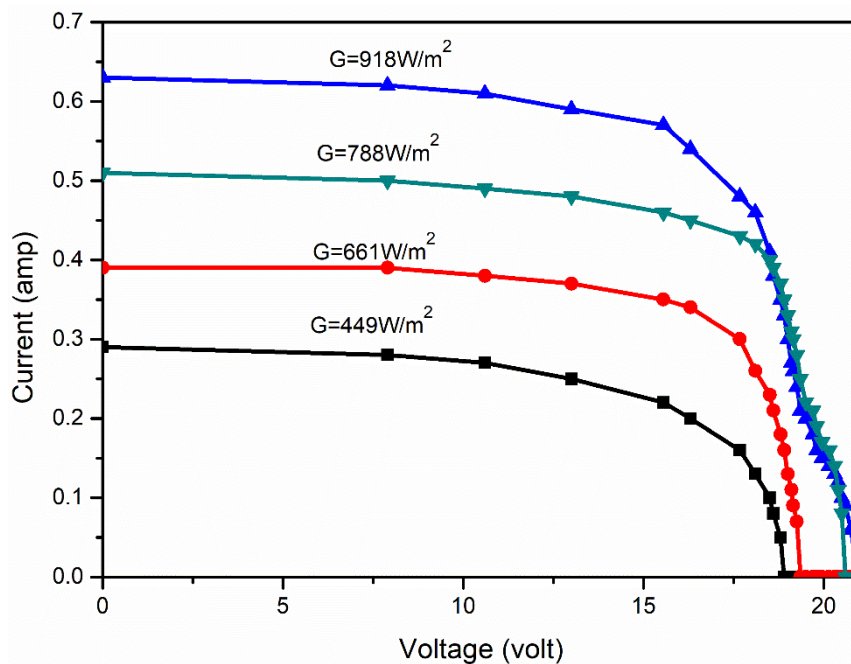


Figure 4.4 I-V characteristic of PV panel under varying solar radiation
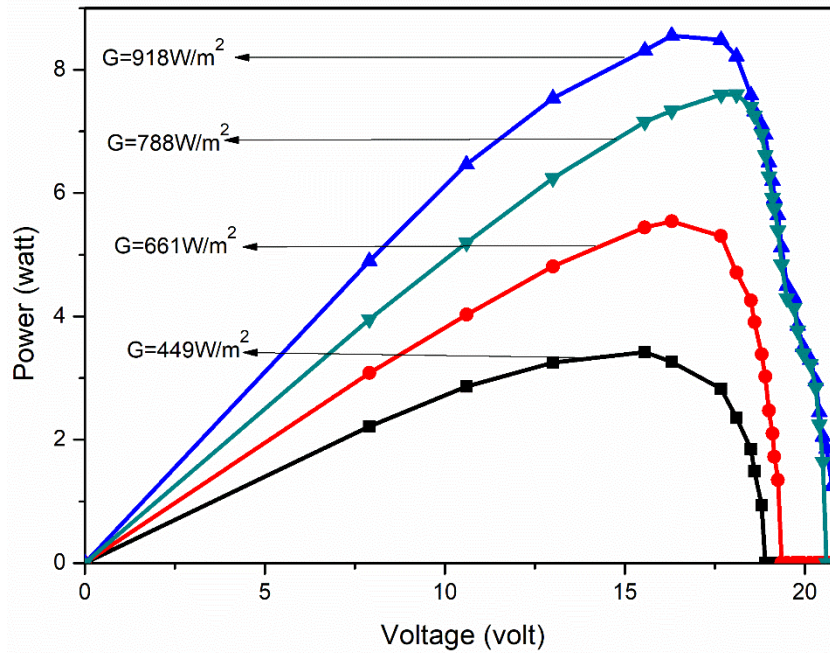
Figure 4.5 P-V characteristic of PV panel under varying solar radiation

A close look at Table 4.11 reveals that the solar radiation falling on the panel surface affects its short circuit current and power output more significantly when compared to its open circuit voltage. This is because of the direct dependency of short circuit current and power output on the solar radiation falling on the panel. On the other hand, open circuit voltage of the panel is proportional to the logarithmic of the solar radiation falling on the panel surface. Figure 4.4 shows that the short circuit current is strongly dependent on the solar radiation falling on the panel surface and this dependency also influences the power output of the panel as depicted in Figure 4.5. The relationship between short circuit current and maximum power output with the solar radiation falling on the panel surface is presented in Figure 4.6 and Figure 4.7. Similarly, the relationship between open circuit voltage and solar radiation falling on the panel surface is shown in Figure 4.8.

From Figure 4.6, Figure 4.7 and Figure 4.8, it is seen that the short circuit current and maximum power output increases linearly and significantly with increase in the solar radiation when compared to its open circuit voltage. Thus, the short circuit current and maximum power output of PV panel is strongly affected by the solar radiation when compared to its open circuit voltage. During the process of the study, it was found that

the short circuit current of the panel is significantly affected by the deposition of dust particle on the panel surface (as discussed in detail in the chapter 6). In the present study the measured data sets are distributed very closely and are lying closer to the straight line. Hence, to draw the relationship between short circuit current and solar radiation, a linear regression technique was used. Table 4.12 gives the data used for the linear regression analysis.
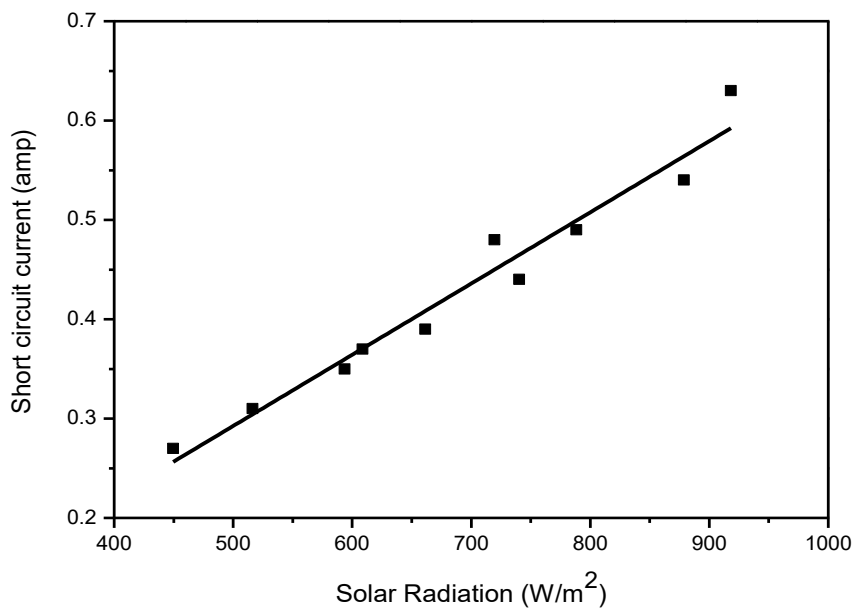


Figure 4.6 Relationship between short circuit current and solar radiation
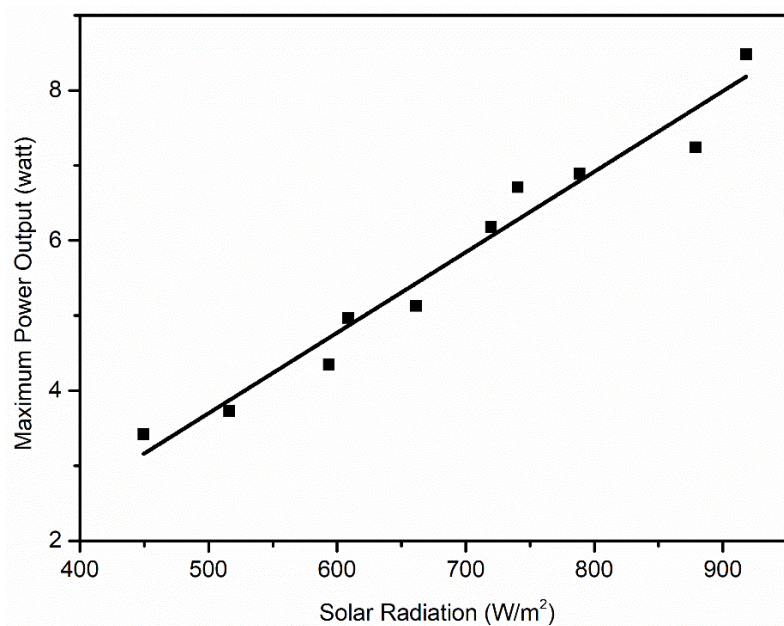


Figure 4.7 Relationship between maximum power output and solar radiation
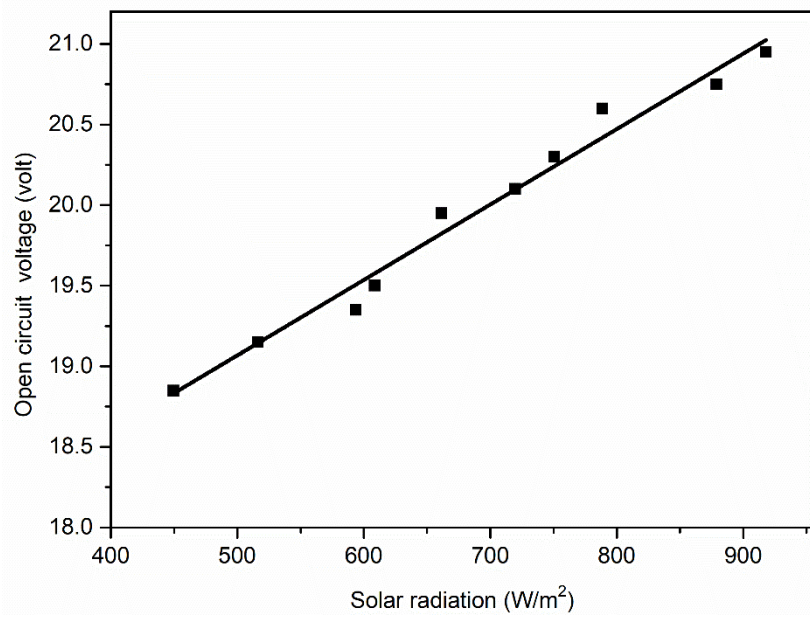
Figure 4.8 Relationship between open circuit voltage and solar radiation

**Table 4.12** Data used for the regression analysis

| Solar radiation (G) | Short circuit current ($I_{SC}$) | $G^2$ | $I_{SC} \times G$ |
|---|---|---|---|
| 449.58 | 0.27 | 202122.20 | 160.03 |
| 516.22 | 0.31 | 266483.10 | 207.80 |
| 593.70 | 0.35 | 352479.70 | 225.19 |
| 608.63 | 0.37 | 370430.50 | 257.98 |
| 661.49 | 0.39 | 437569.00 | 386.36 |
| 719.60 | 0.44 | 517824.20 | 474.48 |
| 750.50 | 0.48 | 548147.70 | 325.76 |
| 788.49 | 0.49 | 621716.50 | 121.39 |
| 878.67 | 0.54 | 772061.00 | 345.41 |
| 918.10 | 0.63 | 842907.60 | 578.40 |

The formulas used for the regression analysis are given by equation (4.1), equation (4.2) and equation (4.3).

$$I_{SC} = a_0 + a_1 G \tag{4.1}$$

$$\sum I_{SC} = n \, a_0 + a_1 \sum G \tag{4.2}$$

$$\sum I_{SC} \times G = a_0 \sum G + a_1 \sum G^2 \tag{4.3}$$

where, $I_{SC}$ = Short circuit current of PV panel (amp),

   G  = Solar radiation falling on the PV panel surface (W/m$^2$),

   n  = Number of observations,

   $a_0$ = Intercept of the line (regression constant), and

   $a_1$ = Slope of the line (regression constant).

A mathematical relation was developed based on equations (4.1), (4.2) and (4.3), which is given by equation (4.4). The regression statistics of the mathematical relation (i.e., equation (4.4)) is presented in Table 4.13. As indicated in Table 4.13, the regression statistics has a very good R square value of 0.9612 and standard error of 0.02306, which is considerably very small (Siddiqui and Bajpai 2012). Thus, the equation (4.4) can be taken as a valid equation, and using it, the short circuit current for a 20W PV panel can be calculated using the known solar radiation falling on its surface.

$$I_{SC} = -0.062+0.0007G \tag{4.4}$$

where, $I_{SC}$ = Short circuit current of PV panel (amp),

   G  = Solar radiation falling on the PV panel surface (W/m$^2$).


Residual analysis is a useful method for the evaluation of the goodness of a fitted model. A residual plot is a graph that shows the residuals on the vertical axis and the independent variable on the horizontal axis. If the points in a residual plot are randomly dispersed around the horizontal axis and not influenced by the residuals in previous observations then a linear regression model is appropriate for the data; otherwise, a non-linear model is more appropriate (Darlington and Hayes 2016; Topp and Gómez 2004).The residual values of developed model are given in Table 4.14. Based on Table 4.14, the residual plot was obtained which is presented in Figure 4.9.

**Table 4.13** Regression statistics of the equation (4.4)

| Sl. No | Parameter | Values |
|--------|-----------|--------|
| 1 | R Square | 0.961243245 |
| 2 | Standard error | 0.023064798 |
| 3 | Observations | 10 |
| 4 | Standard Deviation of residual | 0.0217457 |

**Table 4.14** Residual of the model

| Observation | Observed value | Predicted Y | Residuals (Observed value-Predicted value) | Standard Residuals (Residual/Standard deviation of the residual) |
|---|---|---|---|---|
| 1 | 0.27 | 0.256448069 | 0.013551931 | 0.623200484 |
| 2 | 0.31 | 0.304221679 | 0.005778321 | 0.265722458 |
| 3 | 0.35 | 0.359766386 | -0.009766386 | -0.449118053 |
| 4 | 0.37 | 0.370469568 | -0.000469568 | -0.021593587 |
| 5 | 0.39 | 0.408364421 | -0.018364421 | -0.84450815 |
| 6 | 0.44 | 0.464912776 | -0.024912776 | -1.145641458 |
| 7 | 0.48 | 0.450022951 | 0.029977049 | 1.378527641 |
| 8 | 0.49 | 0.499409566 | -0.009409566 | -0.432709265 |
| 9 | 0.54 | 0.564058788 | -0.024058788 | -1.106369887 |
| 10 | 0.63 | 0.592325796 | 0.037674204 | 1.732489817 |
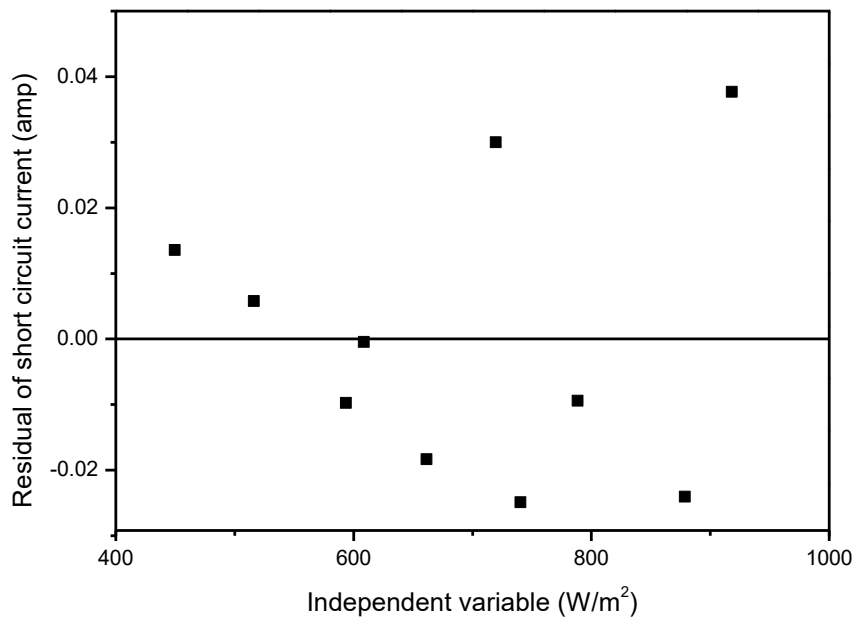


Figure 4.9 Residual plot for the developed mathematical relation

As seen in Figure 4.9, the residuals of the developed model are randomly dispersed around the horizontal axis and not depended on the previous residual, which shows the developed mathematical model is appropriate for the linear regression analysis.

# CHAPTER 5

# EFFECT OF SHADING ON PV PANEL PERFORMANCE

The shading on PV panels may occur due to trees, passing of clouds, deposition of dust particles on the panel surface, nearby permanent structures, shadow of other panels in its vicinity, neighboring buildings etc. The performance of PV panels is affected by the shading on its surface. Therefore, the study of shading effect on PV panel performance is very essential. The study of shading on PV panel performance was carried out in five stages as given below:

i. Effect of shading of panel on its performance using 20 W poly crystalline PV panel.

ii. Effect of single cell shading on the panel performance using 20 W poly crystalline PV panel.

iii. Effect of shading on the performance of PV panel technology, such as mono crystalline and poly crystalline, using 5 W PV panels.

iv. Effect of continuous shading of cells on the temperature variation of an un-shaded cell and glass substrate using 5 W poly crystalline PV panel.

v. Effect of shading strength on the series and parallel configuration of the panels using three numbers of 2.5 W poly crystalline PV panels.

The details of technical specifications of PV panels used in this study are given in Table 5.1.

**Table 5.1** Technical specifications of the PV panels

| Parameter | 20W Panel | 5W Panel | | 2.5W Panel |
|---|---|---|---|---|
| | | Poly crystalline | Mono crystalline | |
| Open circuit voltage (V) | 21.50 | 10.80 | 11.57 | 10.50 |
| Short circuit current (A) | 1.28 | 0.65 | 0.57 | 0.31 |
| Maximum voltage (V) | 17.00 | 8.80 | 9.64 | 8.73 |
| Maximum current (A) | 1.2 | 0.57 | 0.52 | 0.29 |
| Maximum Power (W) | 20 | 5.0 | 5.0 | 2.5 |
| Fill Factor | 0.727 | 0.712 | 0.760 | 0.768 |

## 5.1 EFFECT OF PANEL AND CELL SHADING ON THE PERFORMANCE OF PV PANEL

### 5.1.1 Methodology

The knowledge of shading strength, which is defined as the ratio of the shaded area of the panel to the total area of the panel, was used to investigate the shading effect on the panel performance. The shading of panel surface irrespective of cells is called panel shading and the shading of only cells irrespective of panel surface is called cell shading. The performance of a 20 W poly crystalline PV panel with panel shading was measured for the shading strength of 0%, 25%, 50% and 75%. Figure 5.1, shows the pictorial representation of the panel shading under different shading strengths. Similarly, the effect of single cell shading on the performance of 20 W PV panel was also recorded for the shading strength of 0%, 25%, 50%, 75% and 100%. Figure 5.2 shows the pictorial representation of single cell shading under different shading strengths. To study the electrical responses of panel under different shading conditions a set of solar simulators was used to generate an artificial solar radiation. The solar radiation of 744 W/m$^2$ was maintained during the experiment, which was measured using TM-207 solar power meter.



(a)                                                            (b)
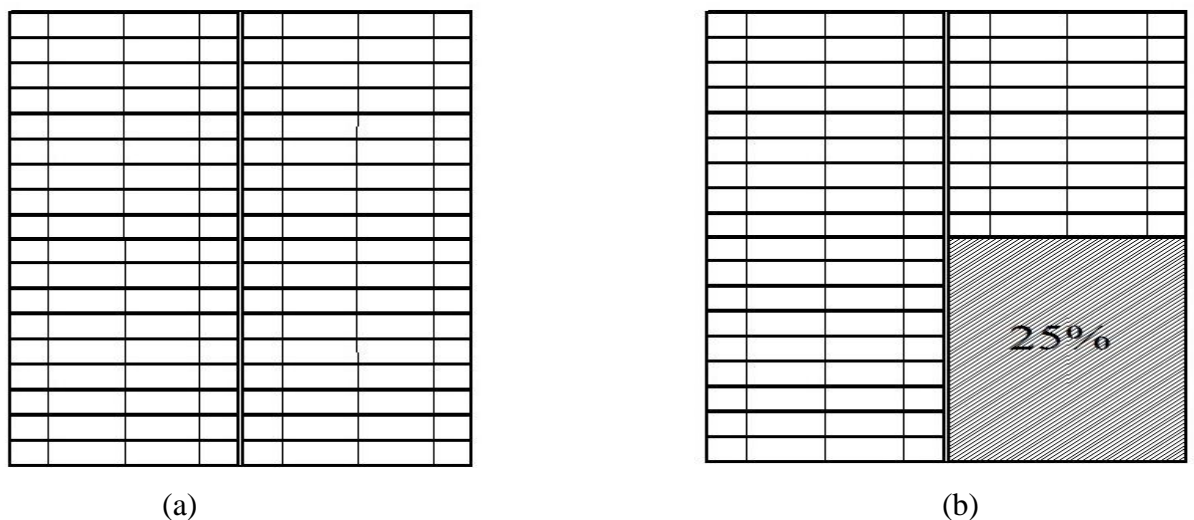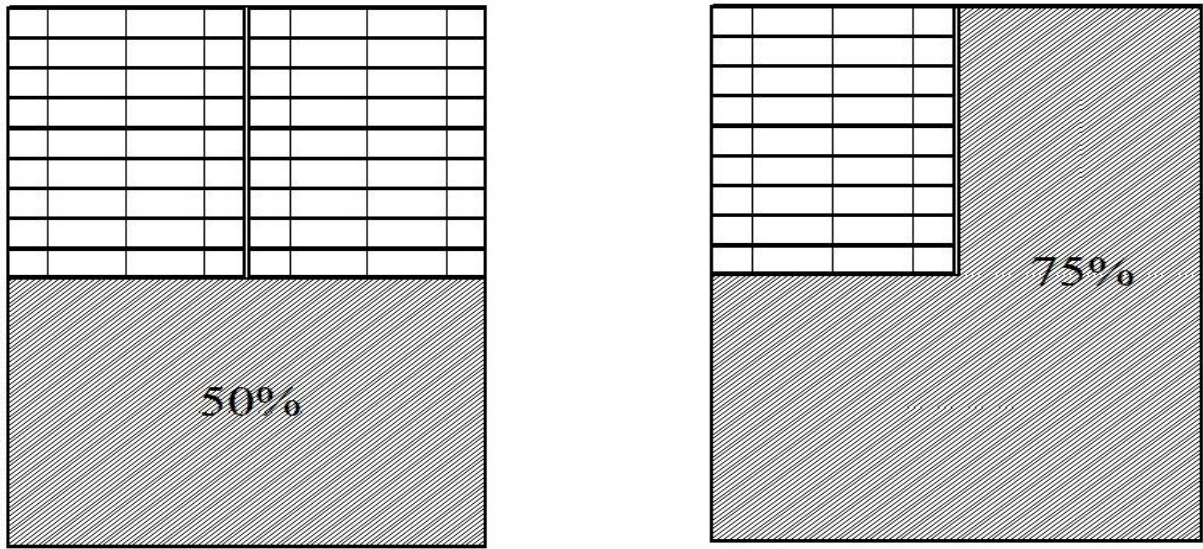
<div align="center">(c)                        (d)</div>

Figure 5.1 Pattern of PV panel shading under different shading strengths of (a) 0% (b) 25% (c) 50% and (d) 75%
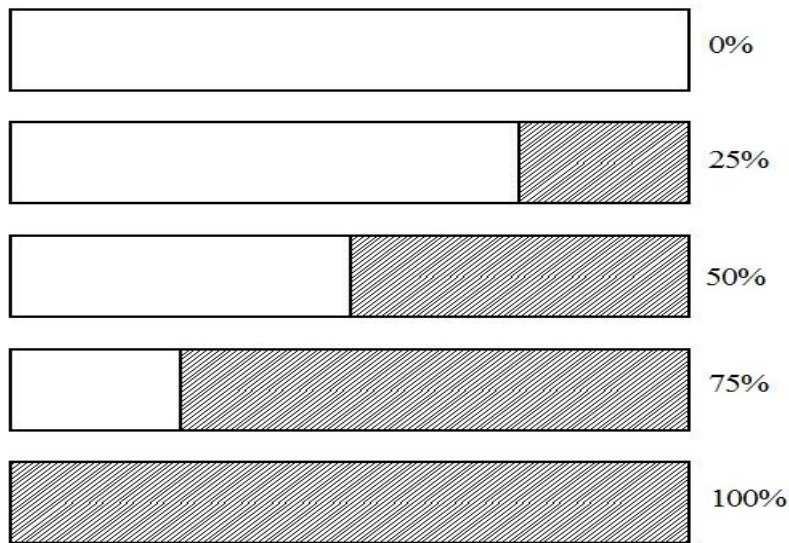


Figure 5.2 Variation of shading strengths on single cell of PV panel

## 5.1.2 Results and Discussion

The reduction in the performance of PV panel due to shading effect was studied in two phases – i) panel shading with varying shading strengths, such as 25%, 50% and 75%, and ii) cell shading with varying shading strengths, such as 25%, 50%, 75% and 100%. The electrical responses of the PV panel, such as current, voltage and power under two condition, i.e., panel shading and cell shading were measured. The electrical responses

of PV panel due to panel shading and cell shading are given in Table 5.2 to Table 5.9 in Appendix II. Based on these measured electrical responses the electrical characteristics of PV panel, such as current-voltage and power-voltage characteristics are plotted which are shown in Figure 5.3, Figure 5.4, Figure 5.5 and Figure 5.6.
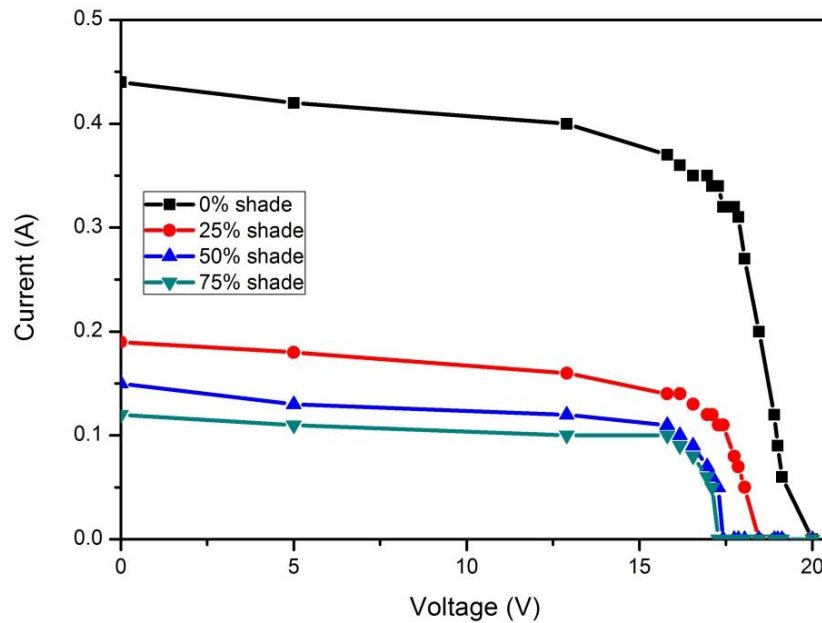


Figure 5.3 I-V characteristic of PV panel under different shading strengths
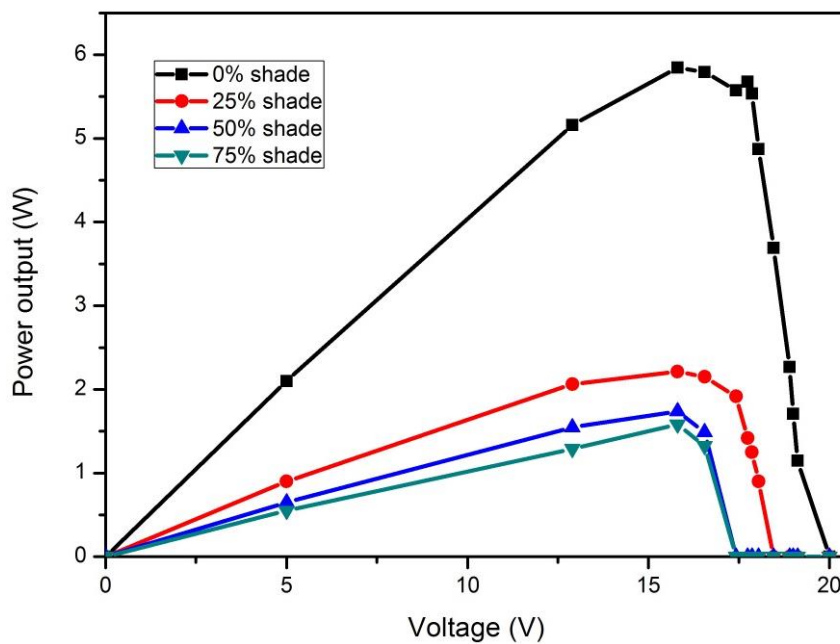


Figure 5.4 P-V characteristic of PV panel under different shading strengths
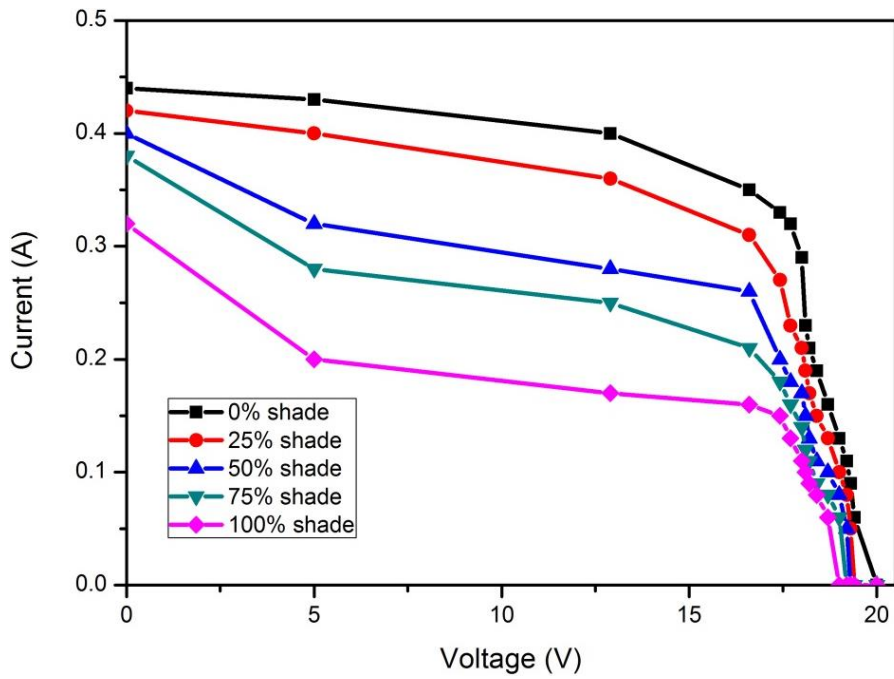
Figure 5.5 I-V characteristic of PV panel under different single cell shading strengths
(with single cell shading)
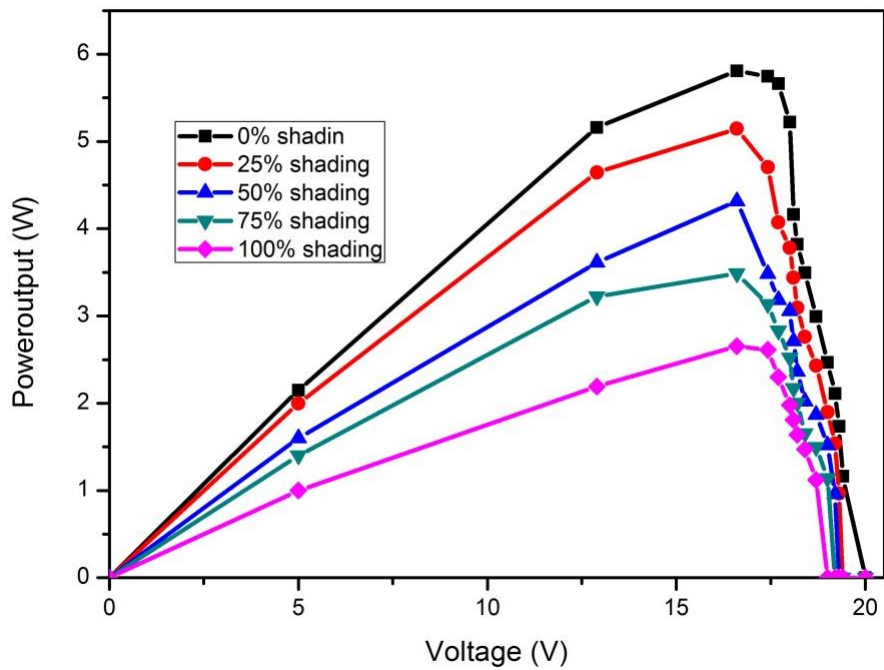


Figure 5.6 P-V characteristic of PV panel under different single cell shading strengths
(with single cell shading)

The panel characteristics as shown in Figure 5.3, Figure 5.4, Figure 5.5 and Figure 5.6 represent a considerable amount of degradation in its performance due to panel shading as well as cell shading. The short circuit current and power output of PV panel are highly influenced by the shading effect when compared to its open circuit voltage. This is because the solar radiation reaching panel surface reduces due to the shading. As discussed in Chapter 4, the solar radiation is directly related to the short circuit current and logarithmically related to the open circuit voltage of the panel. Therefore, the reduction in open circuit voltage of panel due to the reduction in solar radiation is not much significant compared to that of short circuit current and power output. The percentage reduction in the electrical parameters of the panel, such as open circuit voltage, short circuit current and maximum power output due to the panel and cell shading are presented in Table 5.10 and Table 5.11, respectively.

**Table 5.10** Reduction in the panel parameters due to panel shading

| Shading strength (%) | Reduction in open circuit voltage (%) | Reduction in short circuit current (%) | Reduction in maximum power output (%) |
|---|---|---|---|
| 25 | 7.70 | 56.81 | 62.16 |
| 50 | 12.90 | 65.90 | 70.27 |
| 75 | 13.60 | 72.72 | 72.97 |

**Table 5.11** Reduction in the panel parameters due to single cell shading

| Shading strength (%) | Reduction in open circuit voltage (%) | Reduction in short circuit current (%) | Reduction in maximum power output (%) |
|---|---|---|---|
| 25 | 3.0 | 4.54 | 11.42 |
| 50 | 3.5 | 9.09 | 25.71 |
| 75 | 4.0 | 13.63 | 40.0 |
| 100 | 5.0 | 27.27 | 54.28 |

## 5.2 EFFECT OF SHADING ON THE PERFORMANCE OF PV PANEL TECHNOLOGY

### 5.2.1 Methodology

The study of shading on the performance of two kinds of 5 W PV panels, such as mono crystalline and poly crystalline was performed in the laboratory. The constant solar radiation of 1190 W/m$^2$ was maintained during the study, which was measured using

TM-207 solar power meter. The shading strength of 1.56%, 6.25%, 12.5% and 25% were maintained for both the type of panels for their performance study. The electrical responses of PV panels, such as current, voltage and power output were measured by varying output load, for all the defined shading strengths. Further, the electrical responses were also recorded for the un-shaded condition.

Since, both the panels are of different dimensions, the study was also conducted by subjecting these panels to the same level of shading (i.e., 5.2 cm×2 cm). With this amount of shading mono crystalline and poly crystalline PV panels experiences 2.92% and 2.97% shading strengths, respectively. Under this condition, the short circuit current and open circuit voltage of panels were recorded and to evaluate their performance the percentage reduction in short circuit current and open circuit voltage were calculated w.r.t. un-shaded condition.

### 5.2.2 Results and Discussion

The electrical responses of mono crystalline and polycrystalline PV panels, such as current, voltage and power without shading and under 1.56%, 6.25%, 12.5% and 25% shading strengths were measured, which are given in Table 5.12 to Table 5.21 in Appendix II. Based on these measured electrical responses the electrical characteristics i.e., current-voltage (I-V) and power-voltage (P-V) curves were plotted. Figure 5.7 and Figure 5.8 shows the I-V characteristics of mono crystalline and poly crystalline PV panels, respectively. Similarly, Figure 5.9 and Figure 5.10 shows the P-V characteristics of mono crystalline and poly crystalline PV panels, respectively. As depicted in Figure 5.7, Figure 5.8, Figure 5.9 and Figure 5.10, the deformation of current-voltage (I-V) and power-voltage (P-V) characteristic increases with the amount of shading strength, which indicates a considerable amount of degradation in the performance of panels. The maximum power point in the P-V characteristic curves moves towards the lower output voltage. Based on the plotted characteristics of PV panels, the reduction in their output parameters by increasing shading strength were calculated, which is given in Table 5.22. As indicated in Table 5.22, the short circuit current and maximum power output are highly influenced by the shading effect when compared to its open circuit voltage. For example, under 25% shading strength the

reduction in short circuit current of mono crystalline panel was 47.72%, whereas in poly crystalline panel it was as high as 60.86%. Similarly, the reduction in maximum power output for mono crystalline and poly crystalline panels was 41.40% and 61.80%, respectively. But the difference in open circuit voltage was not significant, in fact the reduction in $V_{oc}$ of monocrystalline panel was only 5.26% and that of polycrystalline panel was 6.52%.
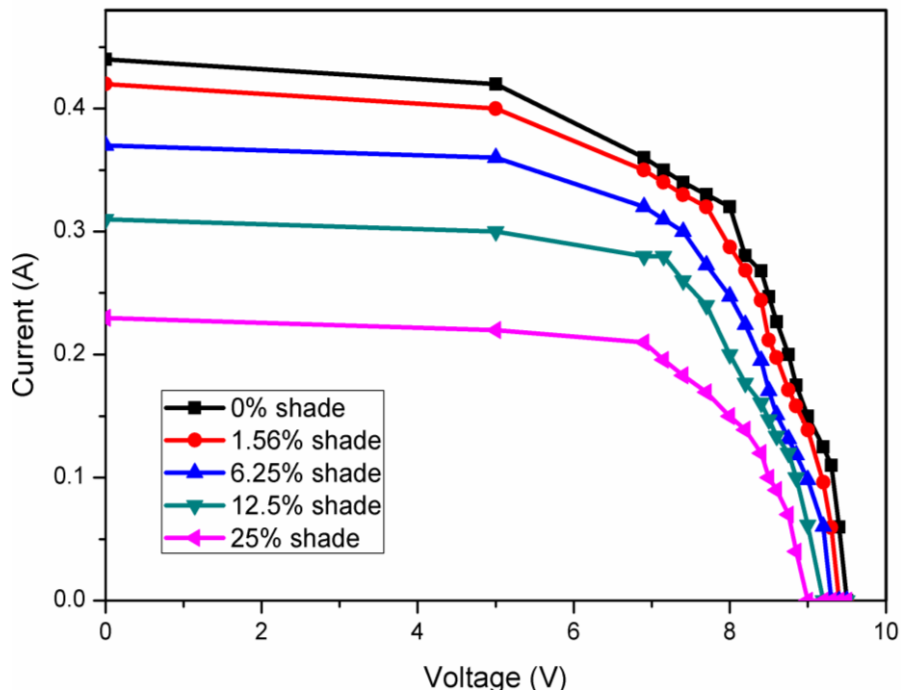


Figure 5.7 I-V characteristics of mono crystalline PV panel
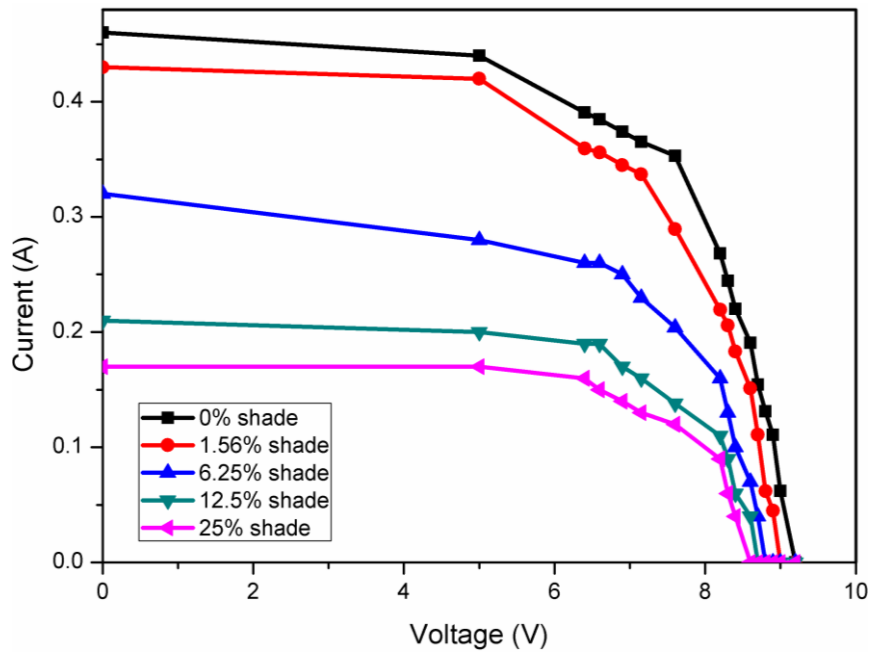
Figure 5.8 I-V characteristics of poly crystalline PV panel
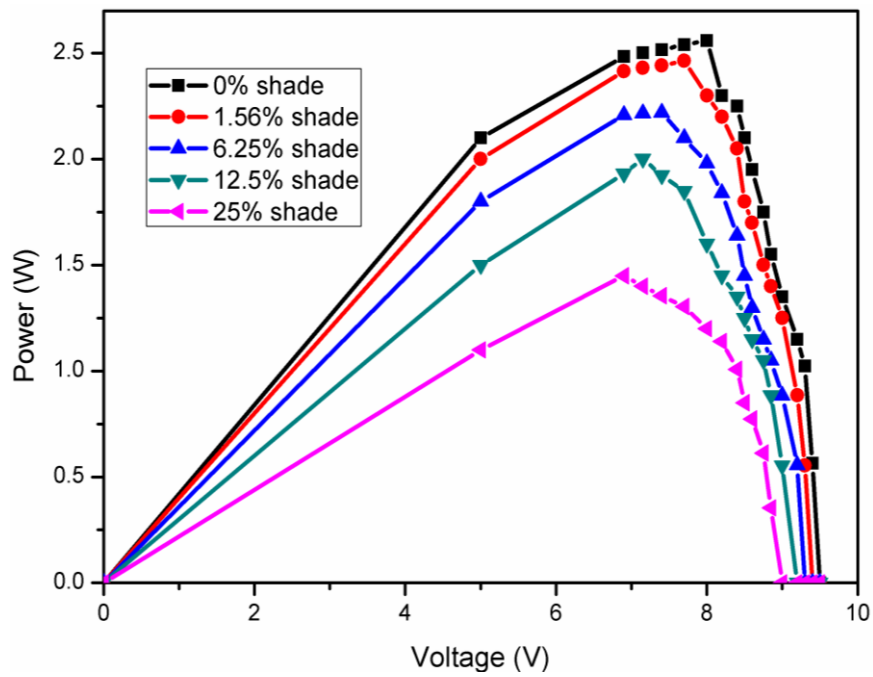


Figure 5.9 P-V characteristics of mono crystalline PV panel
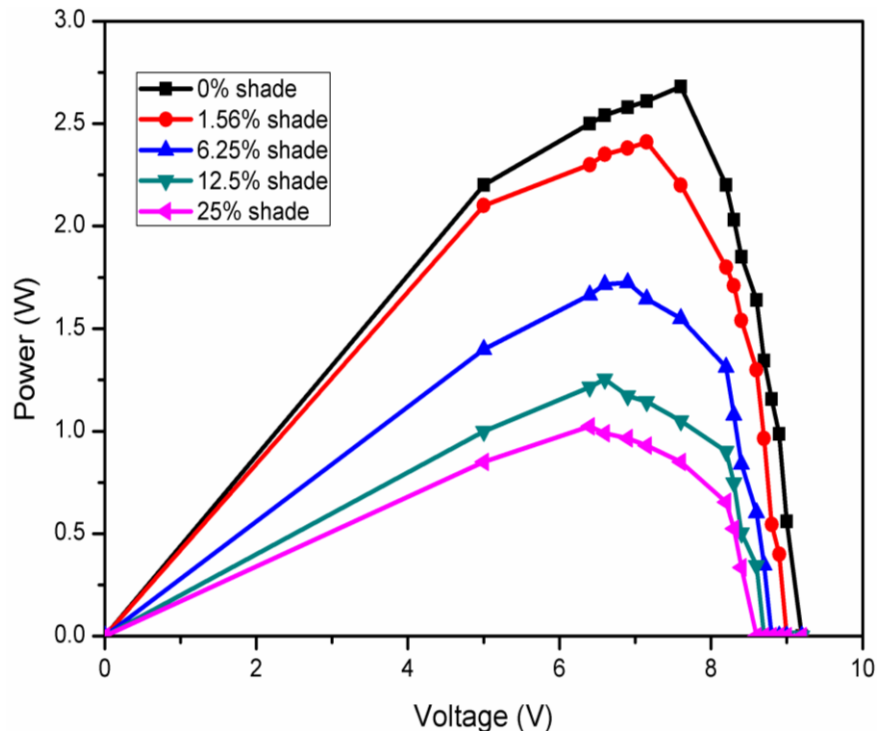
Figure 5.10 P-V characteristics of poly crystalline PV panel

**Table 5.22** Reduction in PV panel output parameters under different shading
strength compared to un-shaded panel

| Shading strength (%) | Mono crystalline panel | | | Poly crystalline panel | | |
|---|---|---|---|---|---|---|
| | Reduction in $I_{sc}$ (%) | Reduction in $V_{oc}$ (%) | Reduction in $P_{max}$ (%) | Reduction in $I_{sc}$ (%) | Reduction in $V_{oc}$ (%) | Reduction in $P_{max}$ (%) |
| 1.56 | 4.53 | 1.05 | 3.75 | 6.52 | 2.18 | 10.07 |
| 6.25 | 15.90 | 2.15 | 13.28 | 30.43 | 3.26 | 35.63 |
| 12.50 | 29.54 | 3.68 | 21.80 | 54.34 | 4.89 | 53.20 |
| 25.00 | 47.72 | 5.26 | 41.40 | 60.86 | 6.52 | 61.80 |

Table 5.23 gives the percentage reduction in short circuit current and open circuit voltage of shaded monocrystalline and polycrystalline panels (i.e., respectively 2.92% and 2.97%) with respect to un-shaded panels. As indicated in Table 5.23, the reduction in $I_{sc}$ and $V_{oc}$ is severe in case of polycrystalline panel when compared to monocrystalline panel. The obtained results as mentioned in Table 5.22 and Table 5.23 demonstrates that the reduction in performance of poly crystalline PV panel is severe when compared to mono crystalline PV panel under the same level of shading condition. Since mono crystalline cells are made out of high grade silicon, they have higher energy conversion efficiency than that of poly crystalline solar cells.

Nevertheless, today the poly crystalline solar cells are more in practice than the mono crystalline solar cells due to less cost and simple production process.

**Table 5.23** Reduction in PV panel output parameters under the same level of shading compared to un-shaded panel

| Parameter | Mono crystalline panel with shading strength of 2.92% | Polycrystalline panel with shading strength of 2.97% |
|---|---|---|
| Reduction in $I_{sc}$ (%) | 9.09 | 23.92 |
| Reduction in $V_{oc}$ (%) | 1.58 | 2.60 |

## 5.3 EFFECT OF CONTINUOUS SHADING OF CELLS ON THE TEMPERATURE VARIATION OF AN UN-SHADED CELL AND GLASS SUBSTRATE OF PV PANEL

In the case of shading, the shaded cells not only influence the performance of the panel, but also affects the temperature of un-shaded cells. Keeping this in view, the temperature of an un-shaded cell was also measured by continuous shading of other cells in the panel.

### 5.3.1 Methodology

A 5 W polycrystalline PV panel consisting of 18 cells was used to measure the temperature variation of an un-shaded cell due to continuous shading of other cells in a panel. Figure 5.11 shows the pictorial view of a 5 W panel. In this study, the temperature variation of one cell (i.e., cell number 18 as shown in Figure 5.11) and the glass surface were monitored by continuous shading of other cells, in steps, one by one (i.e. cell number 1 to 17 as shown in Figure 5.11). The solar radiation was kept constant at 549 W/m$^2$ during the study and the temperature was measured using Pyrometer.

| 1 | | | 10 |
| 2 | | | 11 |
| 3 | | | 12 |
| 4 | | | 13 |
| 5 | | | 14 |
| 6 | | | 15 |
| 7 | | | 16 |
| 8 | | | 17 |
| 9 | | | 18 |
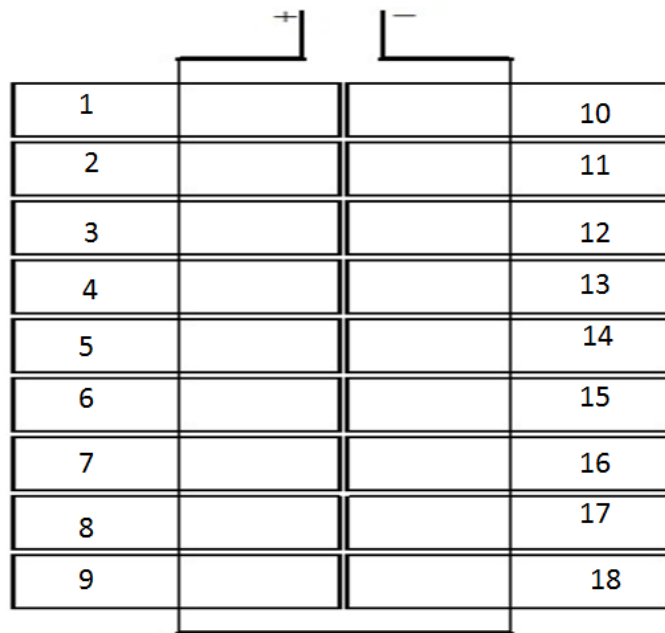
Figure 5.11 Pictorial view of 5W polycrystalline PV panel

### 5.3.2 Results and Discussion

The temperature of the glass surface and an un-shaded cell of a panel were measured at every step of shading as discussed in section 5.3.1, the results of which are given in Table 5.24. Based on these results the graph between temperature and number of shaded cells was plotted, which is shown in Figure 5.12. The rate of change in temperature of un-shaded cell and glass surface was calculated based on equation 5.1.

$$\text{RCTUC or RCTG} = \frac{\Delta T}{T \times N} \times 1000 \tag{5.1}$$

where, RCTUC= Rate of change of temperature of un-shaded cell (%),

RCTG= Rate of change of temperature of glass surface (%),

$\Delta T$= Change in temperature (°C),

T = Temperature of a cell and glass without shading (°C), and

N= Total number of shaded cell.

As depicted in Figure 5.12, the temperature of an un-shaded cell rises at faster rate (at the rate of 1.753%) than the glass temperature (i.e., 0.185%). Thus, the shaded cells in the panel not only affect its performance but also the temperature of un-shaded cell and glass substrate. This rise in temperature can create a local hot spot problem in an un-shaded cell. However, the increment in the temperature of an un-shaded cell is not

linear. This non-linear behaviour may be due to the uneven distribution of solar radiation and erratic generation of current.

**Table 5.24** Temperature of un-shaded cell and glass substrate of PV panel due to continuous shading of other cells in the panel

| No. of shaded cell | Temp of un-shaded cell (°C) | Glass Temperature (°C) |
|---|---|---|
| 0 | 34.55 | 34.90 |
| 1 | 36.45 | 33.00 |
| 2 | 35.75 | 33.10 |
| 3 | 35.60 | 34.20 |
| 4 | 35.10 | 33.40 |
| 5 | 38.95 | 34.00 |
| 6 | 36.15 | 34.50 |
| 7 | 35.85 | 34.20 |
| 8 | 36.50 | 35.50 |
| 9 | 37.20 | 34.30 |
| 10 | 36.75 | 35.20 |
| 11 | 38.60 | 35.20 |
| 12 | 42.20 | 35.10 |
| 13 | 42.85 | 35.50 |
| 14 | 40.90 | 36.00 |
| 15 | 40.65 | 36.30 |
| 16 | 44.05 | 35.80 |
| 17 | 44.85 | 36.00 |
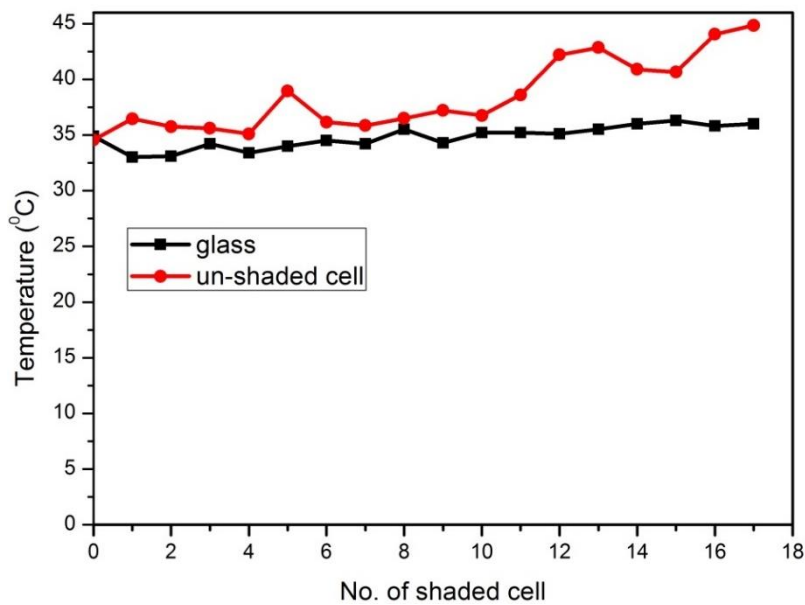


Figure 5.12 Variation of temperature of an un-shaded cell and glass surface of PV panel due to continuous shading

## 5.4 EFFECT OF SHADING STRENGTH ON THE PERFORMANCE OF PV PANELS CONFIGURATION

### 5.4.1 Methodology

The effect of shading on a panel configuration, such as series and parallel were also studied, using three identical 2.5 W polycrystalline PV panels. The electrical responses of both the configurations were measured for three different loads, i.e., of 50 Ω, 70 Ω and 108 Ω with the same shading strength and the same level of solar radiation. The electrical responses were also recorded for an un-shaded condition. The solar radiation of 744 W/m$^2$ was maintained during the experiment. Figure 5.13 shows the shading pattern of series and parallel configurations. In this Figure, the hatched portion represents the shaded area, which is 6.35% of single panel area. Moreover, the position of shading was kept constant for both the configurations.



(a)                                              (b)
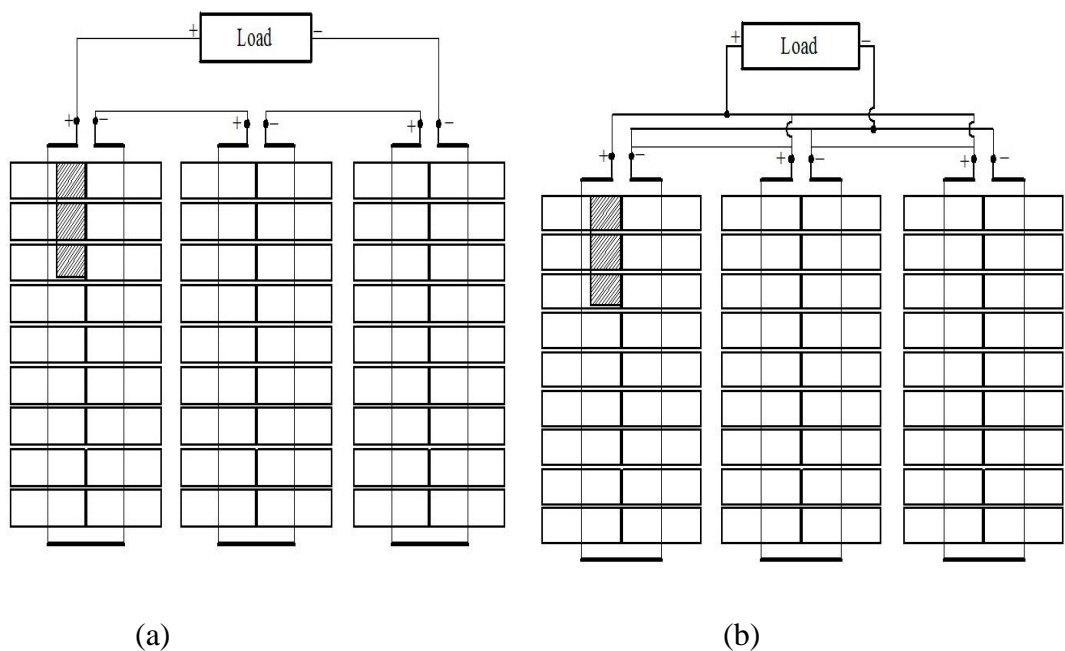
Figure 5.13 Shading of PV panels in (a) series configuration and (b) parallel configuration

### 5.4.2 Results and Discussion

The electrical responses of panels, under different conditions, as discussed in section 5.4.1, were measured in laboratory and the results were tabulated, which are shown in Table 5.25.

**Table 5.25** Electrical parameters for series and parallel configuration under shaded and non-shaded conditions

| Load/ Configuration | Un-shaded condition | | | Shaded condition | | | |
|---|---|---|---|---|---|---|---|
| | Output voltage (in volt) | Output current (in amp) | Output power (in watt) | Output voltage (in volt) | Output current (in amp) | Output power (in watt) | Reduction in output power (in %) |
| **50Ω** | | | | | | | |
| Series | 9.00 | 0.17 | 1.53 | 8.9 | 0.16 | 1.424 | 6.90 |
| Parallel | 8.00 | 0.16 | 1.28 | 7.9 | 0.16 | 1.264 | 1.25 |
| | | | | | | | |
| **70Ω** | | | | | | | |
| Series | 11.30 | 0.16 | 1.80 | 11.00 | 0.15 | 1.65 | 8.30 |
| Parallel | 9.00 | 0.14 | 1.26 | 8.80 | 0.14 | 1.232 | 2.20 |
| | | | | | | | |
| **108Ω** | | | | | | | |
| Series | 17.3 | 0.16 | 2.768 | 15.4 | 0.14 | 2.31 | 16.54 |
| Parallel | 9.75 | 0.09 | 0.8775 | 9.70 | 0.085 | 0.8245 | 6.03 |

Table 5.25 also gives the percentage reduction in power output when both the configurations are suffering from the same level of shading. A close look at these readings reveals that the reduction in output power is severe in the case of series configuration. This is because in series configuration the output current is decided by the reduced current of the shaded panel, which profusely affects the panel power output. On the other hand, in parallel configuration, the output current is decided by its output voltage, and this voltage is not much influenced by the shading. Hence, the reduction in power output due to shading is lesser in parallel configurations when compared to series configurations. As observed in Table 5.25, the reduction in power output increases with the increase in load for both the configurations (i.e., series and parallel). The above study demonstrates that the parallel configuration performs well under the shaded condition when compared to that of series configuration.

# CHAPTER 6

# EFFECT OF DUST ON PV PANEL PERFORMANCE AND CLEANING TECHNIQUE OF DUST FROM PV PANEL SURFACE

The performance of a PV panel is highly affected by the deposition of dust on its surface. To study the effect of dust on PV panel performance a 20 W polycrystalline panel was used with an experimental set-up as discussed in Section 3.1 of Chapter 3. The experiment was carried out to understand the effect of dust mass, dust size and dust type on the performance of a PV panel. A study was also carried out to know the effect of dust deposition on panel surface temperature. As a case study, an experiment was carried out in a surface mine in Hospet Sector of Karnataka State. Further, a technology was evolved for cleaning the surface of PV panel, so as to study the efficiency of panel when it is cleaned regularly.

## 6.1 EFFECT OF DUST MASS ON PV PANEL PERFORMANCE
### 6.1.1 Methodology

To understand the influence of dust deposition on panel surface an experiment was performed in a laboratory using 20 W polycrystalline PV panel (area of the panel is 0.1489 $m^2$) at 722 W/$m^2$ constant solar radiation. Iron ore dusts of size less than 75 μ were used in this study which was prepared using sieve analysis process. The dust was distributed on the panel surface with the help of a strainer. A set of solar simulators were used to generate an artificial solar radiation. A Digital Multi-meter Fluke 178+ and DT830B were used to measure the electrical response of PV panel. The rheostat of rating 320 ohm was used as an output load for PV panel.

Initially the electrical parameters of clean PV panel, such as current, voltage and power were recorded by varying its load using rheostat. To study the effect of dust mass deposition on the panel, iron ore dusts were spread on the panel surface, and its

respective electrical responses were measured as discussed above. This procedure was repeated for ten different mass depositions of dust, such as 1 gm, 2 gm, 3 gm, 4 gm, 5 gm, 6 gm, 7 gm, 8 gm, 9 gm and 10 gm. The measured electrical parameters of all the said conditions are given in Table 6.1 to Table 6.11 in Appendix III.

## 6.1.2 Results and Discussion

Table 6.12 gives the variation in the electrical responses, such as $I_{sc}$, $V_{oc}$ and $P_{max}$ for the ten-different mass depositions on the panel surface along with the clean panel. Based on the measured electrical parameters the PV panel characteristics such as, current-voltage (I-V) and power-voltage (P-V) characteristics were plotted. The I-V and P-V characteristics of the panel for only six panel surface conditions, (i.e., for clean panel, 2 gm, 4 gm, 6 gm, 8 gm and 10 gm dust deposition) were plotted, which are shown in Figure 6.1 and Figure 6.2 (here not considered, for plotting all the eleven panel surface conditions as the graph looks very clumsy). Table 6.13 indicates the reduction in electrical parameters compared to a clean panel due to dust deposition.

**Table 6.12** Electrical responses of PV panel under varying dust deposition on its surface

| Amount of dust deposition (gm) | Dust deposition density (gm/m$^2$) | Open circuit voltage (volt) | Short circuit current (amp) | Maximum power output (watt) |
|---|---|---|---|---|
| Clean surface | Clean surface | 19.30 | 0.48 | 6.60 |
| 1 | 6.72 | 19.15 | 0.46 | 6.28 |
| 2 | 13.43 | 19.00 | 0.44 | 5.96 |
| 3 | 20.14 | 18.85 | 0.42 | 5.64 |
| 4 | 26.86 | 18.70 | 0.38 | 4.99 |
| 5 | 33.58 | 18.40 | 0.34 | 3.85 |
| 6 | 40.29 | 18.10 | 0.28 | 3.23 |
| 7 | 47.01 | 17.90 | 0.25 | 2.94 |
| 8 | 53.72 | 17.50 | 0.24 | 2.79 |
| 9 | 60.44 | 17.35 | 0.18 | 1.79 |
| 10 | 67.15 | 17.20 | 0.16 | 1.66 |

**Table 6.13** Reduction in electrical parameters compared to a clean panel surface

due to dust deposition

| Amount of dust deposition (gm) | Dust deposition density (gm/m²) | Reduction in open circuit voltage (%) | Reduction in short circuit current (%) | Reduction in maximum power output (%) |
|---|---|---|---|---|
| 1 | 6.72 | 0.78 | 4.17 | 4.85 |
| 2 | 13.43 | 1.55 | 8.33 | 9.70 |
| 3 | 20.14 | 2.33 | 12.50 | 14.55 |
| 4 | 26.86 | 3.11 | 20.83 | 24.39 |
| 5 | 33.58 | 4.66 | 29.17 | 41.67 |
| 6 | 40.29 | 6.22 | 41.67 | 51.06 |
| 7 | 47.01 | 7.25 | 47.92 | 55.45 |
| 8 | 53.72 | 9.33 | 50.00 | 57.72 |
| 9 | 60.44 | 10.10 | 62.50 | 72.88 |
| 10 | 67.15 | 10.88 | 66.67 | 74.85 |
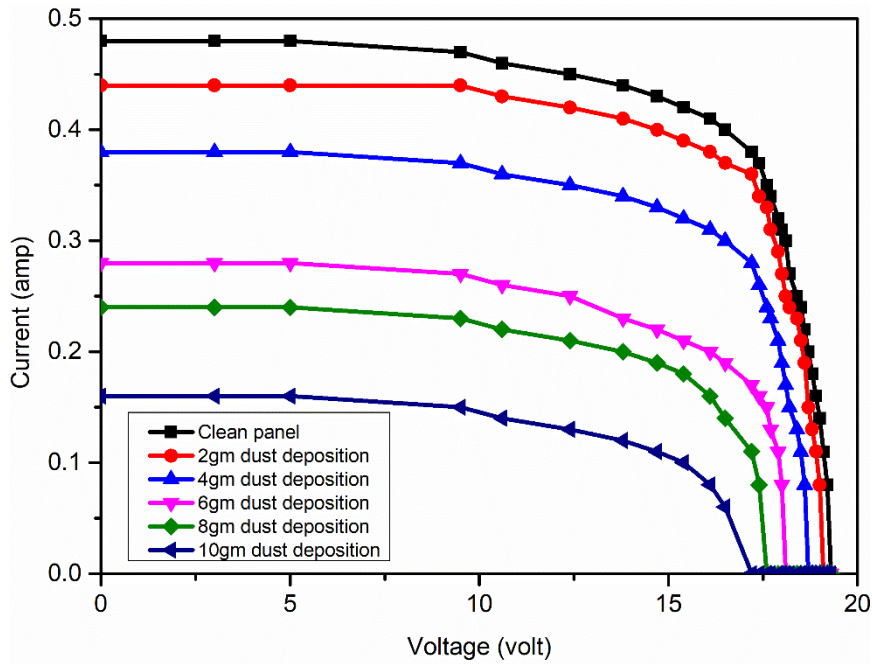


Figure 6.1 I-V characteristics of PV panel under different dust mass deposition
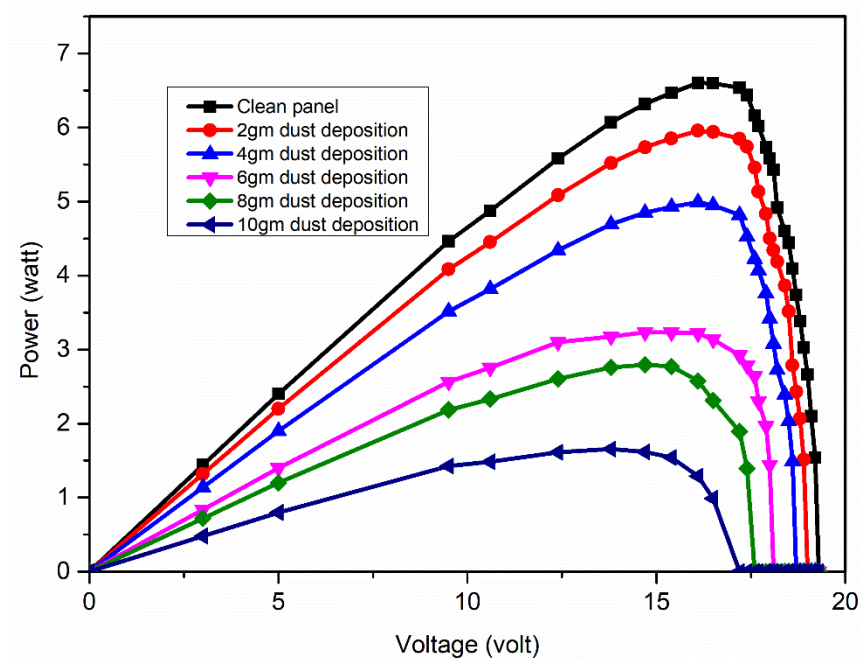
Figure 6.2 P-V characteristics of PV panel under different dust mass deposition

As depicted in Figure 6.1 and Figure 6.2, the open circuit voltage of PV panel is less affected, whereas short circuit current and maximum power output are significantly reduced with increase in the amount dust deposition on the panel surface. The reduction in $I_{sc}$ and $P_{max}$ for 10 gm of dust (67.15 gm/m$^2$ dust density) deposition are respectively 66.67% and 74.84%, whereas the reduction in $V_{oc}$ is observed as 10.88%, which is quite low compared to $I_{sc}$ and $P_{max}$. The obtained results show that the change in open circuit voltage is not affected much by the dust deposition until the layer of dust blocks the sunlight falling on the panel surface completely.

## 6.2 EFFECT OF DUST PARTICLES SIZE ON PANEL PERFORMANCE

### 6.2.1 Methodology

To study the effect of dust particles size on the PV panel performance, laboratory study was conducted using different size of iron ore dust particles as given in Table 6.14.

**Table 6.14** Different size of dust particle

| Sl. No. | Particle Size | Designated as |
|---------|---------------|---------------|
| 1 | Between 600μ to < 850μ | $T_1$ |
| 2 | Between 300μ to < 600μ | $T_2$ |
| 3 | Between 150μ to < 300μ | $T_3$ |
| 4 | Between 75μ to <150μ | $T_4$ |
| 5 | less than 75μ | $T_5$ |

The dusts were distributed over the panel surface in a mass of 5 gm (33.58 gm/m$^2$ dust density) and the electrical responses of the panel were recorded (by measuring output current and voltage of PV panel) under the constant solar radiation of 750 W/m$^2$.

**6.2.2 Results and Discussion**

The electrical responses, such as output current, voltage and power which were measured for five different range of dust particle are given in Table 6.15 to Table 6.20 in Appendix III. The performance of solar panel, under different dust particle size (i.e., $T_1$, $T_2$, $T_3$, $T_4$ and $T_5$) were compared with the performance of a clean panel (which is designated as $T_0$), which was measured under same set of conditions (i.e., same solar radiation). The electrical characteristics of PV panel, such as I-V and P-V characteristics, for all size cases (i.e., $T_1$, $T_2$, $T_3$, $T_4$ and $T_5$) along with the clean panel were plotted, which are given in Figure 6.3 and Figure 6.4. From Figure 6.3, the percentage reduction in short circuit current of the panel was calculated using equation (6.1) for the distribution of different size of dust particles, which are given in Table 6.21.

$$\text{RSCC} = \frac{I_{scclean} - I_{scdusty}}{I_{scclean}} \times 100 \ (\%) \qquad\qquad (6.1)$$

where, RSCC= Reduction in short circuit current (%),

$I_{sc\ clean}$ = Short circuit current of clean panel, and

$I_{sc\ dusty}$ = Short circuit current of dusty panel (amp).

Figure 6.5 shows the variation in short circuit current due to distribution of different size of dust particles on the panel surface. As observed from Figure 6.3, Figure 6.4 and Figure 6.5, the smaller size dust particles show a higher reduction in the panel performance when compared to larger size particles. This is because the smaller dust particles are denser than the larger dust particles (Al-Hasan 1998). Moreover, in the

case of smaller size dust particles the contact force between them are higher compared to larger dust particles (Ranade 1987). Therefore, the degradation in the performance of PV panel is severe in case of smaller size dust particles.
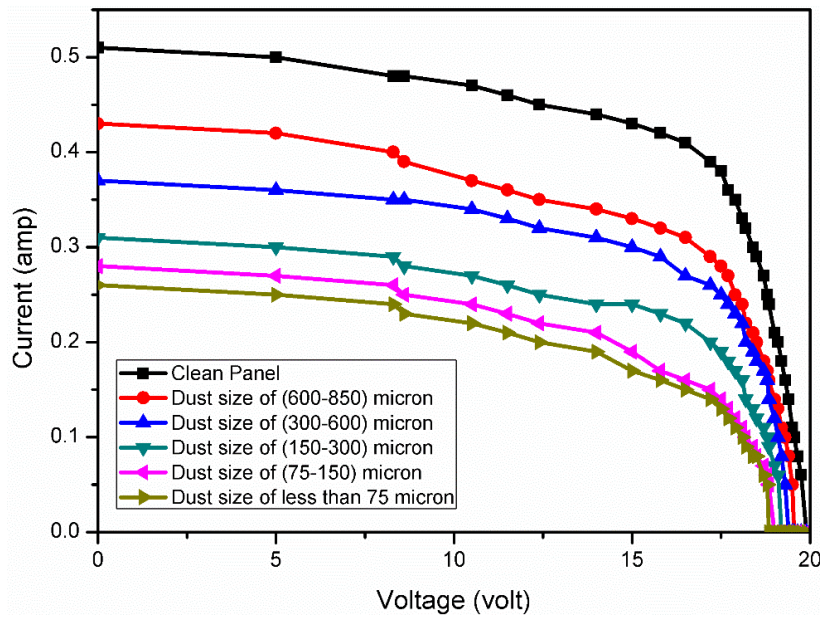


Figure 6.3 I-V characteristics of PV panel on distribution of different size of dust particles
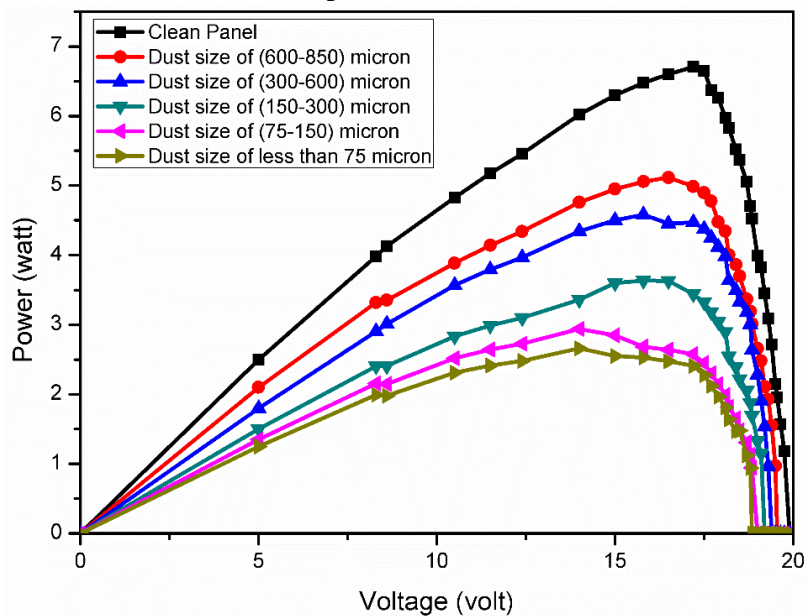


Figure 6.4 P-V characteristics of PV panel on distribution of different size of dust particles

**Table 6.21** Reduction in short circuit current due to deposition of different size of dust particles

| Dust particle size (micron) | Short circuit current (amp) | Reduction in short circuit current $\frac{I_{SCclean} - I_{SCdusty}}{I_{SCclean}} \times 100$ (%) |
|---|---|---|
| $T_0$ | 0.50 | NA |
| $T_1$ | 0.43 | 15.68627 |
| $T_2$ | 0.37 | 27.45098 |
| $T_3$ | 0.31 | 39.21569 |
| $T_4$ | 0.28 | 45.09804 |
| $T_5$ | 0.26 | 49.01961 |
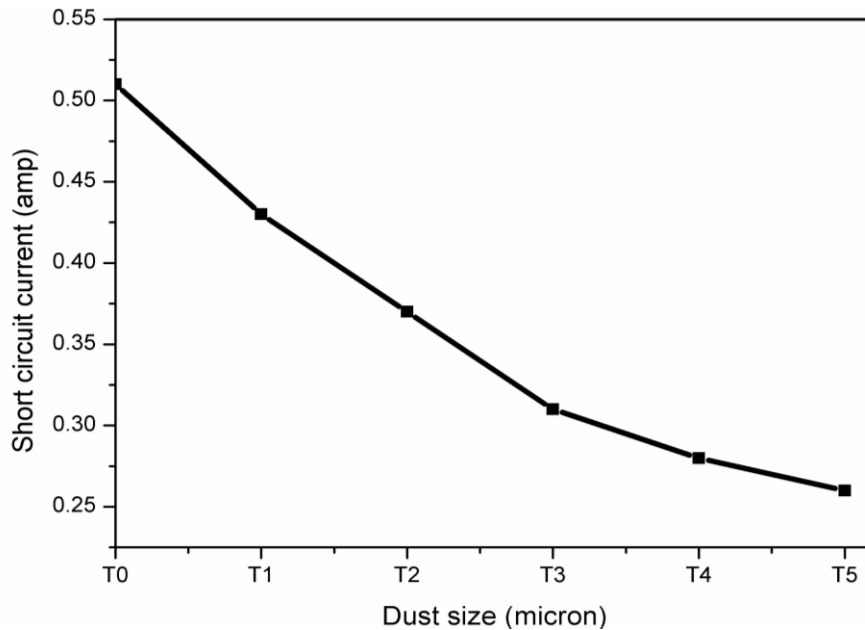


Figure 6.5 Variation in short circuit current due to distribution of different size of dust particles on the PV panel surface

Based on the developed mathematical relation as given in the Section 4.2 of Chapter 4 between short circuit and solar radiation falling on the panel surface, the solar radiation ($G_s$) reaching the PV panel surface for five-different size of dust particles, under consideration, was calculated and is given in Table 6.22. The measured solar radiation reaching a clean panel surface was 750 W/m$^2$ as mentioned earlier and the computed solar radiation reaching a clean panel surface as per developed mathematical relation is 800 W/m$^2$. The relative error between measured and computed solar radiation is 6.66%.

The computed solar radiation of a clean panel (i.e., 800 W/m$^2$) was taken as a reference solar radiation (G$_r$) and the reduction in solar radiation due to deposition of five different size of dust particles was calculated, which is also given in Table 6.22.

**Table 6.22** Variation in short circuit current with dust particles size

| Dust particle size (micron) | Simulated solar radiation Gs (W/m$^2$) | Reduction solar radiation= $\frac{G_r - G_s}{G_r} \times 100$ (%) |
|---|---|---|
| 600μ to < 850μ (T$_1$) | 702.85 | 12.14 |
| 300μ to < 600μ (T$_2$) | 617.14 | 22.85 |
| 150μ to < 300μ (T$_3$) | 531.43 | 33.57 |
| 75μ to <150μ(T$_4$) | 488.57 | 38.92 |
| Less than75μ (T$_5$) | 460.00 | 42.50 |

From the Table 6.22, it is evident that the smaller size dust particles block the solar radiation more prominently compared to larger size dust particles, though the mass distribution is the same. There is a reduction of almost 40% in solar radiation with the decrease in size of dust particles from T$_1$ to T$_5$ (with a relative error of 6.66%). This may be due to the smaller dust particles are denser than the larger dust particles (Al-Hasan 1998).

## 6.3 EFFECT OF DUST POLLUTANT TYPES ON PANEL PERFORMANCE
### 6.3.1 Methodology

To study the effect of dust pollutants types on the performance of PV panel, three different types of dust pollutants, namely red soil dust, limestone dust and iron ore dust of size less than 75 μ were used. The three types of dust pollutants used for the study are shown in Figure 6.6. The dust was distributed on the panel surface with the help of strainer and its electrical responses were measured for a constant solar radiation of 567 W/m$^2$. For each dust type, the measurements were taken for three different quantity of dust distributions, i.e., 5 gm, 8 gm and 11 gm in mass. This procedure was repeated for all three types of dusts. The electrical responses were also recorded for a clean panel.

(a) Limestone             (b) Red soil             (c) Iron ore

Figure 6.6 Three types of dust pollutants used in the experiment

### 6.3.2 Results and Discussion

The electrical responses of all the ten trials (three each for three type of dusts and one for a clean panel) are given in Table 6.23 to Table 6.32 in Appendix III. The electrical characteristics (I-V and P-V) of PV panel for all the three dust pollutants are shown in Figure 6.7, Figure 6.8, Figure 6.9, Figure 6.10, Figure 6.11 and Figure 6.12 which were plotted based on the data given in Table 6.23 to Table 6.32 in Appendix III due to deposition of dust. The reduction in short circuit current ($I_{sc}$), open circuit voltage ($V_{oc}$) and maximum power output ($P_{max}$) respectively were calculated (when compared to a clean panel) for all the three types of dusts, such as iron ore, limestone and red soil. which are presented in Table 6.33, Table 6.34 and Table 6.35 respectively and indicate a significant reduction in short circuit current and maximum power output, whereas the reduction is meagre in case of open circuit voltage, for all the three types of dust pollutants.

The reduction in maximum power output of PV panel due to deposition of iron ore dust, limestone dust and red soil dust is presented in Figure 6.13. As depicted in Figure 6.13, the reduction in maximum power output is higher with the deposition of red soil dust, which is followed by limestone dust and iron ore dust. In the present study it was observed that with the 11gm (73.87 gm/m$^2$ dust density) of dust deposition on the panel

surface, the reduction in maximum power output was high with red soil dust deposition (reduction was 61.20%) which is followed by lime stone dust (reduction was 51.60%) and iron ore dust (reduction was 41.90%). This trend in reduction of maximum power output demonstrates that the performance degradation of PV panel not only depends on the mass of dust but it is also influenced by the type of dust. This variation in degradation of performance of PV panel among different types of dust pollutants may be due to the discrepancy in their reflectance or transmittance of dusts.
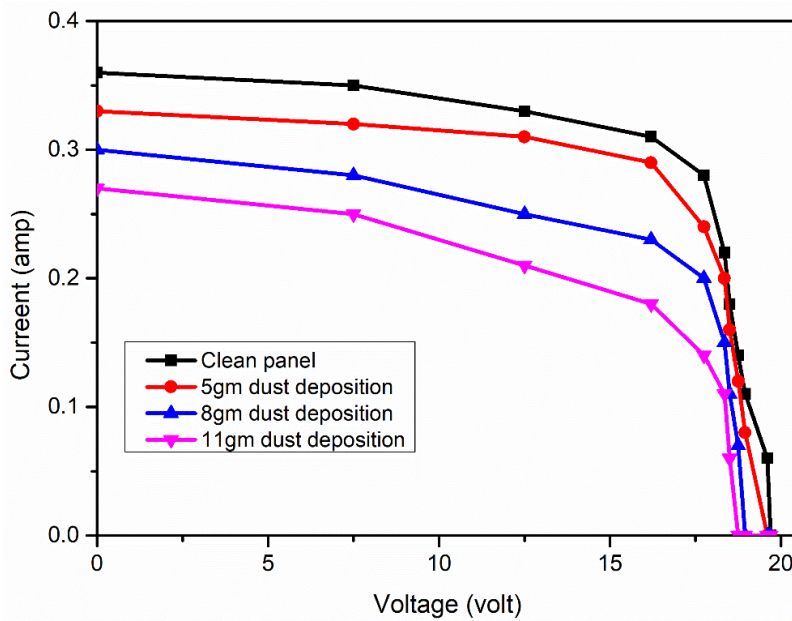


Figure 6.7 I-V characteristics of the PV panel due to deposition of iron ore dust
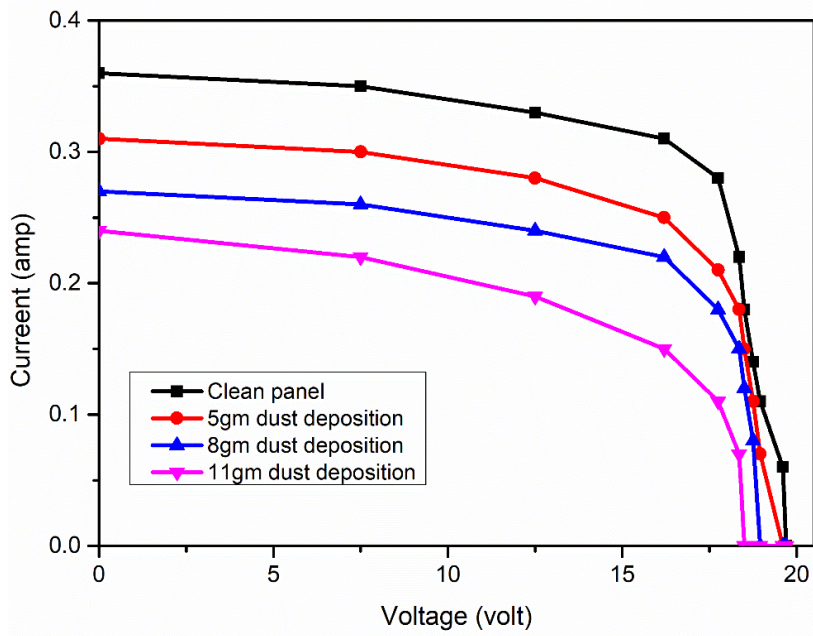


Figure 6.8 I-V characteristics of the PV panel due to deposition of limestone dust
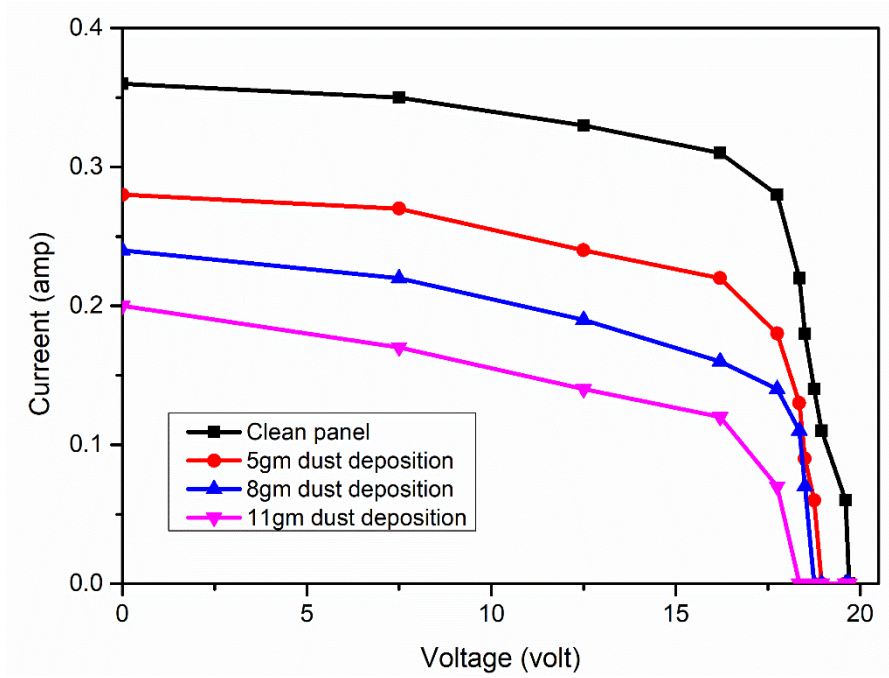
Figure 6.9 I-V characteristics of the PV panel due to deposition of red soil dust
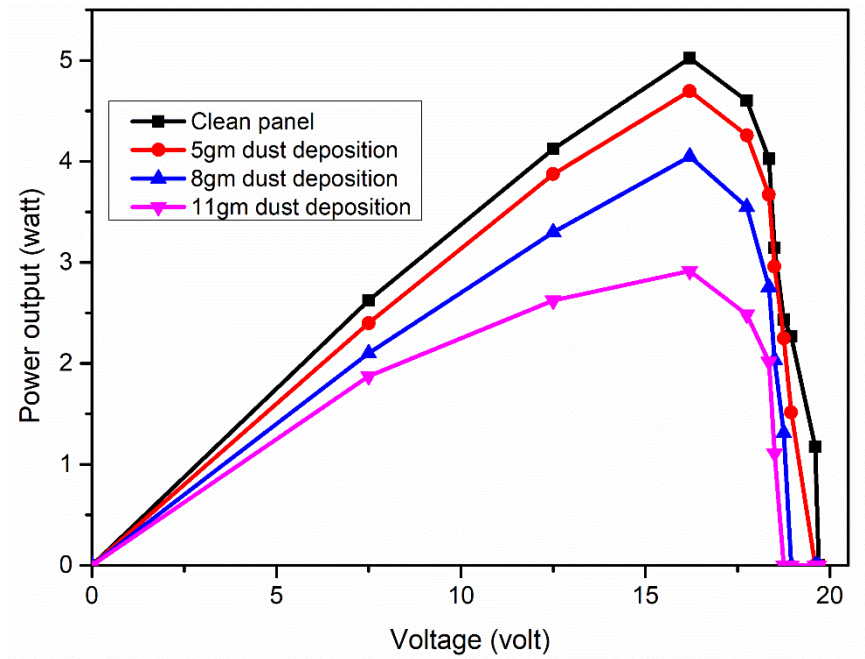


Figure 6.10 P-V characteristics of the PV panel due to deposition of iron ore dust
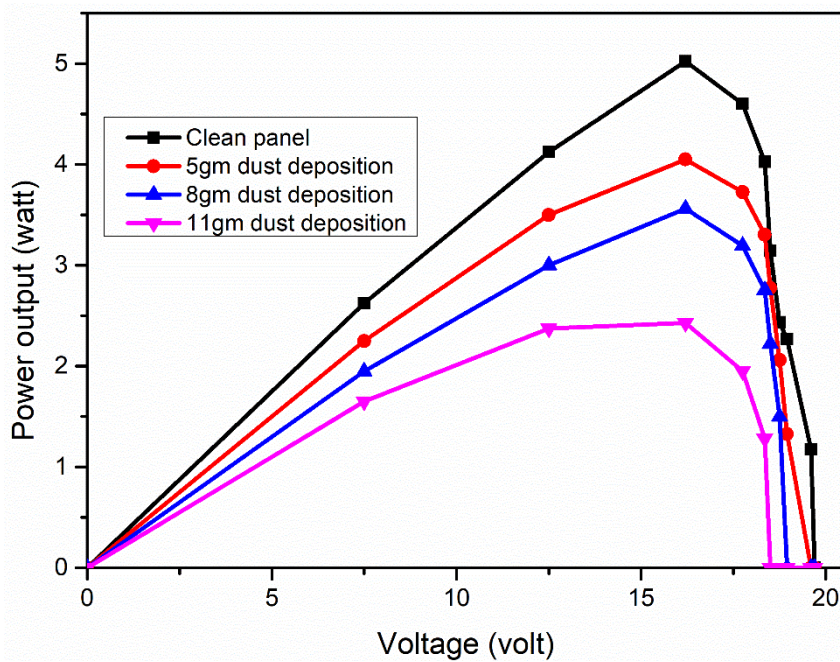
Figure 6.11 P-V characteristics of the PV panel due to deposition of limestone dust
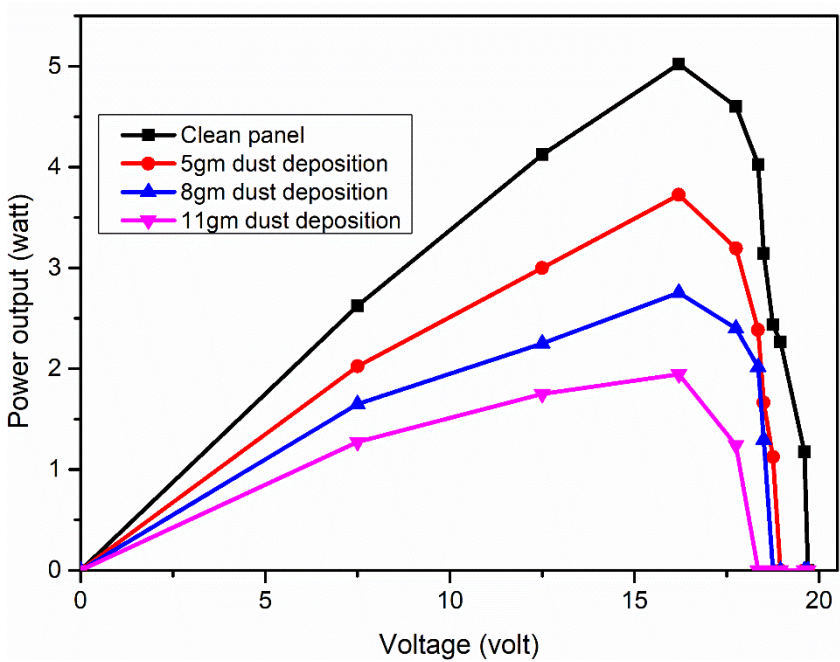


Figure 6.12 P-V characteristics of the PV panel due to deposition of red soil dust

**Table 6.33** Effect of iron ore dust on the PV panel performance

| Mass deposition (gm) | Reduction in short circuit current (%) | Reduction in open circuit voltage (%) | Reduction in maximum power output (%) |
|---|---|---|---|
| 5 | 8.30 | 2.80 | 6.50 |
| 8 | 16.70 | 3.80 | 19.40 |
| 11 | 25.00 | 4.80 | 41.90 |

**Table 6.34** Effect of lime stone dust on the PV panel performance

| Mass deposition (gm) | Reduction in short circuit current (%) | Reduction in open circuit voltage (%) | Reduction in maximum power output (%) |
|---|---|---|---|
| 5 | 13.80 | 3.00 | 19.30 |
| 8 | 25.00 | 4.00 | 29.00 |
| 11 | 33.30 | 6.00 | 51.60 |

**Table 6.35** Effect of red soil dust on the PV panel performance

| Mass deposition (gm) | Reduction in short circuit current (%) | Reduction in open circuit voltage (%) | Reduction in maximum power output (%) |
|---|---|---|---|
| 5 | 22.20 | 3.80 | 25.80 |
| 8 | 33.30 | 4.80 | 45.10 |
| 11 | 44.40 | 6.80 | 61.20 |
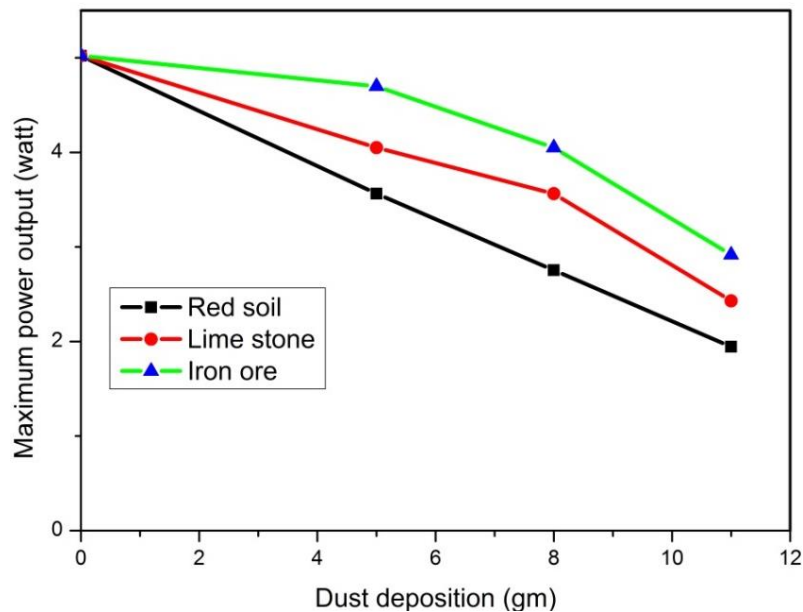


Figure 6.13 Reduction in maximum power output of PV panel w.r.t three type dust deposition

## 6. 4 EFFECT OF DUST ON PV PANEL SURFACE TEMPERATURE

### 6.4.1 Methodology

To study the temperature difference between clean and dusty panel, under the same environmental conditions, a laboratory study was performed using two identical 20 W polycrystalline PV panels. Both the panels were subjected to a constant solar radiation of 1024 W/m$^2$ which was generated artificially, as discussed in Section 4.1 of Chapter 4. This artificial solar radiation was generated using a set of solar simulators (incandescent bulbs). On one panel iron ore dust of 3gm in mass was spread with the help of a strainer which was considered as a dusty panel and the other was kept free from iron ore dust i.e., clean. Thereafter, at every one-minute interval the surface temperatures of both the panels (i.e., clean and dusty) were recorded, using pyrometer, till it reached maximum permissible surface temperature (i.e., 83°C). This procedure was repeated for another two trials i.e. by distributing 5gm and 8gm dust on the dusty panel. The measured values of surface temperature of PV panels for all the four conditions are given in Table 6.36.

**Table 6.36** Measured values of PV panel surface temperatures

| Time (minute) | PV Panel Surface Temperature (°C) | | | |
|---|---|---|---|---|
| | **Clean Panel** | **3gm of dust deposition** | **5gm of dust deposition** | **8gm of dust deposition** |
| 1 | 35 | 35 | 36 | 36.50 |
| 2 | 42 | 43 | 44 | 45 |
| 3 | 47 | 48 | 49 | 50 |
| 4 | 50 | 51 | 53 | 55 |
| 5 | 52 | 54 | 56 | 59 |
| 6 | 55 | 57 | 59 | 64 |
| 7 | 57 | 61 | 62 | 69 |
| 8 | 58 | 63 | 65 | 71 |
| 9 | 60 | 66 | 68 | 74 |
| 10 | 62 | 68 | 70 | 77 |
| 11 | 65 | 70 | 74 | 80 |
| 12 | 66 | 72 | 76 | 84 |

### 6.4.2 Results and Discussion

The recorded surface temperature of clean and dusty (i.e., with 3 gm, 5 gm and 8 gm deposition) PV panels with respect to time were plotted, which is presented in Figure 6.14. As shown in Figure 6.14, the surface temperature of dusty panel is higher than the

clean panel at every measured interval. This is mainly due to the accumulated dust particles on the panel surface which covers the cells of the panel completely or partially thus promotes the reverse biasing of the shaded cell. The reverse biasing of shaded cells enhances the surface temperature of PV panel under dusty condition (Zegaoui et al. 2011). The increase in surface temperature of PV panel due to increase in mass of dust deposition, as illustrated in Figure 6.14, indicates that the surface temperature of PV panel also depends upon the mass of dust deposition. As the amount dust deposition increases the surface temperature of PV panel also increases under the same working condition.
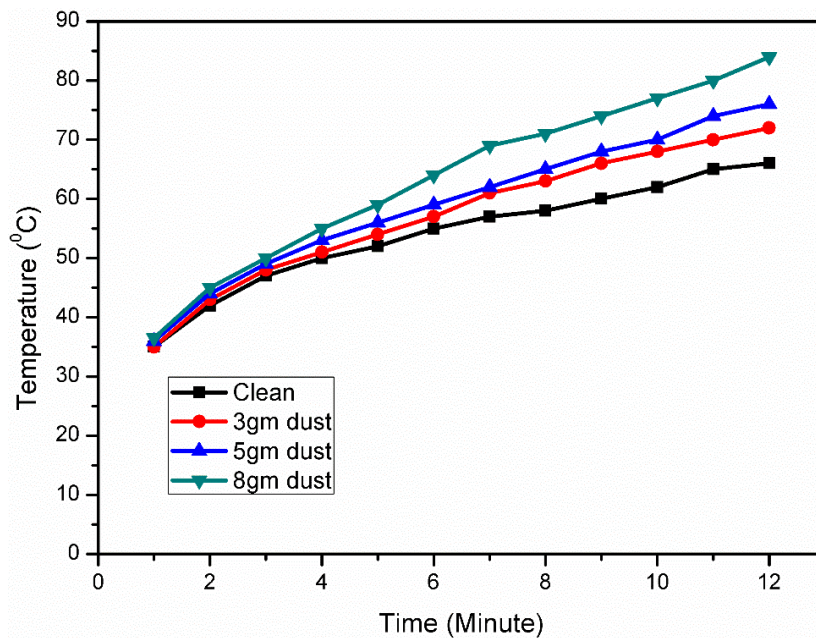


Figure 6.14 Temperature of clean and dusty PV panels

## 6. 5 FIELD AND LABORATORY STUDY AND ITS COMPARISON

The effect of dust deposition on PV panel performance was studied in the field (under natural environmental condition) as well as in the laboratory (under controlled environmental condition). While performing the experiment in the laboratory, as far as possible, due care was taken to replicate the field conditions. The results obtained from the field study were verified with the results obtained from the laboratory studies (with the help of simulated laboratory test set-up). This study helps to draw a scheme for systematic cleaning of panel surface in a dusty environment.

### 6.5.1 Field Study - Perusal of Selected Site

The field study was carried out during the month of January, 2017 in a surface mine in Chitradurga District of Karnataka State, India. This mine is situated at the coordinates of 14° 8' 55.4928" N, 76° 40' 1.1424" E. The site endures the good solar radiation profile. During a sunny day the peak solar radiation of 1182 W/m$^2$ was recorded. Due to high solar radiation, good atmospheric temperature (generally 25ºC to 37ºC) and good wind profile (peak value of 4 m/s), this site could be a good choice for the installation of PV panel.

### 6.5.1.1 Field measurements

To study the effect of dust deposition on the panel surface, two identical 20 W polycrystalline panels were placed in a mine, side by side, which were directed towards the south. The average solar radiation received by these panels was recorded as 1120 W/m$^2$. Among these two panels, one panel was kept uncleaned (which was considered as dusty panel) and other one was cleaned regularly (i.e., every day in the morning, which was considered as clean panel). To measure the mass of dust deposition on the panel surface a filter paper of size equal to that of panel surface, of known weight, was kept beside the clean panel. This filter paper was kept flat and steady. Every day in the morning the filter paper was removed carefully and weighed to know the mass of the deposited dust. Table 6.42 gives the dust deposition on the panel surface for all the five days.

The electrical parameters (i.e., power output, current and voltage) of both the panels were measured for five days (which are given in Table 6.37 to 6.41 in Appendix III) using 320 Ω rheostat and two digital multi-meters (one is used as ammeter and the other one as voltmeter of the circuit).

**Table 6.42** Dust deposition on panel surface

| Day | Day to day dust deposition (gm) | Total dust deposition (gm) |
|---|---|---|
| First Day | 2.58 | 2.58 |
| Second Day | 2.54 | 5.12 |
| Third Day | 2.57 | 7.69 |
| Fourth Day | 2.57 | 10.26 |
| Fifth Day | 2.60 | 12.86 |

**6.5.1.2 Results and discussion**

The electrical responses of a clean and a dusty panel were recorded for five days. The obtained electrical parameters of both the panels were compared to analyse the performance of a panel under two different operating conditions (i.e., clean and dusty environment). Table 6.43 gives the measured electrical responses of both the panels for five days. Based on the readings as indicated in Table 6.43, the reduction in electrical responses of PV panel due to dust deposition were calculated and is presented in Table 6.44.

The performance of a PV panel in a dusty environment can be defined by the term normalised power output (Rosyid 2016). The normalised power output of a PV panel in the dusty environment indicates the performance of a dust panel w.r.t. a clean panel, which is calculated using equation (6.2). The higher value of normalised power output represents the better operation of the panel in dusty environment. The normalised power output of panels was calculated, which is also given in Table 6.44.

$$P_N = \frac{P_d}{P_c} \times 100 \qquad\qquad (6.2)$$

where,

$P_N$= Normalised power output (%),

$P_d$= Power output of dusty panel (watt), and

$P_c$= Power output of clean panel (watt).

As observed from Table 6.44, the reduction in short circuit current ($I_{sc}$) and maximum power output ($P_{max}$) of dusty panel are respectively, 39.58% and 43.18% compared to clean panel, after five days of exposure. Similarly, the reduction in open circuit voltage ($V_{oc}$) of dusty panel is up to 4.35% after five days of its exposure. This emphasizes that the reduction in open circuit voltage due to dust deposition is meagre when compared to short circuit current and power output. Figure 6.15 shows the comparison of I-V characteristics of clean and dusty panels for all the five days of its exposure for outdoor condition. Based on Table 6.44 the reduction in the maximum power output ($P_{max}$) of a PV panel is plotted w.r.t the number of exposure days, which is shown in Figure 6.16.

As depicted in Figure 6.16, the maximum power output of a PV panel reduces with increase in exposure time, under dusty environment. The graphical representation of normalised power output w.r.t number of days of exposure of the panel for the outside environment is presented in Figure 6.17.

**Table 6.43** Measured electrical parameters of clean and dusty panels

| Day | Clean | | | Dusty | | |
|-----|-------|---|---|-------|---|---|
| | Open circuit voltage (volt) | Short circuit current (amp) | Maximum power output (watt) | Open circuit voltage (volt) | Short circuit current (amp) | Maximum power output (watt) |
| 1 | 20.62 | 0.65 | 8.82 | 20.37 | 0.53 | 6.84 |
| 2 | 20.51 | 0.58 | 7.60 | 20.06 | 0.45 | 5.32 |
| 3 | 20.57 | 0.60 | 8.51 | 19.80 | 0.43 | 5.47 |
| 4 | 20.60 | 0.80 | 10.94 | 19.77 | 0.53 | 6.53 |
| 5 | 20.65 | 0.96 | 13.38 | 19.75 | 0.58 | 7.60 |

**Table 6.44** Reduction in electrical responses of a dusty panel compared to a clean panel

| Day | Reduction in open circuit voltage (%) | Reduction in short circuit current (%) | Reduction in maximum power output (%) | Normalised power output (%) | Reduction in normalised power output (%) | Daily reduction in normalised power output (%) |
|-----|------|------|------|------|------|------|
| 1 | 1.21 | 18.46 | 22.41 | 77.55 | 22.45 | 22.45 |
| 2 | 2.10 | 22.41 | 30.00 | 70.00 | 30.00 | 7.55 |
| 3 | 3.74 | 28.33 | 35.71 | 64.27 | 35.73 | 5.73 |
| 4 | 4.02 | 33.75 | 40.28 | 59.68 | 40.32 | 4.59 |
| 5 | 4.35 | 39.58 | 43.18 | 56.80 | 43.20 | 2.88 |

Figure 6.17 represents the performance degradation of a PV panel under the dusty environment. As depicted in Figure 6.17, initially the reduction in the panel performance is predominant, whereas it reduces gradually with the exposure time. There is a sudden decrease in the panel performance on the first day (i.e., percentage decrease on first day was 22.45% which is quite high when compared to succeeding days), which is evidenced by the steep gradient of the curve. The gradient of the curve gradually reduces with time, which represents a slowdown in the reduction of panel performance. This is mainly due to the overlapping of dust particles rather than settling on the panel surface.
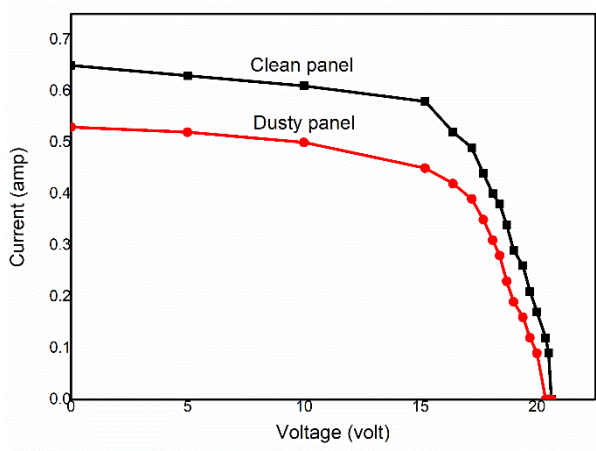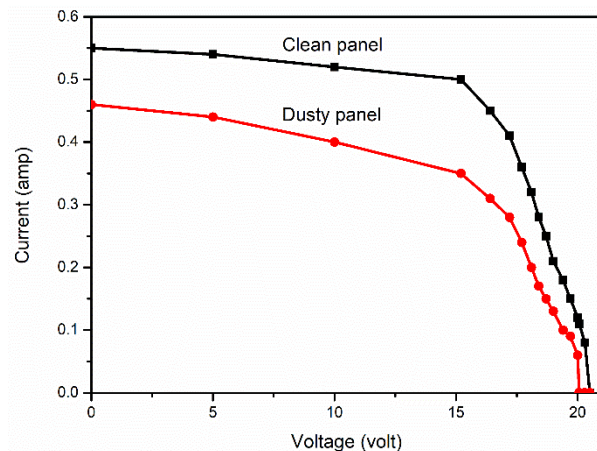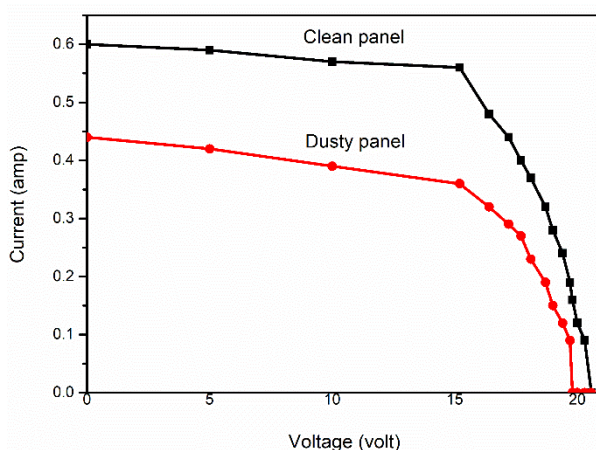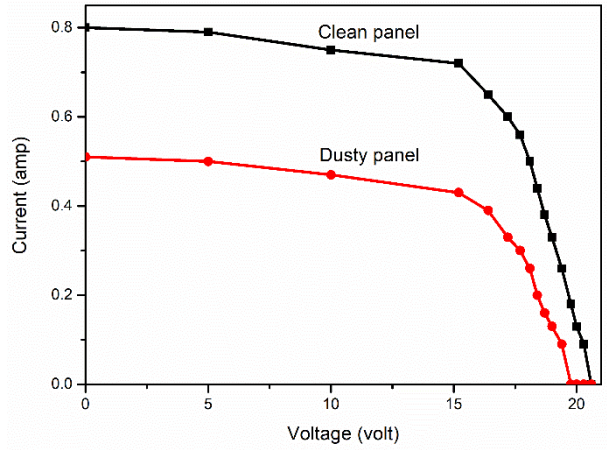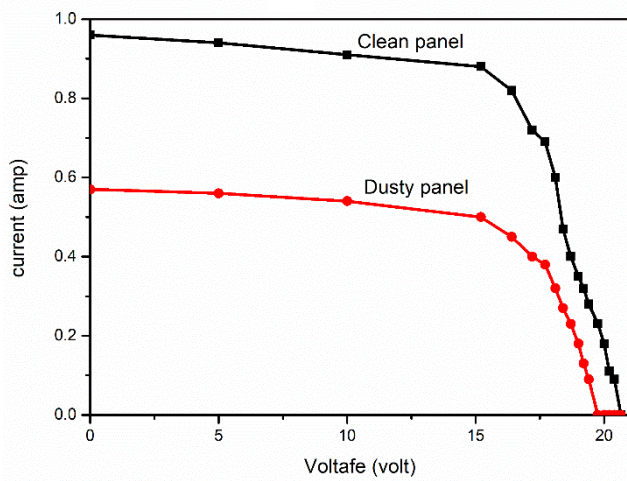
Figure 6.15 Comparison of I-V characteristics of clean and dusty panel in outdoor test condition (a) after one day of exposure (b) after two daysof exposure (c) after three days of exposure (d) after four days of exposure (e) after five days of exposure
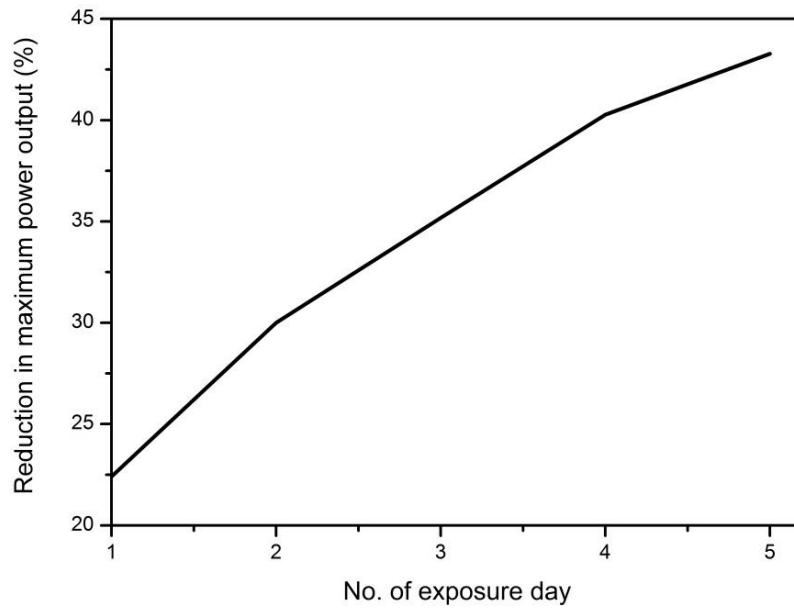
Figure 6.16 Reduction in maximum power output of PV panel w.r.t number of days of exposure
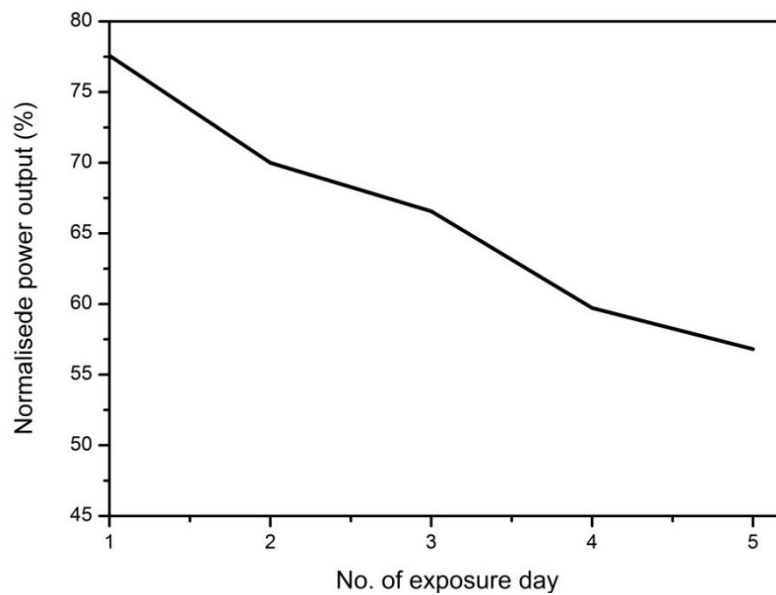


Figure 6.17 Normalised power output of PV panel w.r.t number of days of exposure

## 6.5.2 Laboratory Study - Methodology

In order to perform laboratory studies airborne dust particles were collected from the mines. A polycrystalline 20 W PV panel was used for this study and the solar radiation was maintained at 1082 W/m$^2$. The airborne dust which was collected from the mines was spread over the panel surface and electrical responses of the panel were measured

for five conditions, i.e., with 3 gm, 5 gm, 8 gm. 11 gm and 13 gm of dust deposition. The amount of dust deposition for this study was considered based on the field observation (w.r.t Table 6.42) so as to maintain a glaring comparison between the field and laboratory studies. The electrical responses of a PV panel were recorded by varying amount of dust deposition on the panel surface (based on filed condition as shown in Table 6.42), the results of which are shown in Table 6.45 to Table 6.50 in Appendix III. Table 6.51 gives the measured electrical respnoses of PV panel under varying dust deposition conditions.

### 6.5.2.1 Results and discussion

Based on the recorded electrical responses, the electrical characteristics are plotted, which are shown in Figure 6.18 and Figure 6.19. The reduction in $I_{SC}$, $V_{OC}$ and $P_{MAX}$ were calculated from Figure 6.18 and Figure 6.19, which are shown in Table 6.52. As indicated in Table 6.52, the reduction in short circuit current and maximum power output are respectively, 44% and 45.44% with 13gm of dust deposition on the PV panel surface. However, the reduction in open circuit voltage (i.e., 5.20%) was not found much significant when compared to short circuit current and power output of the PV panel. The reduction in panel performance was observed more in laboratory study as compared to field study. This is because of the controlled environmental conditions prevailing in the laboratory (such as solar radiation, wind speed and temperature) and also suniformity in the distribution of dust particles on the panel surface.

**Table 6.51** Electrical parameters of PV panel with varying dust deposition

| Dust deposition (gm) | Short circuit current (amp) | Open circuit voltage (volt) | Maximum power output (watt) |
|---|---|---|---|
| 0 | 0.50 | 19.20 | 7.24 |
| 3 | 0.41 | 18.50 | 5.70 |
| 5 | 0.38 | 18.35 | 5.24 |
| 8 | 0.34 | 18.28 | 4.62 |
| 11 | 0.30 | 18.20 | 4.00 |
| 13 | 0.28 | 18.15 | 3.95 |

**Table 6.52** Reduction in electrical responses of PV panel due to dust deposition

| Dust deposition (gm) | Reduction in short circuit current (%) | Reduction in open circuit voltage (%) | Reduction in maximum power output (%) |
|---|---|---|---|
| 3 | 18 | 3.60 | 21.27 |
| 5 | 24 | 4.43 | 27.62 |
| 8 | 32 | 4.80 | 36.18 |
| 11 | 40 | 5.20 | 44.75 |
| 13 | 44 | 5.47 | 45.44 |
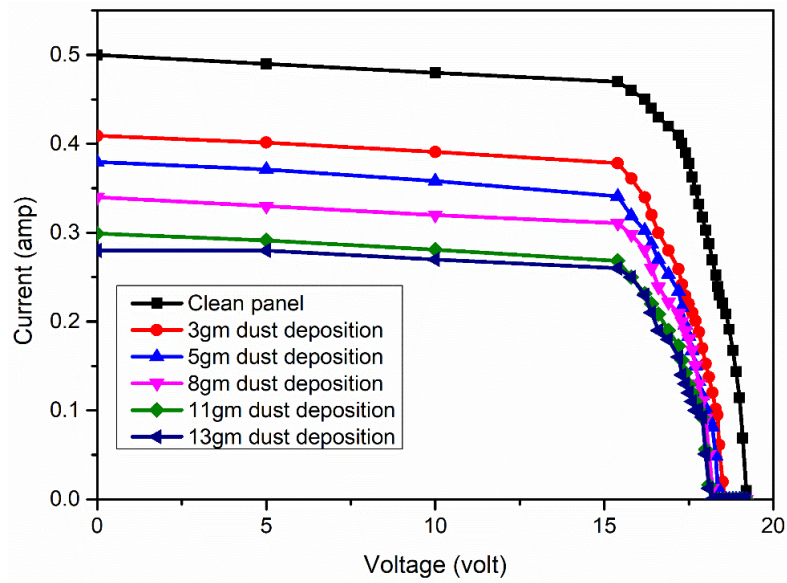


Figure 6.18 I-V characteristics of PV panel under the varying dust deposition condition
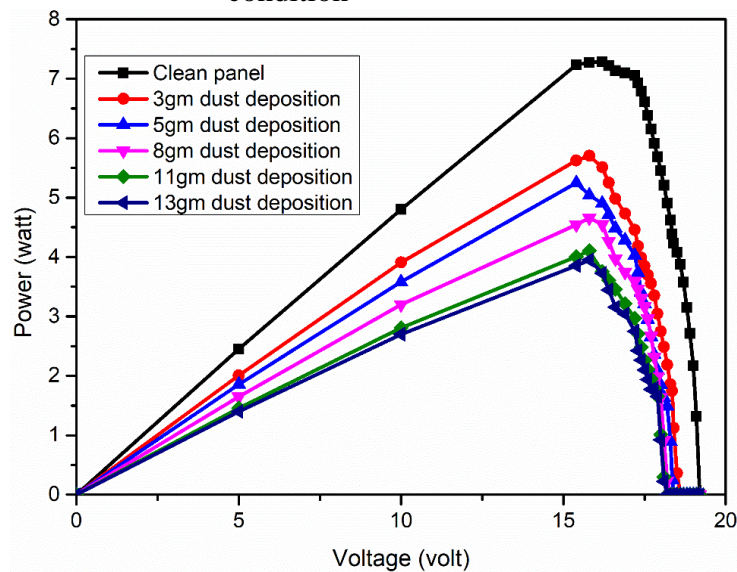


Figure 6.19 P-V characteristics of PV panel under the varying dust deposition condition

## 6.6 PV PANEL SURFACE CLEANING TECHNIQUE

The solar PV panel placed in the outside environment converts the sunlight into electricity. During this process, the performance of the panel gets affected by the accumulation of dust particles on it. Because the dust particles reduce the amount of sunlight reaching the panel surface. Thus, the performance of PV panel reduces, as demonstrated by the field and laboratory studies, as stated in Section 6.5.1.2 and 6.5.2.1. Hence, a cleaning technique for cleaning the panel surface at a regular interval is evolved.

### 6.6.1 Experimental Set-up

Figure 6.20 represents the block diagram of the proposed PV panel surface cleaning technique. This technique consists of a microcontroller, DC motor driver circuit and wiper section. As shown in Figure 6.20, the DC motor gets activation signal from the microcontroller and facilitates the wiper to move up and down on the panel surface to clean the accumulated dust. The schematic circuit diagram of the proposed cleaning technique is presented in Figure 6.21. Figure 6.22 shows the photographic view of the entire set-up. The flow chart of cleaning technique is given in Figure 6.23.
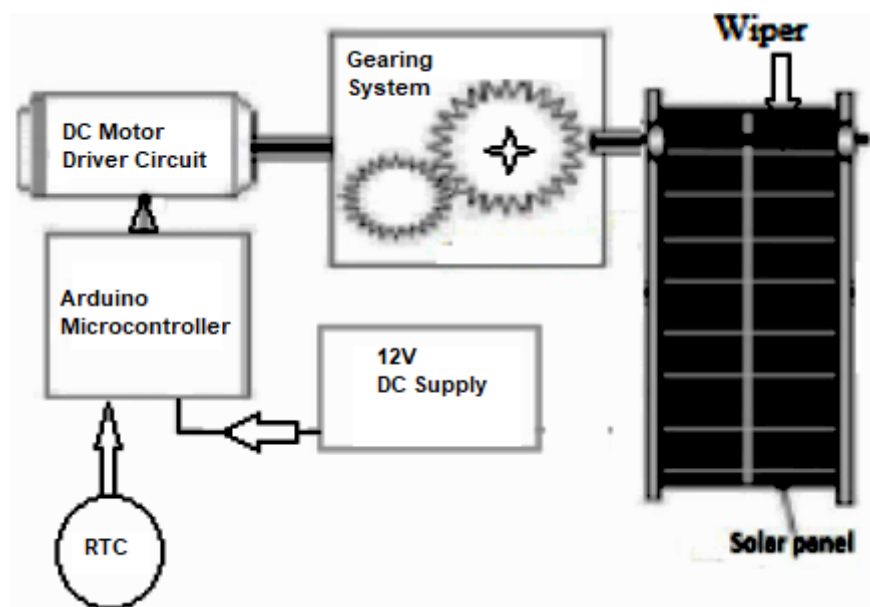


Figure 6.20 Block diagram of PV surface cleaning system
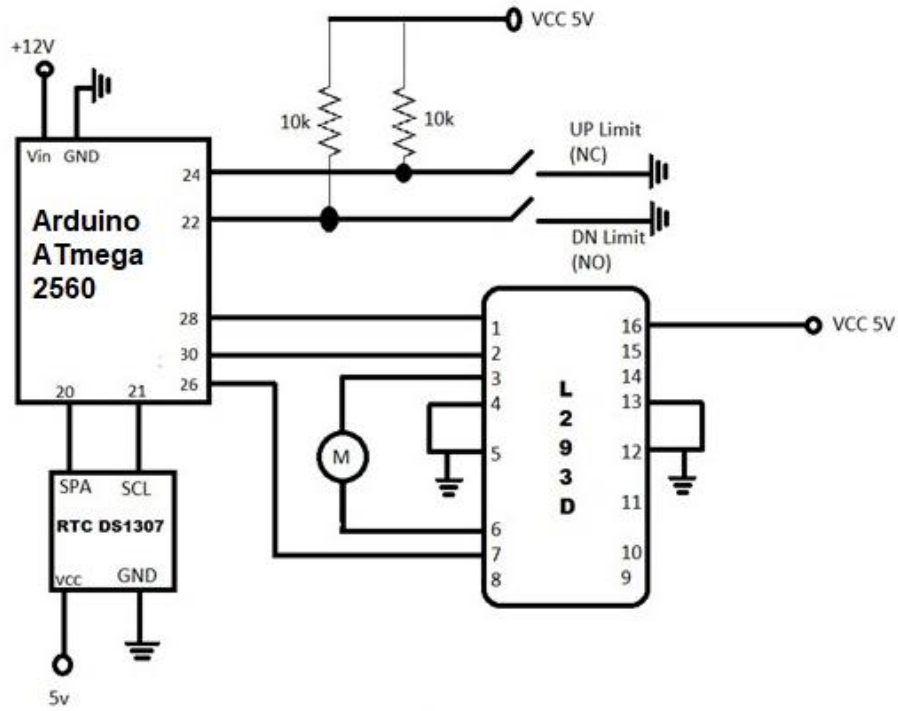
Figure 6.21 Circuit diagram of proposed design
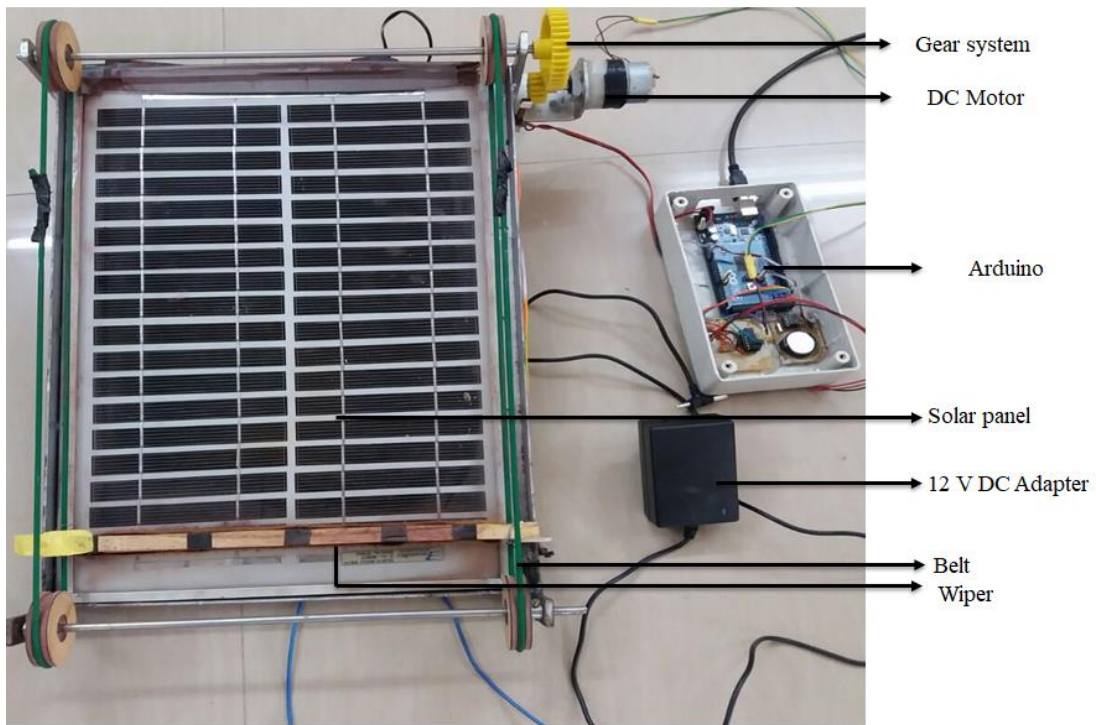


Figure 6.22 Photograph of PV panel surface cleaning system
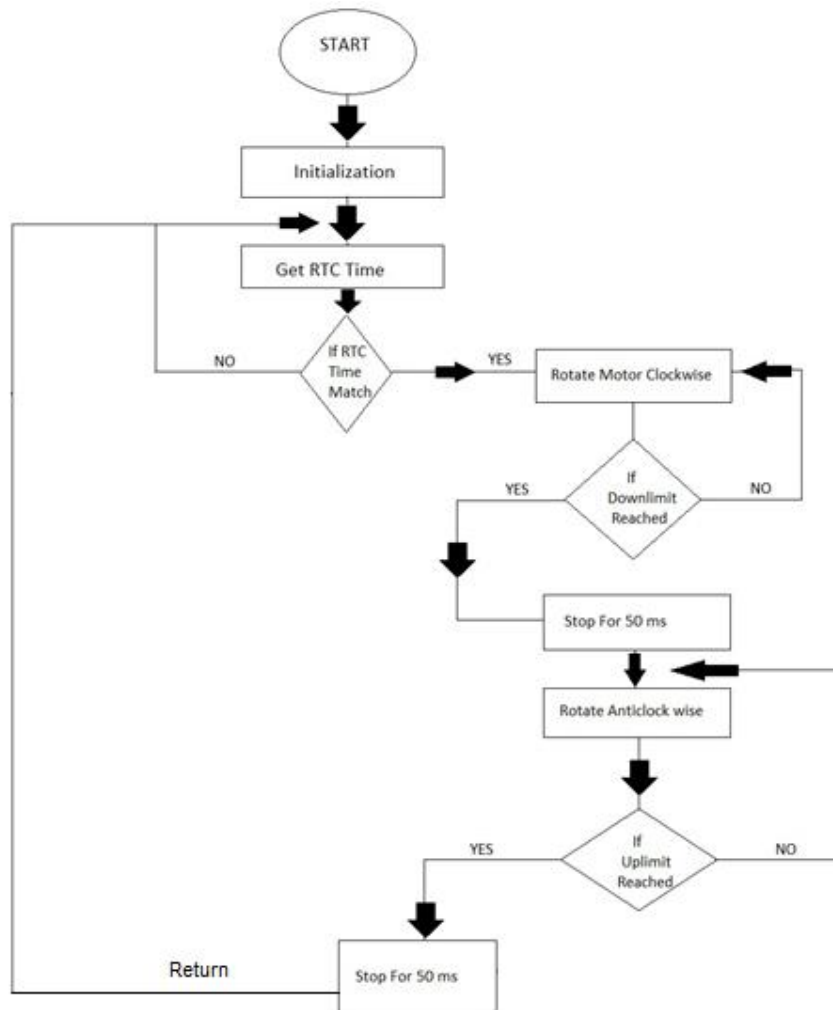
Figure 6.23 Flow chart of dust cleaning system from panel surface

## 6.6.2 Components Used in The Experimental Set-up

The description of the various components which are used in the experimental set-up

of PV panel surface cleaning technique are given in the below sections.

### 6.6.2.1 Solar PV panel

A 10W solar PV panel is used in this study, the technical specifications of which is

presented in Table 6.53, and it is shown in Figure 6.22.

Table 6.53 Technical specifications of 10W PV panel

| Sl. No. | Parameter | Ratings |
|---------|-----------|---------|
| 1 | Open circuit voltage (volt) | 21.50 |
| 2 | Short circuit current (amp) | 0.59 |
| 3 | Maximum voltage (volt) | 17.00 |
| 4 | Maximum current (amp) | 0.56 |
| 5 | Maximum Power (watt) | 10.00 |
| 6 | Fill Factor | 0.75 |

| 7 | Dimension | 340mm $\times$ 280mm |
|---|---|---|

## 6.6.2.2 Arduino microcontroller (Atmega 2560)

Arduino is used as a microcontroller in this study, whose function is to store the desired programme and give the output digital signal to motor driver circuit for controlling the rotation of the motor. The internal structure with pin diagram of Atmega 2560 Arduino is shown in Figure 6.24. It has 54 digital input/output pins (of which 15 can be used as PWM outputs), 16 pins as analog inputs, 4 numbers of Universal Asynchronous Receiver Transmitter (UARTs, i.e., hardware serial ports), a 16 MHz crystal oscillator, a USB connection, a power jack, an in-circuit serial programming (ICSP) header, and a reset button. The description of some pins of Atmega 2560 Arduino with their special functions are discussed in Appendix III. The technical specifications of Atmega 2560 Arduino are given in Table 6.54. The algorithm which was used to operate the cleaning technique is also given in Annexure III.
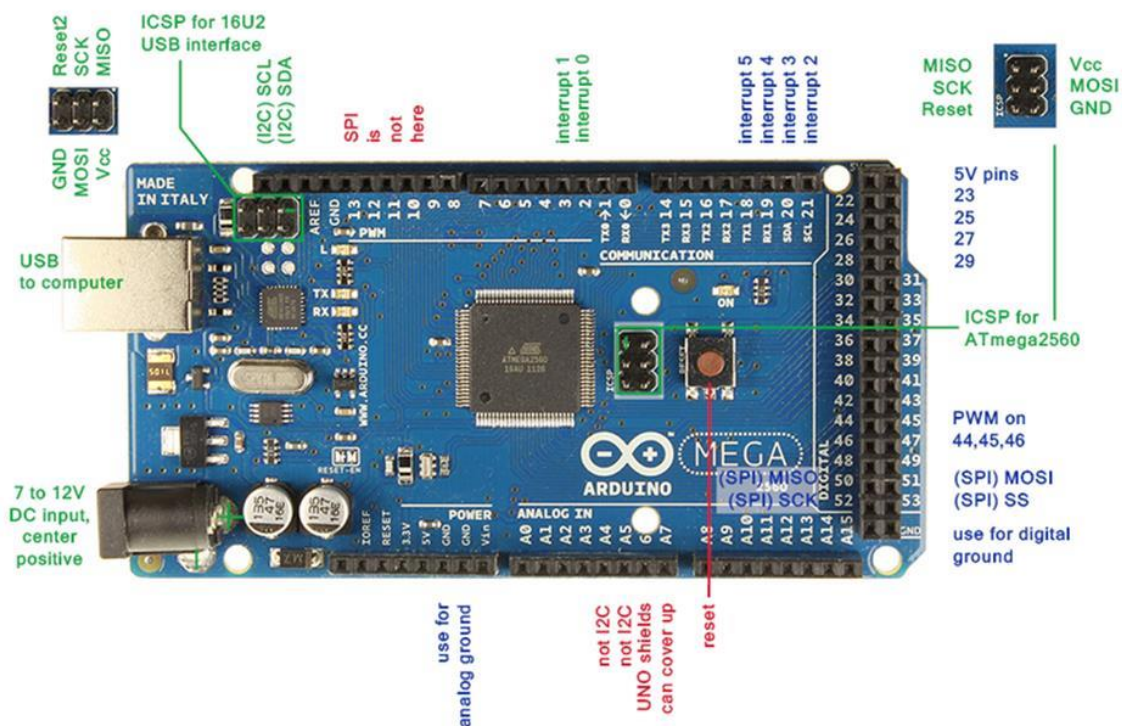


Figure 6.24 Pin diagram of Arduino Atmega 2560

**Table 6.54** Technical specification of Atmega 2560 Arduino

| Sl. No. | Parameters | Specifications |
|---|---|---|
| 1 | Operating Voltage | 5volt |
| 2 | Input Voltage (recommended) | 7-12volt |
| 3 | Minimum Input Voltage | 6volt |
| 4 | Maximum Input Voltage | 20volt |
| 5 | Number of digital I/O Pins | 54 |
| 6 | Number of analog Input Pins | 16 |
| 7 | DC Current per I/O Pin | 40 mA |
| 8 | Flash Memory | 256 KB |
| 9 | SRAM | 8 KB |
| 10 | EEPROM | 4 KB |
| 11 | Clock Speed | 16 MHz |

### 6.6.2.3 Motor Driver Circuit

The integrated circuit (Model: L293D) is used as a motor driver circuit in this set-up, which is a bidirectional motor driver circuit. It is used to drive the motor in upward and downward direction based on the input digital signal received from the Arduino microcontroller. The integrated circuit (IC) and its pin diagram are shown in Figure 6.25 and Figure 6.26. It has 16 pins out of which pin number 1 and 9 are the enable pins, so, when pin number 1 receives 'high' signal/command then all the pins on left side gets activated and similarly, when pin number 9 receives 'high' signal/command then all the pins on right side pins get activated. In Figure 6.26, pin numbers 2,7,15 and 10 are the input pins, 3,6,14 and 11 are the output pins and 4,5,13 and 12 are the ground pins. The pin numbers 8 and 16 are the power supply pins, which have the voltage limit in between 4.5V-36 V.

The input pins on the left side of IC regulates the rotation of motor which is connected to the left side where as the input pins on the right side regulates the rotation of motor connected to the right side. The motors are rotated on the basis of the inputs provided across the input pins as Logic 0 or Logic 1. For rotating the motor in clockwise direction input pins have to be provided with Logic 1 and Logic 0, similarly to rotate the motor in anti-clock wise direction input pins have to be provided with Logic 0 and Logic 1.

In this study motor was connected to the left side of IC through input pin numbers 1 and 7.



Figure 6.25 IC L293D motor driver
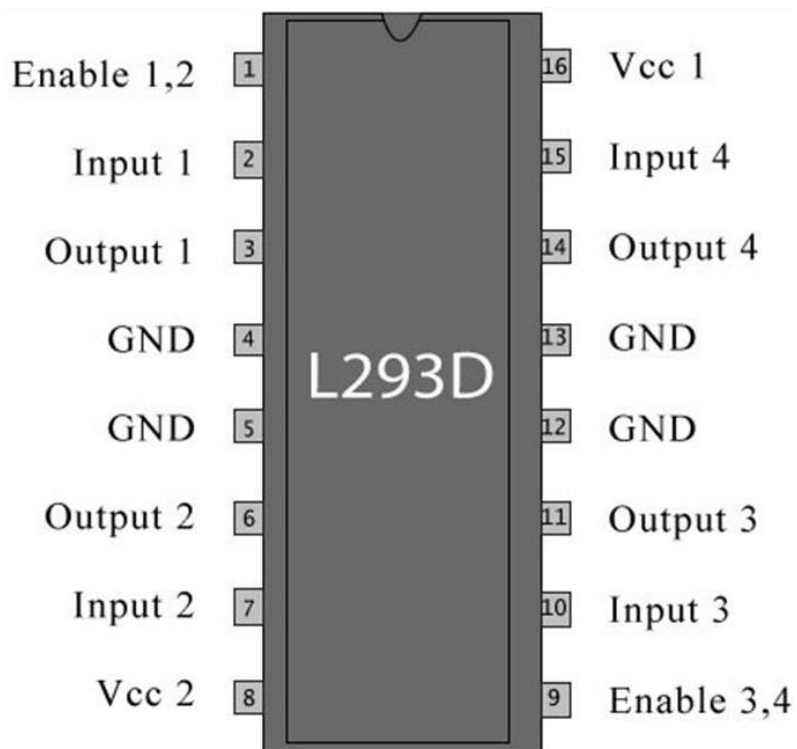


Figure 6.26 Pin diagram of IC L293D

### 6.6.2.4 DC Motor

A direct current motor is an actuator device that converts electrical energy into mechanical energy. In this study, DC gear motor is used to move the wiper up and down on the panel surface in such a way that the wiper cleans the accumulated dust from the panel surface. A photographic view of DC gear motor is illustrated in Figure 6.27 and its technical specifications are given in Table 6.55. The motor was operated at 5 volt and 78 mA load current, and the power consumed was calculated as 0.39 W.
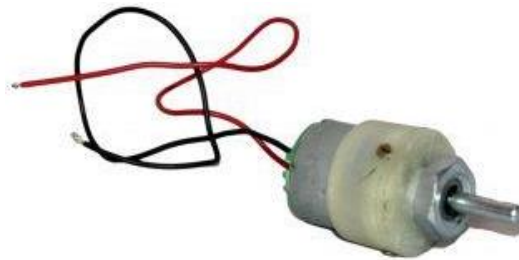


Figure 6.27 DC gear motor

**Table 6.55** Technical specifications of DC motor

| Sl. No. | Parameter | Ratings |
|---|---|---|
| 1 | Voltage limit (volt) | 12.00 |
| 2 | Rotation speed (RPM) | 10.00 |
| 3 | Shaft diameter (mm) | 6.00 |
| 4 | Weight (gm) | 125.00 |
| 5 | Torque (Kg-cm) | 12.00 |
| 6 | No load current (mA) | 60.00 |
| 7 | Full load current (mA) | 300.00 |

### 6.6.2.5 Real Time Clock (RTC)

A Real Time Clock is an electronics device which is used to keep an accurate time to track the current time of programme provider (i.e., personal computer). The photographic view of a real time clock is shown in Figure 6.28.

Figure 6.28 The photograph of real time clock

### 6.6.2.6 DC Power Supply

Since, the recommended input voltage for the Arduino Atmega 2560 is ranging in between 7 V-12 V as given in Table 6.51, to maintain the required input voltage limit, a 12V DC power supply (AC/DC adapter) is used to power the Arduino circuit which is shown in Figure 6.22.

### 6.6.2.7 Wiper

To clean the accumulated dust from the panel surface, a dry sponge wiper is used. The advantage of dry sponge is that the dust and water particles will not stick to it. The photographic view of wiper pieces used in the experiments are shown in Figure 6.22.

### 6.6.2.8 Limit Switch

It is an electromechanical device which activates by the contact of wiper which is sliding over the panel surface. Two such devices are located at the corner on each side of a panel, which activates due to physical contact of wiper when it reaches on either side of panel, thus gets actuated and sends signal to the microcontroller circuit so as to reverse the direction of the movement of the wiper. The photograph of a limit switch is shown in Figure 6.29.



Figure 6.29 Limit switch

### 6.6.2.9 Belt

Two endless belts are mounted along the length of the panel which are supported by set of wheels out of which one set of a wheel is driven by a motor. These belts are carrying the wiper which facilitates its movement over the panel surface which is shown in Figure 6.22.

### 6.6.2.10 Wheels

Two sets of wooden wheels are used to support the belts which carries a wiper which is shown in Figure 6.22.

### 6.6.3 Experimental study

The study was carried out using the developed experimental set-up with the help of a 10 W PV panel (area of the panel is 0.095 $m^2$). The panel was kept under an artificial solar radiation of 442 $W/m^2$. The electrical parameters of the panel, such as current, voltage and output power were measured under this condition. Thereafter, 3 gm of dust was spread over the panel surface with the help of a strainer and its electrical parameters were measured. Now, the wiper was made to move for one cleaning cycle (i.e., from one side to other side and back) and again its electrical parameters were measured. Thus, the electrical parameters of the panel were measured under three-different panel surface conditions, namely clean surface, dusty surface and cleaned surface. The reading of measured electrical parameters under three different panel surface conditions are given in Table 6.56 To Table 6.58 in the Appendix III.

From the measured electrical parameters of PV panel its electrical responses, such as short circuit current, open circuit voltage and maximum power output were tabulated (which are given in Table 6.59). Based on the measured electrical parameters the current-voltage and power-voltage characteristics of the panel were plotted (which are shown in Figure 6.30 and Figure 6.31). The plotted characteristics curves shown in Figure 6.30 and Figure 6.31 clearly indicate that the proposed cleaning system shows an improvement in the panel performance. The increment in the short circuit current, open circuit voltage and maximum power output of a cleaned panel are respectively, 25.00%, 2.80% and 27.98% w. r. t. dusty panel.

**Table 6.59** Measured electrical parameters

| Sl. No | Nature of Panel Surface | Short circuit current (amp) | Open circuit voltage (volt) | Maximum power output (watt) |
|--------|-------------------------|-----------------------------|------------------------------|-----------------------------|
| 1 | Clean Panel | 0.25 | 18.5 | 3.116 |
| 2 | Dusty Panel | 0.16 (36% reduction w.r.t clean panel) | 17.8 (3.78% reduction w.r.t clean panel) | 1.794 (42.42% reduction w.r.t clean panel) |
| 3 | Cleaned Panel | 0.20 (20% reduction w.r.t clean panel / 25.00% improvement w.r.t dusty panel) | 18.3 (1.80% reduction w.r.t clean panel / 2.80% improvement w.r.t dusty panel) | 2.296 (26.31% reduction w.r.t clean panel / 27.98% improvement w.r.t dusty panel)) |
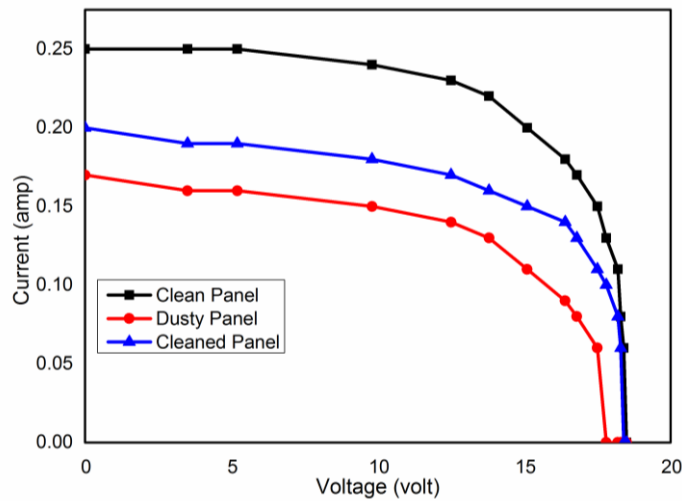


Figure 6.30 I-V characteristics for the three different panel surface conditions
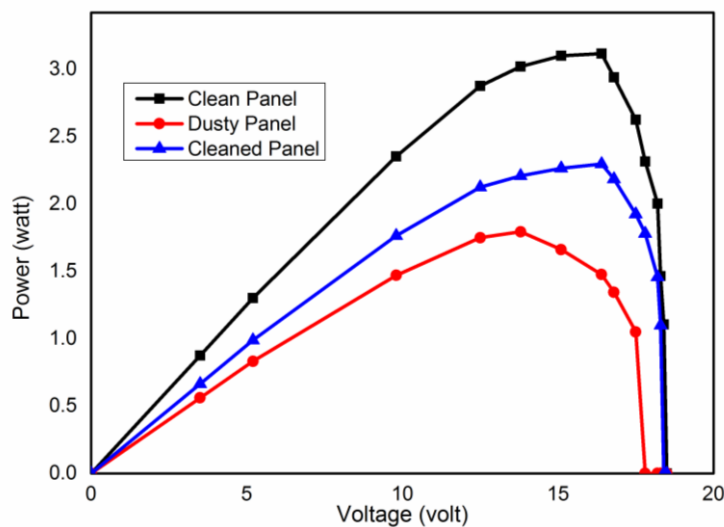


Figure 6.31 P-V characteristics for the three different panel surface conditions

94

# CHAPTER 7

# EFFECT OF TEMPERATURE AND HUMIDITY ON PV PANEL PERFORMANCE

## 7.1 EFFECT OF TEMPERATURE ON PV PANEL PERFORMANCE

### 7.1.1 Methodology

Two types of 5W PV panel (mono and poly crystalline) were used to study the effect of temperature on type (based on technology) of PV panel. This experiment was carried out in the laboratory. The technical specifications of both the panels used in this study are given in Table 7.1. Initially, a mono crystalline PV panel was mounted on the flat frame at zero inclination with the horizontal and subjected to a constant solar radiation of 1182 W/m$^2$. This range of solar radiation was generated and maintained using an experimental setup as discussed in Section 4.1 of Chapter 4. The experimental setups used for heating the panel surface study is shown in Figure 7.1. For measuring electrical responses, the PV panel was connected to a variable rheostat of 320 Ω rating through the ammeter (connected in series) and a voltmeter (connected in parallel). Two Digital Multi-meters (Fluke 178+ and DT830B) were used, one as a voltmeter and the other as an ammeter in the circuit, as shown in Figure 7.2.

To increase the surface temperature of PV panel a set of infrared dryer bulbs were used and its surface temperature was measured with the help of a digital pyrometer. The panel surface temperature was increased from 35ºC to 75ºC and its electrical responses (i.e., current, voltage and output power) were measured at every 10ºC interval. These measured electrical responses of PV panel are given in Table 7.2 to Table 7.6 in Appendix IV. Based on the measured electrical responses, fill factor of the panel was also calculated using equation (7.1). These electrical parameters under the above said condition are given in Table 7.7. Now, the monocrystalline panel was replaced by polycrystalline panel and the entire procedure was repeated. The measured electrical

responses of polycrystalline panel were given in Table 7.8 to Table 7.12 in Appendix IV. The obtained electrical parameters poly crystalline panel, such as open circuit voltage, short circuit current, maximum power output and fill factor (which was calculated) are tabulated which are given in Table 7.13.

The equation used for calculating the fill factor (FF) is given by equation (7.1).

$$FF = \frac{V_m \times I_m}{V_{OC} \times I_{SC}}$$
(7.1)

where,

$V_{oc}$ = open circuit voltage (volt),

$I_{sc}$ = Short circuit current (amp),

$I_m$ = Maximum current (amp), and

$V_m$ = maximum voltage (volt).

**Table 7.1** Technical specifications of 5 W mono crystalline and poly crystalline PV panels

| Sl. No. | Specifications | Rating | |
|---|---|---|---|
| | | **Mono crystalline panel** | **Poly crystalline panel** |
| 1 | Maximum power | 5 watt | 5 watt |
| 2 | Maximum voltage | 9.64 volt | 8.80 volt |
| 3 | Maximum current | 0.52 amp | 0.57 amp |
| 4 | Open circuit voltage | 11.57 volt | 10.80 volt |
| 5 | Short circuit current | 0.57 amp | 0.65 amp |
| 6 | Normal operating cell temperature | (47±2) ℃ | (47±2) ℃ |
| 7 | Tolerance level | 0 to 3% | 0 to 3% |

Figure 7.1 Heating of PV panel surface
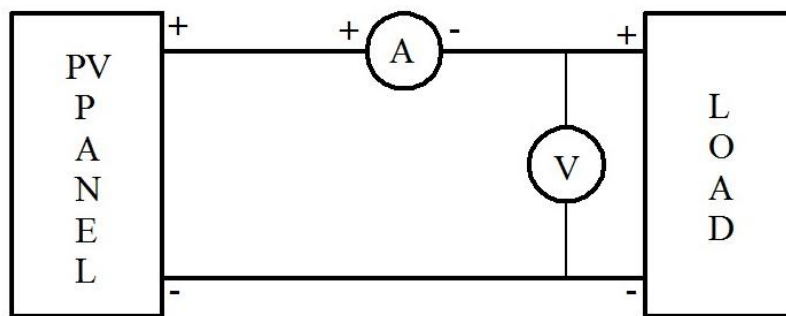


Figure 7.2 Circuit diagram for the measurement of electrical parameters of PV panel

Table 7.7 Electrical responses of mono crystalline PV panel

| Panel surface temperature ($^0$C) | Open circuit voltage (volt) | Short circuit current (amp) | Maximum power output (watt) | Fill factor |
|---|---|---|---|---|
| 35 | 9.95 | 0.350 | 2.511 | 0.721 |
| 45 | 9.60 | 0.3530 | 2.320 | 0.684 |
| 55 | 9.30 | 0.360 | 2.194 | 0.655 |
| 65 | 9.15 | 0.365 | 2.160 | 0.646 |
| 75 | 8.75 | 0.370 | 1.975 | 0.608 |

**Table 7.13** Electrical responses of poly crystalline PV panel

| Panel surface temperature ($^0$C) | Open circuit voltage (volt) | Short circuit current (amp) | Maximum power output (watt) | Fill factor |
|---|---|---|---|---|
| 35 | 9.70 | 0.360 | 2.476 | 0.709 |
| 45 | 9.30 | 0.360 | 2.202 | 0.657 |
| 55 | 8.90 | 0.365 | 2.050 | 0.631 |
| 65 | 8.55 | 0.370 | 1.950 | 0.616 |
| 75 | 8.20 | 0.375 | 1.755 | 0.570 |

### 7.1.2 Results and Discussion

Based on the measured and calculated electrical parameters, as presented in Table 7.7 and Table 7.13, I-V and P-V characteristics of mono crystalline and poly crystalline panels were plotted, which is shown in Figure 7.3, Figure 7.4, Figure 7.5 and Figure 7.6. As represented in Figure 7.3 to Figure 7.6, the plotting of characteristic curves was done w.r.t. only three temperatures i.e., 35ºC, 55ºC and 75ºC. Because by plotting characteristic curve for all the five temperature, the graph looks very clumsy. Figure 7.3 and Figure 7.4 shows the I-V characteristics of mono and poly crystalline panels, respectively. Similarly, Figure 7.5 and Figure 7.6 shows the P-V characteristics of mono and poly crystalline panels, respectively. As depicted in the I-V characteristics of both the panels, there is not much variation in current in lower voltage (the voltage which is less than the maximum output voltage) range, but as the voltage increases there is a sudden drop in the current. These electrical characteristics of PV panel show that the surface temperature of PV panel has a significant impact on its performance.

As presented in Figure 7.3, Figure 7.4, Figure 7.5 and Figure 7.6, the deformation in I-V and P-V characteristic curve increases with the panel surface temperature. The variation in the electrical parameters of PV panel, such as open circuit voltage, short circuit current, maximum power output and fill factor due to increase in its surface temperature from 35ºC to 75ºC is calculated using equation (7.2), equation (7.3), equation (7.4) and equation (7.5), which is tabulated in Table 7.14.

$$\text{Variation in V}_{\text{oc}} = \frac{\Delta V_{oc}}{V_{oc\ 35°C}} \times 100 \tag{7.2}$$

$$\text{Variation in I}_{\text{sc}} = \frac{\Delta I}{I_{sc\ 35°C}} \times 100 \tag{7.3}$$

$$\text{Variation in P}_{\text{m}} = \frac{\Delta P_m}{P_{m\ 35°C}} \times 100 \tag{7.4}$$

$$\text{Variation in FF} = \frac{\Delta FF}{FF_{35°C}} \times 100 \tag{7.5}$$

where,

$\Delta V_{oc}$ = Change in open circuit voltage with the increase in surface temperature from 35°C to 75°C (volt),

$\Delta I_{sc}$ = Change in short circuit current with the increase in surface temperature from 35°C to 75°C (amp),

$\Delta P_m$ = Change in maximum power output with the increase in surface temperature from 35°C to 75°C (watt),

$\Delta FF$ = Change in fill factor with the increase in surface temperature from 35°C to 75°C,

$V_{oc\ 35°C}$ = Open circuit voltage at 35°C surface temperature (volt),

$I_{sc\ 35°C}$ = Short circuit current at 35°C surface temperature (amp),

$P_{m\ 35°C}$ = Maximum power output at 35°C surface temperature (watt),

$FF_{35°C}$ = Fill factor at 35°C surface temperature.

**Table 7.14** Variation in electrical parameters of PV panel due to change in its surface temperature from 35ºC to 75ºC

| Sl. No. | Parameters | Variation of electrical parameters of PV panel (%) | |
|---|---|---|---|
| | | Mono crystalline | Poly crystalline |
| 1 | $V_{oc}$ (reduces) | 12.06 | 15.46 |
| 2 | $I_{sc}$ (increases) | 5.71 | 4.17 |
| 3 | $P_m$ (reduces) | 21.34 | 29.12 |
| 4 | FF (reduces) | 15.67 | 19.60 |

As depicted in Table 7.14, there was a significant reduction in $V_{OC}$ with the increase in the panel surface temperature, whereas a small increment in $I_{SC}$ was observed. Due to the significant reduction in $V_{OC}$ the other electrical parameters, such as maximum power output and fill factor were also reduced. Therefore, the overall performance of

PV panel reduces with the rise in its surface temperature. Also, the reduction in electrical parameters of poly crystalline PV panel is observed higher than the mono crystalline PV panel.

Moreover, as shown in Figure 7.5 and Figure 7.6, the maximum power point (MPP) in the PV characteristic curve moves towards the lower output voltage with the increase in panel surface temperature. Due to this, the maximum power point tracker algorithm would not be able to operate at a particular maximum power point, which reduces the performance of solar charge controller. Hence, the shifting of MPP in the PV curve directly affects the effective operation of the entire PV systems (i.e., PV panel and charge controller).
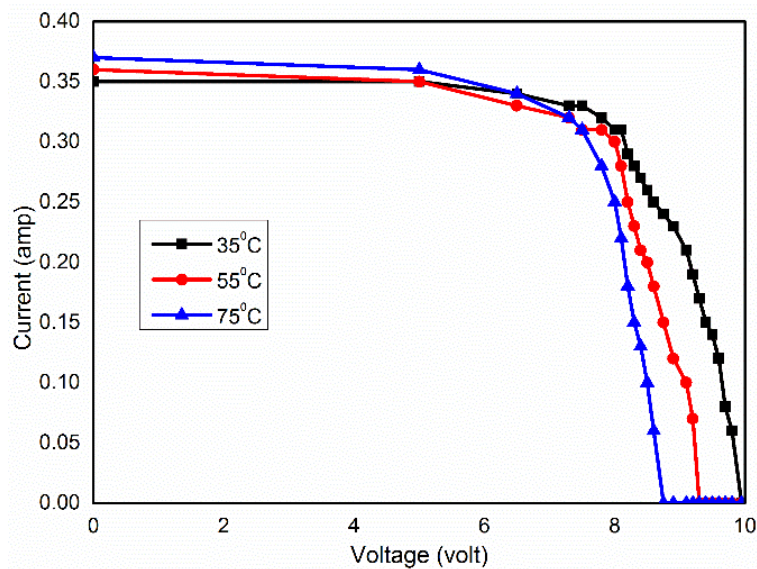


Figure 7.3 I-V characteristics of mono crystalline PV panel under varying surface temperature
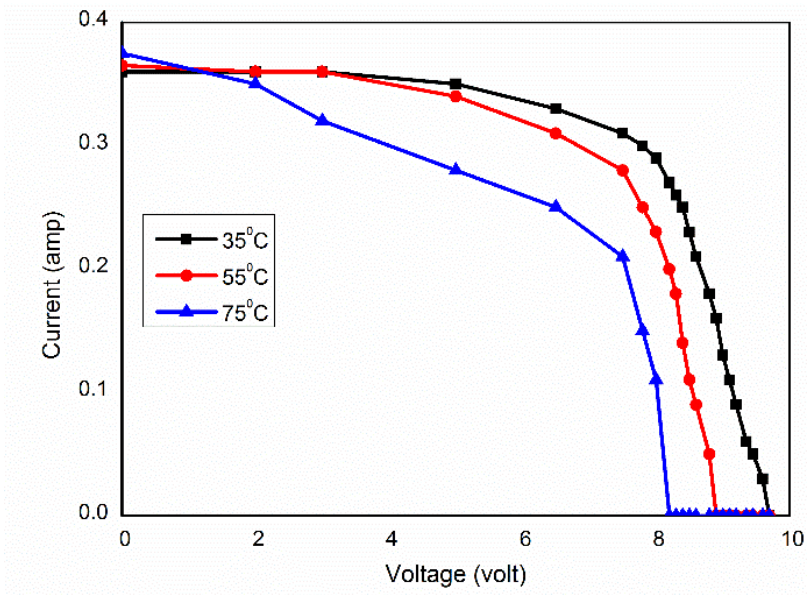
Figure 7.4 I-V characteristics of poly crystalline PV panel under varying surface temperature
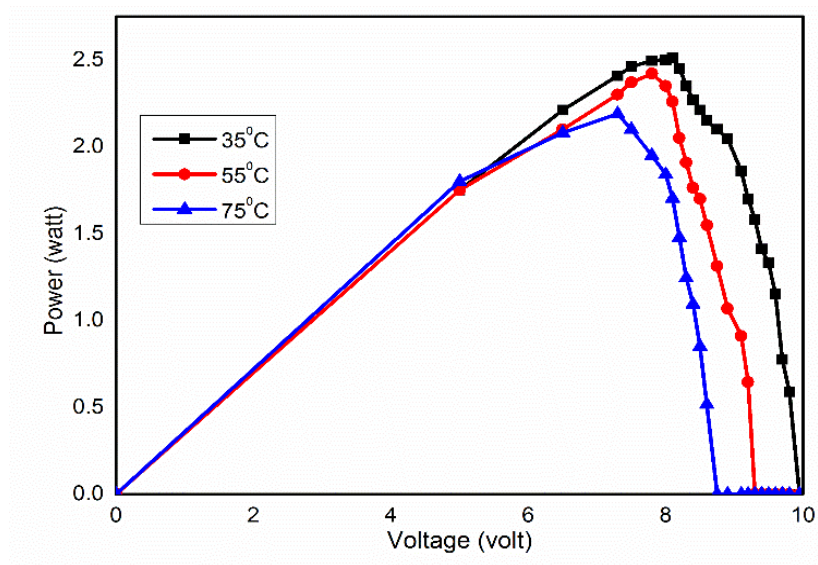


Figure 7.5 P-V characteristics of mono crystalline PV panel under varying surface temperature
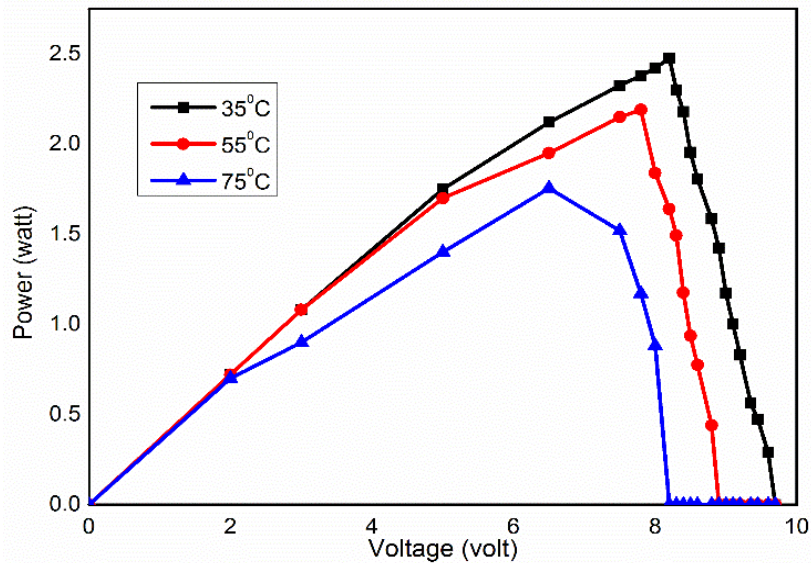
Figure 7.6 P-V characteristics of poly crystalline PV panel under varying surface temperature

## 7.2 EFFECT OF HUMIDITY ON PV PANEL PERFORMANCE

### 7.2.1 Methodology

The experiment was performed on a 20 W poly-crystalline PV panel to study the effect of humidity on PV panel performance. The detailed specifications of the panel are presented in Table 7.15. This panel was subjected to a humid environment, which is artificially generated by a humidifier, in the laboratory. The electrical parameters of PV panel (such as current, voltage and power output) were measured, for a fixed load of 38 Ω, by varying humidity level 65.40% to 98.20%. Table 7.16 indicates the measured electrical parameters of the panel. The percentage reduction in electrical parameters due to increase in humidity level is depicted in Table 7.17.

**Table 7.15** Technical specifications of 20W ploy crystalline PV panel

| Sl. No | Parameter | Ratings |
|--------|-----------|---------|
| 1 | Open circuit voltage | 21.50 volt |
| 2 | Short circuit current | 1.28 amp |
| 3 | Maximum voltage | 17.00 volt |
| 4 | Maximum Power | 20 watt |
| 5 | Maximum current | 1.2 amp |
| 6 | Fill Factor | 0.727 |
| 7 | Normal operating cell temperature | (47±2) ℃ |

**Table 7.16** Measured electrical parameters

| Relative humidity (%) | Short circuit current (amp) | Open circuit voltage (volt) | Output voltage (volt) | Output current (amp) | Output power (watt) |
|---|---|---|---|---|---|
| 65.40 | 0.530 | 19.03 | 17.52 | 0.450 | 7.884 |
| 73.50 | 0.490 | 18.40 | 16.90 | 0.414 | 6.996 |
| 80.40 | 0.460 | 17.90 | 16.52 | 0.387 | 6.393 |
| 85.60 | 0.438 | 17.50 | 16.10 | 0.368 | 5.924 |
| 91.70 | 0.412 | 17.76 | 16.27 | 0.347 | 5.645 |
| 95.10 | 0.398 | 17.15 | 15.80 | 0.335 | 5.293 |
| 98.20 | 0.385 | 16.85 | 15.57 | 0.325 | 5.060 |

**Table 7.17** Reduction in electrical parameters

| Relative humidity (%) | Reduction in short circuit current (%) | Reduction in open circuit voltage (%) | Reduction in output voltage (%) | Reduction in output current (%) | Reduction in output power (%) |
|---|---|---|---|---|---|
| 8.10 | 7.55 | 3.31 | 3.54 | 8.00 | 11.26 |
| 15.00 | 13.20 | 5.94 | 5.71 | 14.00 | 18.91 |
| 20.20 | 17.35 | 8.04 | 8.11 | 18.22 | 24.86 |
| 26.30 | 22.26 | 6.67 | 7.13 | 22.89 | 28.39 |
| 29.70 | 24.90 | 9.88 | 9.82 | 25.56 | 32.86 |
| 32.80 | 27.35 | 11.45 | 11.13 | 27.78 | 35.82 |

## 7.2.2 Results and Discussion

Based on the measured electrical parameter graphs were plotted between humidity Vs short circuit current and humidity Vs power, which are shown in Figure 7.7 and Figure 7.8, respectively. As shown in Figure 7.7 and Figure 7.8, the short circuit current and power output are reducing with an increase in humidity level in the atmosphere. This reduction in short circuit current and output power is mainly due to the presence of water droplets in the atmosphere. When the sun (light) rays hit these water droplets they undergo the phenomena of refraction, reflection and diffraction. Thus, humidity alters the solar radiation reaching panel surface in non-linear manner due to non-uniform distribution and random sizes of water droplets in the atmosphere (Gwandu and Creasey 1995). As a result of this, the effective solar radiation falling on the panel surface reduces with increase in the humidity level. This leads to a large variation in short circuit current, whereas a little variation in open circuit voltage, as observed in Table 7.17.

Hence, the increase in humidity level in the atmosphere degrades the performance of PV panel. The obtained results show that the output power of the PV panel reduces by 35.82% with the increase in humidity level from 65.40% to 98.20% (i.e., with 32.8% increase).
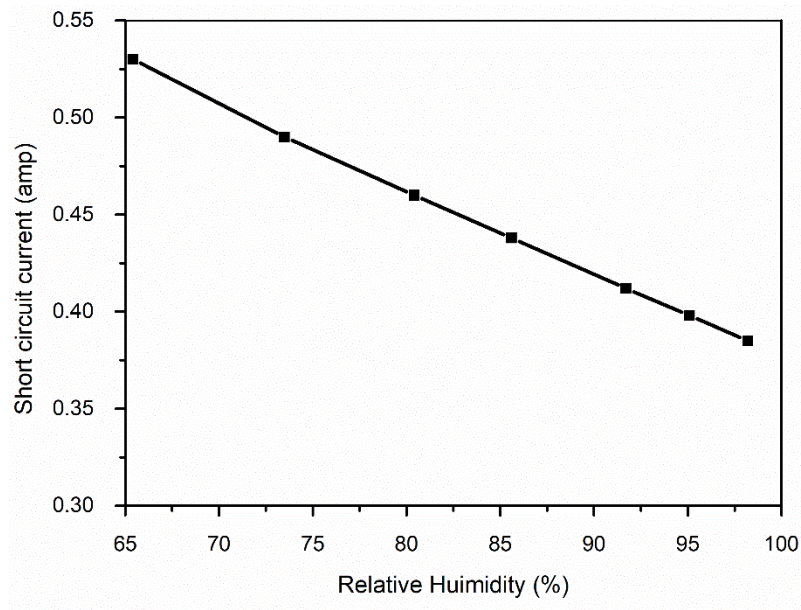


Figure 7.7 Variation in short circuit current with humidity
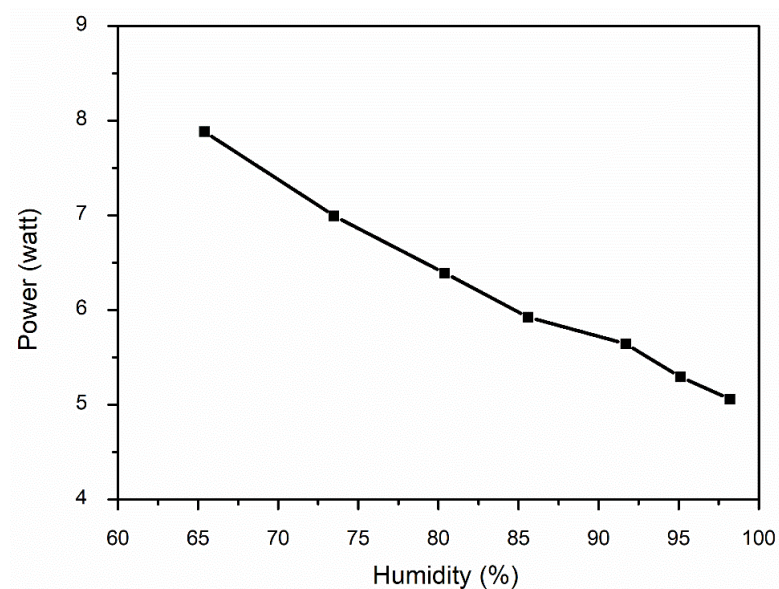


Figure 7.8 Variation in power output with humidity

The variation in open circuit voltage of PV panel with reference to change in humidity level is shown in Figure 7.9. As indicated in Table 7.16 and Figure 7.10, panel

experiences a small increment in open circuit voltage i.e., from 17.50 V to 17.76 V with increase in humidity level from 85.60% to 91.70%. This may be due to the water droplets, trapped inside the glass of the panel which acts like magnifier lenses that focus the sunlight towards the cell (Tan et al. 2010). It is worth mentioning here that the moisture ingression into the cell of the panel reduce the life span of the crystalline cell by delamination, embrittlement and corrosive of encapsulant material of the PV cell (Mekhilef et al. 2012).
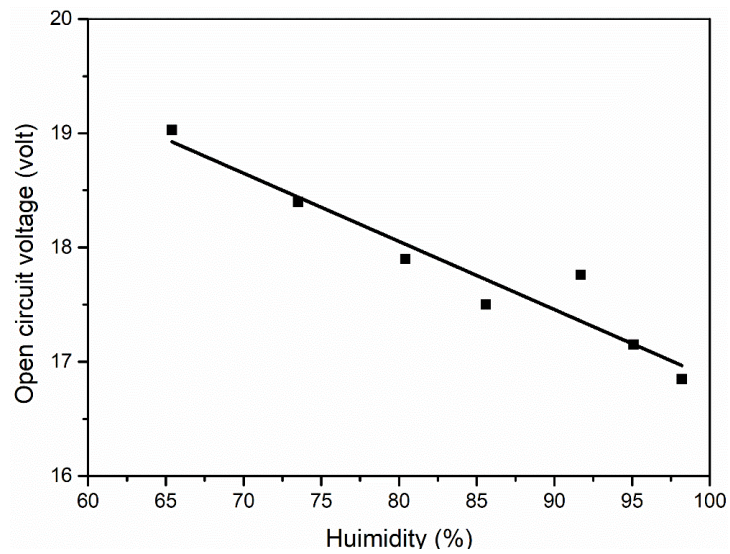


Figure 7.9 Variation in open circuit voltage with humidity

# CHAPTER 8

# EFFECT OF TILT ANGLE ON PV PANEL PERFORMANCE

## 8.1 METHODOLOGY

The mine under study is located in Chitradurga District of Karnataka State, India. It is situated at the coordinates 14° 8' 55.4928" N and 76° 40' 1.1424" E. The site endures good solar radiation profile. During sunny day the peak solar radiation of 1182 W/m$^2$ was recorded. Due to high solar radiation, good atmospheric temperature (generally 25ºC to 37ºC) and good wind profile (peak value of 4m/s) this site could be a good choice for the installation of PV panel.

To study the variation of solar radiation on panel surface at different tilt angle and at different time in a day, a 100 W polycrystalline solar PV panel was installed in a mine near the weather monitoring station (as usual the panel was kept facing towards south direction), which is situated at 883 m RL (i.e., reduced level). The panel consists of 4 strings with 8 cells in each string (i.e., 8×4 cells). Solar radiation on the panel surface was measured using TM-207 solar power meter. The measurements were made by varying the tilt angle of the panel surface, from 0º to 90º (with the horizontal), at an interval of 15º. The readings were recorded from 9 am to 5 pm at every one-hour interval.  For every tilt angle of the panel the solar radiation was measured at each cell (in total there were 32 cells) and thereafter the average radiation falling on the panel surface was calculated. These measurements were made for five days. Also, the output power of PV panel was calculated by measuring its output current and voltage throughout a day, at different tilt angles for all the five days, with the load of 200 Ω. This experiment was carried out in the month of January.

## 8.2 RESULTS AND DISCUSSION

The readings of solar radiation received by the panel surface throughout a day at different tilt angles for all the five days are presented in Table 8.1, Table 8.2, Table 8.3, Table 8.4 and Table 8.5. Based on the measured values, the variation in the pattern of solar radiation w.r.t. the time, at different tilt angles, for all the five days are presented in Figure 8.1, Figure 8.2, Figure 8.3, Figure 8.4 and Figure 8.5. As shown in the Figures 8.1 to 8.5, the maximum solar radiation received by the panel surface is at around 12 noon, for all the tilt angles under considerations. Therefore, with reference to 12 noon, the variation in the pattern of solar radiation w.r.t. tilt angle was plotted, which is shown in Figure 8.6.

**Table 8.1** Solar radiation received by the panel surface at different tilt angles on day one

| Time | Solar radiation (W/m$^2$) | | | | | | |
|------|------|------|------|------|------|------|------|
|      | 0° | 15° | 30° | 45° | 60° | 75° | 90° |
| 9am | 533.20 | 694.10 | 678.33 | 646.78 | 567.90 | 410.15 | 331.28 |
| 10am | 703.57 | 728.81 | 716.19 | 684.64 | 631.00 | 580.52 | 504.80 |
| 11am | 886.56 | 962.28 | 949.66 | 914.95 | 864.47 | 694.10 | 599.45 |
| 12noon | 974.90 | 1135.80 | 1072.70 | 1056.93 | 943.35 | 820.30 | 694.10 |
| 1pm | 949.66 | 1088.48 | 1041.15 | 1009.60 | 930.73 | 772.98 | 662.55 |
| 2pm | 959.12 | 1056.93 | 1009.60 | 978.05 | 883.40 | 709.88 | 599.45 |
| 3pm | 810.84 | 867.63 | 820.30 | 788.75 | 757.20 | 631.00 | 552.13 |
| 4pm | 448.01 | 577.37 | 555.28 | 492.18 | 394.38 | 378.60 | 321.81 |
| 5pm | 236.63 | 302.88 | 233.47 | 220.85 | 176.68 | 126.20 | 110.43 |

**Table 8.2** Solar radiation received by the panel surface at different tilt angles on day two

| Time | Solar radiation (W/m$^2$) | | | | | | |
|------|------|------|------|------|------|------|------|
|      | 0° | 15° | 30° | 45° | 60° | 75° | 90° |
| 9am | 520.58 | 678.33 | 668.86 | 662.55 | 552.13 | 394.38 | 331.28 |
| 10am | 709.88 | 725.65 | 709.88 | 678.33 | 631.00 | 567.90 | 520.58 |
| 11am | 851.85 | 959.12 | 946.50 | 899.18 | 851.85 | 662.55 | 583.68 |
| 12noon | 949.66 | 1120.01 | 1041.15 | 1025.38 | 955.97 | 788.75 | 678.33 |
| 1pm | 930.73 | 1072.70 | 1056.93 | 978.05 | 930.73 | 757.20 | 646.78 |
| 2pm | 905.49 | 1041.15 | 978.05 | 899.18 | 851.85 | 678.33 | 583.68 |
| 3pm | 741.43 | 883.40 | 788.75 | 725.65 | 725.65 | 615.23 | 536.35 |
| 4pm | 457.48 | 599.45 | 552.13 | 520.58 | 410.15 | 394.38 | 331.28 |
| 5pm | 246.09 | 318.66 | 252.40 | 220.85 | 189.30 | 157.75 | 126.20 |

**Table 8.3** Solar radiation received by the panel surface at different tilt angles on day three

| Time | Solar radiation (W/m²) | | | | | | |
|---|---|---|---|---|---|---|---|
| | **0°** | **15°** | **30°** | **45°** | **60°** | **75°** | **90°** |
| 9am | 536.35 | 709.88 | 678.33 | 646.78 | 583.68 | 410.15 | 331.28 |
| 10am | 709.88 | 741.43 | 719.34 | 694.10 | 631.00 | 583.68 | 504.80 |
| 11am | 899.18 | 978.05 | 962.28 | 899.18 | 851.85 | 700.41 | 583.68 |
| 12noon | 978.05 | 1167.35 | 1088.48 | 1072.70 | 946.50 | 836.08 | 694.10 |
| 1pm | 955.97 | 1104.25 | 1056.93 | 1025.38 | 914.95 | 788.75 | 646.78 |
| 2pm | 930.73 | 1041.15 | 1025.38 | 962.28 | 867.63 | 694.10 | 599.45 |
| 3pm | 836.08 | 883.40 | 804.53 | 804.53 | 772.98 | 615.23 | 552.13 |
| 4pm | 448.01 | 567.90 | 552.13 | 492.18 | 410.15 | 394.38 | 315.50 |
| 5pm | 233.47 | 296.57 | 227.16 | 220.85 | 173.53 | 126.20 | 110.43 |

**Table 8.4** Solar radiation received by the panel surface at different tilt angles on day four

| Time | Solar radiation (W/m²) | | | | | | |
|---|---|---|---|---|---|---|---|
| | **0°** | **15°** | **30°** | **45°** | **60°** | **75°** | **90°** |
| 9am | 552.12 | 709.88 | 694.10 | 662.55 | 599.45 | 425.93 | 347.05 |
| 10am | 725.65 | 757.20 | 725.65 | 694.10 | 662.55 | 599.45 | 552.13 |
| 11am | 914.95 | 993.82 | 962.28 | 962.28 | 914.95 | 709.88 | 646.78 |
| 12noon | 1009.6 | 1183.13 | 1104.25 | 1104.25 | 978.05 | 851.85 | 741.43 |
| 1pm | 978.05 | 1088.48 | 1072.70 | 1025.38 | 962.28 | 788.75 | 662.55 |
| 2pm | 962.28 | 1072.70 | 1025.37 | 993.82 | 899.18 | 725.65 | 615.23 |
| 3pm | 836.08 | 883.40 | 851.85 | 820.30 | 772.98 | 662.55 | 567.90 |
| 4pm | 460.63 | 583.68 | 567.90 | 520.58 | 410.15 | 425.93 | 347.05 |
| 5pm | 236.63 | 283.95 | 220.85 | 214.54 | 189.30 | 157.75 | 126.20 |

**Table 8.5** Solar radiation received by the panel surface at different tilt angles on day five

| Time | Solar radiation (W/m$^2$) | | | | | | |
|---|---|---|---|---|---|---|---|
| | **0°** | **15°** | **30°** | **45°** | **60°** | **75°** | **90°** |
| 9am | 520.58 | 694.10 | 662.55 | 631.00 | 567.90 | 410.15 | 347.05 |
| 10am | 694.10 | 725.65 | 694.10 | 662.55 | 631.00 | 567.90 | 489.03 |
| 11am | 883.40 | 962.28 | 946.50 | 899.18 | 851.85 | 662.55 | 599.45 |
| 12noon | 962.28 | 1104.25 | 1041.15 | 1041.15 | 930.73 | 757.20 | 662.55 |
| 1pm | 930.73 | 1072.70 | 993.82 | 978.05 | 899.18 | 725.65 | 615.23 |
| 2pm | 946.50 | 1041.15 | 962.28 | 962.28 | 820.30 | 694.10 | 599.45 |
| 3pm | 804.53 | 820.30 | 788.75 | 757.20 | 694.10 | 599.45 | 536.35 |
| 4pm | 441.70 | 552.13 | 536.35 | 489.02 | 394.38 | 378.60 | 331.28 |
| 5pm | 220.85 | 283.95 | 233.47 | 220.85 | 173.53 | 126.20 | 110.43 |
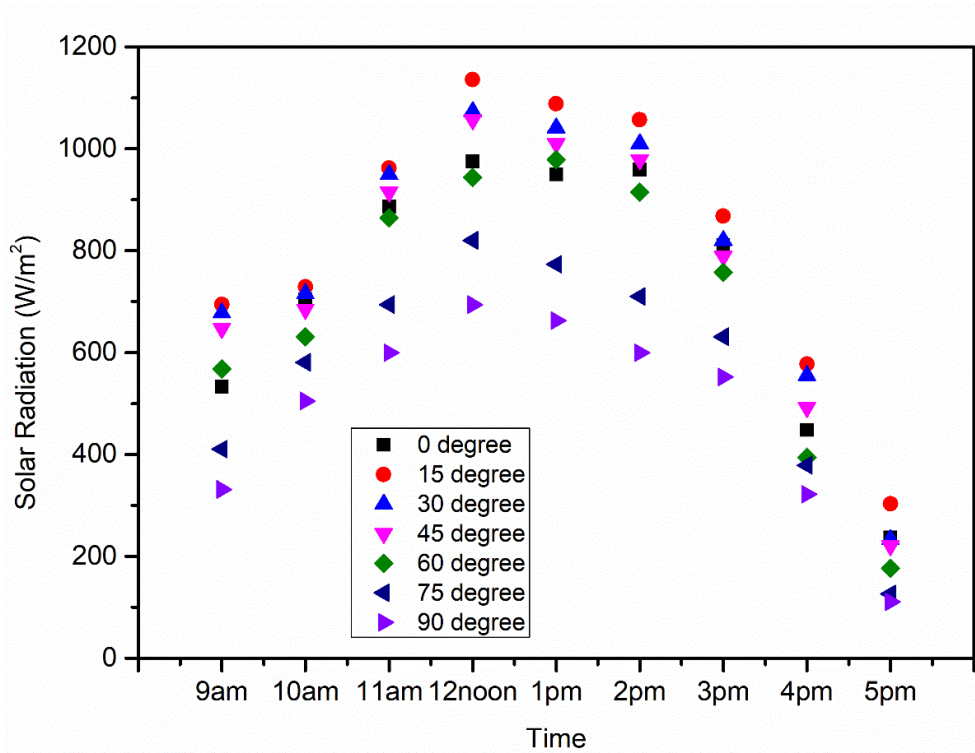


Figure 8.1 Variation of solar radiation in a day at different tilt angles on day one
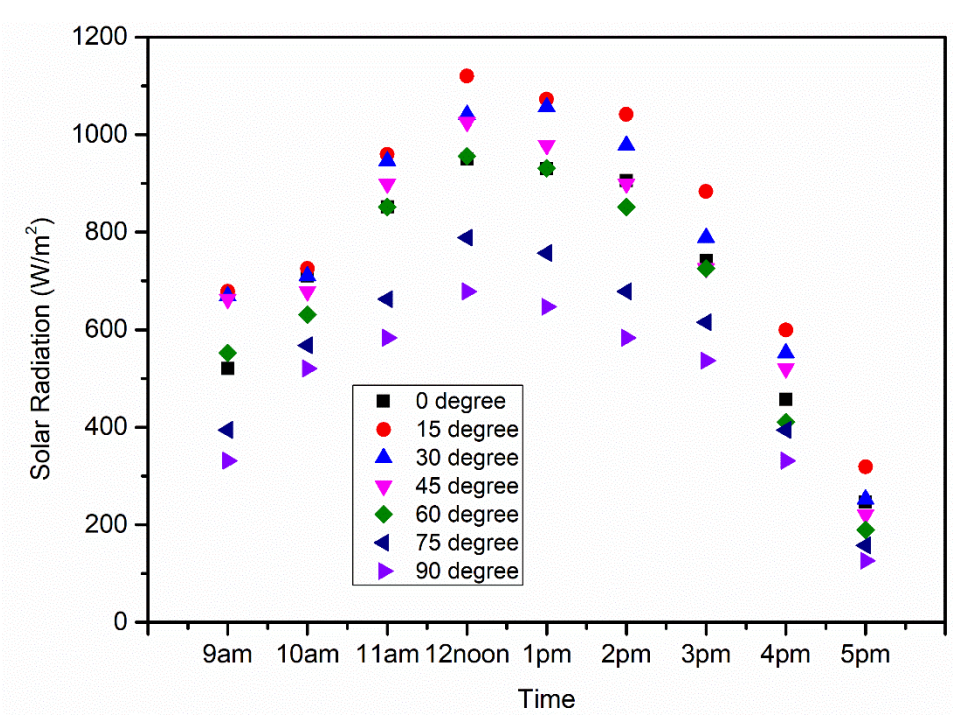
Figure 8.2 Variation of solar radiation in a day at different tilt angles on day two
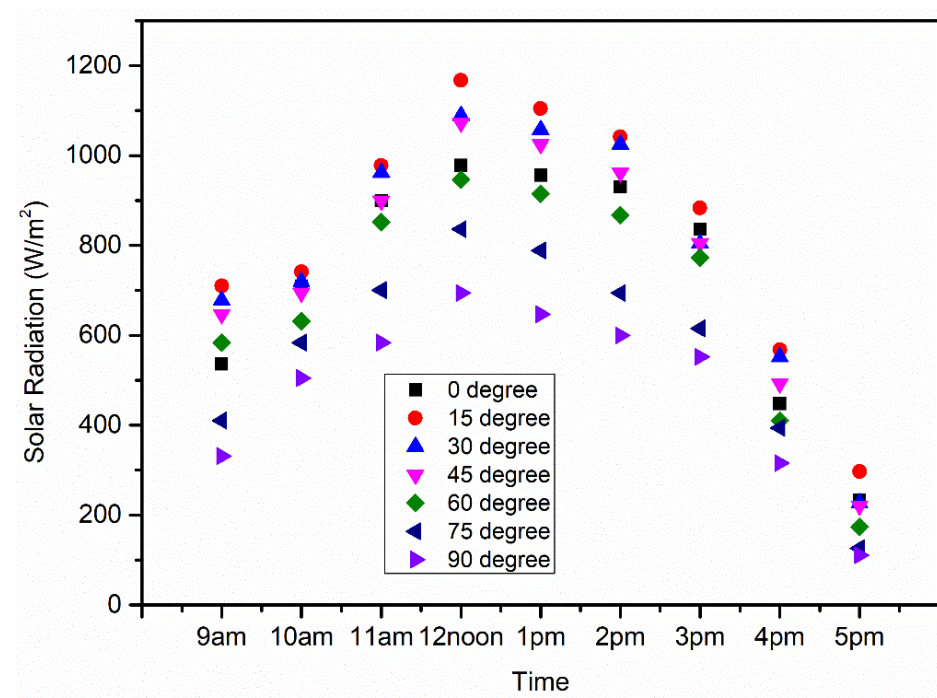


Figure 8.3 Variation of solar radiation in a day at different tilt angles on day three
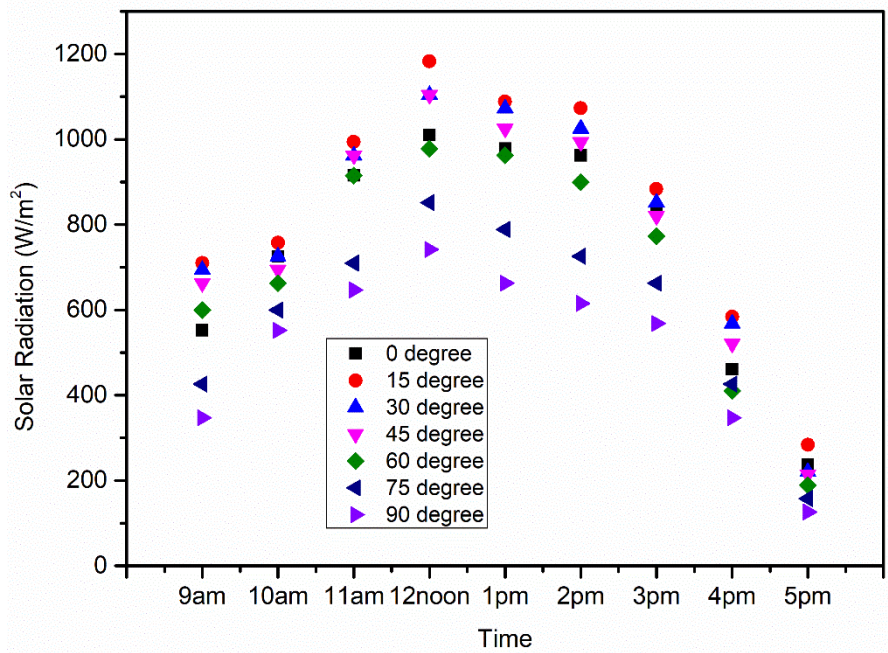
Figure 8.4 Variation of solar radiation in a day at different tilt angles on day four
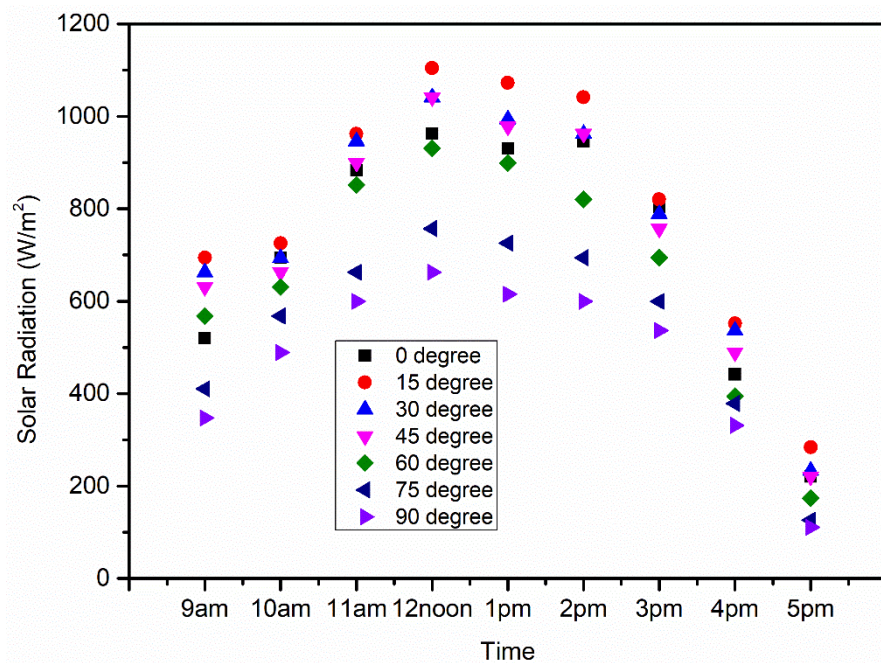


Figure 8.5 Variation of solar radiation in a day at different tilt angles on day five
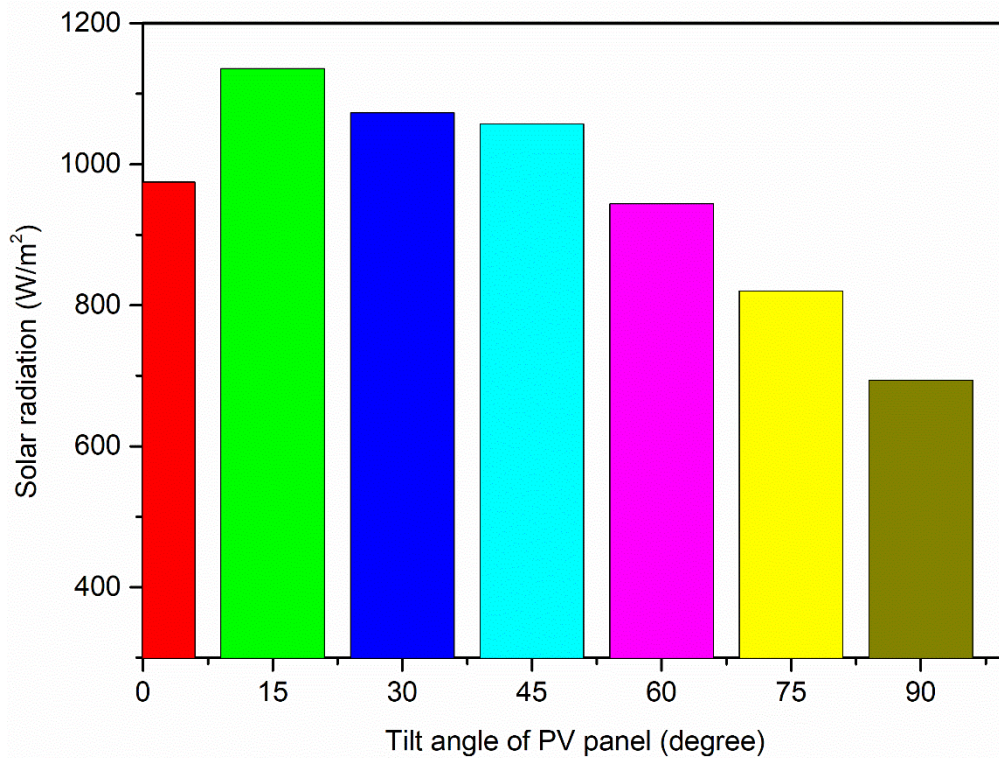
Figure 8.6 Variation of solar radiation w.r.t. tilt angles (at 12 noon)

As indicated in the Figure 8.6, maximum solar radiation is received at 15° tilt angle, of course at 12 noon, as shown in Figure 8.1 to 8.5. The measured values of electrical parameters such as output current and output voltage of the panel, for all the five days, are given in Table 8.6, Table 8.7, Table 8.8, Table 8.9 and Table 8.10 (in Appendix V). Based on the measured electrical parameters, the output power of the panel was calculated, for all the five days, which are given in Table 8.1, Table 8.12, Table 8.13, Table 8.14 and Table 8.15. From Table 8.11 to 8.15, the variation in the pattern of output power of PV panel w.r.t. the time, at different tilt angle, for all the five days are presented, which are shown in Figure 8.7, Figure 8.8, Figure 8.9, Figure 8.10 and Figure 8.11, respectively.

**Table 8.11** Output power of PV panel at different tilt angles on day one

| Time | Output power (watt) | | | | | | |
|---|---|---|---|---|---|---|---|
| | **0°** | **15°** | **30°** | **45°** | **60°** | **75°** | **90°** |
| 9am | 28.10 | 36.10 | 35.80 | 34.10 | 29.90 | 22.40 | 16.10 |
| 10am | 37.15 | 38.48 | 37.80 | 45.90 | 33.20 | 30.65 | 26.60 |
| 11am | 46.80 | 50.80 | 50.10 | 48.31 | 45.62 | 36.64 | 31.68 |
| 12noon | 51.45 | 59.98 | 57.2 | 56.1 | 49.64 | 43.32 | 36.6 |
| 1pm | 50.15 | 56.90 | 54.90 | 53.30 | 48.80 | 40.80 | 34.98 |
| 2pm | 50.60 | 55.80 | 52.90 | 51.48 | 46.64 | 37.48 | 31.65 |
| 3pm | 42.82 | 45.80 | 45.40 | 43.64 | 39.90 | 35.40 | 29.15 |
| 4pm | 23.65 | 30.48 | 30.10 | 26.70 | 21.40 | 20.40 | 17.40 |
| 5pm | 12.50 | 13.90 | 13.40 | 12.10 | 11.10 | 9.70 | 7.10 |

**Table 8.12** Output power of PV panel at different tilt angles on day two

| Time | Output power (watt) | | | | | | |
|---|---|---|---|---|---|---|---|
| | **0°** | **15°** | **30°** | **45°** | **60°** | **75°** | **90°** |
| 9am | 27.49 | 35.82 | 35.31 | 34.98 | 29.152 | 20.82 | 17.49 |
| 10am | 37.48 | 38.31 | 37.48 | 35.82 | 33.32 | 29.99 | 27.49 |
| 11am | 44.98 | 50.64 | 49.98 | 47.48 | 44.98 | 34.98 | 30.81 |
| 12noon | 50.14 | 59.13 | 54.97 | 54.14 | 50.47 | 41.65 | 35.82 |
| 1pm | 49.14 | 56.64 | 55.81 | 51.64 | 49.14 | 39.98 | 34.15 |
| 2pm | 47.81 | 54.97 | 51.64 | 47.48 | 44.98 | 35.815 | 30.82 |
| 3pm | 39.15 | 46.64 | 41.65 | 38.314 | 38.314 | 32.48 | 28.32 |
| 4pm | 24.15 | 31.65 | 29.15 | 27.49 | 21.66 | 20.82 | 17.49 |
| 5pm | 12.99 | 16.82 | 13.32 | 11.66 | 9.99 | 8.33 | 6.66 |

**Table 8.13** Output power of PV panel at different tilt angles on day three

| Time | Output power (watt)) | | | | | | |
|---|---|---|---|---|---|---|---|
| | **0°** | **15°** | **30°** | **45°** | **60°** | **75°** | **90°** |
| 9am | 28.32 | 37.48 | 35.82 | 34.15 | 30.82 | 21.66 | 17.49 |
| 10am | 37.48 | 39.15 | 37.98 | 36.65 | 33.32 | 30.82 | 26.65 |
| 11am | 47.48 | 51.64 | 50.81 | 47.48 | 44.98 | 36.98 | 30.82 |
| 12noon | 51.64 | 61.63 | 57.47 | 56.64 | 49.98 | 44.14 | 36.65 |
| 1pm | 50.47 | 58.30 | 55.81 | 54.14 | 48.31 | 41.64 | 34.15 |
| 2pm | 49.14 | 54.97 | 54.14 | 50.81 | 45.81 | 36.65 | 31.65 |
| 3pm | 44.14 | 46.64 | 42.48 | 42.48 | 40.81 | 32.48 | 29.15 |
| 4pm | 23.65 | 29.99 | 29.15 | 25.99 | 21.66 | 20.82 | 16.66 |
| 5pm | 12.32 | 15.66 | 11.99 | 11.66 | 9.16 | 6.66 | 5.830 |

**Table 8.14** Output power of PV panel at different tilt angles on day four

| Time | Output power (watt) | | | | | | |
|---|---|---|---|---|---|---|---|
| | **0°** | **15°** | **30°** | **45°** | **60°** | **75°** | **90°** |
| 9am | 29.15 | 37.48 | 36.65 | 34.98 | 31.65 | 22.48 | 18.32 |
| 10am | 38.34 | 39.98 | 38.31 | 36.65 | 34.98 | 31.65 | 29.15 |
| 11am | 48.31 | 52.47 | 50.81 | 50.81 | 48.30 | 37.48 | 34.15 |
| 12noon | 53.31 | 62.46 | 58.30 | 58.30 | 51.64 | 44.98 | 39.15 |
| 1pm | 51.64 | 57.47 | 56.64 | 54.14 | 50.81 | 41.65 | 34.98 |
| 2pm | 50.81 | 56.64 | 54.14 | 52.47 | 47.48 | 38.31 | 32.48 |
| 3pm | 44.14 | 46.64 | 44.98 | 43.31 | 40.81 | 34.98 | 29.99 |
| 4pm | 24.32 | 30.82 | 29.99 | 27.48 | 21.66 | 22.49 | 18.32 |
| 5pm | 12.49 | 14.99 | 11.66 | 11.33 | 9.99 | 8.33 | 6.66 |

**Table 8.15** Output power of PV panel at different tilt angles on day five

| Time | Output power (watt) | | | | | | |
|---|---|---|---|---|---|---|---|
| | **0°** | **15°** | **30°** | **45°** | **60°** | **75°** | **90°** |
| 9am | 27.49 | 36.65 | 34.98 | 33.32 | 29.99 | 21.66 | 18.32 |
| 10am | 36.64 | 38.31 | 36.65 | 34.98 | 33.31 | 29.99 | 25.82 |
| 11am | 46.64 | 50.81 | 49.98 | 47.48 | 44.98 | 34.98 | 31.65 |
| 12noon | 50.81 | 58.30 | 54.97 | 54.98 | 49.14 | 39.98 | 34.98 |
| 1pm | 49.14 | 56.64 | 52.47 | 51.64 | 47.48 | 38.31 | 32.48 |
| 2pm | 49.97 | 54.98 | 50.81 | 50.81 | 43.31 | 36.65 | 31.65 |
| 3pm | 42.48 | 43.31 | 41.65 | 39.98 | 36.65 | 31.65 | 28.32 |
| 4pm | 23.32 | 29.15 | 28.32 | 25.82 | 20.82 | 19.99 | 17.49 |
| 5pm | 11.66 | 14.99 | 12.33 | 11.66 | 9.16 | 6.66 | 5.83 |
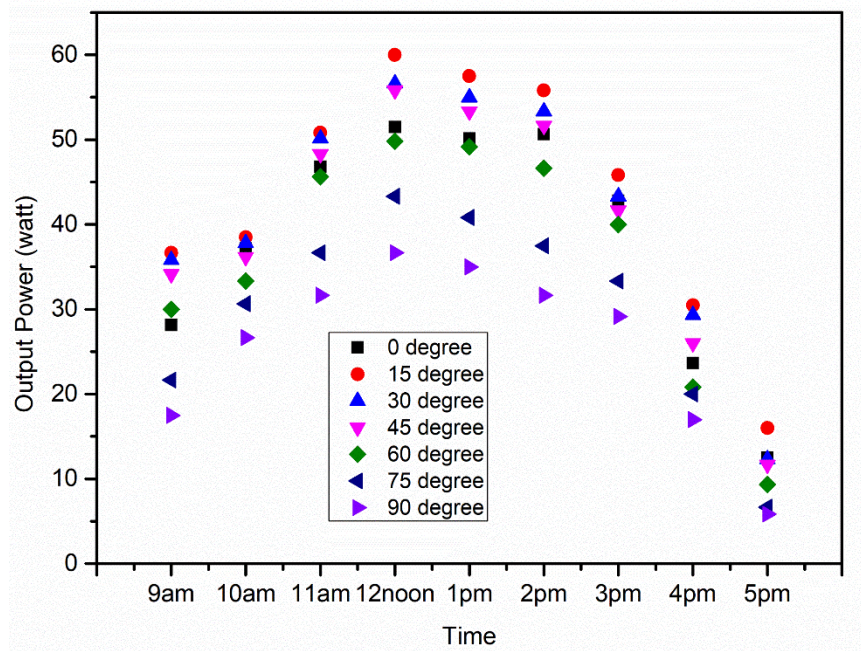
Figure 8.7 Variation of power output of PV panel throughout the day at different tilt angles
for day one
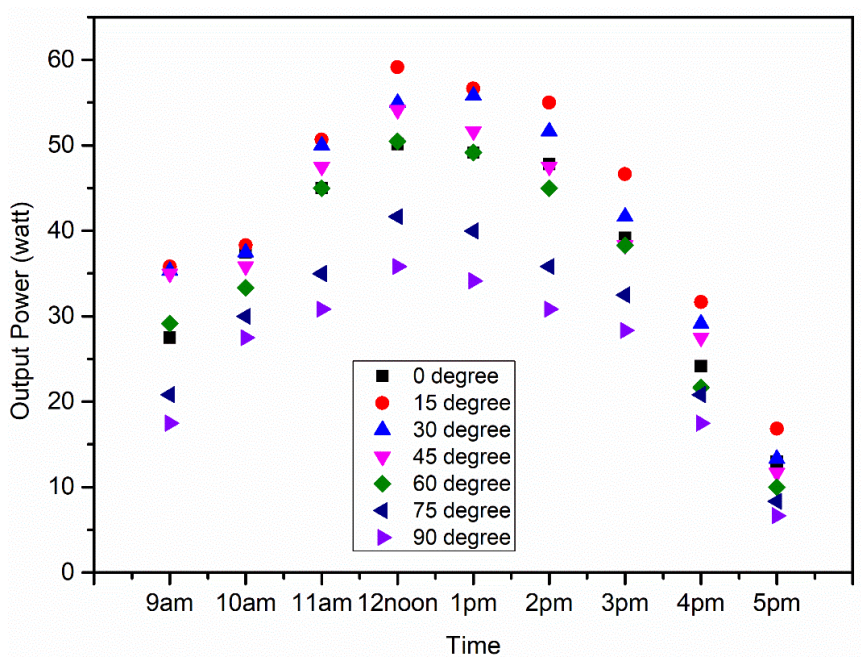


Figure 8.8 Variation of power output of PV panel throughout the day at different tilt angles
for day two
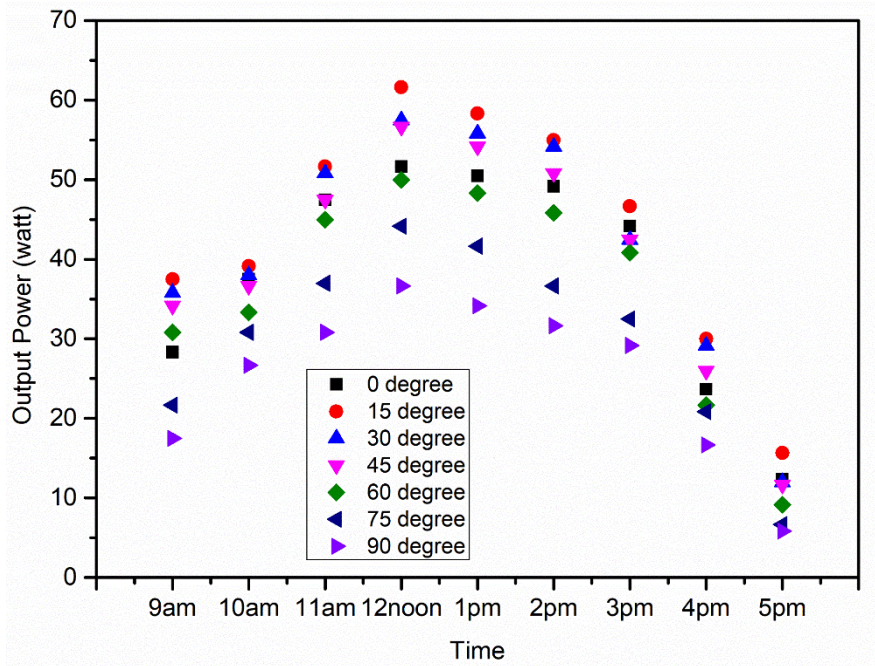
Figure 8.9 Variation of power output of PV panel throughout the day at different tilt angles
for day three
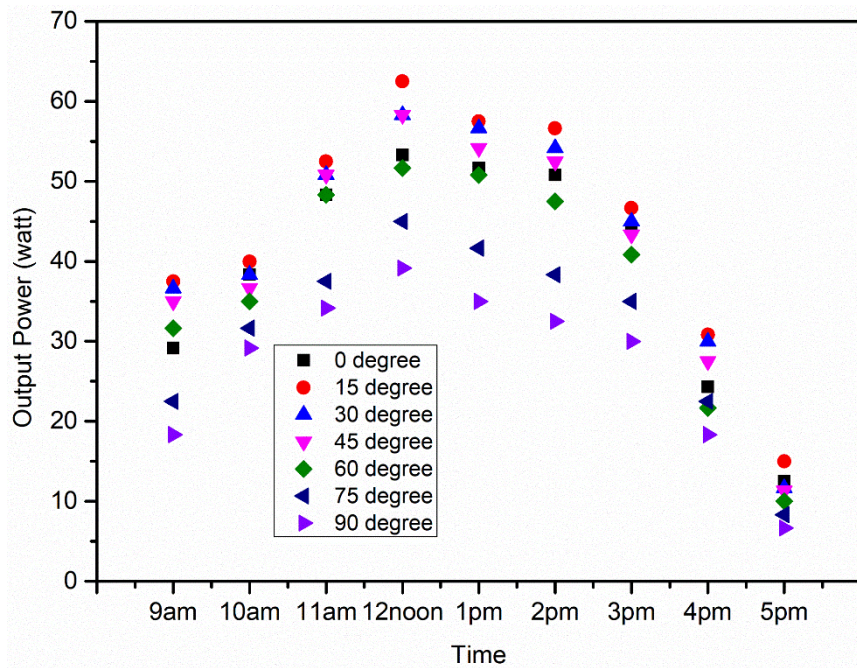


Figure 8.10 Variation of power output of PV panel throughout the day at different tilt angles
for day four

116
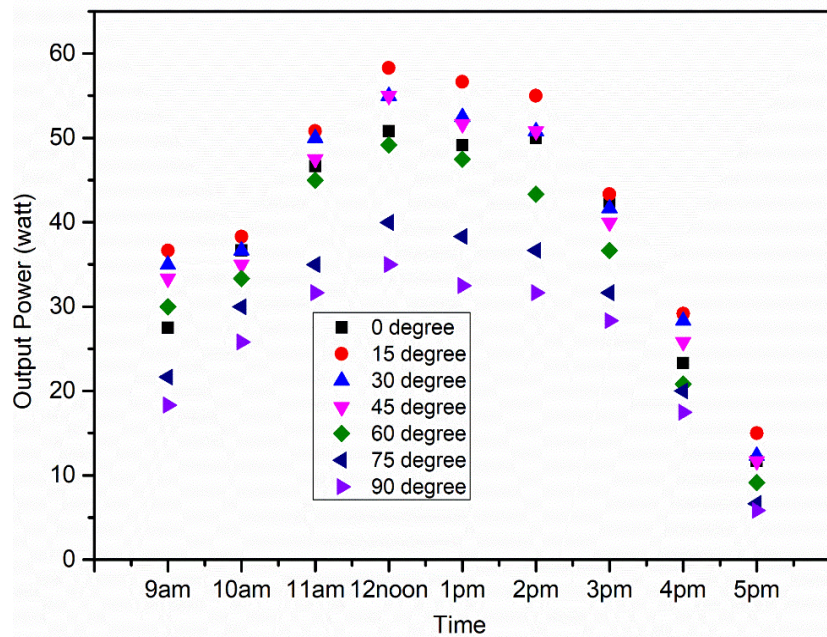
Figure 8.11 Variation of power output of PV panel throughout the day at different tilt angles for day five

As indicated in the Figure 8.1 to Figure 8.11, the maximum output power and solar radiation were obtained from the PV panel at 15° tilt angle, which is also the latitude of the site. Therefore, to receive maximum solar radiation on the panel surface and to extract maximum power from the PV panel, a tilt angle of 15° is recommended as the optimum tilt angle for this site.

# CHAPTER 9

# CONCLUSIONS AND SCOPE FOR FUTURE WORK

## 9.1 CONCLUSIONS

Laboratory experiments were carried out to investigate the effect of particle size of dust, dust pollutants type, shading, temperature and humidity on PV panel performance and also a field study was carried out exclusively to find the effect of dust on PV panel performance. The following conclusions were drawn from the laboratory and field studies:

- The shading on the panel surface affects its short circuit current and maximum power output more significantly when compared to its open circuit voltage. The present study shown that 100% shading of single cell of a 20 W polycrystalline PV panel reduced its short circuit current and maximum power output by 27.27% and 54.28%, respectively, whereas its open circuit voltage was reduced only by 5.00%.

- The present study also demonstrated that the performance degradation of poly crystalline PV panel is more severe when compared to mono crystalline PV panel under the same amount of shading condition. Under the same amount of shading (i.e., shading an area of 5.2 cm×2 cm) the percentage reduction in short circuit current of a 5 W mono and poly crystalline PV panels are 9.09% and 23.92%, respectively. Similarly, the reduction in open circuit voltage of mono and poly crystalline panels are 1.58% and 2.60%, respectively.

- Due to shading the reduction in power output in parallel panel configuration is low when compared to series panel configuration. Three identical 2.5 W polycrystalline PV panels connected in parallel configuration experienced 6.03% reduction due to shading when subjected to 108 Ω output load. Under the same output load and shading conditions, the reduction in power output was 16.54% when the PV panels were connected in series configuration.

- Due to the continuous shading of other cells in a (study carried out using a 20 W polycrystalline) panel the temperature of an un-shaded cell rises at the rate of 1.75% which can create a local hotspot problem in an un-shaded cell.

- The accumulation of dust mass on the PV panel surface reduces its short circuit current and maximum power output more significantly when compared to its open circuit voltage. As per laboratory study, the deposition of 3 gm (20.14 gm/m$^2$ dust density) of iron ore dust reduced short circuit current and maximum power output of PV panel respectively, by 12.50% and 14.54%, whereas the reduction in open circuit voltage was 2.33%, which is quite low compared to short circuit current and maximum power output. Similarly, for the deposition of 10gm (67.15 gm/m$^2$ dust density) of iron ore dust the reduction in short circuit current and maximum power output were respectively, 66.67% and 74.84%, and the reduction in open circuit voltage was only 10.88%. The results of this study reveal that the reduction in open circuit voltage due to dust deposition is not significant, until the layer of deposited dust completely shades the sun light falling on the panel surface.

- The reduction in short circuit current and maximum power output of a dusty panel when compared to a clean panel are respectively, 39.58% and 43.18%, after five days of its exposure to outside regime (in an iron ore mine). In five days, 12.86 gm of dust was deposited on the panel surface. However, the reduction in open circuit voltage was 4.35%, which is quite low when compared to short circuit current and maximum power output.

  From the field study it was also observed that there is an abrupt reduction in the normalised power output (i.e., 22.45% on first day) during the initial stage of dust deposition where as it slowdown in the later stages (i.e., 7.55% on second day, 5.73% on third day, 4.59% on fourth day and 2.88% on fifth day).

  To validate the field results a laboratory study was conducted, with 13gm of an iron ore dust deposition on the panel surface, which showed a reduction of 44% in short circuit current and 45.74% in maximum power output. This laboratory results corroborates with the field results. As stated above, in the laboratory condition also, the reduction in open circuit voltage was quite low (i.e.,5.47%).

- The relation between size of dust particle deposited on the panel surface and the respective reduction in solar radiation reaching the panel surface shows that the smaller size dust particles block the solar radiation more prominently compared to larger size dust particles. For example, dust particle size between 600 μ to less than 850 μ reduced the solar radiation by 12.14%, whereas the reduction was 42.50% with dust particle size less than 75 μ. Hence, this study shows that the smaller size dust particles affects the panel performance more significantly when compared to larger size dust particles.

- Among the three types of dust pollutants i.e., red soil dust, lime stone dust and iron ore dust, with 11 gm (73.87 gm/m$^2$ dust density) of dust deposition on the panel surface, the reduction in maximum power output was high with red soil dust deposition (reduction was 61.20%) which is followed by lime stone dust (reduction was 51.60%) and iron ore dust (reduction was 41.90%). The results of this study reveal that the performance of PV panel not only affected by the mass of dust deposition on its surface but it also influenced by the type of dust pollutants.

- The developed cleaning system for PV panel surface showed an increment in the short circuit current by 25.00%, open circuit voltage by 2.80% and maximum power output by 27.98% when compared to a dusty panel. However, this study has been carried out with the help of a laboratory scale set-up without its cost economics study.

- A study carried out in the laboratory shown that there was a difference of 6 °C in temperature between a clean and a dusty panel (with the deposition of 3 gm iron ore dust) after 10 minutes of their exposure to the solar radiation of intensity 1024 W/m$^2$. Under the same set of conditions, the temperature difference was 8 °C with 5 gm of dust deposition and 15 °C with 8 gm of dust deposition. This shows that the deposition of dust on the PV panel surface increases its surface temperature, which may create a hot spot on the cells (those covered by the dust layer), thus permanently damaging the cells of the panel.

- With the increase in panel surface temperature of a 5 W polycrystalline PV panel, from 35 ℃ to 75 ℃ (i.e., 40 ℃ increase), there was a remarkable reduction in open circuit voltage, maximum power output and fill factor by

15.46%, 29.12% and 19.60%, respectively. On the other hand, the short circuit current was increased by 4.17%. Though there was a slight increment in short circuit current the overall performance of the panel reduced with the increase in panel surface temperature.

Over and above, this study also demonstrated that the maximum power point (MPP) in the P-V curve moves towards the lower output voltage as the surface temperature of PV panel increases. As per literature, this movement of MPP disturbs the operation of solar charge controller, which reduces the overall performance of whole PV systems.

- In general, the increase in humidity level reduces the panel power output. There was 35.82% reduction in power output of a 20 W polycrystalline PV panel with the increase in relative humidity level from 65.40% to 98.20%. However, there was a small increment observed in open circuit voltage from 17.50 V to 17.76 V with increase in relative humidity level from 85.60% to 91.70%. This small increment in open circuit voltage is due to the intrusion of water droplets inside the glass of the panel.

- To receive maximum solar radiation on the panel surface and to extract maximum power from the PV panel a tilt angle of 15° is recommended as the optimum tilt angle for the site which was selected for this study.

## 9.2 SCOPE FOR FUTURE WORK

- The effective cooling mechanism may be developed to cool the PV panel surface so as to improve the performance of PV panel operated in high temperature condition.

- This work may be further extended by studying the temperature and humidity gradient on the panel performance.

- In the present study, a real time clock was used to activate the cleaning mechanism of the PV panel surface. This cleaning mechanism can be further sensitized by using dust sensors.

- A detailed techno-economic analysis of the proposed cleaning technique can be carried out to study the feasibility of the dust cleaning system.

# REFERENCES

Adinoyi, M. J., and Said, S. A. (2013). "Effect of dust accumulation on the power outputs of solar photovoltaic modules." *Renew. Energy*, 60, 633–636.

Ajao, K. R., Ambali, R. M., and Mahmoud, M. O. (2013). "Determination of the Optimal Tilt Angle for Solar Photovoltaic Panel in Ilorin, Nigeria." *J. Eng. Sci. Technol. Rev.*, 6(1), 87–90.

Al-Hasan, A. Y. (1998). "A new correlation for direct beam solar radiation received by photovoltaic panel with sand dust accumulated on its surface." *Sol. Energy*, 63(5), 323–333.

Al-Hasan, A. Y., and Ghoneim, A. A. (2005). "A new correlation between photovoltaic panel's efficiency and amount of sand dust accumulated on their surface." *Int. J. Sustain. Energy*, 24(4), 187–197.

Alonso-Garcia, M. C., Ruiz, J. M., and Chenlo, F. (2006). "Experimental study of mismatch and shading effects in the I–V characteristic of a photovoltaic module." *Sol. Energy Mater. Sol. Cells*, 90(3), 329–340.

Appels, R., Muthirayan, B., Beerten, A., Paesen, R., Driesen, J., and Poortmans, J. (2012). "The effect of dust deposition on photovoltaic modules." *Photovolt. Spec. Conf. PVSC 2012 38th IEEE*, IEEE, 001886–001889.

Arjyadhara, P., Ali, S. M., and Chitralekha, J. (2013). "Analysis of solar PV cell performance with changing irradiance and temperature." *Int. J. Eng. Comput. Sci.*, 2(1), 214–220.

Bahaidarah, H., Subhan, A., Gandhidasan, P., and Rehman, S. (2013). "Performance evaluation of a PV (photovoltaic) module by back surface water cooling for hot climatic conditions." *Energy*, 59, 445–453.

BAKHSH, H., and ITAKO, K. (2015). "Investigation of PV solar panel IV characteristics for real-time hot-spot detection system." *J. Adv. Sci.*, 27(1+ 2), 7–10.

Bayod-Rújula, A. A., Ortego-Bielsa, A., and Martínez-Gracia, A. (2011). "Photovoltaics on flat roofs: energy considerations." *Energy*, 36(4), 1996–2010.

Bishop, J. W. (1988). "Computer simulation of the effects of electrical mismatches in photovoltaic cell interconnection circuits." *Sol. Cells*, 25(1), 73–89.

Bruendlinger, R., Bletterie, B., Milde, M., and Oldenkamp, H. (2006). "Maximum power point tracking performance under partially shaded PV array conditions." *Proc 21st EUPVSEC*, 2157–2160.

Calabrò, E. (2013). "An algorithm to determine the optimum tilt angle of a solar panel from global horizontal solar radiation." J. Renew. Energy, 2013.

Carannante, G., Fraddanno, C., Pagano, M., and Piegari, L. (2009). "Experimental performance of MPPT algorithm for photovoltaic sources subject to inhomogeneous insolation." *IEEE Trans. Ind. Electron.*, 56(11), 4374–4380.

Central Electricity Authority of India Report, Energy Sector, P. (2016). "Government of India." *New Delhi*.

Chakrabarti, S., and Chakrabarti, S. (2002). "Rural electrification programme with solar energy in remote region–a case study in an island." *Energy Policy*, 30(1), 33–42.

Chander, S., Purohit, A., Sharma, A., Nehra, S. P., and Dhaka, M. S. (2015). "Impact of temperature on performance of series and parallel connected mono-crystalline silicon solar cells." *Energy Rep.*, 1, 175–180.

Chegaar, M., and Mialhe, P. (2008). "Effect of atmospheric parameters on the silicon solar cells performance." *J. Electron Devices*, 6(173–176).

Chueco-Fernández, F. J., and Bayod-Rújula, Á. A. (2010). "Power supply for pumping systems in northern Chile: photovoltaics as alternative to grid extension and diesel engines." *Energy*, 35(7), 2909–2921.

Contreras, M. A., Egaas, B., Ramanathan, K., Hiltner, J., Swartzlander, A., Hasoon, F., and Noufi, R. (1999). "Progress toward 20% efficiency in Cu (In, Ga) Se2 polycrystalline thin-film solar cells." *Prog. Photovolt. Res. Appl.*, 7(4), 311–316.

Darwish, Z. A., Kazem, H. A., Sopian, K., Al-Goul, M. A., and Alawadhi, H. (2015). "Effect of dust pollutant type on photovoltaic performance." *Renew. Sustain. Energy Rev.*, 41, 735–744.

Decker, B., and Jahn, U. (1997). "Performance of 170 grid connected PV plants in northern Germany—analysis of yields and optimization potentials." *Sol. Energy*, 59(4–6), 127–133.

Dincer, F. (2011). "The analysis on photovoltaic electricity generation status, potential and policies of the leading countries in solar energy." *Renew. Sustain. Energy Rev.*, 15(1), 713–720.

Dirnberger, D., Müller, B., and Reise, C. (2015). "On the uncertainty of energetic impact on the yield of different PV technologies due to varying spectral irradiance." *Sol. Energy*, 111, 82–96.

Dolara, A., Lazaroiu, G. C., Leva, S., and Manzolini, G. (2013). "Experimental investigation of partial shading scenarios on PV (photovoltaic) modules." *Energy*, 55, 466–475.

El Amrani, A., Mahrane, A., Moussa, F. Y., and Boukennous, Y. (2007). "Solar module fabrication." *Int. J. Photoenergy*, 2007.

Elminir, H. K., Ghitas, A. E., Hamid, R. H., El-Hussainy, F., Beheary, M. M., and Abdel-Moneim, K. M. (2006). "Effect of dust on the transparent cover of solar collectors." *Energy Convers. Manag.*, 47(18), 3192–3203.

El-Shobokshy, M. S., and Hussein, F. M. (1993). "Degradation of photovoltaic cell performance due to dust deposition on to its surface." *Renew. Energy*, 3(6–7), 585–590. El-Shobokshy, M. S., Mujahid, A., and Zakzouk, A. K. M. (1985). "Effects of dust on the performance of concentrator photovoltaic cells." *IEE Proc. Solid-State Electron Devices*, 132(1), 5–8.

Darlington, R. B., and Hayes, A. F. (2016). *Regression analysis and linear models: Concepts, applications, and implementation*. Guilford Publications.

Gandhi, T. A., Gupta, A., and Shyam, B. V. (2014). "Investigation of the effects of dust accumulation, and performance for mono and poly-crystalline silica modules." *Int. J. Renew. Energy Res.*, 4(3).

García, M. A., and Balenzategui, J. L. (2004). "Estimation of photovoltaic module yearly temperature and performance based on nominal operation cell temperature calculations." *Renew. Energy*, 29(12), 1997–2010.

Gevorkian, P. (2007). *Sustainable Energy System Engineering: The Complete Green Building Design Resource*. McGraw Hill Professional.

Ghitas, A. E. (2012). "Studying the effect of spectral variations intensity of the incident solar radiation on the Si solar cells performance." *NRIAG J. Astron. Geophys.*, 1(2), 165–171.

Goetzberger, A., Hebling, C., and Schock, H.-W. (2003). "Photovoltaic materials, history, status and outlook." *Mater. Sci. Eng. R Rep.*, 40(1), 1–46.

Gonzalez, C. C., Arnett, J. C., Ross, R. G., Spencer, R., and Weaver, R. W. (1984). "Determination of hot-spot susceptibility of multistring photovoltaic modules in a central-station application." *Conf Rec IEEE Photovolt. Spec ConfUnited States*, Jet Propulsion Laboratory, Pasadena, California.

Gouvêa, E. C., Sobrinho, P. M., and Souza, T. M. (2017). "Spectral Response of Polycrystalline Silicon Photovoltaic Cells under Real-Use Conditions." *Energies*, 10(8), 1178.

Green, M. A. (1982). "Solar cells: operating principles, technology, and system applications." Englewood Cliffs, NJ, Prentice-Hall, Inc., 1982. 288 p.

Green, M. A. (2002). "Photovoltaic principles." *Phys. E Low-Dimens. Syst. Nanostructures*, 14(1–2), 11–17.

Gwandu, B. A. L., and Creasey, D. J. (1995). "Humidity: a factor in the appropriate positioning of a photovoltaic power station." *Renew. Energy*, 6(3), 313–316.

Haeberlin, H., and Graf, J. D. (1998). "Gradual reduction of PV generator yield due to pollution." *Power W*, 1200, 1400.

Hammond, R., Srinivasan, D., Harris, A., Whitfield, K., and Wohlgemuth, J. (1997). "Effects of soiling on PV module and radiometer performance." *Photovolt. Spec. Conf. 1997 Conf. Rec. Twenty-Sixth IEEE*, IEEE, 1121–1124.

Hee, J. Y., Kumar, L. V., Danner, A. J., Yang, H., and Bhatia, C. S. (2012). "The effect of dust on transmission and self-cleaning property of solar panels." *Energy Procedia*, 15, 421–427.

Herrmann, W., Wiesner, W., and Vaassen, W. (1997). "Hot spot investigations on PV modules-new concepts for a test standard and consequences for module design with respect to bypass diodes." *Photovolt. Spec. Conf. 1997 Conf. Rec. Twenty-Sixth IEEE*, IEEE, 1129–1132.

Hirata, Y., and Tani, T. (1995). "Output variation of photovoltaic modules with environmental factors—I. The effect of spectral solar radiation on photovoltaic module output." *Sol. Energy*, 55(6), 463–468.

Ishaque, K., and Salam, Z. (2013). "A review of maximum power point tracking techniques of PV system for uniform insolation and partial shading condition." *Renew. Sustain. Energy Rev.*, 19, 475–488.

Jager-Waldau, A. (2011). "Progress in chalcopyrite compound semiconductor research for photovoltaic applications and transfer of results into actual solar cell production." *Sol. Energy Mater. Sol. Cells*, 95(6), 1509–1517.

Jiang, H., Lu, L., and Sun, K. (2011). "Experimental investigation of the impact of airborne dust deposition on the performance of solar photovoltaic (PV) modules." *Atmos. Environ.*, 45(25), 4299–4304.

Jones, G. G., and Bouamane, L. (2012). "'Power from Sunshine': A Business History of Solar Energy." Harvard Business School, working paper,12-105.

Kaldellis, J. K., Fragos, P., and Kapsali, M. (2011). "Systematic experimental study of the pollution deposition impact on the energy yield of photovoltaic installations." *Renew. Energy*, 36(10), 2717–2724.

Kaldellis, J. K., and Kapsali, M. (2011). "Simulating the dust effect on the energy performance of photovoltaic generators based on experimental measurements." *Energy*, 36(8), 5154–5161.

Kamanga, B., Mlatho, J. S. P., Mikeka, C., and Kamunda, C. (2014). "Optimum Tilt Angle for Photovoltaic Solar Panels in Zomba District, Malawi." *J. Sol. Energy*, 2014.

Kawamoto, H., and Shibata, T. (2015). "Electrostatic cleaning system for removal of sand from solar panels." *J. Electrost.*, 73, 65–70.

Kazem, H. A., Chaichan, M. T., Al-Shezawi, I. M., Al-Saidi, H. S., Al-Rubkhi, H. S., Al-sinani, K., and Al-Waeli, A. H. (2012). "Effect of Humidity on the PV Performance in Oman."

Khatib, T., Kazem, H., Sopian, K., Buttinger, F., Elmenreich, W., and Albusaidi, A. S. (2013). "Effect of dust deposition on the performance of multi-crystalline photovoltaic modules based on experimental measurements." *Int. J. Renew. Energy Res. IJRER*, 3(4), 850–853.

Kimber, A. (2007). "The effect of soiling on photovoltaic systems located in arid climates." *Proc. 22nd Eur. Photovolt. Sol. Energy Conf.*

Klugmann-Radziemska, E. (2015). "Degradation of electrical performance of a crystalline photovoltaic module due to dust deposition in northern Poland." *Renew. Energy*, 78, 418–426.

Krauter, S. (2004). "Increased electrical yield via water flow over the front of photovoltaic panels." *Sol. Energy Mater. Sol. Cells*, 82(1), 131–137.

Kumar, S., Bhattacharyya, B., and Gupta, V. K. (2014). "Present and Future Energy Scenario in India." *J. Inst. Eng. India Ser. B*, 95(3), 247–254.

Mani, M., and Pillai, R. (2010). "Impact of dust on solar photovoltaic (PV) performance: Research status, challenges and recommendations." *Renew. Sustain. Energy Rev.*, 14(9), 3124–3131.

Mazumder, M., Horenstein, M. N., Stark, J. W., Girouard, P., Sumner, R., Henderson, B., Sadder, O., Hidetaka, I., Biris, A. S., and Sharma, R. (2013). "Characterization of electrodynamic screen performance for dust removal from solar panels and solar hydrogen generators." *IEEE Trans. Ind. Appl.*, 49(4), 1793–1800.

Mekhilef, S., Saidur, R., and Safari, A. (2011). "A review on solar energy use in industries." *Renew. Sustain. Energy Rev.*, 15(4), 1777–1790.

Mekhilef, S., Saidur, R., and Kamalisarvestani, M. (2012). "Effect of dust, humidity and air velocity on efficiency of photovoltaic cells." *Renew. Sustain. Energy Rev.*, 16(5), 2920–2925.

Mekhilef, S., Saidur, R., and Kamalisarvestani, M. (2012). "Effect of dust, humidity and air velocity on efficiency of photovoltaic cells." *Renew. Sustain. Energy Rev.*, 16(5), 2920–2925.

Merten, J., Voz, C., Munoz, A., Asensi, J. M., and Andreu, J. (1999). "The role of the buffer layer in the light of a new equivalent circuit for amorphous silicon solar cells." *Sol. Energy Mater. Sol. Cells*, 57(2), 153–165.

Mhlongo, S. E., and Amponsah-Dacosta, F. (2016). "A review of problems and solutions of abandoned mines in South Africa." *Int. J. Min. Reclam. Environ.*, 30(4), 279–294.

Migan, G.-A. (2013). "Study the operating temperature of a PV module." *Proj. Rep.*

Mohamed, A. O., and Hasan, A. (2012). "Effect of dust accumulation on performance of photovoltaic solar modules in Sahara environment." *J. Basic Appl. Sci. Res.*, 2(11), 11030–11036.

Mohanty, P., Muneer, T., Gago, E. J., and Kotak, Y. (2016). "Solar radiation fundamentals and PV system components." *Sol. Photovolt. Syst. Appl.*, Springer, 7–47.

Molenbroek, E., Waddington, D. W., and Emery, K. A. (1991). "Hot spot susceptibility and testing of PV modules." *Photovolt. Spec. Conf. 1991 Conf. Rec. Twenty Second IEEE*, IEEE, 547–552.

Mukerjee, A. K., and Thakur, N. (2011). *Photovoltaic systems: analysis and design*. PHI Learning Pvt. Ltd, New Delhi.

Nadh, G. A., Vijay, S., and Gupta, A. (2014). "Investigation on the effects of dust accumulation, transmittace on glass plates and performance of mono and poly crystalline silica modules." *Int. J. Renew. Energy Res. IJRER*, 4(3), 628–634.

Ndiaye, A., Kébé, C. M., Ndiaye, P. A., Charki, A., Kobi, A., and Sambou, V. (2013). "Impact of dust on the photovoltaic (PV) modules characteristics after an exposition year in Sahelian environment: The case of Senegal." *Int. J. Phys. Sci.*, 8(21), 1166–1173.

Oliver, M., and Jackson, T. (2001). "Energy and economic evaluation of building-integrated photovoltaics." *Energy*, 26(4), 431–439.

Ozturk, I., Aslan, A., and Kalyoncu, H. (2010). "Energy consumption and economic growth relationship: Evidence from panel data for low and middle income countries." *Energy Policy*, 38(8), 4422–4428.

Panjwani, M. K., and Narejo, G. B. (2014). "Effect of Humidity on the Efficiency of Solar Cell (photovoltaic)." *Int. J. Eng. Res. Gen. Sci.*, 2(4), 499–503.

Patel, H., and Agarwal, V. (2008a). "Maximum power point tracking scheme for PV systems operating under partially shaded conditions." *IEEE Trans. Ind. Electron.*, 55(4), 1689–1698.

Patel, H., and Agarwal, V. (2008b). "MATLAB-based modeling to study the effects of partial shading on PV array characteristics." *IEEE Trans. Energy Convers.*, 23(1), 302–310.

Pavan, A. M., Mellit, A., and De Pieri, D. (2011). "The effect of soiling on energy production for large-scale photovoltaic plants." *Sol. Energy*, 85(5), 1128–1136. "Photovoltaic (PV) - Electrical Calculations." (n.d.). <http://myelectrical.com/notes/entryid/225/photovoltaic-pv-electrical-calculations> (Dec. 25, 2017).

Radziemska, E. (2003). "The effect of temperature on the power drop in crystalline silicon solar cells." *Renew. Energy*, 28(1), 1–12.

Rahman, M. M., Hasanuzzaman, M., and Rahim, N. A. (2014). "Temperature effect of photovoltaic module under partial shading operation condition."

Rajput, D. S., and Sudhakar, K. (2013). "Effect of dust on the performance of solar PV panel." *Int J ChemTech Res*, 5(2), 1083–6.

Ramabadran, R., and Mathur, B. (2009). "Effect of shading on series and parallel connected solar PV modules." *Mod. Appl. Sci.*, 3(10), 32.

Ranade, M. B. (1987). "Adhesion and removal of fine particles on surfaces." *Aerosol Sci. Technol.*, 7(2), 161–176.

Rosyid, O. A. (2016). "Comparative performance testing of photovoltaic modules in tropical climates of Indonesia." *AIP Conf. Proc.*, AIP Publishing, 020004.

Said, S. A., and Walwil, H. M. (2014). "Fundamental studies on dust fouling effects on PV module performance." *Sol. Energy*, 107, 328–337.

Saidan, M., Albaali, A. G., Alasis, E., and Kaldellis, J. K. (2016). "Experimental study on the effect of dust deposition on solar photovoltaic panels in desert environment." *Renew. Energy*, 92, 499–505.

Sayigh, A. (2009). "Withdrawn: Worldwide progress in renewable energy." *Renew. Energy*.

Sayyah, A., Horenstein, M. N., and Mazumder, M. K. (2014). "Energy yield loss caused by dust deposition on photovoltaic panels." *Sol. Energy*, 107, 576–604.
Sera, D., and Baghzouz, Y. (2008). "On the impact of partial shading on PV output power." *WSEASIASME Int. Conf. Renew. Energy Sources RES08*.

Shah, A., Torres, P., Tscharner, R., Wyrsch, N., and Keppner, H. (1999). "Photovoltaic Technology: The Case for Thin-Film Solar Cells." *Science*, 285(5428), 692–698.

Siddiqui, R., and Bajpai, U. (2012). "Correlation between thicknesses of dust collected on photovoltaic module and difference in efficiencies in composite climate." *Int. J. Energy Environ. Eng.*, 3(1), 26.

Silvestre, S., and Chouder, A. (2008). "Effects of shadowing on photovoltaic module performance." *Prog. Photovolt. Res. Appl.*, 16(2), 141–149.

Simon, J., and Mosey, G. (n.d.). *Feasibility Study of Economics and Performance of Solar Photovoltaics at the VAG Mine Site in Eden and Lowell*. Vermont.
Solanki, C. S. (2015). *Solar photovoltaics: fundamentals, technologies and applications*. PHI Learning Pvt. Ltd.

"Solar cell." (2017). *Wikipedia*, https://en.wikipedia.org/wiki/Solar_cell. (Nov. 15,2017).

Song, J., and Choi, Y. (2015). "Design of photovoltaic systems to power aerators for natural purification of acid mine drainage." *Renew. Energy*, 83, 759–766.

Song, J., and Choi, Y. (2016). "Analysis of wind power potentials at abandoned mine promotion districts in Korea." *Geosystem Eng.*, 19(2), 77–82.

Song, J., Choi, Y., and Yoon, S.-H. (2015). "Analysis of photovoltaic potential at abandoned mine promotion districts in Korea." *Geosystem Eng.*, 18(3), 168–172.

Sukhatme, K., and Sukhatme, S. P. (1996). *Solar energy: principles of thermal collection and storage*. Tata McGraw-Hill Education.

Sulaiman, S. A., Singh, A. K., Mokhtar, M. M. M., and Bou-Rabee, M. A. (2014). "Influence of dirt accumulation on performance of PV panels." *Energy Procedia*, 50, 50–56.

Sun, Y., Chen, S., Xie, L., Hong, R., and Shen, H. (2014). "Investigating the impact of shading effect on the characteristics of a large-scale grid-connected PV power plant in northwest china." *Int. J. Photoenergy*, 2014.
Tabish, S., and Ashraf, I. (2017). "Simulation of partial shading on solar photovoltaic modules with experimental verification." *Int. J. Ambient Energy*, 38(2), 161–170.

Tan, C. M., Chen, B. K. E., and Toh, K. P. (2010). "Humidity study of a-Si PV cell." *Microelectron. Reliab.*, 50(9), 1871–1874.

Tejwani, R., and Solanki, C. S. (2010). "360 sun tracking with automated cleaning system for solar PV modules." *Photovolt. Spec. Conf. PVSC 2010 35th IEEE*, IEEE, 002895–002898.

Tian, W., Wang, Y., Ren, J., and Zhu, L. (2007). "Effect of urban climate on building integrated photovoltaics performance." *Energy Convers. Manag.*, 48(1), 1–8.

Tripathi, A. K. (2014). "Application of Solar Energy for Lighting in Opencast Mines." MTech thesis, National Institute of Technology Rourkela, India.

Tripathi, A. K., Aruna, M., and Murthy, S. N. (2017). "Performance Evaluation of PV Panel Under Dusty Condition." *Int. J. Renew. Energy Dev.*, 6(3), 225.

Tripathi, A. K., Aruna, M., and Murthy, Ch. S.N. (2017). "Performance of a PV panel under different shading strengths." *Int. J. Ambient Energy*, 1–6.

Topp, R., and Gómez, G. (2004). "Residual analysis in linear regression models with an interval-censored covariate." *Stat. Med.*, 23(21), 3377–3391.

Van Sark, W., Brandsen, G. W., Fleuster, M., and Hekkert, M. P. (2007). "Analysis of the silicon market: Will thin films profit?" *Energy Policy*, 35(6), 3121–3125.

Vengatesh, R. P., and Rajan, S. E. (2016). "Analysis of PV module connected in different configurations under uniform and non-uniform solar radiations." *Int. J. Green Energy*, 13(14), 1507–1516.

Vergura, S., Acciani, G., and Falcone, O. (2012). "A finite-element approach to analyze the thermal effect of defects on silicon-based PV cells." *IEEE Trans. Ind. Electron.*, 59(10), 3860–3867.

Villalva, M. G., Gazoli, J. R., and Ruppert Filho, E. (2009). "Comprehensive approach to modeling and simulation of photovoltaic arrays." *IEEE Trans. Power Electron.*, 24(5), 1198–1208.
Virtuani, A., Pavanello, D., and Friesen, G. (2010). "Overview of temperature coefficients of different thin film photovoltaic technologies." *5th World Conf. Photovolt. Energy Convers.*, 6–10.

Vlahinić-Dizdarević, N., and Žiković, S. (2010). "The role of energy in economic growth: the case of Croatia." *Zb. Rad. Ekon. Fak. U Rijeci Časopis Za Ekon. Teor. Praksu*, 28(1), 35–60.

Weller, B., Hemmerle, C., Jakubetz, S., and Unnewehr, S. (2010). *Detail Practice: Photovoltaics: Technology, Architecture, Installation*. Walter de Gruyter.
Wu, X. (2004). "High-efficiency polycrystalline CdTe thin-film solar cells." *Sol. Energy*, 77(6), 803–814.

Zabel, G., and Economics, E. (2009). "Peak People: The Interrelationship between Population Growth and Energy Resources." *Energy Bull.*, 20.

Zegaoui, A., Petit, P., Aillerie, M., Sawicki, J. P., Belarbi, A. W., Krachai, M. D., and Charles, J. P. (2011). "Photovoltaic cell/panel/array characterizations and modeling considering both reverse and direct modes." *Energy Procedia*, 6, 695–703.

Zorrilla-Casanova, J., Piliougine, M., Carretero, J., Bernaola-Galván, P., Carpena, P., Mora-López, L., and Sidrach-de-Cardona, M. (2013). "Losses produced by soiling in the incoming radiation to photovoltaic modules." *Prog. Photovolt. Res. Appl.*, 21(4), 790–796.

# APPENDIX-I

Table 4.1 Values of electrical parameters of PV panel under 449.58 W/m$^2$

| Voltage (volt) | Current (amp) | Power (watt) |
|----------------|---------------|--------------|
| 0 | 0.27 | 0 |
| 7.9 | 0.23 | 1.817 |
| 10.6 | 0.25 | 2.65 |
| 13 | 0.23 | 2.99 |
| 15.55 | 0.22 | 3.421 |
| 16.3 | 0.2 | 3.26 |
| 17.67 | 0.16 | 2.8272 |
| 18.1 | 0.13 | 2.353 |
| 18.5 | 0.1 | 1.85 |
| 18.6 | 0.08 | 1.488 |
| 18.7 | 0.05 | 0.935 |
| 18.85 | 0 | 0 |

Table 4.2 Values of electrical parameters of PV panel under 516.22 W/m$^2$

| Voltage (volt) | Current (amp) | Power (watt) |
|----------------|---------------|--------------|
| 0 | 0.31 | 0 |
| 7.9 | 0.3 | 2.37 |
| 10.6 | 0.29 | 3.074 |
| 13 | 0.27 | 3.51 |
| 15.55 | 0.24 | 3.732 |
| 16.3 | 0.22 | 3.586 |
| 17.67 | 0.2 | 3.534 |
| 18.1 | 0.19 | 3.439 |
| 18.5 | 0.17 | 3.145 |
| 18.6 | 0.16 | 2.976 |
| 18.8 | 0.14 | 2.632 |
| 18.9 | 0.1 | 1.89 |
| 19 | 0.08 | 1.52 |
| 19.1 | 0.06 | 1.146 |
| 19.15 | 0 | 0 |

Table 4.3 Values of electrical parameters of PV panel under 593.70 W/m$^2$

| Voltage (volt) | Current (amp) | Power (watt) |
|----------------|---------------|--------------|
| 0.00 | 0.35 | 0 |
| 7.90 | 0.34 | 2.686 |
| 10.60 | 0.32 | 3.392 |
| 13.00 | 0.30 | 3.9 |
| 15.55 | 0.28 | 4.354 |

| | | |
|---|---|---|
| 16.30 | 0.26 | 4.238 |
| 17.67 | 0.23 | 4.0641 |
| 18.10 | 0.21 | 3.801 |
| 18.50 | 0.19 | 3.515 |
| 18.60 | 0.18 | 3.348 |
| 18.80 | 0.17 | 3.196 |
| 18.90 | 0.15 | 2.835 |
| 19.00 | 0.13 | 2.47 |
| 19.10 | 0.11 | 2.101 |
| 19.15 | 0.09 | 1.7235 |
| 19.25 | 0.07 | 1.3475 |
| 19.35 | 0.00 | 0 |

Table 4.4 Values of electrical parameters of PV panel under 608.66 W/m$^2$

| Voltage (volt) | Current (amp) | Power (watt) |
|---|---|---|
| 0 | 0.37 | 0 |
| 7.9 | 0.35 | 2.765 |
| 10.6 | 0.34 | 3.604 |
| 13 | 0.33 | 4.29 |
| 15.55 | 0.32 | 4.976 |
| 17.67 | 0.26 | 4.5942 |
| 18.1 | 0.22 | 3.982 |
| 18.5 | 0.17 | 3.145 |
| 18.6 | 0.15 | 2.79 |
| 18.8 | 0.13 | 2.444 |
| 18.9 | 0.12 | 2.268 |
| 19 | 0.11 | 2.09 |
| 19.1 | 0.1 | 1.91 |
| 19.15 | 0.09 | 1.7235 |
| 19.25 | 0.08 | 1.54 |
| 19.35 | 0.06 | 1.161 |
| 19.5 | 0 | 0 |

Table 4.5 Values of electrical parameters of PV panel under 661.51 W/m$^2$

| Voltage (volt) | Current (amp) | Power (watt) |
|---|---|---|
| 0 | 0.39 | 0 |
| 7.9 | 0.38 | 3.002 |
| 10.6 | 0.37 | 3.922 |
| 13 | 0.35 | 4.55 |

| | | |
|---|---|---|
| 15.55 | 0.33 | 5.1315 |
| 16.3 | 0.3 | 4.89 |
| 17.67 | 0.27 | 4.7709 |
| 18.1 | 0.25 | 4.525 |
| 18.5 | 0.22 | 4.07 |
| 18.6 | 0.21 | 3.906 |
| 18.8 | 0.19 | 3.572 |
| 18.9 | 0.18 | 3.402 |
| 19 | 0.17 | 3.23 |
| 19.1 | 0.15 | 2.865 |
| 19.15 | 0.14 | 2.681 |
| 19.25 | 0.13 | 2.5025 |
| 19.35 | 0.12 | 2.322 |
| 19.5 | 0.11 | 2.145 |
| 19.7 | 0.1 | 1.97 |
| 19.8 | 0.08 | 1.584 |
| 19.95 | 0 | 0 |

Table 4.6 Values of electrical parameters of PV panel under 719.60 W/m$^2$

| Voltage (volt) | Current (amp) | Power (watt) |
|---|---|---|
| 0 | 0.44 | 0 |
| 7.9 | 0.43 | 3.397 |
| 10.6 | 0.42 | 4.452 |
| 13 | 0.4 | 5.2 |
| 15.55 | 0.37 | 5.7535 |
| 17.67 | 0.35 | 6.1845 |
| 18.1 | 0.33 | 5.973 |
| 18.5 | 0.31 | 5.735 |
| 18.6 | 0.29 | 5.394 |
| 18.8 | 0.26 | 4.888 |
| 18.9 | 0.23 | 4.347 |
| 19 | 0.21 | 3.99 |
| 19.1 | 0.19 | 3.629 |
| 19.15 | 0.18 | 3.447 |
| 19.25 | 0.16 | 3.08 |
| 19.35 | 0.14 | 2.709 |
| 19.5 | 0.12 | 2.34 |
| 19.7 | 0.1 | 1.97 |
| 19.85 | 0.08 | 1.588 |
| 20 | 0.06 | 1.2 |
| 20.1 | 0 | 0 |

Table 4.7 Values of electrical parameters of PV panel under 750.50 W/m$^2$

| Voltage (volt) | Current (amp) | Power (watt) |
|---|---|---|
| 0 | 0.48 | 0 |
| 7.9 | 0.47 | 3.713 |
| 10.6 | 0.46 | 4.876 |
| 13 | 0.44 | 5.72 |
| 15.55 | 0.42 | 6.531 |
| 17.67 | 0.38 | 6.7146 |
| 18.1 | 0.36 | 6.516 |
| 18.5 | 0.33 | 6.105 |
| 18.6 | 0.31 | 5.766 |
| 18.8 | 0.29 | 5.452 |
| 18.9 | 0.27 | 5.103 |
| 19 | 0.24 | 4.56 |
| 19.1 | 0.22 | 4.202 |
| 19.15 | 0.21 | 4.0215 |
| 19.25 | 0.18 | 3.465 |
| 19.35 | 0.16 | 3.096 |
| 19.5 | 0.14 | 2.73 |
| 19.7 | 0.12 | 2.364 |
| 19.85 | 0.11 | 2.1835 |
| 20 | 0.08 | 1.6 |
| 20.15 | 0.06 | 1.209 |
| 20.3 | 0 | 0 |

Table 4.8 Values of electrical parameters of PV panel under 788.50 W/m$^2$

| Voltage (volt) | Current (amp) | Power (watt) |
|---|---|---|
| 0 | 0.49 | 0 |
| 7.9 | 0.48 | 3.792 |
| 10.6 | 0.47 | 4.982 |
| 13 | 0.45 | 5.85 |
| 15.55 | 0.43 | 6.6865 |
| 16.3 | 0.41 | 6.683 |
| 17.67 | 0.39 | 6.8913 |
| 18.1 | 0.37 | 6.697 |
| 18.5 | 0.35 | 6.475 |
| 18.6 | 0.34 | 6.324 |
| 18.8 | 0.32 | 6.016 |

| | | |
|---|---|---|
| 18.9 | 0.31 | 5.859 |
| 19 | 0.3 | 5.7 |
| 19.1 | 0.29 | 5.539 |
| 19.15 | 0.28 | 5.362 |
| 19.25 | 0.27 | 5.1975 |
| 19.35 | 0.25 | 4.8375 |
| 19.5 | 0.22 | 4.29 |
| 19.7 | 0.21 | 4.137 |
| 19.85 | 0.19 | 3.7715 |
| 20 | 0.17 | 3.4 |
| 20.15 | 0.16 | 3.224 |
| 20.3 | 0.14 | 2.842 |
| 20.4 | 0.11 | 2.244 |
| 20.5 | 0.08 | 1.64 |
| 20.6 | 0 | 0 |

Table 4.9 Values of electrical parameters of PV panel under 878.67 W/m$^2$

| Voltage (volt) | Current (amp) | Power (watt) |
|---|---|---|
| 0 | 0.54 | 0 |
| 7.9 | 0.53 | 4.187 |
| 10.6 | 0.52 | 5.512 |
| 13 | 0.48 | 6.24 |
| 15.55 | 0.46 | 7.153 |
| 17.67 | 0.41 | 7.2447 |
| 18.1 | 0.38 | 6.878 |
| 18.5 | 0.35 | 6.475 |
| 18.6 | 0.32 | 5.952 |
| 18.8 | 0.29 | 5.452 |
| 18.9 | 0.26 | 4.914 |
| 19 | 0.22 | 4.18 |
| 19.1 | 0.2 | 3.82 |
| 19.15 | 0.19 | 3.6385 |
| 19.25 | 0.18 | 3.465 |
| 19.35 | 0.17 | 3.2895 |
| 19.5 | 0.16 | 3.12 |
| 19.7 | 0.15 | 2.955 |
| 19.85 | 0.14 | 2.779 |
| 20 | 0.13 | 2.6 |
| 20.15 | 0.12 | 2.418 |

| | | |
|---|---|---|
| 20.3 | 0.11 | 2.233 |
| 20.5 | 0.09 | 1.845 |
| 20.6 | 0.06 | 1.236 |
| 20.75 | 0 | 0 |

Table 4.10 Values of electrical parameters of PV panel under 918.10 W/m$^2$

| Voltage (volt) | Current (amp) | Power (watt) |
|---|---|---|
| 0 | 0.63 | 0 |
| 7.9 | 0.62 | 4.898 |
| 10.6 | 0.61 | 6.466 |
| 13 | 0.58 | 7.54 |
| 15.55 | 0.55 | 8.5525 |
| 16.3 | 0.51 | 8.313 |
| 17.67 | 0.48 | 8.4816 |
| 18.1 | 0.46 | 8.326 |
| 18.5 | 0.41 | 7.585 |
| 18.6 | 0.38 | 7.068 |
| 18.8 | 0.35 | 6.58 |
| 18.9 | 0.33 | 6.237 |
| 19 | 0.3 | 5.7 |
| 19.1 | 0.27 | 5.157 |
| 19.15 | 0.26 | 4.979 |
| 19.25 | 0.24 | 4.62 |
| 19.35 | 0.21 | 4.0635 |
| 19.5 | 0.2 | 3.9 |
| 19.7 | 0.18 | 3.546 |
| 19.8 | 0.16 | 3.168 |
| 19.95 | 0.15 | 2.9925 |
| 20.15 | 0.14 | 2.821 |
| 20.3 | 0.13 | 2.639 |
| 20.4 | 0.12 | 2.448 |
| 20.5 | 0.1 | 2.05 |
| 20.6 | 0.09 | 1.854 |
| 20.75 | 0.06 | 1.245 |
| 20.95 | 0 | 0 |

# APPENDIX-II

Table 5.2 Values of electrical responses of PV panel under no shading condition

| Voltage (volt) | Current (amp) | Power (watt) |
|---|---|---|
| 0 | 0.44 | 0 |
| 5.00 | 0.42 | 2.1 |
| 12.90 | 0.4 | 5.16 |
| 15.80 | 0.36 | 5.68 |
| 16.17 | 0.36 | 5.82 |
| 16.55 | 0.35 | 5.84 |
| 16.96 | 0.35 | 5.93 |
| 17.10 | 0.34 | 5.81 |
| 17.28 | 0.34 | 5.87 |
| 17.42 | 0.32 | 5.57 |
| 17.74 | 0.32 | 5.67 |
| 17.86 | 0.31 | 5.53 |
| 18.04 | 0.27 | 4.87 |
| 18.46 | 0.2 | 3.69 |
| 18.90 | 0.12 | 2.26 |
| 19.00 | 0.09 | 1.71 |
| 19.12 | 0.06 | 1.14 |
| 20.00 | 0 | 0 |

Table 5.3 Values of electrical responses of PV panel under 25% shading strength condition of panel shading

| Voltage (volt) | Current (amp) | Power (watt) |
|---|---|---|
| 0 | 0.19 | 0 |
| 5.00 | 0.18 | 0.90 |
| 12.90 | 0.16 | 2.06 |
| 15.80 | 0.14 | 2.21 |
| 16.17 | 0.14 | 2.26 |
| 16.55 | 0.13 | 2.15 |
| 16.96 | 0.12 | 2.03 |
| 17.10 | 0.12 | 2.05 |
| 17.28 | 0.11 | 1.90 |
| 17.42 | 0.11 | 1.91 |
| 17.74 | 0.08 | 1.41 |
| 17.86 | 0.07 | 1.25 |
| 18.04 | 0.05 | 0.90 |
| 18.46 | 0 | 0 |
| 18.90 | 0 | 0 |
| 19.00 | 0 | 0 |
| 19.12 | 0 | 0 |
| 20.00 | 0 | 0 |

Table 5.4 Values of electrical responses of PV panel under 50% shading strength condition of panel shading

| Voltage (volt) | Current (amp) | Power (watt) |
|---|---|---|
| 0 | 0.15 | 0 |
| 5.00 | 0.13 | 0.65 |
| 12.90 | 0.12 | 1.55 |
| 15.80 | 0.11 | 1.74 |
| 16.17 | 0.1 | 1.62 |
| 16.55 | 0.09 | 1.49 |
| 16.96 | 0.07 | 1.19 |
| 17.10 | 0.06 | 1.02 |
| 17.28 | 0.05 | 0.86 |
| 17.42 | 0 | 0 |
| 17.74 | 0 | 0 |
| 17.86 | 0 | 0 |
| 18.04 | 0 | 0 |
| 18.46 | 0 | 0 |
| 18.90 | 0 | 0 |
| 19.00 | 0 | 0 |
| 19.12 | 0 | 0 |
| 20.00 | 0 | 0 |

Table 5.5 Values of electrical responses of PV panel under 75% shading strength condition of panel shading

| Voltage (volt) | Current (amp) | Power (watt) |
|---|---|---|
| 0 | 0.12 | 0 |
| 5.00 | 0.11 | 0.55 |
| 12.90 | 0.1 | 1.29 |
| 15.80 | 0.1 | 1.58 |
| 16.17 | 0.09 | 1.46 |
| 16.55 | 0.08 | 1.32 |
| 16.96 | 0.06 | 1.02 |
| 17.10 | 0.05 | 0.86 |
| 17.28 | 0 | 0 |
| 17.42 | 0 | 0 |
| 17.74 | 0 | 0 |
| 17.86 | 0 | 0 |
| 18.04 | 0 | 0 |
| 18.46 | 0 | 0 |
| 18.90 | 0 | 0 |
| 19.00 | 0 | 0 |

| | | |
|---|---|---|
| 19.12 | 0 | 0 |
| 20.00 | 0 | 0 |

Table 5.6 Values of electrical responses of PV panel under 25% shading strength
condition of single cell

| Voltage (volt) | Current (amp) | Power (watt) |
|---|---|---|
| 0 | 0.42 | 0 |
| 5.00 | 0.40 | 2 |
| 12.90 | 0.36 | 4.644 |
| 16.60 | 0.31 | 5.146 |
| 17.42 | 0.27 | 4.7034 |
| 17.70 | 0.23 | 4.071 |
| 18.00 | 0.21 | 3.78 |
| 18.10 | 0.19 | 3.439 |
| 18.20 | 0.17 | 3.094 |
| 18.40 | 0.15 | 2.76 |
| 18.70 | 0.13 | 2.431 |
| 19.00 | 0.1 | 1.9 |
| 19.20 | 0.08 | 1.536 |
| 19.30 | 0.05 | 0.965 |
| 19.40 | 0 | 0 |
| 20.00 | 0 | 0 |

Table 5.7 Values of electrical responses of PV panel under 50% shading strength
condition of single cell

| Voltage (volt) | Current (amp) | Power (watt) |
|---|---|---|
| 0 | 0.40 | 0 |
| 5.00 | 0.32 | 1.60 |
| 12.90 | 0.28 | 3.61 |
| 16.60 | 0.26 | 4.32 |
| 17.42 | 0.2 | 3.48 |
| 17.70 | 0.18 | 3.19 |
| 18.00 | 0.17 | 3.06 |
| 18.10 | 0.15 | 2.72 |
| 18.20 | 0.13 | 2.37 |
| 18.40 | 0.11 | 2.02 |
| 18.70 | 0.1 | 1.87 |
| 19.00 | 0.08 | 1.52 |
| 19.20 | 0.05 | 0.96 |
| 19.30 | 0 | 0 |
| 19.40 | 0 | 0 |

| | | |
|---|---|---|
| 20.00 | 0 | 0 |

Table 5.8 Values of electrical responses of PV panel under 75% shading strength condition of single cell

| Voltage (volt) | Current (amp) | Power (watt) |
|---|---|---|
| 0 | 0.38 | 0 |
| 5.00 | 0.28 | 1.40 |
| 12.90 | 0.25 | 3.23 |
| 16.60 | 0.21 | 3.49 |
| 17.42 | 0.18 | 3.14 |
| 17.70 | 0.16 | 2.83 |
| 18.00 | 0.14 | 2.52 |
| 18.10 | 0.12 | 2.17 |
| 18.20 | 0.11 | 2.01 |
| 18.40 | 0.09 | 1.66 |
| 18.70 | 0.08 | 1.50 |
| 19.00 | 0.06 | 1.14 |
| 19.20 | 0 | 0 |
| 19.30 | 0 | 0 |
| 19.40 | 0 | 0 |
| 20.00 | 0 | 0 |

Table 5.9 Values of electrical responses of PV panel under 100% shading strength condition of single cell

| Voltage (volt) | Current (amp) | Power (watt) |
|---|---|---|
| 0 | 0.32 | 0 |
| 5.00 | 0.2 | 1 |
| 12.90 | 0.17 | 2.19 |
| 16.60 | 0.16 | 2.66 |
| 17.42 | 0.15 | 2.61 |
| 17.70 | 0.13 | 2.30 |
| 18.00 | 0.11 | 1.98 |
| 18.10 | 0.1 | 1.81 |
| 18.20 | 0.09 | 1.64 |
| 18.40 | 0.08 | 1.47 |
| 18.70 | 0.06 | 1.12 |
| 19.00 | 0 | 0 |
| 19.20 | 0 | 0 |
| 19.30 | 0 | 0 |
| 19.40 | 0 | 0 |
| 20.00 | 0 | 0 |

Table 5.12 Values of electrical responses of mono crystalline PV panel under no
shading strength condition

| Voltage (volt) | Current (amp) | Power (watt) |
|---|---|---|
| 0 | 0.44 | 0 |
| 5.00 | 0.42 | 2.1 |
| 6.90 | 0.36 | 2.48 |
| 7.15 | 0.35 | 2.50 |
| 7.40 | 0.34 | 2.51 |
| 7.70 | 0.33 | 2.54 |
| 8.00 | 0.32 | 2.56 |
| 8.20 | 0.28 | 2.30 |
| 8.40 | 0.26 | 2.25 |
| 8.50 | 0.24 | 2.100 |
| 8.60 | 0.22 | 1.95 |
| 8.75 | 0.20 | 1.75 |
| 8.85 | 0.18 | 1.55 |
| 9.00 | 0.15 | 1.35 |
| 9.20 | 0.13 | 1.15 |
| 9.30 | 0.11 | 1.02 |
| 9.40 | 0.06 | 0.56 |
| 9.50 | 0 | 0 |

Table 5.13 Values of electrical responses of mono crystalline PV panel under 1.56%
shading strength condition

| Voltage (volt) | Current (amp) | Power (watt) |
|---|---|---|
| 0 | 0.42 | 0 |
| 5.00 | 0.4 | 2 |
| 6.90 | 0.35 | 2.42 |
| 7.15 | 0.34 | 2.43 |
| 7.40 | 0.33 | 2.44 |
| 7.70 | 0.32 | 2.46 |
| 8.00 | 0.29 | 2.30 |
| 8.20 | 0.27 | 2.20 |
| 8.40 | 0.24 | 2.05 |
| 8.50 | 0.22 | 1.80 |
| 8.60 | 0.20 | 1.70 |
| 8.75 | 0.17 | 1.50 |
| 8.85 | 0.15 | 1.40 |
| 9.00 | 0.14 | 1.25 |

| | | |
|---|---|---|
| 9.20 | 0.10 | 0.89 |
| 9.30 | 0.06 | 0.55 |
| 9.40 | 0 | 0 |
| 9.50 | 0 | 0 |

Table 5.14 Values of electrical responses of mono crystalline PV panel under 6.25% shading strength condition

| Voltage (volt) | Current (amp) | Power (watt) |
|---|---|---|
| 0 | 0.37 | 0 |
| 5.00 | 0.36 | 1.80 |
| 6.90 | 0.32 | 2.21 |
| 7.15 | 0.31 | 2.22 |
| 7.40 | 0.3 | 2.22 |
| 7.70 | 0.27 | 2.10 |
| 8.00 | 0.24 | 1.98 |
| 8.20 | 0.22 | 1.84 |
| 8.40 | 0.20 | 1.64 |
| 8.50 | 0.17 | 1.45 |
| 8.60 | 0.15 | 1.30 |
| 8.75 | 0.13 | 1.15 |
| 8.85 | 0.12 | 1.05 |
| 9.00 | 0.09 | 0.89 |
| 9.20 | 0.06 | 0.56 |
| 9.30 | 0 | 0 |
| 9.40 | 0 | 0 |
| 9.50 | 0 | 0 |

Table 5.15 Values of electrical responses of mono crystalline PV panel under 12.5% shading strength condition

| Voltage (volt) | Current (amp) | Power (watt) |
|---|---|---|
| 0 | 0.31 | 0 |
| 5.00 | 0.3 | 1.5 |
| 6.90 | 0.28 | 1.93 |
| 7.15 | 0.28 | 2.00 |
| 7.40 | 0.26 | 1.92 |
| 7.70 | 0.24 | 1.85 |
| 8.00 | 0.2 | 1.60 |
| 8.20 | 0.18 | 1.45 |
| 8.40 | 0.16 | 1.35 |

| | | |
|---|---|---|
| 8.50 | 0.15 | 1.25 |
| 8.60 | 0.13 | 1.15 |
| 8.75 | 0.12 | 1.05 |
| 8.85 | 0.10 | 0.89 |
| 9.00 | 0.06 | 0.55 |
| 9.20 | 0 | 0 |
| 9.30 | 0 | 0 |
| 9.40 | 0 | 0 |
| 9.50 | 0 | 0 |

Table 5.16 Values of electrical responses of mono crystalline PV panel under 25% shading strength condition

| Voltage (volt) | Current (amp) | Power (watt) |
|---|---|---|
| 0 | 0.23 | 0 |
| 5.0 | 0.22 | 1.1 |
| 6.90 | 0.21 | 1.45 |
| 7.15 | 0.20 | 1.40 |
| 7.40 | 0.18 | 1.36 |
| 7.70 | 0.17 | 1.30 |
| 8.00 | 0.15 | 1.20 |
| 8.20 | 0.14 | 1.14 |
| 8.40 | 0.12 | 1.01 |
| 8.50 | 0.10 | 0.85 |
| 8.60 | 0.09 | 0.77 |
| 8.75 | 0.07 | 0.61 |
| 8.85 | 0.04 | 0.35 |
| 9.00 | 0 | 0 |
| 9.20 | 0 | 0 |
| 9.30 | 0 | 0 |
| 9.40 | 0 | 0 |
| 9.50 | 0 | 0 |

Table 5.17 Values of electrical responses of poly crystalline PV panel under no shading strength condition

| Voltage (volt) | Current (amp) | Power (watt) |
|---|---|---|
| 0 | 0.46 | 0 |
| 5.00 | 0.44 | 2.20 |
| 6.40 | 0.39 | 2.50 |
| 6.60 | 0.38 | 2.54 |
| 6.90 | 0.37 | 2.58 |

| | | |
|---|---|---|
| 7.15 | 0.36 | 2.61 |
| 7.60 | 0.35 | 2.68 |
| 8.20 | 0.26 | 2.20 |
| 8.30 | 0.24 | 2.03 |
| 8.40 | 0.22 | 1.85 |
| 8.60 | 0.19 | 1.64 |
| 8.70 | 0.15 | 1.35 |
| 8.80 | 0.13 | 1.16 |
| 8.90 | 0.11 | 0.99 |
| 9.00 | 0.06 | 0.56 |
| 9.20 | 0 | 0 |

Table 5.18 Values of electrical responses of poly crystalline PV panel under 1.56% shading strength condition

| Voltage (volt) | Current (amp) | Power (watt) |
|---|---|---|
| 0 | 0.43 | 0 |
| 5.00 | 0.42 | 2.10 |
| 6.40 | 0.36 | 2.30 |
| 6.60 | 0.35 | 2.35 |
| 6.90 | 0.34 | 2.38 |
| 7.15 | 0.34 | 2.41 |
| 7.60 | 0.29 | 2.20 |
| 8.20 | 0.22 | 1.80 |
| 8.30 | 0.21 | 1.71 |
| 8.40 | 0.18 | 1.54 |
| 8.60 | 0.15 | 1.30 |
| 8.70 | 0.11 | 0.97 |
| 8.80 | 0.06 | 0.54 |
| 8.90 | 0.04 | 0.40 |
| 9.00 | 0 | 0 |
| 9.20 | 0 | 0 |

Table 5.19 Values of electrical responses of poly crystalline PV panel under 6.25% shading strength condition

| Voltage (volt) | Current (amp) | Power (watt) |
|---|---|---|
| 0 | 0.32 | 0 |
| 5.00 | 0.28 | 1.40 |
| 6.40 | 0.26 | 1.67 |
| 6.60 | 0.26 | 1.72 |

| | | |
|---|---|---|
| 6.90 | 0.25 | 1.73 |
| 7.15 | 0.23 | 1.65 |
| 7.60 | 0.20 | 1.55 |
| 8.20 | 0.16 | 1.31 |
| 8.30 | 0.13 | 1.08 |
| 8.40 | 0.10 | 0.84 |
| 8.60 | 0.08 | 0.69 |
| 8.70 | 0.05 | 0.44 |
| 8.80 | 0.03 | 0.26 |
| 8.90 | 0 | 0 |
| 9.00 | 0 | 0 |
| 9.20 | 0 | 0 |

Table 5.20 Values of electrical responses of poly crystalline PV panel under 12.5% shading strength condition

| Voltage (volt) | Current (amp) | Power (watt) |
|---|---|---|
| 0 | 0.21 | 0 |
| 5.00 | 0.20 | 1 |
| 6.40 | 0.19 | 1.22 |
| 6.60 | 0.19 | 1.26 |
| 6.90 | 0.17 | 1.17 |
| 7.15 | 0.16 | 1.14 |
| 7.60 | 0.14 | 1.05 |
| 8.20 | 0.11 | 0.90 |
| 8.30 | 0.09 | 0.75 |
| 8.40 | 0.06 | 0.50 |
| 8.60 | 0.04 | 0.34 |
| 8.70 | 0 | 0 |
| 8.80 | 0 | 0 |
| 8.90 | 0 | 0 |
| 9.00 | 0 | 0 |
| 9.20 | 0 | 0 |

Table 5.21 Values of electrical responses of poly crystalline PV panel under 25% shading strength condition

| Voltage (volt) | Current (amp) | Power (watt) |
|---|---|---|
| 0 | 0.17 | 0 |
| 5.00 | 0.17 | 0.85 |
| 6.40 | 0.16 | 1.02 |

| | | |
|------|------|------|
| 6.60 | 0.15 | 0.99 |
| 6.90 | 0.14 | 0.97 |
| 7.15 | 0.13 | 0.93 |
| 7.60 | 0.12 | 0.85 |
| 8.20 | 0.08 | 0.65 |
| 8.30 | 0.06 | 0.52 |
| 8.40 | 0.04 | 0.33 |
| 8.60 | 0 | 0 |
| 8.70 | 0 | 0 |
| 8.80 | 0 | 0 |
| 8.90 | 0 | 0 |
| 9.00 | 0 | 0 |
| 9.20 | 0 | 0 |

# APPENDIX-III

## VI.I Tables Used in Chapter-6

Table 6.1 Measured electrical parameters for the clean panel surface at 722 W/m$^2$

| Voltage (volt) | Current (amp) | Power (watt) |
|---|---|---|
| 0 | 0.48 | 0 |
| 3.00 | 0.48 | 1.44 |
| 5.00 | 0.48 | 2.4 |
| 9.50 | 0.47 | 4.465 |
| 10.60 | 0.46 | 4.876 |
| 12.40 | 0.45 | 5.58 |
| 13.80 | 0.44 | 6.072 |
| 14.70 | 0.43 | 6.321 |
| 15.40 | 0.42 | 6.468 |
| 16.10 | 0.41 | 6.601 |
| 16.50 | 0.4 | 6.6 |
| 17.20 | 0.38 | 6.536 |
| 17.40 | 0.37 | 6.438 |
| 17.60 | 0.35 | 6.16 |
| 17.70 | 0.34 | 6.018 |
| 17.90 | 0.32 | 5.728 |
| 18.00 | 0.31 | 5.58 |
| 18.10 | 0.3 | 5.43 |
| 18.20 | 0.27 | 4.914 |
| 18.40 | 0.25 | 4.6 |
| 18.50 | 0.24 | 4.44 |
| 18.60 | 0.22 | 4.092 |
| 18.70 | 0.2 | 3.74 |
| 18.80 | 0.18 | 3.384 |
| 18.90 | 0.16 | 3.024 |
| 19.00 | 0.14 | 2.66 |
| 19.10 | 0.11 | 2.101 |
| 19.20 | 0.08 | 1.536 |
| 19.30 | 0 | 0 |

Table 6.2 Measured electrical parameters for the deposition of 1 gm iron ore dust on PV panel surface

| Voltage (volt) | Current (amp) | Power (watt) |
|---|---|---|
| 0 | 0.46 | 0 |
| 3.00 | 0.46 | 1.38 |
| 5.00 | 0.46 | 2.3 |

| Voltage (volt) | Current (amp) | Power (watt) |
|---|---|---|
| 9.50 | 0.45 | 4.275 |
| 10.60 | 0.44 | 4.664 |
| 12.40 | 0.43 | 5.332 |
| 13.80 | 0.42 | 5.796 |
| 14.70 | 0.41 | 6.027 |
| 15.40 | 0.4 | 6.16 |
| 16.10 | 0.39 | 6.279 |
| 16.50 | 0.38 | 6.27 |
| 17.20 | 0.36 | 6.192 |
| 17.40 | 0.35 | 6.09 |
| 17.60 | 0.33 | 5.808 |
| 17.70 | 0.32 | 5.664 |
| 17.90 | 0.3 | 5.37 |
| 18.00 | 0.29 | 5.22 |
| 18.10 | 0.27 | 4.887 |
| 18.20 | 0.26 | 4.732 |
| 18.40 | 0.24 | 4.416 |
| 18.50 | 0.22 | 4.07 |
| 18.60 | 0.2 | 3.72 |
| 18.70 | 0.17 | 3.179 |
| 18.80 | 0.14 | 2.632 |
| 18.90 | 0.12 | 2.268 |
| 19.00 | 0.1 | 1.9 |
| 19.10 | 0.06 | 1.146 |
| 19.20 | 0 | 0 |
| 19.30 | 0 | 0 |

Table 6.3 Measured electrical parameters for the deposition of 2 gm iron ore dust on PV panel surface

| Voltage (volt) | Current (amp) | Power (watt) |
|---|---|---|
| 0 | 0.44 | 0 |
| 3.00 | 0.44 | 1.32 |
| 5.00 | 0.44 | 2.2 |
| 9.50 | 0.43 | 4.085 |
| 10.60 | 0.42 | 4.452 |
| 12.40 | 0.41 | 5.084 |
| 13.80 | 0.4 | 5.52 |
| 14.70 | 0.39 | 5.733 |
| 15.40 | 0.38 | 5.852 |
| 16.10 | 0.37 | 5.957 |
| 16.50 | 0.36 | 5.94 |

| Voltage | Current | Power |
|---|---|---|
| 17.20 | 0.34 | 5.848 |
| 17.40 | 0.33 | 5.742 |
| 17.60 | 0.31 | 5.456 |
| 17.70 | 0.29 | 5.133 |
| 17.90 | 0.27 | 4.833 |
| 18.00 | 0.25 | 4.5 |
| 18.10 | 0.24 | 4.344 |
| 18.20 | 0.23 | 4.186 |
| 18.40 | 0.21 | 3.864 |
| 18.50 | 0.19 | 3.515 |
| 18.60 | 0.15 | 2.79 |
| 18.70 | 0.13 | 2.431 |
| 18.80 | 0.11 | 2.068 |
| 18.90 | 0.08 | 1.512 |
| 19.00 | 0 | 0 |
| 19.10 | 0 | 0 |
| 19.20 | 0 | 0 |
| 19.30 | 0 | 0 |

Table 6.4 Measured electrical parameters for the deposition of 3 gm iron ore dust on PV panel surface

| Voltage (volt) | Current (amp) | Power (watt) |
|---|---|---|
| 0 | 0.42 | 0 |
| 3.00 | 0.42 | 1.26 |
| 5.00 | 0.42 | 2.1 |
| 9.50 | 0.41 | 3.895 |
| 10.60 | 0.4 | 4.24 |
| 12.40 | 0.39 | 4.836 |
| 13.80 | 0.38 | 5.244 |
| 14.70 | 0.37 | 5.439 |
| 15.40 | 0.36 | 5.544 |
| 16.10 | 0.35 | 5.635 |
| 16.50 | 0.34 | 5.61 |
| 17.20 | 0.32 | 5.504 |
| 17.40 | 0.31 | 5.394 |
| 17.60 | 0.29 | 5.104 |
| 17.70 | 0.27 | 4.779 |
| 17.90 | 0.25 | 4.475 |
| 18.00 | 0.23 | 4.14 |
| 18.10 | 0.2 | 3.62 |
| 18.20 | 0.18 | 3.276 |

| Voltage (volt) | Current (amp) | Power (watt) |
|---|---|---|
| 18.40 | 0.16 | 2.944 |
| 18.50 | 0.14 | 2.59 |
| 18.60 | 0.12 | 2.232 |
| 18.70 | 0.1 | 1.87 |
| 18.80 | 0.06 | 1.128 |
| 18.90 | 0 | 0 |
| 19.00 | 0 | 0 |
| 19.10 | 0 | 0 |
| 19.20 | 0 | 0 |
| 19.30 | 0 | 0 |

Table 6.5 Measured electrical parameters for the deposition of 4 gm iron ore dust on PV panel surface

| Voltage (volt) | Current (amp) | Power (watt) |
|---|---|---|
| 0 | 0.38 | 0 |
| 3.00 | 0.38 | 1.14 |
| 5.00 | 0.38 | 1.9 |
| 9.50 | 0.37 | 3.515 |
| 10.60 | 0.36 | 3.816 |
| 12.40 | 0.35 | 4.34 |
| 13.80 | 0.34 | 4.692 |
| 14.70 | 0.33 | 4.851 |
| 15.40 | 0.32 | 4.928 |
| 16.10 | 0.31 | 4.991 |
| 16.50 | 0.3 | 4.95 |
| 17.20 | 0.28 | 4.816 |
| 17.40 | 0.26 | 4.524 |
| 17.60 | 0.24 | 4.224 |
| 17.70 | 0.23 | 4.071 |
| 17.90 | 0.21 | 3.759 |
| 18.00 | 0.19 | 3.42 |
| 18.10 | 0.17 | 3.077 |
| 18.20 | 0.15 | 2.73 |
| 18.40 | 0.13 | 2.392 |
| 18.50 | 0.11 | 2.035 |
| 18.60 | 0.08 | 1.488 |
| 18.70 | 0 | 0 |
| 18.80 | 0 | 0 |
| 18.90 | 0 | 0 |
| 19.00 | 0 | 0 |
| 19.10 | 0 | 0 |

| Voltage (volt) | Current (amp) | Power (watt) |
|:---:|:---:|:---:|
| 19.20 | 0 | 0 |
| 19.30 | 0 | 0 |

Table 6.6 Measured electrical parameters for the deposition of 5 gm iron ore dust on PV panel surface

| Voltage (volt) | Current (amp) | Power (watt) |
|:---:|:---:|:---:|
| 0 | 0.34 | 0 |
| 3.00 | 0.34 | 1.02 |
| 5.00 | 0.34 | 1.7 |
| 9.50 | 0.33 | 3.135 |
| 10.60 | 0.32 | 3.392 |
| 12.40 | 0.29 | 3.596 |
| 13.80 | 0.27 | 3.726 |
| 14.70 | 0.26 | 3.822 |
| 15.40 | 0.25 | 3.85 |
| 16.10 | 0.23 | 3.703 |
| 16.50 | 0.22 | 3.63 |
| 17.20 | 0.2 | 3.44 |
| 17.40 | 0.18 | 3.132 |
| 17.60 | 0.17 | 2.992 |
| 17.70 | 0.16 | 2.832 |
| 17.90 | 0.13 | 2.327 |
| 18.00 | 0.12 | 2.16 |
| 18.10 | 0.1 | 1.81 |
| 18.20 | 0.07 | 1.274 |
| 18.40 | 0 | 0 |
| 18.50 | 0 | 0 |
| 18.60 | 0 | 0 |
| 18.70 | 0 | 0 |
| 18.80 | 0 | 0 |
| 18.90 | 0 | 0 |
| 19.00 | 0 | 0 |
| 19.10 | 0 | 0 |
| 19.20 | 0 | 0 |
| 19.30 | 0 | 0 |

Table 6.7 Measured electrical parameters for the deposition of 6 gm iron ore dust on PV panel surface

| Voltage (volt) | Current (amp) | Power (watt) |
|---|---|---|
| 0 | 0.28 | 0 |
| 3.00 | 0.28 | 0.84 |
| 5.00 | 0.28 | 1.4 |
| 9.50 | 0.27 | 2.565 |
| 10.60 | 0.26 | 2.756 |
| 12.40 | 0.25 | 3.1 |
| 13.80 | 0.23 | 3.174 |
| 14.70 | 0.22 | 3.234 |
| 15.40 | 0.21 | 3.234 |
| 16.10 | 0.2 | 3.22 |
| 16.50 | 0.19 | 3.135 |
| 17.20 | 0.17 | 2.924 |
| 17.40 | 0.16 | 2.784 |
| 17.60 | 0.15 | 2.64 |
| 17.70 | 0.13 | 2.301 |
| 17.90 | 0.11 | 1.969 |
| 18.00 | 0.08 | 1.44 |
| 18.10 | 0 | 0 |
| 18.20 | 0 | 0 |
| 18.40 | 0 | 0 |
| 18.50 | 0 | 0 |
| 18.60 | 0 | 0 |
| 18.70 | 0 | 0 |
| 18.80 | 0 | 0 |
| 18.90 | 0 | 0 |
| 19.00 | 0 | 0 |
| 19.10 | 0 | 0 |
| 19.20 | 0 | 0 |
| 19.30 | 0 | 0 |

Table 6.8 Measured electrical parameters for the deposition of 7 gm iron ore dust on PV panel surface

| Voltage (volt) | Current (amp) | Power (watt) |
|---|---|---|
| 0 | 0.25 | 0 |
| 3.00 | 0.25 | 0.75 |
| 5.00 | 0.25 | 1.25 |
| 9.50 | 0.24 | 2.28 |

| | | |
|---|---|---|
| 10.60 | 0.23 | 2.438 |
| 12.40 | 0.22 | 2.728 |
| 13.80 | 0.21 | 2.898 |
| 14.70 | 0.2 | 2.94 |
| 15.40 | 0.19 | 2.926 |
| 16.10 | 0.17 | 2.737 |
| 16.50 | 0.16 | 2.64 |
| 17.20 | 0.14 | 2.408 |
| 17.40 | 0.12 | 2.088 |
| 17.60 | 0.1 | 1.76 |
| 17.70 | 0.08 | 1.416 |
| 17.90 | 0 | 0 |
| 18.00 | 0 | 0 |
| 18.10 | 0 | 0 |
| 18.20 | 0 | 0 |
| 18.40 | 0 | 0 |
| 18.50 | 0 | 0 |
| 18.60 | 0 | 0 |
| 18.70 | 0 | 0 |
| 18.80 | 0 | 0 |
| 18.90 | 0 | 0 |
| 19.00 | 0 | 0 |
| 19.10 | 0 | 0 |
| 19.20 | 0 | 0 |
| 19.30 | 0 | 0 |

Table 6.9 Measured electrical parameters for the deposition of 8 gm iron ore dust on PV panel surface

| Voltage (volt) | Current (amp) | Power (watt) |
|---|---|---|
| 0 | 0.24 | 0 |
| 3.00 | 0.24 | 0.72 |
| 5.00 | 0.24 | 1.2 |
| 9.50 | 0.23 | 2.185 |
| 10.60 | 0.22 | 2.332 |
| 12.40 | 0.21 | 2.604 |
| 13.80 | 0.2 | 2.76 |
| 14.70 | 0.19 | 2.793 |
| 15.40 | 0.18 | 2.772 |
| 16.10 | 0.16 | 2.576 |
| 16.50 | 0.14 | 2.31 |
| 17.20 | 0.11 | 1.892 |

| | | |
|---|---|---|
| 17.40 | 0.08 | 1.392 |
| 17.60 | 0 | 0 |
| 17.70 | 0 | 0 |
| 17.90 | 0 | 0 |
| 18.00 | 0 | 0 |
| 18.10 | 0 | 0 |
| 18.20 | 0 | 0 |
| 18.40 | 0 | 0 |
| 18.50 | 0 | 0 |
| 18.60 | 0 | 0 |
| 18.70 | 0 | 0 |
| 18.80 | 0 | 0 |
| 18.90 | 0 | 0 |
| 19.00 | 0 | 0 |
| 19.10 | 0 | 0 |
| 19.20 | 0 | 0 |
| 19.30 | 0 | 0 |

Table 6.10 Measured electrical parameters for the deposition of 9 gm iron ore dust on PV panel surface

| Voltage (volt) | Current (amp) | Power (watt) |
|---|---|---|
| 0 | 0.18 | 0 |
| 3.00 | 0.18 | 0.54 |
| 5.00 | 0.18 | 0.9 |
| 9.50 | 0.17 | 1.615 |
| 10.60 | 0.16 | 1.696 |
| 12.40 | 0.14 | 1.736 |
| 13.80 | 0.13 | 1.794 |
| 14.70 | 0.12 | 1.764 |
| 15.40 | 0.11 | 1.694 |
| 16.10 | 0.1 | 1.61 |
| 16.50 | 0.09 | 1.485 |
| 17.20 | 0.06 | 1.032 |
| 17.40 | 0 | 0 |
| 17.60 | 0 | 0 |
| 17.70 | 0 | 0 |
| 17.90 | 0 | 0 |
| 18.00 | 0 | 0 |
| 18.10 | 0 | 0 |
| 18.20 | 0 | 0 |
| 18.40 | 0 | 0 |

| | | |
|---|---|---|
| 18.50 | 0 | 0 |
| 18.60 | 0 | 0 |
| 18.70 | 0 | 0 |
| 18.80 | 0 | 0 |
| 18.90 | 0 | 0 |
| 19.00 | 0 | 0 |
| 19.10 | 0 | 0 |
| 19.20 | 0 | 0 |
| 19.30 | 0 | 0 |

Table 6.11 Measured electrical parameters for the deposition of 10 gm iron ore dust on PV panel surface

| Voltage (volt) | Current (amp) | Power (watt) |
|---|---|---|
| 0 | 0.16 | 0 |
| 3 | 0.16 | 0.48 |
| 5 | 0.16 | 0.8 |
| 9.5 | 0.15 | 1.425 |
| 10.6 | 0.14 | 1.484 |
| 12.4 | 0.13 | 1.612 |
| 13.8 | 0.12 | 1.656 |
| 14.7 | 0.11 | 1.617 |
| 15.4 | 0.1 | 1.54 |
| 16.1 | 0.08 | 1.288 |
| 16.5 | 0.06 | 0.99 |
| 17.2 | 0 | 0 |
| 17.4 | 0 | 0 |
| 17.6 | 0 | 0 |
| 17.7 | 0 | 0 |
| 17.9 | 0 | 0 |
| 18 | 0 | 0 |
| 18.1 | 0 | 0 |
| 18.2 | 0 | 0 |
| 18.4 | 0 | 0 |
| 18.5 | 0 | 0 |
| 18.6 | 0 | 0 |
| 18.7 | 0 | 0 |
| 18.8 | 0 | 0 |
| 18.9 | 0 | 0 |
| 19 | 0 | 0 |
| 19.1 | 0 | 0 |
| 19.2 | 0 | 0 |

| 19.3 | 0 | 0 |
| --- | --- | --- |

Table 6.15 Readings of the electrical parameters for the clean panel surface at 750 W/m$^2$

| Voltage (volt) | Current (amp) | Power (watt) |
| --- | --- | --- |
| 0 | 0.51 | 0 |
| 5.00 | 0.5 | 2.5 |
| 8.30 | 0.48 | 3.984 |
| 8.60 | 0.48 | 4.128 |
| 10.50 | 0.46 | 4.83 |
| 11.50 | 0.45 | 5.175 |
| 12.40 | 0.44 | 5.456 |
| 14.00 | 0.43 | 6.02 |
| 15.0 | 0.42 | 6.3 |
| 15.80 | 0.41 | 6.478 |
| 16.50 | 0.4 | 6.6 |
| 17.20 | 0.39 | 6.708 |
| 17.50 | 0.38 | 6.65 |
| 17.70 | 0.36 | 6.372 |
| 17.90 | 0.35 | 6.265 |
| 18.10 | 0.33 | 5.973 |
| 18.20 | 0.32 | 5.824 |
| 18.40 | 0.3 | 5.52 |
| 18.50 | 0.29 | 5.365 |
| 18.70 | 0.27 | 5.049 |
| 18.80 | 0.25 | 4.7 |
| 18.85 | 0.24 | 4.524 |
| 19.00 | 0.21 | 3.99 |
| 19.10 | 0.2 | 3.82 |
| 19.20 | 0.18 | 3.456 |
| 19.30 | 0.16 | 3.088 |
| 19.40 | 0.14 | 2.716 |
| 19.50 | 0.11 | 2.145 |
| 19.55 | 0.1 | 1.955 |
| 19.65 | 0.08 | 1.572 |
| 19.75 | 0.06 | 1.185 |
| 19.90 | 0 | 0 |

Table 6.16 Readings of the electrical parameters for the dust particles between 600 μ

to less than 850 μ

| Voltage (volt) | Current (amp) | Power (watt) |
|---|---|---|
| 0 | 0.43 | 0 |
| 5.00 | 0.42 | 2.1 |
| 8.30 | 0.40 | 3.32 |
| 8.60 | 0.39 | 3.354 |
| 10.50 | 0.37 | 3.885 |
| 11.50 | 0.36 | 4.14 |
| 12.40 | 0.35 | 4.34 |
| 14.00 | 0.34 | 4.76 |
| 15.0 | 0.33 | 4.95 |
| 15.80 | 0.32 | 5.056 |
| 16.50 | 0.31 | 5.115 |
| 17.20 | 0.29 | 4.988 |
| 17.50 | 0.28 | 4.9 |
| 17.70 | 0.27 | 4.779 |
| 17.90 | 0.25 | 4.475 |
| 18.10 | 0.24 | 4.344 |
| 18.20 | 0.22 | 4.004 |
| 18.40 | 0.21 | 3.864 |
| 18.50 | 0.20 | 3.7 |
| 18.70 | 0.18 | 3.366 |
| 18.80 | 0.17 | 3.196 |
| 18.85 | 0.16 | 3.016 |
| 19.00 | 0.14 | 2.66 |
| 19.10 | 0.13 | 2.483 |
| 19.20 | 0.11 | 2.112 |
| 19.30 | 0.10 | 1.93 |
| 19.40 | 0.08 | 1.552 |
| 19.50 | 0.05 | 0.975 |
| 19.55 | 0 | 0 |
| 19.65 | 0 | 0 |
| 19.75 | 0 | 0 |
| 19.90 | 0 | 0 |

Table 6.17 Readings of the electrical parameters for the dust particles between 300 μ

to less than 600 μ

| Voltage (volt) | Current (amp) | Power (watt) |
|---|---|---|
| 0 | 0.37 | 0 |
| 5.00 | 0.36 | 1.8 |
| 8.30 | 0.35 | 2.905 |
| 8.60 | 0.35 | 3.01 |

| | | |
|---|---|---|
| 10.50 | 0.34 | 3.57 |
| 11.50 | 0.33 | 3.795 |
| 12.40 | 0.32 | 3.968 |
| 14.00 | 0.31 | 4.34 |
| 15.0 | 0.30 | 4.5 |
| 15.80 | 0.29 | 4.582 |
| 16.50 | 0.27 | 4.455 |
| 17.20 | 0.26 | 4.472 |
| 17.50 | 0.25 | 4.375 |
| 17.70 | 0.24 | 4.248 |
| 17.90 | 0.23 | 4.117 |
| 18.10 | 0.22 | 3.982 |
| 18.20 | 0.20 | 3.64 |
| 18.40 | 0.19 | 3.496 |
| 18.50 | 0.18 | 3.33 |
| 18.70 | 0.17 | 3.179 |
| 18.80 | 0.16 | 3.008 |
| 18.85 | 0.14 | 2.639 |
| 19.00 | 0.12 | 2.28 |
| 19.10 | **0.10** | 1.91 |
| 19.20 | 0.08 | 1.536 |
| 19.30 | 0.05 | 0.965 |
| 19.40 | 0 | 0 |
| 19.50 | 0 | 0 |
| 19.55 | 0 | 0 |
| 19.65 | 0 | 0 |
| 19.75 | 0 | 0 |
| 19.90 | 0 | 0 |

Table 6.18 Readings of the electrical parameters for the dust particles between 150μ

to less than 300μ

| Voltage (volt) | Current (amp) | Power (watt) |
|---|---|---|
| 0 | 0.31 | 0 |
| 5.00 | 0.30 | 1.50 |
| 8.30 | 0.29 | 2.407 |
| 8.60 | 0.28 | 2.408 |
| 10.50 | 0.27 | 2.835 |
| 11.50 | 0.26 | 2.99 |
| 12.40 | 0.25 | 3.1 |
| 14.00 | 0.24 | 3.36 |
| 15.0 | 0.24 | 3.6 |
| 15.80 | 0.23 | 3.634 |
| 16.50 | 0.22 | 3.63 |

| Voltage (volt) | Current (amp) | Power (watt) |
|---|---|---|
| 17.20 | 0.20 | 3.44 |
| 17.50 | 0.19 | 3.325 |
| 17.70 | 0.18 | 3.186 |
| 17.90 | 0.17 | 3.043 |
| 18.10 | 0.16 | 2.896 |
| 18.20 | 0.14 | 2.548 |
| 18.40 | 0.13 | 2.392 |
| 18.50 | 0.12 | 2.22 |
| 18.70 | 0.11 | 2.057 |
| 18.80 | 0.10 | 1.88 |
| 18.85 | 0.09 | 1.6965 |
| 19.00 | 0.07 | 1.33 |
| 19.10 | 0.06 | 1.146 |
| 19.20 | 0 | 0 |
| 19.30 | 0 | 0 |
| 19.40 | 0 | 0 |
| 19.50 | 0 | 0 |
| 19.55 | 0 | 0 |
| 19.65 | 0 | 0 |
| 19.75 | 0 | 0 |
| 19.90 | 0 | 0 |

Table 6.19 Readings of the electrical parameters for the dust particles between 75 μ to less than 150 μ

| Voltage (volt) | Current (amp) | Power (watt) |
|---|---|---|
| 0 | 0.28 | 0 |
| 5.00 | 0.27 | 1.35 |
| 8.30 | 0.26 | 2.158 |
| 8.60 | 0.25 | 2.15 |
| 10.50 | 0.24 | 2.52 |
| 11.50 | 0.23 | 2.645 |
| 12.40 | 0.22 | 2.728 |
| 14.00 | 0.21 | 2.94 |
| 15.0 | 0.19 | 2.85 |
| 15.80 | 0.17 | 2.686 |
| 16.50 | 0.16 | 2.64 |
| 17.20 | 0.15 | 2.58 |
| 17.50 | 0.14 | 2.45 |
| 17.70 | 0.13 | 2.301 |
| 17.90 | 0.12 | 2.148 |
| 18.10 | 0.11 | 1.991 |
| 18.20 | 0.10 | 1.82 |
| 18.40 | 0.09 | 1.656 |
| 18.50 | 0.08 | 1.48 |

| Voltage | Current | Power |
|---|---|---|
| 18.70 | 0.07 | 1.309 |
| 18.80 | 0.06 | 1.128 |
| 18.85 | 0.05 | 0.9425 |
| 19.00 | 0 | 0 |
| 19.10 | 0 | 0 |
| 19.20 | 0 | 0 |
| 19.30 | 0 | 0 |
| 19.40 | 0 | 0 |
| 19.50 | 0 | 0 |
| 19.55 | 0 | 0 |
| 19.65 | 0 | 0 |
| 19.75 | 0 | 0 |
| 19.90 | 0 | 0 |

Table 6.20 Readings of the electrical parameters for the dust particles less than 75 μ

| Voltage (volt) | Current (amp) | Power (watt) |
|---|---|---|
| 0 | 0.26 | 0 |
| 5.00 | 0.25 | 1.25 |
| 8.30 | 0.24 | 1.992 |
| 8.60 | 0.23 | 1.978 |
| 10.50 | 0.22 | 2.31 |
| 11.50 | 0.21 | 2.415 |
| 12.40 | 0.20 | 2.48 |
| 14.00 | 0.19 | 2.66 |
| 15.0 | 0.17 | 2.55 |
| 15.80 | 0.16 | 2.528 |
| 16.50 | 0.15 | 2.475 |
| 17.20 | 0.14 | 2.408 |
| 17.50 | 0.13 | 2.275 |
| 17.70 | 0.12 | 2.124 |
| 17.90 | 0.11 | 1.969 |
| 18.10 | 0.10 | 1.81 |
| 18.20 | 0.09 | 1.638 |
| 18.40 | 0.08 | 1.472 |
| 18.50 | 0.08 | 1.48 |
| 18.70 | 0.06 | 1.122 |
| 18.80 | 0.05 | 0.94 |
| 18.85 | 0 | 0 |
| 19.00 | 0 | 0 |
| 19.10 | 0 | 0 |
| 19.20 | 0 | 0 |
| 19.30 | 0 | 0 |
| 19.40 | 0 | 0 |
| 19.50 | 0 | 0 |
| 19.55 | 0 | 0 |

| | | |
|---|---|---|
| 19.65 | 0 | 0 |
| 19.75 | 0 | 0 |
| 19.90 | 0 | 0 |

Table 6.23 Readings of the electrical parameters for the clean panel surface at 567 W/m$^2$

| Voltage (volt) | Current (amp) | Power (watt) |
|---|---|---|
| 0 | 0.36 | 0 |
| 7.50 | 0.35 | 2.625 |
| 12.50 | 0.33 | 4.125 |
| 16.20 | 0.31 | 5.022 |
| 17.75 | 0.27 | 4.79 |
| 18.35 | 0.22 | 4.026 |
| 18.50 | 0.17 | 3.145 |
| 18.75 | 0.13 | 2.4375 |
| 18.95 | 0.12 | 2.268 |
| 19.60 | 0.06 | 1.176 |
| 19.70 | 0 | 0 |

Table 6.24 Readings of the electrical parameters for the red soil of 5 gm dust deposition on its surface

| Voltage (volt) | Current (amp) | Power (watt) |
|---|---|---|
| 0 | 0.28 | 0 |
| 7.50 | 0.27 | 2.025 |
| 12.50 | 0.24 | 3 |
| 16.20 | 0.22 | 3.564 |
| 17.75 | 0.18 | 3.195 |
| 18.35 | 0.13 | 2.3855 |
| 18.50 | 0.09 | 1.665 |
| 18.75 | 0.06 | 1.125 |
| 18.95 | 0 | 0 |
| 19.60 | 0 | 0 |
| 19.70 | 0 | 0 |

Table 6.25 Readings of the electrical parameters for the red soil of 8 gm dust deposition on its surface

| Voltage (volt) | Current (amp) | Power (watt) |
|---|---|---|
| 0 | 0.24 | 0 |

| | | |
|---|---|---|
| 7.50 | 0.22 | 1.65 |
| 12.50 | 0.18 | 2.25 |
| 16.20 | 0.17 | 2.754 |
| 17.75 | 0.14 | 2.485 |
| 18.35 | 0.11 | 2.0185 |
| 18.50 | 0.07 | 1.295 |
| 18.75 | 0 | 0 |
| 18.95 | 0 | 0 |
| 19.60 | 0 | 0 |
| 19.70 | 0 | 0 |

Table 6.26 Readings of the electrical parameters for the red soil of 11 gm dust deposition on its surface

| Voltage (volt) | Current (amp) | Power (watt) |
|---|---|---|
| 0 | 0.2 | 0 |
| 7.50 | 0.17 | 1.275 |
| 12.50 | 0.14 | 1.75 |
| 16.20 | 0.12 | 1.944 |
| 17.75 | 0.07 | 1.2425 |
| 18.35 | 0 | 0 |
| 18.50 | 0 | 0 |
| 18.75 | 0 | 0 |
| 18.95 | 0 | 0 |
| 19.60 | 0 | 0 |
| 19.70 | 0 | 0 |

Table 6.27 Readings of the electrical parameters for the lime stone of 5 gm dust deposition on its surface

| Voltage (volt) | Current (amp) | Power (watt) |
|---|---|---|
| 0 | 0.31 | 0 |
| 7.50 | 0.3 | 2.25 |
| 12.50 | 0.28 | 3.5 |
| 16.20 | 0.25 | 4.05 |
| 17.75 | 0.21 | 3.7275 |
| 18.35 | 0.18 | 3.303 |
| 18.50 | 0.15 | 2.775 |
| 18.75 | 0.11 | 2.0625 |
| 18.95 | 0.07 | 1.3265 |
| 19.60 | 0 | 0 |

| Voltage (volt) | Current (amp) | Power (watt) |
|:---:|:---:|:---:|
| 19.70 | 0 | 0 |

Table 6.28 Readings of the electrical parameters for the lime stone of 8 gm dust deposition on its surface

| Voltage (volt) | Current (amp) | Power (watt) |
|:---:|:---:|:---:|
| 0 | 0.27 | 0 |
| 7.50 | 0.26 | 1.95 |
| 12.50 | 0.24 | 3 |
| 16.20 | 0.22 | 3.564 |
| 17.75 | 0.18 | 3.195 |
| 18.35 | 0.15 | 2.7525 |
| 18.50 | 0.12 | 2.22 |
| 18.75 | 0.08 | 1.5 |
| 18.95 | 0 | 0 |
| 19.60 | 0 | 0 |
| 19.70 | 0 | 0 |

Table 6.29 Readings of the electrical parameters for the lime stone of 11 gm dust deposition on its surface

| Voltage (volt) | Current (amp) | Power (watt) |
|:---:|:---:|:---:|
| 0 | 0.24 | 0 |
| 7.50 | 0.22 | 1.65 |
| 12.50 | 0.19 | 2.375 |
| 16.20 | 0.15 | 2.43 |
| 17.75 | 0.11 | 1.9525 |
| 18.35 | 0.07 | 1.2845 |
| 18.50 | 0 | 0 |
| 18.75 | 0 | 0 |
| 18.95 | 0 | 0 |
| 19.60 | 0 | 0 |
| 19.70 | 0 | 0 |

Table 6.30 Readings of the electrical parameters for the iron ore of 5 gm dust deposition on its surface

| Voltage (volt) | Current (amp) | Power (watt) |
|:---:|:---:|:---:|
| 0 | 0.33 | 0 |

| | | |
|---|---|---|
| 7.50 | 0.32 | 2.4 |
| 12.50 | 0.31 | 3.875 |
| 16.20 | 0.29 | 4.698 |
| 17.75 | 0.24 | 4.26 |
| 18.35 | 0.2 | 3.67 |
| 18.50 | 0.16 | 2.96 |
| 18.75 | 0.12 | 2.25 |
| 18.95 | 0.08 | 1.516 |
| 19.60 | 0 | 0 |
| 19.70 | 0 | 0 |

Table 6.31 Readings of the electrical parameters for the iron ore of 8 gm dust deposition on its surface

| Voltage (volt) | Current (amp) | Power (watt) |
|---|---|---|
| 0 | 0.3 | 0 |
| 7.50 | 0.28 | 2.1 |
| 12.50 | 0.25 | 3.125 |
| 16.20 | 0.25 | 4.05 |
| 17.75 | 0.2 | 3.55 |
| 18.35 | 0.15 | 2.7525 |
| 18.50 | 0.11 | 2.035 |
| 18.75 | 0.07 | 1.3125 |
| 18.95 | 0 | 0 |
| 19.60 | 0 | 0 |
| 19.70 | 0 | 0 |

Table 6.32 Readings of the electrical parameters for the iron ore of 11 gm dust deposition on its surface

| Voltage (volt) | Current (amp) | Power (watt) |
|---|---|---|
| 0 | 0.27 | 0 |
| 7.50 | 0.25 | 1.875 |
| 12.50 | 0.21 | 2.625 |
| 16.20 | 0.18 | 2.916 |
| 17.75 | 0.14 | 2.485 |
| 18.35 | 0.11 | 2.0185 |
| 18.50 | 0.06 | 1.11 |
| 18.75 | 0 | 0 |
| 18.95 | 0 | 0 |
| 19.60 | 0 | 0 |

| Voltage | | |
|---------|---|---|
| 19.70 | 0 | 0 |

Table 6.37 Measured values of currents and voltages of clean and dusty PV panel for the day one

| Voltage (volt) | Current of clean panel (amp) | Current of dusty panel (amp) |
|---|---|---|
| 0 | 0.65 | 0.53 |
| 5 | 0.63 | 0.52 |
| 10 | 0.61 | 0.5 |
| 15.2 | 0.58 | 0.45 |
| 16.4 | 0.52 | 0.42 |
| 17.2 | 0.49 | 0.39 |
| 17.7 | 0.44 | 0.35 |
| 18.1 | 0.4 | 0.31 |
| 18.4 | 0.38 | 0.28 |
| 18.7 | 0.34 | 0.23 |
| 19 | 0.29 | 0.19 |
| 19.4 | 0.26 | 0.16 |
| 19.7 | 0.21 | 0.12 |
| 20 | 0.17 | 0.09 |
| 20.37 | 0.12 | 0 |
| 20.5 | 0.09 | 0 |
| 20.62 | 0 | 0 |

Table 6.38 Measured values of currents and voltages of clean and dusty PV panel for the day two

| Voltage (volt) | Current of clean panel (amp) | Current of dusty panel (amp) |
|---|---|---|
| 0 | 0.51 | 0.39 |
| 5 | 0.5 | 0.38 |
| 10 | 0.48 | 0.36 |
| 15.2 | 0.46 | 0.35 |
| 16.4 | 0.42 | 0.31 |
| 17.2 | 0.38 | 0.28 |
| 17.7 | 0.35 | 0.24 |
| 18.1 | 0.32 | 0.2 |
| 18.4 | 0.28 | 0.17 |
| 18.7 | 0.25 | 0.15 |
| 19 | 0.21 | 0.13 |
| 19.4 | 0.18 | 0.1 |

| | | |
|---|---|---|
| 19.7 | 0.15 | 0.09 |
| 20 | 0.12 | 0.06 |
| 20.06 | 0.11 | 0 |
| 20.3 | 0.08 | 0 |
| 20.5 | 0 | 0 |

Table 6.39 Measured values of currents and voltages of clean and dusty PV panel for the day three

| Voltage (volt) | Current of clean panel (amp) | Current of dusty panel (amp) |
|---|---|---|
| 0 | 0.6 | 0.42 |
| 5 | 0.59 | 0.41 |
| 10 | 0.57 | 0.39 |
| 15.2 | 0.52 | 0.37 |
| 16.4 | 0.48 | 0.32 |
| 17.2 | 0.44 | 0.29 |
| 17.7 | 0.4 | 0.27 |
| 18.1 | 0.37 | 0.23 |
| 18.7 | 0.32 | 0.19 |
| 19 | 0.28 | 0.15 |
| 19.4 | 0.24 | 0.12 |
| 19.7 | 0.19 | 0.09 |
| 19.8 | 0.16 | 0 |
| 20 | 0.12 | 0 |
| 20.3 | 0.09 | 0 |
| 20.57 | 0 | 0 |

Table 6.40 Measured values of currents and voltages of clean and dusty PV panel for the day four

| Voltage (volt) | Current of clean panel (amp) | Current of dusty panel (amp) |
|---|---|---|
| 0 | 0.8 | 0.51 |
| 5 | 0.79 | 0.5 |
| 10 | 0.75 | 0.47 |
| 15.2 | 0.72 | 0.44 |
| 16.4 | 0.69 | 0.4 |
| 17.2 | 0.64 | 0.37 |
| 17.7 | 0.56 | 0.3 |
| 18.1 | 0.5 | 0.26 |
| 18.4 | 0.44 | 0.2 |

| | | |
|---|---|---|
| 18.7 | 0.38 | 0.16 |
| 19 | 0.33 | 0.13 |
| 19.4 | 0.26 | 0.09 |
| 19.77 | 0.18 | 0 |
| 20 | 0.13 | 0 |
| 20.3 | 0.09 | 0 |
| 20.6 | 0 | 0 |

Table 6.41 Measured values of currents and voltages of clean and dusty PV panel for the day four

| Voltage (volt) | Current of clean panel (amp) | Current of dusty panel (amp) |
|---|---|---|
| 0 | 0.96 | 0.57 |
| 5 | 0.94 | 0.56 |
| 10 | 0.91 | 0.54 |
| 15.2 | 0.88 | 0.5 |
| 16.4 | 0.82 | 0.45 |
| 17.2 | 0.72 | 0.4 |
| 17.7 | 0.69 | 0.38 |
| 18.1 | 0.6 | 0.32 |
| 18.4 | 0.47 | 0.27 |
| 18.7 | 0.4 | 0.23 |
| 19 | 0.35 | 0.18 |
| 19.2 | 0.32 | 0.13 |
| 19.4 | 0.28 | 0.09 |
| 19.75 | 0.23 | 0 |
| 20 | 0.18 | 0 |
| 20.2 | 0.11 | 0 |
| 20.4 | 0.09 | 0 |
| 20.65 | 0 | 0 |

Table 6.45 Readings of the electrical parameters for the clean panel surface at 1082W/m$^2$

| Voltage (volt) | Current (amp) | Power (watt) |
|---|---|---|
| 0 | 0.5 | 0 |
| 5.00 | 0.49 | 2.45 |
| 10.00 | 0.48 | 4.8 |
| 15.40 | 0.47 | 7.238 |
| 15.80 | 0.456 | 7.204 |
| 16.20 | 0.444 | 7.192 |

| | | |
|---|---|---|
| 16.40 | 0.435 | 7.134 |
| 16.60 | 0.43 | 7.138 |
| 16.90 | 0.42 | 7.098 |
| 17.20 | 0.41 | 7.052 |
| 17.30 | 0.40 | 6.92 |
| 17.40 | 0.39 | 6.786 |
| 17.50 | 0.38 | 6.65 |
| 17.60 | 0.36 | 6.336 |
| 17.70 | 0.35 | 6.195 |
| 17.80 | 0.33 | 5.874 |
| 17.90 | 0.32 | 5.728 |
| 18.00 | 0.30 | 5.4 |
| 18.10 | 0.29 | 5.249 |
| 18.20 | 0.27 | 4.914 |
| 18.30 | 0.25 | 4.575 |
| 18.35 | 0.24 | 4.404 |
| 18.40 | 0.23 | 4.232 |
| 18.50 | 0.22 | 4.07 |
| 18.60 | 0.21 | 3.906 |
| 18.70 | 0.19 | 3.553 |
| 18.80 | 0.17 | 3.196 |
| 18.90 | 0.14 | 2.646 |
| 19.00 | 0.11 | 2.09 |
| 19.10 | 0.06 | 1.146 |
| 19.20 | 0 | 0 |

Table 6.46 Readings of the electrical parameters for 3 gm of dust deposition on the panel surface

| Voltage (volt) | Current (amp) | Power (watt) |
|---|---|---|
| 0 | 0.4 | 0 |
| 5.00 | 0.40 | 2.00 |
| 10.00 | 0.39 | 3.90 |
| 15.40 | 0.36 | 5.54 |
| 15.80 | 0.36 | 5.70 |
| 16.20 | 0.34 | 5.50 |
| 16.40 | 0.32 | 5.24 |
| 16.60 | 0.3 | 4.98 |
| 16.90 | 0.28 | 4.73 |
| 17.20 | 0.26 | 4.46 |
| 17.30 | 0.24 | 4.18 |
| 17.40 | 0.23 | 3.98 |

| | | |
|---|---|---|
| 17.50 | 0.22 | 3.85 |
| 17.60 | 0.21 | 3.69 |
| 17.70 | 0.20 | 3.55 |
| 17.80 | 0.19 | 3.35 |
| 17.90 | 0.17 | 3.04 |
| 18.00 | 0.15 | 2.74 |
| 18.10 | 0.14 | 2.48 |
| 18.20 | 0.12 | 2.18 |
| 18.30 | 0.10 | 1.86 |
| 18.35 | 0.09 | 1.74 |
| 18.40 | 0.06 | 1.12 |
| 18.50 | 0.04 | 0.36 |
| 18.60 | 0 | 0 |
| 18.70 | 0 | 0 |
| 18.80 | 0 | 0 |
| 18.90 | 0 | 0 |
| 19.00 | 0 | 0 |
| 19.10 | 0 | 0 |
| 19.20 | 0 | 0 |

Table 6.47 Readings of the electrical parameters for 5 gm of dust deposition on the panel surface

| Voltage (volt) | Current (amp) | Power (watt) |
|---|---|---|
| 0 | 0.38 | 0 |
| 5.00 | 0.37 | 1.85 |
| 10.00 | 0.36 | 3.58 |
| 15.40 | 0.34 | 5.24 |
| 15.80 | 0.32 | 5.04 |
| 16.20 | 0.30 | 4.90 |
| 16.40 | 0.29 | 4.71 |
| 16.60 | 0.27 | 4.48 |
| 16.90 | 0.25 | 4.28 |
| 17.20 | 0.23 | 4.02 |
| 17.30 | 0.22 | 3.73 |
| 17.40 | 0.20 | 3.40 |
| 17.50 | 0.18 | 3.21 |
| 17.60 | 0.17 | 2.94 |
| 17.70 | 0.15 | 2.65 |
| 17.80 | 0.13 | 2.36 |
| 17.90 | 0.12 | 2.08 |
| 18.00 | 0.10 | 1.84 |

| | | |
|---|---|---|
| 18.10 | 0.09 | 1.63 |
| 18.20 | 0.08 | 1.49 |
| 18.30 | 0.05 | 0.89 |
| 18.35 | 0.04 | 0.25 |
| 18.40 | 0 | 0 |
| 18.50 | 0 | 0 |
| 18.60 | 0 | 0 |
| 18.70 | 0 | 0 |
| 18.80 | 0 | 0 |
| 18.90 | 0 | 0 |
| 19.00 | 0 | 0 |
| 19.10 | 0 | 0 |
| 19.20 | 0 | 0 |

Table 6.48 Readings of the electrical parameters for 8 gm of dust deposition on the panel surface

| Voltage (volt) | Current (amp) | Power (watt) |
|---|---|---|
| 0 | 0.34 | 0 |
| 5.00 | 0.33 | 1.65 |
| 10.00 | 0.32 | 3.2 |
| 15.40 | 0.3 | 4.62 |
| 15.80 | 0.28 | 4.42 |
| 16.20 | 0.27 | 4.37 |
| 16.40 | 0.26 | 4.26 |
| 16.60 | 0.24 | 3.96 |
| 16.90 | 0.22 | 3.74 |
| 17.20 | 0.21 | 3.59 |
| 17.30 | 0.20 | 3.46 |
| 17.40 | 0.19 | 3.31 |
| 17.50 | 0.18 | 3.16 |
| 17.60 | 0.17 | 2.96 |
| 17.70 | 0.15 | 2.67 |
| 17.80 | 0.13 | 2.31 |
| 17.90 | 0.11 | 1.98 |
| 18.00 | 0.09 | 1.63 |
| 18.10 | 0.05 | 0.92 |
| 18.20 | 0.004 | 0.23 |
| 18.30 | 0 | 0 |
| 18.35 | 0 | 0 |
| 18.40 | 0 | 0 |
| 18.50 | 0 | 0 |

| Voltage | Current | Power |
|---|---|---|
| 18.60 | 0 | 0 |
| 18.70 | 0 | 0 |
| 18.80 | 0 | 0 |
| 18.90 | 0 | 0 |
| 19.00 | 0 | 0 |
| 19.10 | 0 | 0 |
| 19.20 | 0 | 0 |

Table 6.49 Readings of the electrical parameters for 11 gm of dust deposition on the panel surface

| Voltage (volt) | Current (amp) | Power (watt) |
|---|---|---|
| 0 | 0.30 | 0 |
| 5.00 | 0.29 | 1.45 |
| 10.00 | 0.280 | 2.80 |
| 15.40 | 0.26 | 4.00 |
| 15.80 | 0.25 | 3.95 |
| 16.20 | 0.23 | 3.75 |
| 16.40 | 0.22 | 3.60 |
| 16.60 | 0.21 | 3.46 |
| 16.90 | 0.19 | 3.21 |
| 17.20 | 0.17 | 2.96 |
| 17.30 | 0.16 | 2.70 |
| 17.40 | 0.14 | 2.48 |
| 17.50 | 0.12 | 2.25 |
| 17.60 | 0.12 | 2.11 |
| 17.70 | 0.11 | 1.94 |
| 17.80 | 0.10 | 1.79 |
| 17.90 | 0.09 | 1.66 |
| 18.00 | 0.05 | 1.01 |
| 18.10 | 0.04 | 0.29 |
| 18.20 | 0 | 0 |
| 18.30 | 0 | 0 |
| 18.35 | 0 | 0 |
| 18.40 | 0 | 0 |
| 18.50 | 0 | 0 |
| 18.60 | 0 | 0 |
| 18.70 | 0 | 0 |
| 18.80 | 0 | 0 |
| 18.90 | 0 | 0 |
| 19.00 | 0 | 0 |
| 19.10 | 0 | 0 |

| Voltage (volt) | Current (amp) | Power (watt) |
|---|---|---|
| 19.20 | 0 | 0 |

Table 6.50 Readings of the electrical parameters for 13 gm of dust deposition on the panel surface

| Voltage (volt) | Current (amp) | Power (watt) |
|---|---|---|
| 0 | 0.28 | 0 |
| 5.00 | 0.28 | 1.4 |
| 10.00 | 0.27 | 2.7 |
| 15.40 | 0.25 | 3.85 |
| 15.80 | 0.25 | 3.95 |
| 16.20 | 0.23 | 3.73 |
| 16.40 | 0.21 | 3.44 |
| 16.60 | 0.19 | 3.15 |
| 16.90 | 0.18 | 3.04 |
| 17.20 | 0.16 | 2.75 |
| 17.30 | 0.14 | 2.42 |
| 17.40 | 0.13 | 2.26 |
| 17.50 | 0.12 | 2.10 |
| 17.60 | 0.11 | 1.94 |
| 17.70 | 0.1 | 1.77 |
| 17.80 | 0.10 | 1.79 |
| 17.90 | 0.09 | 1.66 |
| 18.00 | 0.05 | 0.92 |
| 18.10 | 0.03 | 0.22 |
| 18.20 | 0 | 0 |
| 18.30 | 0 | 0 |
| 18.35 | 0 | 0 |
| 18.40 | 0 | 0 |
| 18.50 | 0 | 0 |
| 18.60 | 0 | 0 |
| 18.70 | 0 | 0 |
| 18.80 | 0 | 0 |
| 18.90 | 0 | 0 |
| 19.00 | 0 | 0 |
| 19.10 | 0 | 0 |
| 19.20 | 0 | 0 |

Table 6.56 Readings of the electrical parameters for the clean panel

| Voltage (volt) | Current (amp) | Power (watt) |
|---|---|---|

| | | |
|---|---|---|
| 0 | 0.25 | 0 |
| 3.50 | 0.24 | 0.84 |
| 5.20 | 0.23 | 1.20 |
| 9.80 | 0.22 | 2.16 |
| 12.50 | 0.2 | 2.50 |
| 13.80 | 0.19 | 2.62 |
| 15.10 | 0.18 | 2.72 |
| 16.40 | 0.16 | 2.62 |
| 16.80 | 0.15 | 2.52 |
| 17.50 | 0.14 | 2.45 |
| 17.80 | 0.13 | 2.31 |
| 18.20 | 0.12 | 2.18 |
| 18.30 | 0.11 | 2.01 |
| 18.40 | 0.08 | 1.47 |
| 18.50 | 0.06 | 1.11 |

Table 6.57 Readings of the electrical parameters of the dusty panel with 3gm of mass deposition

| Voltage (volt) | Current (amp) | Power (watt) |
|---|---|---|
| 0 | 0.17 | 0 |
| 3.50 | 0.16 | 0.56 |
| 5.20 | 0.15 | 0.78 |
| 9.80 | 0.14 | 1.37 |
| 12.50 | 0.13 | 1.63 |
| 13.80 | 0.12 | 1.66 |
| 15.10 | 0.11 | 1.66 |
| 16.40 | 0.1 | 1.64 |
| 16.80 | 0.08 | 1.34 |
| 17.50 | 0.06 | 1.05 |
| 17.80 | 0 | 0 |
| 18.20 | 0 | 0 |
| 18.30 | 0 | 0 |
| 18.40 | 0 | 0 |
| 18.50 | 0 | 0 |

Table 6.58 Readings of the electrical parameters for the cleaned panel

| Voltage (volt) | Current (amp) | Power (watt) |
| --- | --- | --- |
| 0 | 0.2 | 0 |
| 3.50 | 0.19 | 0.67 |
| 5.20 | 0.18 | 0.94 |
| 9.80 | 0.17 | 1.67 |
| 12.50 | 0.16 | 2.00 |
| 13.80 | 0.15 | 2.07 |
| 15.10 | 0.14 | 2.11 |
| 16.40 | 0.13 | 2.13 |
| 16.80 | 0.12 | 2.02 |
| 17.50 | 0.11 | 1.93 |
| 17.80 | 0.1 | 1.78 |
| 18.20 | 0.08 | 1.46 |
| 18.30 | 0.06 | 1.10 |
| 18.40 | 0 | 0 |
| 18.50 | 0 | 0 |

## VI.II Input and Output Pins of Arduino Atmega 2560

Each of the 54 digital pins on the Mega can be used as an input or output, using pin Mode (),

digital Write (), and digital Read () functions. They operate at 5 volts. Each pin can provide or

receive a maximum of 40 mA and has an internal pull-up resistor (disconnected by default) of

20-50 k$\Omega$. In addition, some pins have specialized functions:

 **Serial: 0 (RX) and 1 (TX); Serial 1: 19 (RX) and 18 (TX); Serial 2: 17 (RX) and 16**

**(TX); Serial 3: 15 (RX) and 14 (TX).** Used to receive (RX) and transmit (TX) TTL serial data. Pins 0 and 1 are also connected to the corresponding pins of the ATmega16U2 USB-to-TTL Serial chip.

**External Interrupts: 2 (interrupt 0), 3 (interrupt 1), 18 (interrupt 5), 19 (interrupt**

**4), 20 (interrupt 3), and 21 (interrupt 2).** These pins can be configured to trigger an interrupt on a low value, a rising or falling edge, or a change in value. See the Attach Interrupt () function for details.

**PWM: 2 to 13 and 44 to 46.** Provide 8-bit PWM output with the analogWrite() function.

**SPI: 50 (MISO), 51 (MOSI), 52 (SCK), 53 (SS).** These pins support SPI communication using the SPI library. The SPI pins are also broken out on the ICSP header, which is physically compatible with the Uno, Duemilanove and Diecimila.

**LED: 13.** There is a built-in LED connected to digital pin 13. When the pin is HIGH value, the LED is on, when the pin is LOW, it's off.

**TWI: 20 (SDA) and 21 (SCL).** Support TWI communication using the Wire library. Note that these pins are not in the same location as the TWI pins on the Duemilanove or Diecimila. The Mega2560 has 16 analog inputs, each of which provide 10 bits of resolution (i.e., 1024\different values). By default, they measure from ground to 5 volts, though is it possibly to\change the upper end of their range using the AREF pin and analog Reference () function. There are a couple of other pins on the board:

**AREF.** Reference voltage for the analog inputs. Used with analog Reference ().

**Reset.** Bring this line LOW to reset the microcontroller. Typically used to add a reset button to shields which block the one on the board.

**VI.III Arduino Algorithm**

The algorithm which was used to operate the cleaning techniques is given in Annexure VI.

const int uplimit = 24;  // up limit switch fixed to pin 24

const int dnlimit = 22;  // down limit switch fixed to pin 22

Both swtches will be high

int up,dn;  // Declaring two variable up, dn to store value

const int en = 28;

```
const int in2 = 30;
const int in1 = 26;
#include <Wire.h>  // Invoke header file which support two wire interface
#include "RTClib.h"  // Connecting RTC
RTC_DS1307 rtc; // Connecting DS1307N IC
int HOUR,MIN;  // Declaring two variables hours and minutes
int am_time_hr=17;  //  Initializing the time to ON the motor during AM
int am_time_min=53;
int pm_time_hr=00;   // Initializing the time to ON the motor during PM
int pm_time_min=00;
void setup()
{
#ifdef AVR // Define Advance Virtual RISC
Wire.begin();      // Start Two wire interface
#else
Wire1.begin(); // Shield I2C pins connect to alt I2C bus on Arduino Due
#endif
rtc.begin();   // Start the clock
rtc.adjust(DateTime(__DATE__,__TIME__)); // Adjust current time and date
delay(1000);   // Small delay to stabilize the clock
pinMode(uplimit, INPUT);  // Switches output as input to IC
pinMode(dnlimit, INPUT);
pinMode(en, OUTPUT);   // Controller output as input to IC
pinMode(in1, OUTPUT);
pinMode(in2, OUTPUT);
Serial.begin(9600);  //  Display on screen
delay(1000);
}
void loop()
{
DateTime now = rtc.now(); // Read from RTC
HOUR=now.hour(); // New Hour
```

```
MIN=now.minute();  // New Min
Serial.print(HOUR);  // Print Hour in computer
Serial.print(":");
Serial.print(MIN);  // Print Min in computer
Serial.print(":");
Serial.println(now.second());  // Print sec in computer
delay(1000);  // For every sec display time
if(((HOUR == am_time_hr) && (MIN == am_time_min)) || ((HOUR ==
pm_time_hr) && (MIN == pm_time_min)))
{
Serial.println("Cleaning Started");  // Prints on screen when condition is satisfied
for(int i=0; i<1; i++)  // initialization, condition, increment
{
  digitalWrite(en, HIGH);
  digitalWrite(in1, HIGH);
  digitalWrite(in2, LOW);
do
  {
  dn=digitalRead(dnlimit);
  }while(dn == LOW);
digitalWrite(en, LOW);
  digitalWrite(in1, LOW);
  digitalWrite(in2, LOW);
delay(50);
 digitalWrite(en, HIGH);
  digitalWrite(in1, LOW);
  digitalWrite(in2, HIGH);
  do
  {
  up=digitalRead(uplimit);
  }while(up == HIGH);
  delay(50);
```

```
 digitalWrite(en, LOW);
 digitalWrite(in1, LOW);
 digitalWrite(in2, LOW);
 }
delay(30000);
Serial.println("Cleaning completed"); // Display cleaning completed after condition
processing completes
}
}
```

# APPENDIX-IV

Table 7.2 Measured electrical responses of monocrystalline PV panel at 35ºC

| Voltage (volt) | Current (amp) | Power (watt) |
| --- | --- | --- |
| 0 | 0.35 | 0 |
| 5 | 0.35 | 1.75 |
| 6.5 | 0.34 | 2.21 |
| 7.3 | 0.33 | 2.41 |
| 7.5 | 0.33 | 2.48 |
| 7.8 | 0.32 | 2.49 |
| 8 | 0.31 | 2.48 |
| 8.1 | 0.31 | 2.51 |
| 8.2 | 0.29 | 2.38 |
| 8.3 | 0.28 | 2.32 |
| 8.4 | 0.27 | 2.27 |
| 8.5 | 0.26 | 2.21 |
| 8.6 | 0.25 | 2.15 |
| 8.75 | 0.24 | 2.1 |
| 8.9 | 0.23 | 2.05 |
| 9.1 | 0.21 | 1.91 |
| 9.2 | 0.19 | 1.75 |
| 9.3 | 0.17 | 1.58 |
| 9.4 | 0.15 | 1.41 |
| 9.5 | 0.14 | 1.33 |
| 9.6 | 0.12 | 1.15 |
| 9.7 | 0.08 | 0.78 |
| 9.8 | 0.06 | 0.59 |
| 9.95 | 0 | 0 |

Table 7.3 Measured electrical responses of monocrystalline PV panel at 45ºC

| Voltage (volt) | Current (amp) | Power (watt) |
| --- | --- | --- |
| 0 | 0.35 | 0 |
| 5.00 | 0.34 | 1.70 |
| 6.50 | 0.33 | 2.15 |
| 7.30 | 0.31 | 2.26 |
| 7.50 | 0.30 | 2.25 |
| 7.80 | 0.29 | 2.26 |
| 8.00 | 0.29 | 2.32 |
| 8.10 | 0.28 | 2.27 |
| 8.20 | 0.27 | 2.21 |
| 8.30 | 0.26 | 2.16 |
| 8.40 | 0.25 | 2.10 |
| 8.50 | 0.24 | 2.04 |
| 8.60 | 0.22 | 1.89 |

| Voltage (volt) | Current (amp) | Power (watt) |
|---|---|---|
| 8.75 | 0.20 | 1.75 |
| 8.90 | 0.18 | 1.60 |
| 9.10 | 0.16 | 1.46 |
| 9.20 | 0.14 | 1.29 |
| 9.30 | 0.12 | 1.12 |
| 9.40 | 0.10 | 0.94 |
| 9.50 | 0.07 | 0.67 |
| 9.60 | 0 | 0 |
| 9.70 | 0 | 0 |
| 9.8 | 0 | 0 |
| 9.95 | 0 | 0 |

Table 7.4 Measured electrical responses of monocrystalline PV panel at 55ºC

| Voltage (volt) | Current (amp) | Power (watt) |
|---|---|---|
| 0 | 0.36 | 0 |
| 5.00 | 0.35 | 1.75 |
| 6.50 | 0.33 | 2.15 |
| 7.30 | 0.29 | 2.12 |
| 7.50 | 0.28 | 2.10 |
| 7.80 | 0.28 | 2.18 |
| 8.00 | 0.27 | 2.16 |
| 8.10 | 0.26 | 2.11 |
| 8.20 | 0.25 | 2.05 |
| 8.30 | 0.23 | 1.91 |
| 8.40 | 0.21 | 1.76 |
| 8.50 | 0.20 | 1.70 |
| 8.60 | 0.18 | 1.55 |
| 8.75 | 0.15 | 1.31 |
| 8.90 | 0.12 | 1.07 |
| 9.10 | 0.10 | 0.91 |
| 9.20 | 0.07 | 0.64 |
| 9.30 | 0 | 0 |
| 9.40 | 0 | 0 |
| 9.50 | 0 | 0 |
| 9.60 | 0 | 0 |
| 9.70 | 0 | 0 |
| 9.8 | 0 | 0 |
| 9.95 | 0 | 0 |

Table 7.5 Measured electrical responses of monocrystalline PV panel at 65°C

| Voltage (volt) | Current (amp) | Power (watt) |
|:---:|:---:|:---:|
| 0 | 0.365 | 0 |
| 5.00 | 0.35 | 1.75 |
| 6.50 | 0.32 | 2.08 |
| 7.30 | 0.29 | 2.12 |
| 7.50 | 0.29 | 2.18 |
| 7.80 | 0.27 | 2.11 |
| 8.00 | 0.26 | 2.08 |
| 8.10 | 0.25 | 2.03 |
| 8.20 | 0.22 | 1.80 |
| 8.30 | 0.19 | 1.58 |
| 8.40 | 0.16 | 1.34 |
| 8.50 | 0.14 | 1.19 |
| 8.60 | 0.12 | 1.03 |
| 8.75 | 0.10 | 0.88 |
| 8.90 | 0.08 | 0.71 |
| 9.10 | 0 | 0 |
| 9.20 | 0 | 0 |
| 9.30 | 0 | 0 |
| 9.40 | 0 | 0 |
| 9.50 | 0 | 0 |
| 9.60 | 0 | 0 |
| 9.70 | 0 | 0 |
| 9.8 | 0 | 0 |
| 9.95 | 0 | 0 |

Table 7.6 Measured electrical responses of monocrystalline PV panel at 75°C

| Voltage (volt) | Current (amp) | Power (watt) |
|:---:|:---:|:---:|
| 0 | 0.37 | 0 |
| 5.00 | 0.36 | 1.80 |
| 6.50 | 0.30 | 1.95 |
| 7.30 | 0.27 | 1.97 |
| 7.50 | 0.25 | 1.88 |
| 7.80 | 0.23 | 1.79 |
| 8.00 | 0.21 | 1.68 |
| 8.10 | 0.2 | 1.62 |
| 8.20 | 0.18 | 1.48 |
| 8.30 | 0.15 | 1.25 |
| 8.40 | 0.13 | 1.09 |

| | | |
|---|---|---|
| 8.50 | 0.10 | 0.85 |
| 8.60 | 0.06 | 0.52 |
| 8.75 | 0 | 0 |
| 8.90 | 0 | 0 |
| 9.10 | 0 | 0 |
| 9.20 | 0 | 0 |
| 9.30 | 0 | 0 |
| 9.40 | 0 | 0 |
| 9.50 | 0 | 0 |
| 9.60 | 0 | 0 |
| 9.70 | 0 | 0 |
| 9.8 | 0 | 0 |
| 9.95 | 0 | 0 |

Table 7.8 Measured electrical responses of polycrystalline PV panel at 35ºC

| Voltage (volt) | Current (amp) | Power (watt) |
|---|---|---|
| 0 | 0.36 | 0 |
| 2.00 | 0.36 | 0.72 |
| 3.00 | 0.36 | 1.08 |
| 5.00 | 0.35 | 1.75 |
| 6.50 | 0.32 | 2.08 |
| 7.50 | 0.31 | 2.33 |
| 7.80 | 0.30 | 2.34 |
| 8.00 | 0.30 | 2.4 |
| 8.20 | 0.302 | 2.48 |
| 8.30 | 0.26 | 2.16 |
| 8.40 | 0.25 | 2.10 |
| 8.50 | 0.23 | 1.96 |
| 8.60 | 0.21 | 1.81 |
| 8.80 | 0.18 | 1.58 |
| 8.90 | 0.16 | 1.42 |
| 9.00 | 0.13 | 1.17 |
| 9.10 | 0.11 | 1.00 |
| 9.20 | 0.09 | 0.83 |
| 9.35 | 0.06 | 0.56 |
| 9.45 | 0.05 | 0.47 |
| 9.60 | 0.03 | 0.29 |
| 9.70 | 0 | 0 |

Table 7.9 Measured electrical responses of polycrystalline PV panel at 45ºC

| Voltage (volt) | Current (amp) | Power (watt) |
|---|---|---|
| 0 | 0.36 | 0 |
| 2.00 | 0.36 | 0.72 |
| 3.00 | 0.36 | 1.08 |
| 5.00 | 0.35 | 1.75 |
| 6.50 | 0.31 | 2.02 |
| 7.50 | 0.30 | 2.25 |
| 7.80 | 0.29 | 2.26 |
| 8.00 | 0.29 | 2.33 |
| 8.20 | 0.25 | 2.05 |
| 8.30 | 0.22 | 1.83 |
| 8.40 | 0.19 | 1.59 |
| 8.50 | 0.17 | 1.45 |
| 8.60 | 0.14 | 1.20 |
| 8.80 | 0.11 | 0.97 |
| 8.90 | 0.09 | 0.80 |
| 9.00 | 0.08 | 0.72 |
| 9.10 | 0.06 | 0.55 |
| 9.20 | 0.03 | 0.28 |
| 9.35 | 0 | 0 |
| 9.45 | 0 | 0 |
| 9.60 | 0 | 0 |
| 9.70 | 0 | 0 |

Table 7.10 Measured electrical responses of polycrystalline PV panel at 55ºC

| Voltage (volt) | Current (amp) | Power (watt) |
|---|---|---|
| 0 | 0.365 | 0 |
| 2.00 | 0.36 | 0.72 |
| 3.00 | 0.36 | 1.08 |
| 5.00 | 0.34 | 1.70 |
| 6.50 | 0.30 | 1.95 |
| 7.50 | 0.28 | 2.10 |
| 7.80 | 0.279 | 2.18 |
| 8.00 | 0.23 | 1.84 |
| 8.20 | 0.2 | 1.64 |
| 8.30 | 0.18 | 1.49 |
| 8.40 | 0.14 | 1.18 |
| 8.50 | 0.11 | 0.94 |

| | | |
|---|---|---|
| 8.60 | 0.09 | 0.77 |
| 8.80 | 0.05 | 0.44 |
| 8.90 | 0 | 0 |
| 9.00 | 0 | 0 |
| 9.10 | 0 | 0 |
| 9.20 | 0 | 0 |
| 9.35 | 0 | 0 |
| 9.45 | 0 | 0 |
| 9.60 | 0 | 0 |
| 9.70 | 0 | 0 |

Table 7.11 Measured electrical responses of polycrystalline PV panel at 65ºC

| Voltage (volt) | Current (amp) | Power (watt) |
|---|---|---|
| 0 | 0.37 | 0 |
| 2.00 | 0.36 | 0.72 |
| 3.00 | 0.36 | 1.08 |
| 5.00 | 0.31 | 1.55 |
| 6.50 | 0.28 | 1.82 |
| 7.50 | 0.27 | 2.03 |
| 7.80 | 0.24 | 1.87 |
| 8.00 | 0.2 | 1.60 |
| 8.20 | 0.14 | 1.15 |
| 8.30 | 0.09 | 0.75 |
| 8.40 | 0.05 | 0.42 |
| 8.50 | 0 | 0 |
| 8.60 | 0 | 0 |
| 8.80 | 0 | 0 |
| 8.90 | 0 | 0 |
| 9.00 | 0 | 0 |
| 9.10 | 0 | 0 |
| 9.20 | 0 | 0 |
| 9.35 | 0 | 0 |
| 9.45 | 0 | 0 |
| 9.60 | 0 | 0 |
| 9.70 | 0 | 0 |

Table 7.12 Measured electrical responses of polycrystalline PV panel at 75ºC

| Voltage (volt) | Current (amp) | Power (watt) |
|---|---|---|
| 0 | 0.375 | 0 |
| 2.00 | 0.35 | 0.70 |
| 3.00 | 0.3 | 0.90 |
| 5.00 | 0.28 | 1.40 |
| 6.50 | 0.27 | 1.76 |
| 7.50 | 0.21 | 1.58 |
| 7.80 | 0.15 | 1.17 |
| 8.00 | 0.11 | 0.88 |
| 8.20 | 0 | 0 |
| 8.30 | 0 | 0 |
| 8.40 | 0 | 0 |
| 8.50 | 0 | 0 |
| 8.60 | 0 | 0 |
| 8.80 | 0 | 0 |
| 8.90 | 0 | 0 |
| 9.00 | 0 | 0 |
| 9.10 | 0 | 0 |
| 9.20 | 0 | 0 |
| 9.35 | 0 | 0 |
| 9.45 | 0 | 0 |
| 9.60 | 0 | 0 |
| 9.70 | 0 | 0 |

# APPENDIX-V

Table 8.6 Measured values of output voltage and current for day one

| Time | 0° | | 15° | | 30° | | 45° | | 60° | | 75° | | 90° | |
|---|---|---|---|---|---|---|---|---|---|---|---|---|---|---|
| | V (volt) | I (amp) | V (volt) | I (amp) | V (volt) | I (amp) | V (volt) | I (amp) | V (volt) | I (amp) | V (volt) | I (amp) | V (volt) | I (amp) |
| 9am | 15.40 | 1.82 | 15.80 | 2.28 | 15.70 | 2.28 | 15.60 | 2.19 | 15.50 | 1.93 | 15.10 | 1.48 | 14.80 | 1.09 |
| 10am | 15.80 | 2.35 | 15.90 | 2.42 | 15.80 | 2.39 | 15.70 | 2.92 | 15.60 | 2.13 | 15.50 | 1.98 | 15.30 | 1.74 |
| 11am | 16.40 | 2.85 | 16.80 | 3.02 | 16.80 | 2.98 | 16.40 | 2.95 | 16.40 | 2.78 | 15.80 | 2.32 | 15.50 | 2.04 |
| 12noon | 16.80 | 3.06 | 17.10 | 3.51 | 16.90 | 3.38 | 16.50 | 3.4 | 16.80 | 2.95 | 16.10 | 2.69 | 15.80 | 2.32 |
| 1pm | 16.60 | 3.02 | 16.90 | 3.37 | 16.40 | 3.35 | 16.40 | 3.25 | 16.90 | 2.89 | 15.90 | 2.57 | 15.70 | 2.23 |
| 2pm | 16.62 | 3.04 | 16.80 | 3.32 | 16.60 | 3.19 | 16.20 | 3.18 | 16.80 | 2.78 | 15.80 | 2.37 | 15.50 | 2.04 |
| 3pm | 16.20 | 2.64 | 16.40 | 2.79 | 16.10 | 2.82 | 15.90 | 2.74 | 15.90 | 2.51 | 15.60 | 2.27 | 15.50 | 1.88 |
| 4pm | 15.10 | 1.57 | 15.50 | 1.97 | 15.50 | 1.94 | 15.30 | 1.75 | 15.10 | 1.42 | 15.00 | 1.36 | 14.80 | 1.18 |
| 5pm | 14.40 | 0.87 | 14.50 | 0.96 | 14.40 | 0.93 | 14.20 | 0.85 | 13.90 | 0.8 | 13.70 | 0.71 | 13.70 | 0.52 |

Table 8.7 Measured values of output voltage and current for day two

| Time | 0° | | 15° | | 30° | | 45° | | 60° | | 75° | | 90° | |
|---|---|---|---|---|---|---|---|---|---|---|---|---|---|---|
| | V (volt) | I (amp) | V (volt) | I (amp) | V (volt) | I (amp) | V (volt) | I (amp) | V (volt) | I (amp) | V (volt) | I (amp) | V (volt) | I (amp) |
| 9am | 15.40 | 1.78 | 15.70 | 2.28 | 15.70 | 2.25 | 15.60 | 2.24 | 15.40 | 1.89 | 15.10 | 1.38 | 15.00 | 1.17 |
| 10am | 15.80 | 2.37 | 15.90 | 2.41 | 15.90 | 2.36 | 15.70 | 2.28 | 15.60 | 2.14 | 15.50 | 1.93 | 15.30 | 1.80 |
| 11am | 16.20 | 2.78 | 16.80 | 3.01 | 16.70 | 2.99 | 16.60 | 2.86 | 16.10 | 2.79 | 15.70 | 2.23 | 15.00 | 2.05 |
| 12noon | 16.80 | 2.98 | 17.80 | 3.32 | 17.10 | 3.21 | 17.10 | 3.17 | 16.60 | 3.04 | 15.90 | 2.62 | 15.80 | 2.27 |
| 1pm | 16.50 | 2.98 | 17.40 | 3.26 | 17.40 | 3.21 | 16.80 | 3.07 | 16.50 | 2.98 | 15.80 | 2.53 | 15.70 | 2.18 |
| 2pm | 16.40 | 2.92 | 17.10 | 3.21 | 16.90 | 3.06 | 16.70 | 2.84 | 16.10 | 2.79 | 15.70 | 2.28 | 15.40 | 2.00 |
| 3pm | 15.90 | 2.46 | 16.30 | 2.86 | 15.90 | 2.62 | 15.90 | 2.41 | 15.80 | 2.42 | 15.50 | 2.1 | 15.30 | 1.85 |
| 4pm | 15.20 | 1.59 | 15.40 | 2.06 | 15.40 | 1.89 | 15.20 | 1.81 | 15.10 | 1.43 | 15.10 | 1.38 | 15.00 | 1.17 |
| 5pm | 14.40 | 0.9 | 14.50 | 1.16 | 14.40 | 0.93 | 14.40 | 0.81 | 14.10 | 0.71 | 13.80 | 0.6 | 13.60 | 0.49 |

Table 8.8 Measured values of output voltage and current for day three

| Time | 0° | | 15° | | 30° | | 45° | | 60° | | 75° | | 90° | |
|------|---|---|---|---|---|---|---|---|---|---|---|---|---|---|
| | V (volt) | I (amp) | V (volt) | I (amp) | V (volt) | I (amp) | V (volt) | I (amp) | V (volt) | I (amp) | V (volt) | I (amp) | V (volt) | I (amp) |
| 9am | 15.40 | 1.84 | 15.70 | 2.39 | 15.80 | 2.27 | 15.70 | 2.18 | 15.70 | 1.96 | 15.10 | 1.43 | 15.10 | 1.16 |
| 10am | 15.80 | 2.37 | 15.90 | 2.46 | 15.90 | 2.39 | 15.80 | 2.32 | 15.80 | 2.11 | 15.50 | 1.99 | 15.30 | 1.74 |
| 11am | 16.40 | 2.89 | 16.80 | 3.07 | 16.60 | 3.06 | 16.70 | 2.84 | 16.70 | 2.69 | 15.80 | 2.34 | 15.40 | 2.00 |
| 12noon | 16.80 | 3.07 | 18.00 | 3.42 | 17.50 | 3.28 | 17.50 | 3.24 | 17.50 | 2.86 | 16.10 | 2.74 | 15.80 | 2.32 |
| 1pm | 16.60 | 3.04 | 17.70 | 3.29 | 17.20 | 3.24 | 17.10 | 3.17 | 17.10 | 2.83 | 15.90 | 2.62 | 15.70 | 2.18 |
| 2pm | 16.50 | 2.98 | 17.10 | 3.21 | 17.10 | 3.17 | 16.80 | 3.02 | 16.80 | 2.73 | 15.70 | 2.33 | 15.50 | 2.04 |
| 3pm | 16.10 | 2.74 | 16.20 | 2.88 | 16.10 | 2.64 | 15.90 | 2.67 | 15.90 | 2.57 | 15.50 | 2.1 | 15.40 | 1.89 |
| 4pm | 15.10 | 1.57 | 15.40 | 1.95 | 15.40 | 1.89 | 15.10 | 1.72 | 15.10 | 1.43 | 15.10 | 1.38 | 15.00 | 1.11 |
| 5pm | 14.40 | 0.86 | 14.50 | 1.08 | 14.40 | 0.83 | 14.40 | 0.81 | 14.40 | 0.64 | 13.80 | 0.48 | 13.60 | 0.43 |

Table 8.9 Measured values of output voltage and current for day four

| Time | 0° | | 15° | | 30° | | 45° | | 60° | | 75° | | 90° | |
|---|---|---|---|---|---|---|---|---|---|---|---|---|---|---|
| | V (volt) | I (amp) | V (volt) | I (amp) | V (volt) | I (amp) | V (volt) | I (amp) | V (volt) | I (amp) | V (volt) | I (amp) | V (volt) | I (amp) |
| 9am | 15.50 | 1.88 | 15.80 | 2.37 | 15.80 | 2.32 | 15.70 | 2.23 | 15.50 | 2.04 | 15.10 | 1.49 | 15.10 | 1.21 |
| 10am | 15.80 | 2.42 | 15.90 | 2.51 | 15.80 | 2.42 | 15.80 | 2.32 | 15.70 | 2.23 | 15.50 | 2.04 | 15.40 | 1.89 |
| 11am | 16.50 | 2.93 | 16.80 | 3.12 | 16.80 | 3.02 | 16.80 | 3.02 | 16.50 | 2.93 | 15.80 | 2.37 | 15.70 | 2.18 |
| 12noon | 16.90 | 3.15 | 18.10 | 3.45 | 17.60 | 3.31 | 17.60 | 3.31 | 16.90 | 3.06 | 16.10 | 2.79 | 15.90 | 2.46 |
| 1pm | 16.80 | 3.07 | 17.50 | 3.28 | 17.50 | 3.24 | 17.10 | 3.17 | 16.80 | 3.02 | 15.90 | 2.62 | 15.70 | 2.23 |
| 2pm | 16.80 | 3.02 | 17.50 | 3.24 | 17.10 | 3.17 | 16.90 | 3.1 | 16.30 | 2.91 | 15.80 | 2.42 | 15.60 | 2.08 |
| 3pm | 16.10 | 2.74 | 16.20 | 2.88 | 16.10 | 2.79 | 16.10 | 2.69 | 15.90 | 2.57 | 15.50 | 2.26 | 15.20 | 1.97 |
| 4pm | 15.20 | 1.60 | 15.50 | 1.99 | 15.40 | 1.95 | 15.20 | 1.81 | 15.10 | 1.43 | 15.10 | 1.49 | 15.10 | 1.21 |
| 5pm | 14.40 | 0.87 | 14.50 | 1.03 | 14.40 | 0.81 | 14.30 | 0.79 | 14.10 | 0.71 | 13.80 | 0.6 | 13.60 | 0.49 |

Table 8.10 Measured values of output voltage and current for day five

| Time | 0° | | 15° | | 30° | | 45° | | 60° | | 75° | | 90° | |
|---|---|---|---|---|---|---|---|---|---|---|---|---|---|---|
| | V (volt) | I (amp) | V (volt) | I (amp) | V (volt) | I (amp) | V (volt) | I (amp) | V (volt) | I (amp) | V (volt) | I (amp) | V (volt) | I (amp) |
| 9am | 15.30 | 1.80 | 15.80 | 2.32 | 15.70 | 2.23 | 15.50 | 2.15 | 15.40 | 1.95 | 15.10 | 1.43 | 15.10 | 1.21 |
| 10am | 15.80 | 2.32 | 15.90 | 2.41 | 15.80 | 2.32 | 15.70 | 2.23 | 15.60 | 2.14 | 15.40 | 1.95 | 15.20 | 1.70 |
| 11am | 16.40 | 2.84 | 16.80 | 3.02 | 16.80 | 2.97 | 16.60 | 2.86 | 16.10 | 2.79 | 15.70 | 2.23 | 15.50 | 2.04 |
| 12noon | 16.60 | 3.06 | 17.60 | 3.31 | 16.90 | 3.25 | 16.90 | 3.25 | 16.60 | 2.96 | 15.90 | 2.51 | 15.70 | 2.23 |
| 1pm | 16.50 | 2.98 | 17.50 | 3.24 | 16.80 | 3.12 | 16.80 | 3.07 | 16.60 | 2.86 | 15.90 | 2.41 | 15.60 | 2.08 |
| 2pm | 16.50 | 3.03 | 16.90 | 3.25 | 16.60 | 3.06 | 16.60 | 3.06 | 16.10 | 2.69 | 15.80 | 2.32 | 15.50 | 2.04 |
| 3pm | 15.90 | 2.67 | 16.10 | 2.69 | 15.90 | 2.62 | 15.90 | 2.51 | 15.80 | 2.32 | 15.50 | 2.04 | 15.40 | 1.84 |
| 4pm | 15.10 | 1.54 | 15.50 | 1.88 | 15.40 | 1.84 | 15.20 | 1.70 | 15.10 | 1.38 | 15.10 | 1.32 | 15.10 | 1.16 |
| 5pm | 14.40 | 0.81 | 14.50 | 1.03 | 14.40 | 0.86 | 14.40 | 0.81 | 14.10 | 0.65 | 13.80 | 0.48 | 13.60 | 0.43 |

## List of Publications based on PhD Research Work

| Sl. No. | Title of the paper | Authors (in the same order as in the paper. Underline the Research Scholar's name) | Name of the Journal/ Conference | Year of Publication | Category * |
|---|---|---|---|---|---|
| 1 | Influence of Mine Environmental Parameters on the Performance of Solar Energy System-A Review | Abhishek Kumar Tripathi, Ch.S.N.Murthy and M. Aruna | Concurrent Advances in Mechanical Engineering | 2016 | 1 |
| 2 | Performance of a PV panel under different shading strengths | Abhishek Kumar Tripathi, M. Aruna and Ch.S.N.Murthy | International Journal of Ambient Energy (Taylor and Francis) | 2017 | 1 |
| 3 | Performance Evaluation of PV Panel Under Dusty Condition | Abhishek Kumar Tripathi, M. Aruna and Ch.S.N.Murthy | International Journal of Renewable Energy Development | 2017 | 1 |
| 4 | Output Power Loss of Photovoltaic Panel Due to Dust and Temperature | Abhishek Kumar Tripathi, M. Aruna and Ch.S.N.Murthy | International Journal of Renewable Energy Research | 2017 | 1 |
| 5 | Experimental Investigation of Dust Effect on PV Module Performance | Abhishek Kumar Tripathi, Ch.S.N.Murthy and M. Aruna | Global Journal of Research in Engineering | 2017 | 1 |
| 6 | Performance Degradation of PV Module Due to Different Types of Dust Pollutants | Abhishek Kumar Tripathi, M. Aruna and Ch.S.N.Murthy | 2nd International Conference on Renewable Energy and Environmental Management (ICREEM 2017) at Phuket | 2017 | 3 |
| 7 | Effect of Shading on PV Panel Technology | Abhishek Kumar Tripathi, M. Aruna and Ch.S.N.Murthy | IEEE International Conference on Energy, Communication, Data Analytics and Soft Computing (ICECDS- 2017) | 2017 | 3 |
| 8 | Performance Analysis of PV Panel Under Varying Surface Temperature | Abhishek Kumar Tripathi, Ch.S.N.Murthy and M. Aruna | MATEC Web of Conferences ,RiMES 2017 | 2018 | 3 |

* Category: 1: Journal paper, full paper reviewed      2: Journal paper, Abstract reviews 3: Conference/Symposium paper, full paper reviewed
        4: Conference/Symposium paper, abstract reviewed      5: others (including papers in Workshops, NITK Research Bulletins, Short notes etc.)


**Abhishek Kumar Tripathi**
PhD Research Scholar
Name & Signature, with Date

**Prof. Ch.S.N. Murthy**
Research Guide
Name & Signature, with Date

**Dr. M. Aruna**
Research Guide
Name & Signature, with Date

**BIO-DATA**

**Name**      :    Abhishek Kumar Tripathi

**Date of Birth**   :   27-09-1991

**Address**      :    Assistant Professor, Department of

                       Mining Engineering, A.K.S. University,

                       Satna, Madhya Pradesh, India-485001

**E-mail**       :    abhinitrkl12@gmail.com

**Mobile**      :    +91-9098840971

**Academic Qualifications**

| Degree | University/Board | Year of Passing |
| --- | --- | --- |
| Ph.D in Mining Engineering | N.I.T.K, Surathkal | Pursuing |
| M.Tech in Mining Engineering | N.I.T, Rourkela | 2014 |
| B.E. in Electrical Engineering | B.I.T, Durg | 2012 |
| (10+2) Higher Secondary | CGBSE | 2008 |
| (10) High School | CGBSE | 2006 |

**Professional Experiences**

➢ Worked as an Assistance Professor in Godavari Institute of Engineering and Technology, Rajahmundry, in the session of 2014-2015.

➢ Presently working as an Assistant Professor in A.K.S. University Satna, Madhya Pradesh, India.

**OTHER QUALIFIED EXAMS: (**2 times)
GATE                                                                                                     2012
Branch: Electrical Engineering
Organizer: IIT, Delhi, India

**Publications (Citation: 06, Scopus ID: 57193692186)**

**Journal Publications**

1. **Abhishek Kumar Tripathi**, M. Aruna and Ch.S.N.Murthy (2017). "Performance of a PV panel under different shading strengths". International Journal of Ambient Energy (Taylor and Francis). (*Scopus Index, ESCI by Web of Science and more*)

2. **Abhishek Kumar Tripathi**, M. Aruna and Ch.S.N.Murthy (2017). "Performance Evaluation of PV Panel Under Dusty Condition". International Journal of Renewable Energy Development, 6(3), 225-233. (*ESCI by Web of Science and more*)

3. **Abhishek Kumar Tripathi**, M. Aruna and Ch.S.N.Murthy (2017). "Output Power Loss of Photovoltaic Panel Due to Dust and Temperature". International Journal of Renewable Energy Research (IJRER), 7(1), 439-442. (*Scopus Index, ESCI by Web of Science and more*)

4. **Abhishek Kumar Tripathi**, Ch.S.N.Murthy and M. Aruna and (2017). "Experimental Investigation of Dust Effect on PV Module Performance". Global Journal of Research in Engineering, 17(3), 35-39. (*EBSCO, Google Scholar and more*)

5. M.Aruna, N. Laxmipathy, **Abhishek Kumar Tripathi** and Ch.S.N.Murthy (2017). "Application of LED in Surface Mines- A Case Study". International Journal of Current Advanced Research, 6(5), 3783-3786. (*Crossref, Index of Copernicus, Google Scholar and more*)

6. **Abhishek Kumar Tripathi**, Ch.S.N.Murthy and M.Aruna (2016)."Influence of Mine Environmental Parameters on the Performance of Solar Energy System-A Review". Concurrent Advances in Mechanical Engineering, Vol. 2(1), pp. 1-5. (*Crossref, Index of Copernicus, Google Scholar and more*)

7. Shashwati Ray, **Abhishek Kumar Tripathi,** Gourav Shankar (2017). "Design and Performance Analysis of Solar Tracking PV System", International Journal

of Green Energy (Taylor& Francis). (***Under Review***).*(SCI, Scopus Index, ESCI by Web of Science and more)*

8. **Abhishek Kumar Tripathi**,M. Aruna and Ch.S.N.Murthy (2018). "Performance Degradation of PV Module Due to Different Types of Dust Pollutants" Advanced Science Letter, American Scientific Publisher. (***Accepted***) (*Scopus Index, ESCI by Web of Science and more*)

9. **Abhishek Kumar Tripathi**, M. Aruna and Ch.S.N. Murthy (2018). "Output Power Enhancement of Solar PV Panel Using Solar Tracking System". Recent Advance in Electrical and Electronics Engineering, Bentham Science Publication. (***Accepted***) (*Scopus Index, ESCI by Web of Science and more*)

## Conference Publications

1. **Abhishek Kumar Tripathi**, Ch.S.N.Murthy and M.Aruna (2018). "Performance Analysis of PV Panel Under Varying Surface Temperature", MATEC Web of Conferences. Vol. 144. EDP Sciences, 2018, International Conference on Research in Mechanical Engineering Sciences (RIMES), Decmber 21-23 2017, Manipal Institute of Technology, Manipal, Karnataka, India. (*Scopus Index*)

2. **Abhishek Kumar Tripathi**, M. Aruna and Ch.S.N.Murthy (2017). "Effect of Shading on PV Panel Technology". IEEE International Conference on Energy, Communication, Data Analytics and Soft Computing (ICECDS), August 1-2 2017, SKR Engineering College, Chennai. (*Scopus Index*)

3. Shashwati Ray and **Abhishek Kumar Tripathi** (2016). "Design and development of Tilted Single Axis and Azimuth-Altitude Dual Axis Solar Tracking systems".1stIEEE International Conference on Power Electronics, Intelligent Control and Energy Systems (ICPEICES-2016), July 4 -6, 2016, New Delhi By Delhi Technical University, Delhi, India. (*SCI, Scopus and more*)

4. **Abhishek Kumar Tripathi** and Ch.S.N.Murthy (2016). "Application of Solar Energy in Open Cast Mines- Case Study". National Seminar on Recent Practices and Innovations in Mining Industry, 19th -20th February 2016, Department of Mining Engineering NIT Raipur.

5. **Abhishek Kumar Tripathi** and H.B. Sahu (2015). "Application of Solar Energy for Lighting in Open Cast Mines". BITCON-2015 Innovations for National Development National Conference on: Theme of Concerned Department by BIT Durg Chhattisgarh

6. **Abhishek Kumar Tripathi** and H.B. Sahu (2014). "Application of Solar Energy in Mining Industry- A Case Study". Advances in Nanotechnology and Renewable Energy (NCNRE) April 28-29, 2014 by Jamia Millia Islamia, New Delhi

## REFERENCES

1. Dr. Ch. S. N. Murthy
   Professor, Dept. of Mining Engg.
   National Institute of Technology Karnataka, Surathkal
   575025, India
   chsn58@gmail.com

2. Dr. M. Aruna
   Associate Professor, Dept. of Mining Engg.
   National Institute of Technology Karnataka, Surathkal
   575025, India
   arunamangalpady@gmail.com

3. Dr. Shaswati Ray
   Professor, Dept. of Electrical Engineering
   Bhilai Institute of Technology Durg, Chhattisgarh
   491001, India
   shashwatiray@yahoo.com